

MANIPULATION OF POST-HARVEST  
PHYSIOLOGY IN BROCCOLI THROUGH AN  
OPTIMISED *AGROBACTERIUM*  
*RHIZOGENES*-MEDIATED  
TRANSFORMATION PROTOCOL

by

JAMES DAVID HIGGINS

A thesis submitted to the Faculty of Science  
of The University of Birmingham  
for the degree of  
DOCTOR OF PHILOSOPHY

School of Biosciences  
The University of Birmingham  
January 2002

UNIVERSITY OF  
BIRMINGHAM

**University of Birmingham Research Archive**

**e-theses repository**

This unpublished thesis/dissertation is copyright of the author and/or third parties. The intellectual property rights of the author or third parties in respect of this work are as defined by The Copyright Designs and Patents Act 1988 or as modified by any successor legislation.

Any use made of information contained in this thesis/dissertation must be in accordance with that legislation and must be properly acknowledged. Further distribution or reproduction in any format is prohibited without the permission of the copyright holder.

## Abstract

The aim of this project was to down-regulate *ACC oxidase (ACO) 1* and *2* and *ACC synthase (ACS)* in broccoli (*Brassica oleracea* var. *italica*) to lengthen post-harvest shelf-life. The *ACO 1* and *2* and *ACS* cDNAs of broccoli were ligated into pSCV1.0 in sense and antisense orientations in relation to a CaMV 35S promoter and *nos* terminator. They were electroporated into the *Agrobacterium rhizogenes* co-integrate strain LBA 9402 pRi1855::GFP, and used to co-transform GDDH33, a doubled haploid line derived from the calabrese cultivar Green Duke. 150 transgenic hairy roots were identified by GFP fluorescence, and 18 were regenerated into whole plants. Four of these lines showed severe *rol* phenotype, which did not appear to be related to T<sub>L</sub>-DNA insert copy number. The floral buds from T<sub>0</sub> broccoli heads were assayed for post-harvest production of ethylene and chlorophyll levels. T<sub>0</sub> lines with *ACC oxidase 1* and *2* constructs produced significantly less ethylene than the control plants, and chlorophyll loss was significantly reduced. A positive correlation between post-harvest bud ethylene production and chlorophyll loss was described by the equation  $y = 0.2386x - 23.041$ . There were two copies of *aco1* and *aco2* in the *Brassica oleracea* genome of which one was mapped for each to linkage group 1 and 8, respectively.

**Key Words:** broccoli, *Agrobacterium rhizogenes*, transformation, ACC oxidase, ACC synthase, ethylene, shelf-life

## **Acknowledgements**

I would first like to thank BBSRC and HRI for financially supporting my research over the past 3 years, and Horticulture Research International, Wellesbourne, and the University of Birmingham for providing me the opportunity to do this work.

At HRI, the glasshouse staff for watering my plants, and taking care of aphid problems. For Linda Doyle and Sandy McClement for pollinating and harvesting seeds from the T<sub>0</sub> plants.

I would like to thank Graham King and his group, Graham Teakle, Guy Barker and Rowena Naylor for assisting my work with the mapping.

I would also like to thank the breeding/transformation group of Helen Robinson, Noel Cogan, Lesley Griffiths, Jason Pole, and Liz Harvey for making my time at HRI enjoyable.

On a more personal level, I would like to thank Anne Morton who helped me with the Brassica DNA extractions in her own time, and Dez Barbara who also assisted beyond the call of duty. This thesis would not have been complete without their help. I would also like to thank Tony Roberts, Vinodh, Alex and Emily for making their laboratory a pleasant environment.

My special thanks go to Ian Puddephat, Dez Barbara and John Newbury who have supported me throughout the 3 years with scientific advice, moral support and humour when necessary.

My last acknowledgement goes to Jane Byrne and Erik Kop who have made the last 3 years fun.

## Table of Contents

1.0 General Introduction .....	1
1.1 Introduction .....	2
1.2 Genetic Improvement of Crop Plants .....	4
1.3 Transformation of <i>Brassica</i> .....	6
1.4 Senescence of Broccoli .....	12
1.5 Ethylene Biosynthesis .....	13
1.5.1 ACC synthase .....	14
1.5.2 ACC oxidase .....	14
1.6 Signalling .....	15
1.7 Antisense Technology.....	19
1.8 Isolation of ACC genes .....	21
1.9 Tissue specific expression of <i>ACC oxidases</i> in broccoli .....	23
1.10 Tomato fruit ripening and broccoli post-harvest senescence .....	25
1.11 Project Aims.....	27
2.0 Construction of <i>Brassica oleracea</i> ACC oxidase and ACC synthase sense and antisense gene cassettes .....	28
2.1 Introduction .....	29
2.2 Materials and Methods.....	33
2.2.1 Cloning Strategy.....	33
2.2.2 Plasmids.....	34
2.2.2.1 The <i>ACC oxidase</i> and <i>ACC synthase</i> cDNAs.....	34
2.2.2.2 Binary Vectors .....	35
2.2.2.3 Plasmid extraction.....	35

2.2.3 Bacterial strains and media .....	38
2.2.4 Enzymes and DNA .....	38
2.2.5 Cloning Strategy .....	41
2.2.5.1 Removing <i>gus</i> from pBI121 .....	41
2.2.5.2 Replacing <i>gus</i> with synthetic linker .....	41
2.2.5.3 Transferring CaMV 35S-linker-nos cassette from pBI121 to pSCV1.0 .....	43
2.2.5.4 Inserting the <i>Brassica oleracea ACC oxidase 1</i> and 2 cDNAs into pJ1.0 by blunt-ended cloning .....	44
2.2.5.5 pMOSBlue kit .....	46
2.2.5.6 Inserting <i>Brassica oleracea ACC synthase</i> cDNAs into pJ1.0 ...	46
2.2.5.7 Checking transformants for inserts .....	47
2.2.5.8 Control Plasmid .....	50
2.2.5.9 Producing and storing <i>E. coli</i> and <i>A. rhizogenes</i> stocks with the 7 constructs .....	51
2.3. Results .....	52
2.4. Discussion .....	61
3.0 Transformation of GDDH33 with <i>Agrobacterium rhizogenes</i> .....	63
3.1 Introduction .....	64
3.2 Materials and Methods .....	69
3.2.1 Plant material and culture conditions .....	69
3.2.2 Plant transformation .....	69
3.2.3 Identification of transformed 'hairy roots' .....	71
3.2.4 GUS detection .....	71
3.2.5 PCR .....	71

3.2.6 Shoot Regeneration from established root clones selected by GFP fluorescence .....	74
3.2.7 DNA extraction .....	74
3.2.8 Endonuclease restriction digest of genomic DNA.....	75
3.2.9 Southern Blot.....	76
3.2.10 Hybridisation between N+ filters and $\alpha^{32}\text{P}$ dCTP labelled DNA probes .....	77
3.2.11 Seeds .....	78
3.2.12 Statistical Analysis.....	78
3.3 Results .....	79
3.3.1 Constructs .....	79
3.3.2 Inoculation treatment.....	80
3.3.3 gfp reporter gene .....	82
3.3.4 Co-transformation.....	82
3.3.5 Regeneration.....	84
3.3.6 Determining stable insertion of the T-DNAs into the plant genome ...	86
3.3.7 Transgenic plant phenotype .....	102
3.3.8 Seed production of the transgenic lines .....	105
3.4 Discussion.....	110
4.0 Analysis of broccoli bud post-harvest ethylene production and chlorophyll levels.....	120
4.1 Introduction .....	121
4.2 Materials and Methods.....	127
4.2.1 Harvested broccoli heads.....	127
4.2.2 Ethylene Measurements.....	129

4.2.3 Chlorophyll Measurements.....	130
4.2.4 Measuring dry weight of broccoli buds .....	131
4.2.5 Data Analysis .....	131
4.3 Results .....	133
4.3.1 Tissue to be assayed .....	133
4.3.2 Controls for standardising the analysis of ethylene and chlorophyll	133
4.3.2.1 Calculating ethylene concentrations .....	133
4.3.2.2 Analysis of pre/post harvest ethylene production and chlorophyll levels in broccoli buds of non-transformed GDDH33 .....	134
4.3.3 Analysis of post-harvest ethylene production and chlorophyll levels of non-transformed GDDH33 and the transgenic lines.....	136
4.4 Discussion.....	150
5.0 Identifying <i>Brassica oleracea</i> ACC oxidases .....	159
5.1 Introduction .....	160
5.2 Materials and Methods.....	163
5.2.1 PCR.....	163
5.2.2 Bacterial Artificial Chromosomes (BACs) .....	165
5.2.3 Southern Blots and filters .....	166
5.2.4 Hybridisation between N+ filters and $\alpha$ <sup>32</sup> p dCTP labelled DNA probes .....	167
5.2.5 Genetic Mapping .....	167
5.2.6 Cloning and sequencing PCR fragments .....	168
5.2.7 Analyses of sequences .....	169
5.3 Results .....	170

5.3.1 Identifying Brassica oleracea BACs containing ACC oxidase genes	170
5.3.1.1 Isolating BACs containing ACC oxidases	170
5.3.1.2 Identifying ACC oxidases from BACs isolated	171
5.3.2 Genetic Mapping of Brassica oleracea aco1 and aco2 genes	180
5.3.3 Analysis of nucleotide sequences of closely related genes to Brassica oleracea aco1 and aco2	186
5.4 Discussion	187
6.0 General Discussion	190
6.1 Assessing the strategies	191
6.1.1. Constructs	191
6.1.2 Transformation and regeneration	193
6.1.3 Ethylene and chlorophyll	195
6.1.4 The aco1 and aco2 genes	196
6.2 A role for ethylene	197
6.3 Future work	198
6.3.1 Fully understand the role and expression of the aco and acs genes	198
6.3.2 Biochemical aspect	198
6.3.3 Improved silencing of aco and acs in broccoli	199
6.3.4 Conventional breeding	200
6.3.5 Other ways to improve shelf-life	200
7.0 Appendices	202
8.0 References	210

## List of Figures

<b>Figure 1.1</b> The Agrobacterium infection process.....	8
<b>Figure 1.2</b> Biosynthesis of ethylene .....	16
<b>Figure 1.3</b> Proposed model of the ethylene signal transduction pathway .....	17
<b>Figure 1.4</b> The proposed mechanism for gene silencing by antisense mRNA .....	20
<b>Figure 2.1</b> Circular map of pBI121 .....	36
<b>Figure 2.2</b> Circular map of pSCV1.0 .....	37
<b>Figure 2.3</b> Schematic diagram of primer pairings for cDNA inserts in antisense and sense orientations for <i>aco1</i> , <i>aco2</i> and <i>acs</i> . .....	49
<b>Figure 2.4</b> (a) T-DNA region of pJ1.0 with restriction sites. (b) Restriction endonuclease digest confirming the integrity of the backbone plasmid, pJ1.0.....	52
<b>Figure 2.5</b> PCR products to determine presence and orientation of insert....	54
<b>Figure 2.6</b> PCR products to determine orientation of <i>aco2</i> and <i>acs</i> inserts.	55
<b>Figure 2.7</b> Confirmation of cDNA inserts.....	57
<b>Figure 2.8</b> Confirmation of cDNA inserts and <i>nos</i> terminator .....	59
<b>Figure 3.1</b> The T <sub>L</sub> -DNA of the agropine <i>Ri</i> plasmid pRi1855::GFP. ....	67
<b>Figure 3.2</b> The effect of treatment on construct transformation efficiency. ....	81
<b>Figure 3.3</b> Nine-week-old GFP fluorescing root/callus. ....	83
<b>Figure 3.4</b> Six-week-old GUS positive co-transformed root. ....	83
<b>Figure 3.5</b> The morphogenesis from root callus to plantlet. ....	85
<b>Figure 3.6</b> PCR of genomic DNA from the transgenic plants to confirm insertion of the T-DNA constructs from the binary plasmid.....	88

<b>Figure 3.7</b> PCR of the <i>gfp</i> gene from genomic DNA of the transgenic lines to confirm insertion of the T <sub>L</sub> -DNA region of the virulence plasmid.....	88
<b>Figure 3.8</b> Genomic DNA from <i>aco1</i> and <i>aco2</i> transgenic lines digested with <i>Sst</i> I restriction endonuclease and run on a 0.8% (w/v) agarose gel at 50V for 18h. ....	93
<b>Figure 3.9</b> Genomic DNA from <i>acs</i> and GUS transgenic lines digested with <i>Sst</i> I restriction endonuclease and run on a 0.8% (w/v) agarose gel at 50V for 18h. ....	94
<b>Figure 3.10</b> Autoradiograph of the hybridisation between the <i>Brassica oleracea</i> L. var. <i>italica aco1</i> 283bp 3'UTR DNA probe and the digested genomic DNA of Figure 3.8.....	95
<b>Figure 3.11</b> Autoradiograph of the hybridisation between the <i>Brassica oleracea</i> L. var. <i>italica aco2</i> 252bp 3'UTR DNA probe and the digested genomic DNA of Figure 3.8.....	96
<b>Figure 3.12</b> Autoradiograph of the hybridisation between the <i>Brassica oleracea</i> L. var. <i>italica acs</i> full length cDNA probe and the digested genomic DNA of Figure 3.9.....	97
<b>Figure 3.13</b> Autoradiograph of the hybridisation between the 390bp <i>gus</i> DNA probe and the digested genomic DNA of Figure 3.9. ....	98
<b>Figure 3.14</b> Autoradiograph of the hybridisation between the 494bp GFP DNA probe and the digested genomic DNA of Figure 3.8. ....	99
<b>Figure 3.15</b> Autoradiograph of the hybridisation between the 494bp GFP DNA probe and the digested genomic DNA of Figure 3.9. ....	100
<b>Figure 3.16</b> Heading broccoli plants that have been regenerated from GFP fluorescing roots, through a tissue culture phase.....	103

<b>Figure 3.17</b> Determination of <i>gfp</i> inserts by PCR of 67 28/00 <i>aco1A</i> 3 T <sub>1</sub> progeny grown from seed. ....	107
<b>Figure 3.18</b> Determination of <i>aco1A</i> inserts by PCR of 67 28/00 <i>aco1A</i> 3 T <sub>1</sub> progeny grown from seed. ....	108
<b>Figure 4.1</b> (a) Gas chromatograph; (b) Glass container with broccoli buds evolving ethylene; (c) Injecting 1ml air sample taken from (b); (d) Chlorophyll diffusing from broccoli buds in 5mls methanol. ....	132
<b>Figure 4.2</b> The rate of diffusion of chlorophyll at 20°C in the dark, from 0.2g broccoli buds in 5ml methanol. ....	134
<b>Figure 4.3</b> Ethylene production by harvested/non-harvested untransformed GDDH33 broccoli buds. ....	135
<b>Figure 4.4</b> Chlorophyll levels of harvested/non-harvested untransformed GDDH33 broccoli buds. ....	136
<b>Figure 4.5</b> Post-harvest ethylene production and chlorophyll levels of buds from untransformed GDDH33. ....	144
<b>Figure 4.6</b> Post-harvest ethylene production and chlorophyll levels of buds from GDDH33 transformed with <i>gus</i> control constructs. ....	144
<b>Figure 4.7</b> Post-harvest ethylene production and chlorophyll levels of buds from GDDH33 transformed with <i>ACC oxidase 1</i> antisense constructs. ....	145
<b>Figure 4.8</b> Post-harvest ethylene production and chlorophyll levels of buds from GDDH33 transformed with <i>ACC oxidase 1</i> sense constructs. ....	145
<b>Figure 4.9</b> Post-harvest ethylene production and chlorophyll levels of buds from GDDH33 transformed with <i>ACC oxidase 2</i> antisense constructs. ....	146
<b>Figure 4.10</b> Post-harvest ethylene production and chlorophyll levels of buds from GDDH33 transformed with <i>ACC oxidase 2</i> sense constructs. ....	146

<b>Figure 4.11</b> Post-harvest ethylene production and chlorophyll levels of buds from GDDH33 transformed with <i>ACC synthase</i> antisense constructs. .	147
<b>Figure 4.12</b> Post-harvest ethylene production of buds from two lines of GDDH33 transformed with <i>ACC synthase</i> antisense constructs. ....	147
<b>Figure 4.13</b> Post-harvest ethylene production and chlorophyll levels of buds from GDDH33 transformed with <i>ACC synthase</i> sense construct.....	148
<b>Figure 4.14</b> Relationship between post-harvest ethylene production and chlorophyll loss of buds from transformed and untransformed GDDH33. ....	148
<b>Figure 4.15</b> Broccoli heads post- harvest.....	149
<b>Figure 5.1</b> Schematic diagram of the predicted <i>Brassica oleracea</i> L. var. <i>italica</i> <i>ACC oxidase 1</i> gene.....	165
<b>Figure 5.2</b> Schematic diagram of the predicted <i>Brassica oleracea</i> L. var. <i>italica</i> <i>ACC oxidase 2</i> gene.....	165
<b>Figure 5.3</b> Autoradiograph showing hybridisation between the <i>Brassica oleracea</i> BAC library filter 1, (a) and filter 2, (b) and the <i>Brassica oleracea</i> var. <i>italica</i> <i>ACC oxidase 2</i> full length cDNA (Pogson <i>et al.</i> , 1995a).....	170
<b>Figure 5.4</b> Autoradiograph showing hybridisation between the <i>B. oleracea</i> <i>ACC oxidase 1</i> cDNA (Pogson <i>et al.</i> , 1995a) 3' UTR 283bp probe and the <i>EcoRI</i> RFLP BAC filter.....	172
<b>Figure 5.5</b> Autoradiograph hybridisation between the <i>B. oleracea</i> <i>ACC oxidase 2</i> cDNA (Pogson <i>et al.</i> , 1995a) 3' UTR 252bp probe and the <i>EcoRI</i> RFLP BAC filter.....	173

<b>Figure 5.6</b> Electrophoretogram showing the products of a PCR between the BAC DNA and <i>aco1</i> specific primers (2 and 3) and <i>aco2</i> specific primers (2 and 4).	175
<b>Figure 5.7</b> <i>Brassica oleracea</i> ACC oxidases 1 and 2 intron 1 aligned to determine possible homology.	176
<b>Figure 5.8</b> <i>Brassica oleracea</i> ACC oxidases 1 and 2 intron 2 aligned to determine possible homology.	176
<b>Figure 5.9</b> Electrophoretogram showing the PCR products from primers 5 and 7 on BAC's 3, 4, 12 and 20.	177
<b>Figure 5.10</b> Electrophoretogram showing PCR products from all BACs with primers 5 and 7, and, 9 and 10.	178
<b>Figure 5.11</b> Autoradiograph showing the hybridisation between the <i>Brassica oleracea</i> BAC <i>Eco</i> RI RFLP filter and the <i>Brassica oleracea aco1</i> intron 2 probe.	179
<b>Figure 5.12</b> Autoradiograph showing the hybridisation between the <i>B. oleracea</i> ACC oxidase1 cDNA 3' UTR 283bp probe and the AG mapping filter.	181
<b>Figure 5.13</b> Autoradiograph showing the hybridisation between the <i>B. oleracea</i> ACC oxidase1 cDNA 3' UTR 283bp probe and the NG mapping filter.	182
<b>Figure 5.14</b> Autoradiograph showing the hybridisation between the <i>B. oleracea</i> ACC oxidase2 cDNA 3' UTR 252bp probe and the AG mapping filter.	183

**Figure 5.15** Autoradiograph showing the hybridisation between the *B. oleracea* ACC oxidase2 cDNA 3' UTR 252bp probe and the NG mapping filter..... 184

**Figure 5.16** The linkage map positions of *aco1* and *aco2* in *Brassica oleracea* for the loci that could be scored by *EcoRI* RFLP polymorphism. .... 185

## List of tables

<b>Table 1.1</b> Genetically modified traits on the horizon .....	5
<b>Table 2.1</b> Oligonucleotide sequences used in these experiments .....	39
<b>Table 2.2</b> PCR reaction components.....	40
<b>Table 2.3</b> PCR program.....	40
<b>Table 2.4</b> Predicted PCR product sizes for the insertion of ACC cDNAs in sense or antisense orientations into pJ1.0.....	48
<b>Table 3.1</b> Oligonucleotide sequences used as primers for the verification of T-DNA insertion and making DNA probes for hybridisation. ....	72
<b>Table 3.2</b> PCR reaction components.....	73
<b>Table 3.3</b> PCR program.....	73
<b>Table 3.4</b> Transformation efficiency of LBA 9402 pRi1855::GFP carrying binary plasmids with the <i>B. oleracea</i> var. <i>italica</i> ACC cDNA constructs on GDDH33. ....	79
<b>Table 3.5</b> Transgenic lines regenerated into whole plants.....	84
<b>Table 3.6</b> Summary of the PCR and autoradiograph data for confirming the presence of T-DNAs in lines regenerated through tissue culture.....	101
<b>Table 3.7</b> The effect of the <i>rol</i> genes on transgenic plant morphology. ....	104
<b>Table 3.8</b> The total numbers of transgenic plants produced from all constructs with the effect of the <i>rol</i> genes on mortality. ....	105
<b>Table 3.9</b> The number of seeds recovered from transgenic lines with their particular <i>rol</i> phenotype .....	106
<b>Table 3.10</b> Segregation of T-DNA inserts in the T <sub>(1)</sub> progeny of 28/00 <i>aco1A</i> 3 .....	109

<b>Table 4.1</b> Transgenic lines regenerated by tissue culture .....	128
<b>Table 4.2</b> The concentration of chlorophyll (Chl) in the cuvette was calculated using simultaneous equations, based on the absorbance readings at 645 and 663nm (Hipkins and Baker, 1986). .....	131
<b>Table 4.3</b> Ethylene levels of GDDH33 buds post-harvest as nanolitres per gram bud (dry weight) per hour.....	137
<b>Table 4.4</b> Chlorophyll values of GDDH33 buds post-harvest as micrograms per gram bud (fresh weight).....	137
<b>Table 5.1</b> Oligonucleotide sequences used for primers to determine gene polymorphisms and produce DNA probes . .....	163
<b>Table 5.2</b> PCR reaction components.....	164
<b>Table 5.3</b> PCR program.....	164
<b>Table 5.4</b> The codes of the <i>B. oleracea</i> BAC colonies that hybridised to the <i>B. oleracea ACC oxidase 2</i> full length cDNA probe. ....	171

# **1.0 General Introduction**

## 1.1 Introduction

*Brassica oleracea* is a highly polymorphic species encompassing a wide range of important vegetable fodder crops, including cabbage (var. *capitata*), brussels sprouts (var. *gemmifera*), broccoli (var. *italica*), cauliflower (var. *botrytis*), kohlrabi (var. *gongylodes*), and kale (vars, *medullosa*, *ramosa* and *acephala*) (Hodgkin, 1995). It is a diploid species with  $2n = 2x = 18$ , and a nuclear DNA content of  $1.81 \times 10^{-12}$ g (Verma and Rees, 1974). *Brassica oleracea* is an outbreeding species with a sporophytic self-incompatibility system (Thompson, 1957). The wild species is commonly biennial or perennial, but annual crops also exist such as summer cauliflower and calabrese (Hodgkin, 1995).

The general view has long been that the early evolution of the different cultivated types took place in the mediterranean area (Helm, 1963). However, while much of the early selection may have occurred here, the evidence currently suggests that the species from which modern crops are derived is the wild *B. oleracea* and not the mediterranean species. As a result of their molecular studies, Song *et al.* (1988) propose that the cultivated morphotypes originated from a single ancient progenitor that was similar to wild *B. oleracea*. This then became widely spread along the coasts of the Mediterranean and North Atlantic and the different forms evolved in different areas through selection and adaptation to various climates (Hodgkin, 1995).

The term 'broccoli' has been applied to the young floral shoots of several *Brassica* crops as diverse as cabbages and turnips, but usually refers to heading and sprouting forms belonging to the *Brassica oleracea* L. var. *italica* group. These include Purple, and White Sprouting Broccoli, Purple

Cape, Purple Sicilian, and Black Broccoli varieties (Gray, 1993). The calabrese-broccoli is now the major crop within the italica group and in breeding terms, the most developed (Gray, 1982). It is derived from biennial, Italian green sprouting broccoli from the Calabrian region of Italy (Crisp *et al.*, 1986). Calabrese has become a specialist crop in the USA, Japan and Europe, and is marketed as a quality vegetable (Gray, 1993). There now exist many cultivars, the majority of which are F1 hybrids. These have been intensively selected for rapid maturity so that the crop is now effectively an annual one with an increased terminal head size, which has changed the crop from a sprouting plant virtually to a heading one. Gray (1993) states that improvements in quality and extending the maturity range of horticultural crops will be more important than further increases in productivity.

Broccoli is one of the most successful 'new' crops in the United Kingdom. The crop value of home produced marketed broccoli has doubled from £18.9m to £44.9m in the last 10 years (DEFRA statistics, 2000), where there has been an overall decline of marketed *Brassicas*. The home grown crop does not satisfy demand and there are significant imports (29,000 tonnes with a value of £14m). The UK crop is either processed (frozen) or marketed fresh. There is convincing information from industry that crops of the same variety treated in the same way after harvest, vary in their post-harvest performance (D. Pink, pers. comm. HRI-Wellesbourne). This lack of predictability results in the major retailers specifying a product life of only two days from delivery to 'purchase before date', and a further two days 'best consumed by' in an attempt to ensure a 'quality' product for the consumer.

This short post-harvest life results in significant waste for the retailer (a cost borne by the consumer) and consumers themselves.

## **1.2 Genetic Improvement of Crop Plants**

Genetic improvement of crop species has always been a major goal in breeding programmes. Sexual crossing between species and selection of desirable traits has led to the high yielding varieties of the present day. However, this may take many generations and time to remove unwanted characteristics and is limited by inter-species barriers. Genetic manipulation by transformation has been developed over the past twenty years as a means to facilitate direct gene transfer between two unrelated species as well as within species. Dominant useful agronomic traits may be transferred directly and rapidly offering potential for both gene function studies and crop improvement strategies. Table 1.1 lists the main areas targeted for genetic improvement by direct gene transfer.

**Table 1.1** Genetically modified traits on the horizon  
(after Chrispeels and Sadava, 1994)

<p><b>Pest and Weed Management</b></p> <p>Herbicide tolerance virus resistance Insect resistance Bacterial resistance Fungal resistance</p>	<p><b>Plant Breeding</b></p> <p>Male sterility High-methionine and high-lysine seeds Forage rich in sulphur amino acids</p>
<p><b>Agronomic Properties</b></p> <p>Altering cold sensitivity Improving salt tolerance Improving water stress tolerance</p>	<p><b>Molecular Farming</b></p> <p>Oils Starch Plastic Enzymes Pharmaceuticals</p>
<p><b>Postharvest Qualities</b></p> <p>Delay of fruit ripening Delay of flower senescence High-solids tomatoes High-starch potatoes Sweeter vegetables</p>	<p><b>Detoxifying contaminated soils</b></p>

At present, in the United States there have been environmental field releases for *Brassica oleracea* crops with insect resistance and male sterility genes. The insect resistance gene (*CryIA*) is derived from the soil bacterium *Bacillus thuringiensis* (*Bt*). It codes for a crystal endotoxin which when ingested by the target pest causes disruption of the gut wall leading to eventual starvation (Aronson and Shai, 2001). The advantage of inserting the gene into the crop is that it targets the pest specifically unlike pesticides, and does not affect other species of insects. However, like chemical pesticides it also provides a constant selection pressure for the pest species to overcome and will therefore need to be managed in an integrated system (Weisz *et al.*, 1994). Introduction of male sterility genes into *Brassica oleracea* is useful for

the production of hybrid seeds that may produce higher yielding plants. It is difficult to produce hybrid seeds in *Brassica* because the male and female structures are present in the same flower. American seed companies have used an RNase gene from *Bacillus amyloliquefaciens* (Barnase) to destroy the RNA in the pollen making cells, and thus making the plants male sterile (<http://www.nbiap.vt.edu/cfdocs/fieldtests3.cfm>).

At present, it is estimated that there are hundreds of transgenic varieties commercially available, mostly of soybean, corn, cotton and canola. According to the International Service for the Acquisition of Agri-biotech Applications (ISAAA), the global area of transgenic crops increased by more than 25-fold, from 1.7 million hectares in 1996 to 44.2 million hectares in 2000. Of the top four countries that grew 99% of the global transgenic crop area, the USA grew 68%, Argentina 23%, Canada 7%, and China 1% (James, 2000). In 2000, over 99% of the transgenic acreage was devoted to just two traits – herbicide and insect resistance.

### **1.3 Transformation of *Brassica***

*Brassica* and related species are fairly easy to handle in tissue culture systems making this genus a suitable subject for exploiting techniques for genetic transformation for breeding purposes (Poulsen, 1996). The first step is to introduce 'foreign' DNA into the cells/tissue of interest. This is followed by selection of the transformed cells on a suitable medium with plant growth regulators to induce regeneration into a whole novel plant.

Techniques developed to introduce DNA into *Brassica* plant cells have involved direct gene transfer, in which naked DNA is introduced into

protoplasts or intact cells via microinjection or electroporation; bombardment with DNA coated particles using a particle gun (Puddephat *et al.*, 1996); or to utilise the natural gene transfer capacity of *Agrobacterium*. The latter has been the most effective method for producing stable transformants that segregate in Mendelian fashion.

Crown gall disease and hairy root disease are neoplastic growths on plants incited by virulent strains of *Agrobacterium tumefaciens* and *Agrobacterium rhizogenes*, respectively. Transfer DNA or (T-DNA) is carried on the tumour-inducing (*Ti*) plasmid of *A. tumefaciens* and root-inducing (*Ri*) plasmid of *A. rhizogenes*. The T-DNA is transferred to the plant where it integrates into the plant nuclear DNA (Gelvin, 1990).

Integration of the T-DNA into the host genome (Figure 1.1) depends on a complex series of chemical signals between the *Agrobacterium* and the plant (Gelvin, 2000). These signals include neutral and acidic sugars, phenolic compounds, opines, Vir (virulence) proteins, and the T-DNA that is ultimately transferred from the bacterium to the plant cell (Gelvin, 2000). The T-DNA transfer process initiates when *Agrobacterium* perceives certain phenolic and sugar compounds from wounded cells (Hooykaas and Beijersbergen, 1994). In the presence of these phenolic compounds, the VirA sensory protein becomes phosphorylated. The active VirA protein then transphosphorylates the VirG protein which initiates *vir* gene transcription (Jin *et al.*, 1990a,b). Most of the induced Vir proteins are directly involved in T-DNA processing from the *Ti/Ri*- plasmids, and the subsequent transfer of T-DNA from the bacterium to the plant (Gelvin, 2000). VirD1 and VirD2 are responsible for nicking the *Ti/Ri*-plasmids at 25bp directly repeated sequences called T-DNA

borders that flank the T-DNA (Filichkin and Gelvin, 1993). The VirD2 protein strongly associates with the nicked strand, so that the T-DNA enters the plant cell as protein/nucleic acid complex (Gelvin, 2000). It is probable that the VirD2 and VirE2 protein are important in guiding the T-strand into the plant cell nucleus and integrating it into the genome (Gelvin, 2000).

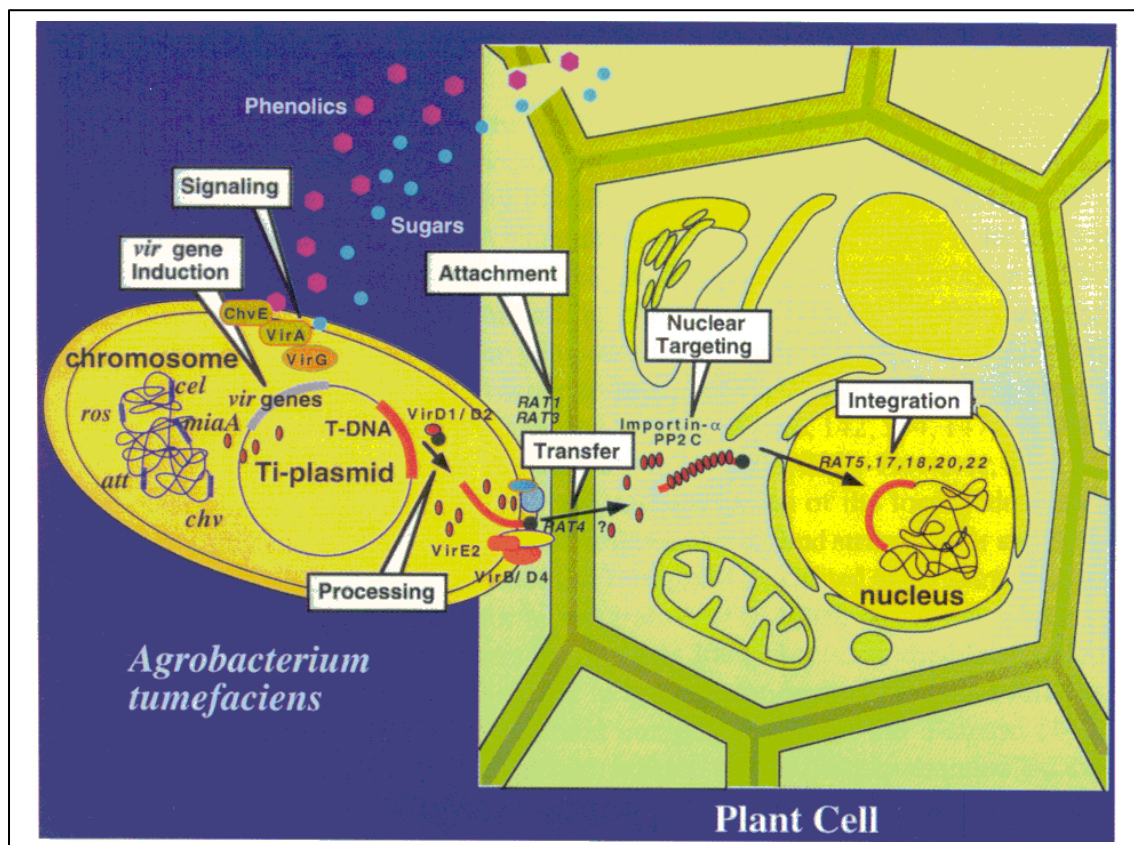


**Figure 1.1** The *Agrobacterium* infection process.

Critical steps that occur to or within the bacterium (chemical signalling, *vir* gene induction, and T-DNA processing) and within the plant cell (bacteria attachment, T-DNA transfer, nuclear targeting, and T-DNA integration) are highlighted along with genes and/or proteins known to mediate these events (after Gelvin, 2000).

It is advantageous to distinguish phenotypically similar transformed plants from non-transformed plants by means of selection. Selection requires

the use of genes that function as selectable markers to permit the recovery of transformed cells and tissues, and genes that act as reporters of transgene expression. The most common selectable markers are based on antibiotic resistance genes, such as *nptII* for neomycin phosphotransferase, which detoxifies a number of aminoglycoside antibiotics, including neomycin and kanamycin (Puddephat *et al.*, 1996). The most widely used reporter gene, the *gus* gene encoding for  $\beta$ -glucuronidase, allows *in situ* histological assessment of transgene expression, but the assay is toxic to the plant. A potentially promising *in vivo* reporter gene is the green fluorescent protein (GFP) from the bioluminescent jellyfish *Aequorea victoria* (Sheen *et al.*, 1995). GFP expression is cell autonomous and independent of cell type and location. Fluorescence is achieved by excitation of the GFP protein with blue or UV light, emitting visible light that may be observed by the naked eye. GFP does not require any exogenous substrates (Chrispeels and Sadava, 1994; Delagrave *et al.*, 1995; Gray *et al.*, 1992, Heim *et al.*, 1994) or produce an endotoxic product when targeted to the endoplasmic reticulum (Haseloff *et al.*, 1997). Therefore, histological *in vivo* studies may be carried out without loss of tissue.

The choice of regulatory sequences for the control of transgene expression is still somewhat limited. Most experiments on engineered pest and disease resistance have used constitutive promoters, most often the cauliflower mosaic virus (CaMV) 35S sequence. Ideally, plant-derived promoters may be more acceptable to regulatory authorities than virus derived promoters (Pierpoint, 1995), but would need to offer the same advantages.

The most successful Brassica tissue for transformation and regeneration appears to be that of explants composed of, or derived from, meristematic tissues at the early stages of plant development (Puddephat *et al.*, 1996). Cells transformed by wild-type *A. rhizogenes* strains may be readily identifiable by virtue of hairy root formation. These roots are cellular clones originating from a single transformed cell (Tempe and Casse-Delbart, 1987) and are capable of regenerating into whole plants (Tepfer, 1990). In most cases, *B. oleracea* explants inoculated with *A. rhizogenes* form roots between one and three weeks after inoculation (Hosoki *et al.*, 1991). Typically, hairy roots exhibit rapid, phytohormone independent growth, with extensive plagiotropic branching. The regeneration of shoots from hairy-roots is achieved by the treatment of cytokinins and auxins. Regeneration frequencies of root clones from broccoli are low, averaging 11% (Hosoki *et al.*, 1991) (for a full review see Puddephat *et al.*, 1996).

The *Agrobacterium rhizogenes* *Ri*-plasmid is necessary for the successful transformation of the host plant. Outside the T<sub>L</sub>(left) -DNA borders the *Ri*-plasmid carries genes specific for T<sub>L</sub> -DNA transfer, such as the *Vir* genes and, within the borders, genes that elicit neoplastic root growth. The T<sub>L</sub> region includes four genes: *rolA*, *rolB*, *rolC*, *rolD* (see Figure 3.1)(White *et al.*, 1985; Zambryski *et al.*, 1989). The first three are important for hairy root production from transformed cells, and the morphological aberrations observed in transformed plants (Schmulling *et al.*, 1988). In most plants *rolB* is capable of inducing root formation on its own (Schmulling *et al.*, 1988). Although *rolA* and *rolB* can induce aberrations in transformed plants, it appears that *rolC* is responsible for many of the most severe features

including reduced chlorophyll content, smaller than normal wrinkled leaves, dwarfing, loss of apical dominance and various forms of flowering abnormalities (Schmulling *et al.*, 1988). The deleterious effects of *rolC* may be avoided by developing an *A. rhizogenes* vector system in which this gene has been eliminated. Senior *et al.*, (1995) used a *rolA* mutant to transform *Antirrhinum*, producing a semi-dwarf phenotype. This approach with a *rolC* mutant may lead to the production of phenotypically normal transgenic plants.

As a scientifically and more socially acceptable approach, co-transformation in which marker genes and genes of interest are located on separate T-DNAs, allows the use of a selectable marker during plant regeneration followed by recovery of progeny which contain the desired gene(s) but lack a marker gene (Puddephat *et al.*, 2001). If transgenes have been inserted into the plant genome at physically unlinked loci, the gene of interest can be segregated from the selectable marker in the next generation. Independent T-DNA insertion has been achieved with co-transformation, using one plasmid with multiple T-DNAs (Depicker *et al.*, 1985; Komari *et al.*, 1996) or separate plasmids with different T-DNAs that are contained in either one (Komari *et al.*, 1996) or more *Agrobacterium* strains (Depicker *et al.*, 1985). Puddephat *et al.* (2001) used a co-transformation strategy based on one *Agrobacterium* strain, harbouring two plasmids, each carrying separate T-DNAs. Puddephat *et al.* (2001) recovered phenotypically normal transgenic *Brassica oleracea* plants from *Agrobacterium rhizogenes*-mediated co-transformation and selection of transformed hairy roots by the GUS assay. There had been sufficient independent integration of T-DNAs at unlinked sites

for the marker genes to segregate from the genes of interest in the progeny of the T<sub>0</sub> plants.

#### **1.4 Senescence of Broccoli**

Senescence is a complex, highly regulated plant developmental phase that results in the co-ordinated degradation of molecules. Genes known to be upregulated in this process encode degradative enzymes such as proteases and nucleases, and enzymes involved in lipid and carbohydrate metabolism. This leads to an ordered series of events involving cessation of photosynthesis, breakdown of chlorophyll and removal of amino acids (Buchanan-Wollaston, 1997).

Broccoli is a floral vegetable that is harvested when the flowering heads are immature and growing rapidly. The head of broccoli is composed of hundreds of immature florets arranged in whorls on a fleshy stem. Each broccoli floret is composed of male and female reproductive structures surrounded by immature petals and enclosed within chlorophyll-containing sepals (Pogson *et al.*, 1995a). At the time of harvest the florets are closed and unpollinated. Vegetables harvested when immature and before growth has ceased experience a disruption of energy, nutrient, and hormone supplies and consequently senesce rapidly (King and Morris, 1994a,b). An estimate by Pogson and Morris (1997) is that 1% of dry mass is respired per hour after harvest. Fresh broccoli is therefore highly perishable, with a storage life of 3 to 4 weeks in air at 0°C (Makhlouf *et al.*, 1989) and 2 to 3 days in air at 20°C (Wang, 1977). As broccoli deteriorates, the head yellows due to degradation of chlorophyll (Wang, 1977). The characteristic sepal yellowing is the first

visual sign of senescence but the final stage of this process. The major catabolic breakdown and oxidation of macromolecules has already occurred leaving the tissue with poor nutrient status, recognised by the consumer. The branchlets and florets also lose turgor and become flaccid due to water loss (Brennan and Shewfelt, 1989). King and Morris (1994b) found that the stress imposed by harvest, trimming, transportation and washing procedures greatly accelerated senescence.

Lieberman and Hardenburg (1954) suggested that yellowing in broccoli florets may be due to endogenous ethylene. There was no visible yellowing of broccoli placed in nitrogen atmospheres, under which conditions ethylene was not evolved. The proposition by Lieberman and Hardenburg was supported by Wang (1977) who delayed chlorophyll loss using ethylene biosynthetic inhibitors (aminoethoxyvinylglycine -AVG) and inhibitors of ethylene action (silver ions). Tian *et al.* (1994) observed that removing the reproductive structures (stamens and pistil) greatly reduced sepal yellowing. The reproductive structures produced more than double the amount of ethylene than other tissues in the floret.

### **1.5 Ethylene Biosynthesis**

Ethylene is produced by plant tissues in amounts ranging from almost none up to 500 nl/g/h (Burg, 1962). It is biologically active in trace amounts (as little as 10-100 nl/l of air). Ethylene production is induced during several developmental stages, including fruit ripening, seed germination, leaf and flower senescence, and abscission. It is also induced by external factors, such as wounding, anaerobiosis, viral infection, auxin treatment, chilling injury,

drought, Cd<sup>2+</sup> and Li<sup>+</sup> ions and mechanical stress (Abeles, 1973; Yang and Hoffman, 1984). Ethylene biosynthesis occurs via the enzymes ACC synthase and ACC oxidase, which catalyse the conversions of S-adenosylmethionine to 1-aminocyclopropane-1-carboxylic acid (ACC) and ACC to ethylene, respectively (see Figure 1.2) (Yang and Hoffman, 1984).

### 1.5.1 ACC synthase

After the discovery that ACC is the immediate precursor of ethylene, it became clear that *ACC synthase* played an important role in regulating the production of ethylene. The induction of ethylene production by a variety of means was reported to be due to *de novo* synthesis of this enzyme (Kende, 1989), although other reports state that its activity may be post-translationally controlled (Morgan and Drew, 1997). There is an emerging picture that *ACC synthase* is encoded by a highly divergent multigene family. In tomato, for example, ACC synthase is encoded by at least seven genes, two of which are expressed during fruit ripening (Van der Straeten *et al.*, 1990; Morgan and Drew, 1997; Oetiker *et al.*, 1997). Similarly, in *Arabidopsis* and rice, *ACC synthase* genes are differentially expressed in response to developmental, hormonal and environmental stimuli (Liang *et al.*, 1992).

### 1.5.2 ACC oxidase

*ACC oxidase* is constitutively expressed in most vegetative tissues (Yang and Hoffman, 1984) and is induced to higher levels during fruit ripening (Gray *et al.*, 1992). In senescing broccoli, the concomitant increase of ACC oxidase activity was suppressed by cycloheximide (an inhibitor of translation),

suggesting increased ACC oxidase activity results from the *de novo* synthesis of the enzyme protein, as with ACC synthase (Kasai *et al.*, 1998). A cDNA encoding ACC oxidase was first cloned from tomato fruit (Slater *et al.*, 1985). It encodes a 37KDa dioxygenase that belongs to the superfamily of Fe<sup>2+</sup>/ascorbate oxidases, which also require CO<sub>2</sub> and O<sub>2</sub> as co-substrates (McGarvey *et al.*, 1992).

## 1.6 Signalling

Molecular genetic analysis of ethylene signalling in *Arabidopsis thaliana*, has led to the identification of a number of genetic loci that are required for normal ethylene responses (McGrath and Ecker, 1998). The elucidation of this biochemical pathway has been achieved with ethylene insensitive mutants and mutants with constitutive ethylene responses. A mutation in the ETR1 gene allowed the elucidation that ethylene is perceived by a histidine kinase membrane bound receptor protein (see Figure 1.3). Ethylene binding results in the inactivation of a MAP kinase cascade that is regulated by another kinase, CTR1. Inactivation of this inhibitory MAP kinase cascade allows activation of the ethylene signalling cascade. It is proposed that this cascade amplifies the ethylene signal and leads to the transcription of target genes that play important roles in developmental phases including senescence.

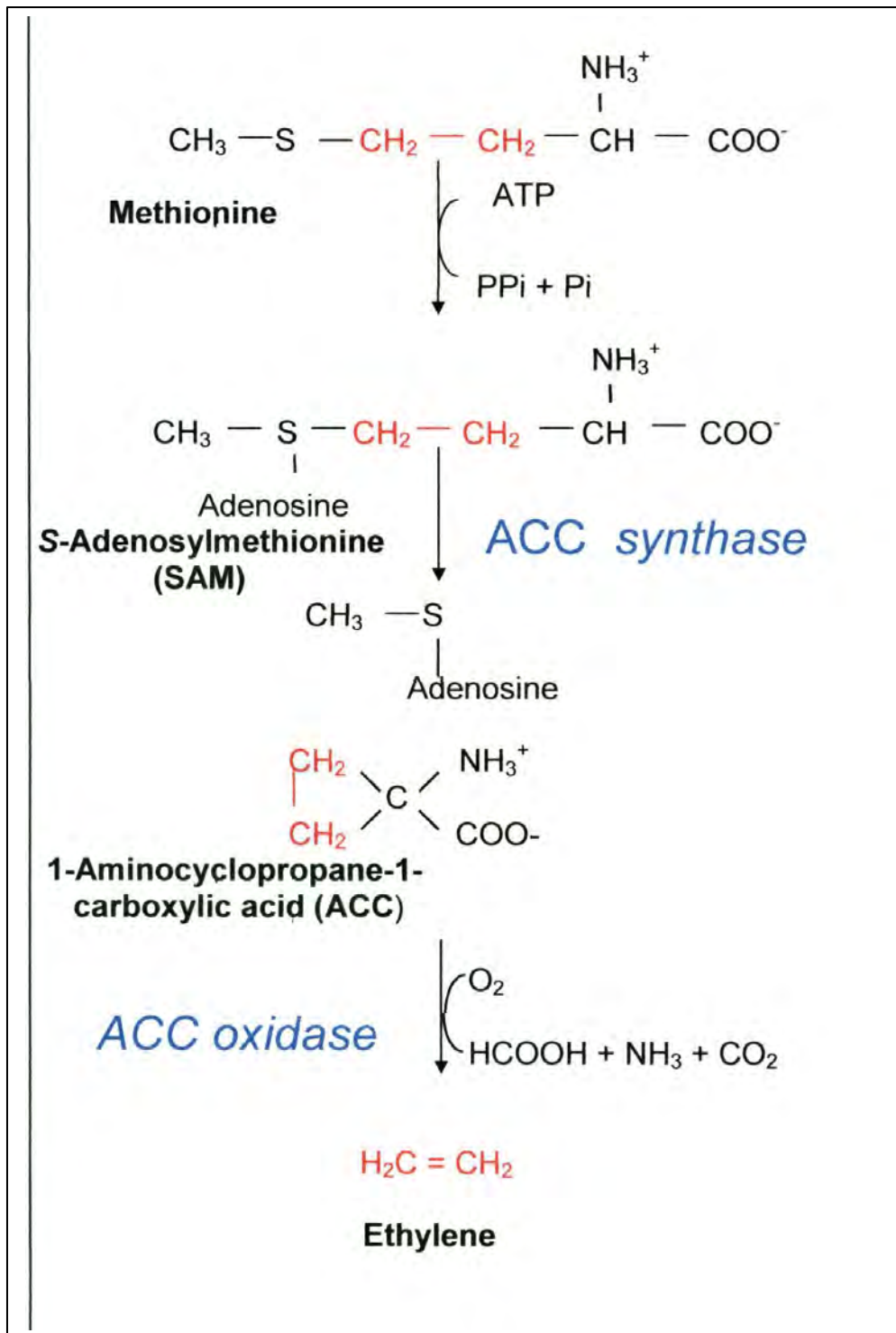


**Figure 1.2** Biosynthesis of ethylene (after Yang and Hoffman, 1984)

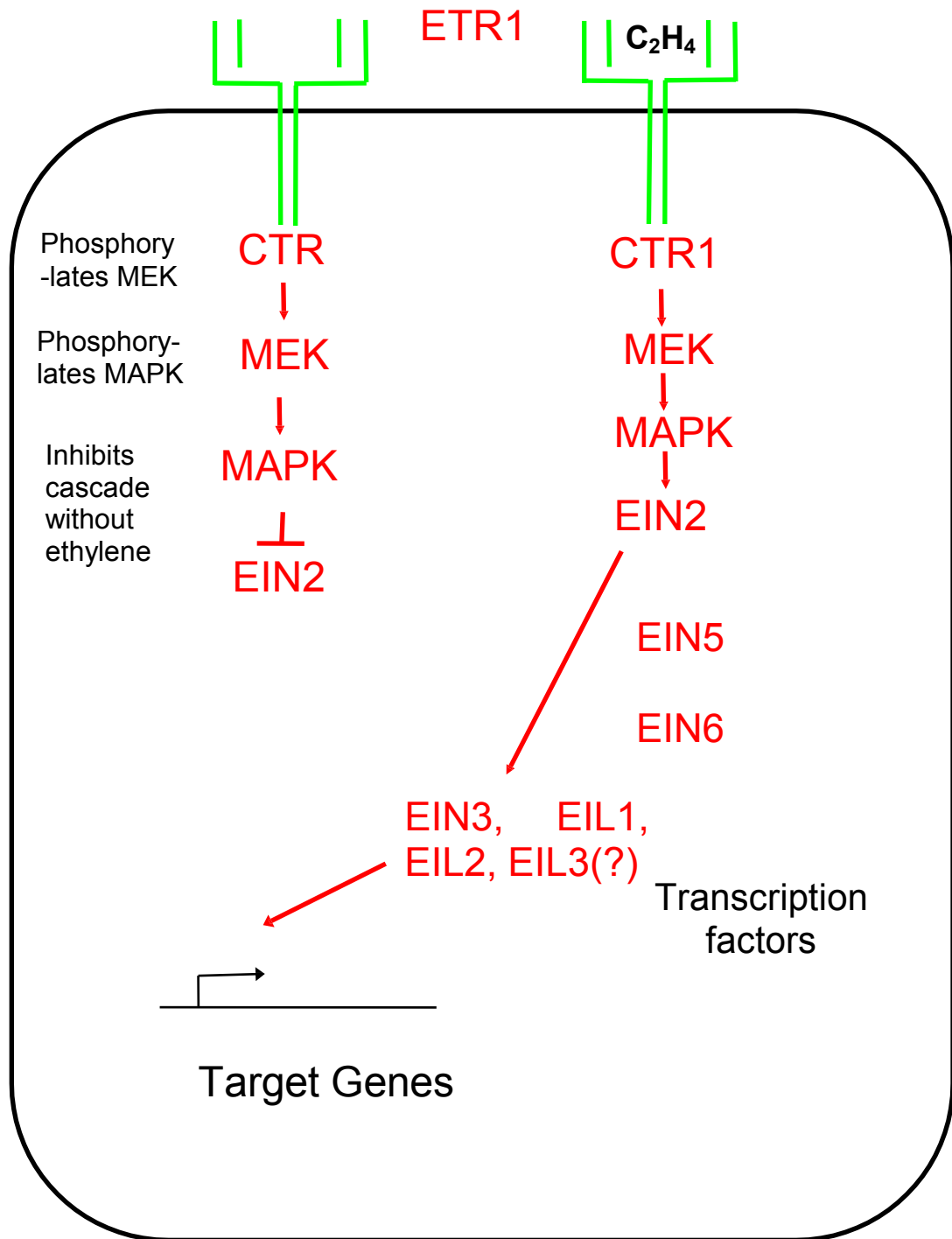


**Figure 1.3** Proposed model of the ethylene signal transduction pathway (after McGrath and Ecker, 1998). Binding of ethylene by the receptor complex inhibits activity of the MAP kinase cascade, allowing transmission of the ethylene signal. CTR1=constitutive triple response; EIN = ethylene insensitive mutant; EIL = EIN-like; ETR= ethylene resistant; MAPK = mitogen activated protein kinase; MEK= MAPK kinase kinase

Using the *Arabidopsis* ethylene receptor ETR1 as a probe, Payton and co-workers (Payton *et al.*, 1996) isolated the tomato homolog *tETR*. They showed that mRNA of *etr1* was undetectable in unripe fruit or pre-senescent flowers, but increased in abundance during the early stages of ripening, flower senescence in abscission zones, and was greatly reduced in fruit of ripening mutants deficient in ethylene synthesis or response. More recent work by Sato-Nara *et al.* (1999) on muskmelon (*Cucumis melo*) also found a stage- and tissue-specific expression of the ethylene receptor during fruit development. They suggest that as the receptors have an inhibitory effect on the signalling cascade, if more are expressed at a specific time there would need to be more ethylene produced to compensate. It follows that if there was a large ethylene burst, with little receptor expression, the cascade would be activated, but possibly to a lesser extent than if there were greater numbers of receptors. Also, if great numbers of receptors were expressed, but with little ethylene, there would be potentially greater inhibition of the signal cascade.

Large numbers of ethylene receptor proteins are prevalent at the climacteric point of fruit development in the melon fruit. There are other reports indicating that receptors increase while tissue sensitivity of ethylene is increasing (Vriezen *et al.*, 1997; Wilkinson *et al.*, 1995). In this light, it is interesting that Makhlouf *et al.* (1989) described the post-harvest senescence of broccoli as climacteric since florets became yellow as respiration and ethylene production increased.

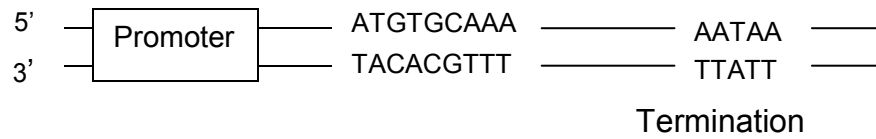
The work over the last 20 years with the elucidation of ethylene biosynthesis and signalling pathway suggests that there are three main controls for the physiological responses invoked by ethylene. These are ACC

*synthase*, known as the rate limiting enzyme in the biosynthetic pathway; *ACC oxidase*, which catalyses the final substrate ACC into ethylene and; the ethylene receptor which may have varying degrees of sensitivity to ethylene depending on developmental phase of the plant.

### **1.7 Antisense Technology**

Antisense technology has proved a powerful tool for understanding genetic control in plants through gene silencing. The technique was developed by D. Grierson and colleagues at Sutton Bonington (University of Nottingham) to understand the genetics behind fruit ripening of tomato (*Lycopersicon esculentum*). Hamilton *et al.* (1990) used a tomato *ACC oxidase* cDNA known as pTOM13, inserted into a binary vector in the antisense orientation, between the CaMV 35S promoter and its terminator. Figure 1.4 illustrates the means by which antisense are thought to down-regulate genes expression at the mRNA level.

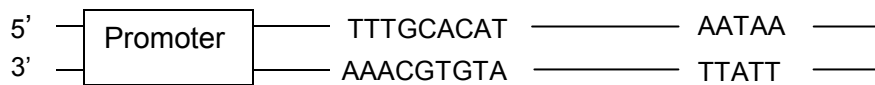
(i) Sense gene



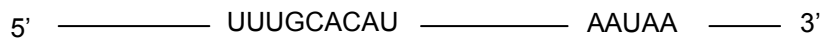
(ii) Sense mRNA



(iii) Antisense gene: the coding region of the normal gene in reverse orientation



(iv) Antisense mRNA



(v) Double stranded mRNA formed between sense and antisense mRNA

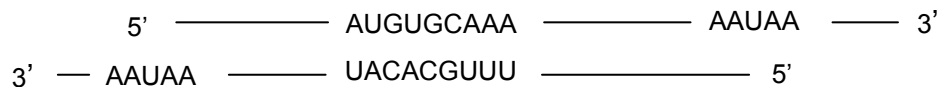


**Figure 1.4** The proposed mechanism for gene silencing by antisense mRNA (after Bryant, 1988).

The theory illustrated in Figure 1.4 proposes that an RNA duplex forms between the sense and antisense strands. The double stranded RNA molecules are not translated (through the ribosomes) and are exposed to native dsRNases within the cytoplasm. The silencing relies on an excess of the antisense mRNAs in the cell to prevent translation of the normal mRNAs. Hamilton *et al.* (1990) found that neither sense nor antisense transcripts were detected in ripening fruit with the pTOM13 construct. *ACC oxidase* activity was reduced by 93% in transgenic plants with two copies of the antisense construct. This permitted normal development of fruit ripening without the extreme softening, cracking and spoilage associated with over-ripening. In

addition, the senescence of the leaves was delayed for 7-10 days. Olson *et al.* (1991) used a tomato *ACC synthase* antisense construct *LE-ACC2*. Interestingly, this resulted in an almost complete inhibition of mRNA expression for the two *ACC synthase* genes (*LE-ACC2* and *LE-ACC4*), and the fruits never ripened. The antisense phenotype can be reversed by treatment with ethylene or propylene, an ethylene analog (Oeller *et al.*, 1991). The antisense approach has been used to down-regulate the ripening genes responsible for the cell wall degrading enzymes polygalacturonase and pectinesterase (Picton *et al.*, 1995) leading to the first biotechnology product based on gene silencing, the 'Flavr Savr' tomato, marketed in the United States by Calgene in 1994 (Grierson *et al.*, 1996).

### **1.8 Isolation of ACC genes**

The initial experiment by Hamilton *et al.* (1990) with pTOM13 where an antisense *ACC oxidase* gene inhibited the synthesis of the hormone ethylene was a major step towards cloning the genes and characterising the elusive ethylene biosynthetic enzymes. The original cloned DNA sequence has been used as a cDNA probe to isolate homologs from numerous other species. The major targets for gene isolation appear to be climacteric fruits such as banana, melon, apple, pear and apricot (LopezGomez *et al.*, 1997; Guis *et al.*, 1997; Bolitho *et al.*, 1997; Kato and Hyodo, 1999; MbeguieAMbeguie *et al.*, 1999). It is clear from a sequence analysis database (BLAST search, <http://www.ncbi.nlm.nih.gov/BLAST/>) that of these genes occur in a great number of other species including *Arabidopsis* and tobacco, two genetic model plants

as well as crop species such as cereals (rice- *Oryza sativa*), legumes (bean- *Phaseolus vulgaris*) as well as *Brassica* species.

Following the isolation of these genes there have been a number of antisense gene-silencing experiments in tomato melon and tobacco to understand gene function (Ayub *et al.*, 1996; Knoester *et al.*, 1997).

In 1995, B. Pogson, and co-workers C. Downs and K. Davies at the Institute for Crop & Food Research, New Zealand isolated two *ACC oxidase* genes and a cDNA clone encoding *ACC synthase* from *Brassica oleracea* (Pogson *et al.*, 1995a). The *ACC synthase* had a transcript of approximately 1700 bp with an open reading frame of 491 amino acids. The transcript abundance did not change in florets post-harvest and was detected in similar abundance in green and senescing tissues (Pogson *et al.*, 1995b). Reports suggest that this enzyme may be post-translationally regulated (Morgan and Drew, 1997). It appears that an *ACC synthase*-inactivase exists which must be phosphorylated for activity. This raises the possibility that some of the very rapid effects on ethylene biosynthesis may initially occur by alteration of an existing pool of *ACC synthase*.

Pogson *et al.* (1995a) used a cDNA clone encoding *ACC oxidase* from *Brassica juncea* (mustard, Pua *et al.*, 1992) to probe a broccoli (*B. oleracea* L. cv. Shogun) 48h post-harvest cDNA library. Two cDNAs with high homology to *ACC oxidases* in the databases were isolated and named *aco1* and *aco2*. The lengths of the *aco1* and *aco2* were 1237 and 1232bp, respectively. Commencing at the first Met, the predicted open reading frames of *aco1* and *aco2* were 320 and 321 amino acids, respectively. *aco1* and *aco2* shared nucleotide identity of 83% in their putative translated regions and 48% in the

3' untranslated regions. The short 5' untranslated regions shared no homology.

### **1.9 Tissue specific expression of ACC oxidases in broccoli**

Transcripts corresponding to *aco1*, but not *aco2*, were detected in florets and, at low levels, in leaf tissues frozen immediately after harvest (Pogson *et al.*, 1995a). The abundance of both *aco1* and *aco2* transcripts increased in florets during the post-harvest period and was accompanied by an increase in ethylene production.

In stamens, neither *aco1* nor *aco2* transcripts were detected at harvest (Pogson *et al.*, 1995a). Transcripts for *aco1* were also not detected in the stamens post-harvest, whereas *aco2* transcript levels increased markedly at 24 h and again at 48 h after harvest. In female reproductive structures, neither transcript was detected at harvest. However, high levels of *aco2* transcript were detected at 24 h but not 48 h after harvest. A closer inspection showed that *aco2* transcripts significantly increased 2 h after harvest in whole florets (Pogson *et al.*, 1995a). Pogson *et al.* (1995a) results were supported by evidence from Kasai *et al.* (1996) that ACC oxidase activity in florets rapidly increased to reach a peak, followed by a sharp decline to a low level as senescence progressed. This paralleled the pattern of ethylene production. Pogson *et al.* (1995a) found a large increase in *aco2* transcripts following ABA treatment, suggesting that changes in water relations and ABA concentrations may form part of the response to harvest.

These results indicated to Pogson *et al.* (1995a) that *aco1* was unlikely to initiate chlorophyll loss associated with broccoli senescence and that its

probable role was the generation of the 'basal ethylene' produced before harvest. They suggested that the ethylene produced was a consequence of rapid and large increases of *aco2* transcripts within the reproductive structures and this is one of the main signals influencing sepal yellowing.

In mature carnation, different parts of the flower produce disparate amounts of ethylene during senescence (Woodson, 1987). In unpollinated flowers, ethylene synthesis may occur simultaneously in all floral organs. After pollination, however, there is a rapid induction of ethylene synthesis in the style, followed a few hours later by greater ethylene synthesis in the petals, leading to premature senescence (Nichols, 1977). The pattern of senescence in carnation is similar to that of broccoli. It has been reported that reproductive development is often associated with leaf senescence in intact plants (Thayer *et al.*, 1987). Pogson and Morris (1997) suggest that a possible reason for induction of ethylene production may be maintenance of the reproductive organs through mobilising metabolites from surrounding tissue, such as sepals. Rather than maintaining floral organs post-harvest, it seems more likely that broccoli is forced into premature senescence by the stresses at harvest such as loss of water relations, lack of nutrients and cellular damage (Pogson *et al.*, 1995a). Once senescence is initiated from the stress-related ethylene production, it continues in a genetically programmed way as during normal senescence to support the fertilised embryo (seed) with nutrients. This effect is exacerbated due to the high stress conditions of harvest and rapid metabolism of nutrients from an ever decreasing pool.

### 1.10 Tomato fruit ripening and broccoli post-harvest senescence

It is difficult to understand the relationship between tomato fruit ripening and broccoli post-harvest senescence without comparing and contrasting the underlying mechanisms. It is not simply a case of comparing a tissue undergoing ripening with one at the latter developmental stages undergoing senescence. Broccoli is an immature plant at harvest that is forced into premature senescence.

The onset of tomato fruit ripening is characterised by a climacteric rapid increase in ethylene production. This increases the respiration rate leading to the metabolism of macromolecules and a characteristic change from green to orange/red colouration. Application of exogenous ethylene to pre-climacteric fruit such as tomato hastens the ripening process. Makhoul *et al.* (1989) indicated that broccoli may be classified as climacteric, since florets became yellow as respiration and ethylene production increased. It is clear that *ACC oxidase* is up-regulated in both broccoli and tomato, correlating with the level of ethylene. It appears that *ACC synthase* is also up-regulated in tomato fruit ripening, and possibly in broccoli. Up-regulation of both these genes results in a burst of ethylene leading to higher respiration rates and metabolism of macromolecules (King and Morris, 1994a,b). Chlorophyll molecules are broken down, starch hydrolysed into sugars, proteins and lipid molecules are subsequently degraded. However, fruit ripening is developmentally regulated so that the chloroplasts are converted to the carotenoid rich chromoplasts to protect from oxidation products and the pool of nutrients is not respired so rapidly. The harvested broccoli has no more nutrient supply and quickly depletes available pools. It is characterized by a

change from chlorophyll-rich green colour to the yellow colour where carbon based molecules have been oxidised leaving reduced nitrogen molecules, and the accumulation of ammonia.

The capability of tissues to synthesise large quantities of ethylene in response to ethylene is referred to as autocatalytic ethylene production (Yang and Oetiker, 1998). It is characteristic of ripening fruits and senescing tissues where ethylene is produced. It has been reported that the positive-feedback response is due to the upregulation of *ACC oxidases*, and in tomato also *ACC synthases* (Kasai, 1996; Cordes, 1989). Interestingly, it was reported that the promoters of such genes contained highly conserved motifs (AGCCGCC) known as GCC boxes. Ethylene-responsive element-binding proteins that belong to a specific class of basic class leucine zippers are able to bind to such regions and induce transcription of down-stream sequences (Hao *et al.*, 1998; Buttner and Singh, 1997). It is possible that this mechanism may contribute to the climacteric increase of ethylene and post-harvest production in broccoli.

Finally, broccoli senescence occurs in vegetative tissue so useful comparisons with leaf senescence may be drawn. John *et al.* (1995) introduced an *ACC oxidase* antisense construct into tomato, which inhibited *ACC oxidase* expression and ethylene synthesis. This clearly delayed leaf senescence by between 10 –14 days, but did not induce a sustained stay-green phenotype as with some of the tomato fruit. John *et al.* (1995) suggest that once senescence begins it proceeds normally and that ethylene may be a significant factor in the timing of senescence.

### 1.11 Project Aims

The literature reports that ethylene has a major role in the rapid senescence of broccoli, and that blocking the key enzymes of synthesis may reduce the rate of yellowing. The cDNAs for the biosynthetic enzymes *ACC oxidase 1*, *ACC oxidase 2*, and *ACC synthase*, have been isolated from *Brassica oleracea* var. *italica* (Shogun) (Pogson *et al.*, 1995a,b).

The main aim of this project is to down-regulate the ACC oxidase and ACC synthase enzymes in *Brassica oleracea* var. *italica* with native cDNAs inserted in the antisense orientation, and to up-regulate these enzymes with sense constructs. This aim may be divided into three main objectives.

- 1). Produce *ACC oxidase 1* and *2*, and *ACC synthase* sense and antisense constructs.
- 2). Transform suitable broccoli cultivar, and regenerate tissue into whole plants with the possibility of producing marker-free plants.
- 3). Analyse transformed plants for ethylene production and factors coupled with senescence such as chlorophyll levels.

If successful, it will be possible to determine the role of ethylene in senescence of broccoli, and the importance of the ACC enzymes in this process. The project may also produce an increased shelf-life phenotype of broccoli through delayed sepal yellowing.

**2.0 Construction of *Brassica oleracea* ACC oxidase and ACC synthase sense and antisense gene cassettes**

## 2.1 Introduction

Broccoli (*Brassica oleracea* L. var. *italica*) is a floral vegetable that when harvested senesces rapidly from a chlorophyll-rich green hue to one with pronounced sepal yellowing (Tian *et al.*, 1994). Post-harvest senescence is characterised by a complex breakdown and oxidation of carbohydrates, proteins and lipids and loss of product quality. In an attempt to ensure a 'quality' product for the consumer, major retailers specify a product life of only two days from delivery to 'purchase before date', and a further two days 'best consumed by'. This short post-harvest life results in significant waste for the retailer, a cost borne by the consumer.

The gaseous hormone ethylene appears to play a major role in post-harvest sepal yellowing as chlorophyll loss is associated with an increase in floret ethylene synthesis (Tian *et al.*, 1994). Ethylene biosynthetic inhibitors such as aminoethoxyvinylglycine and inhibitors of ethylene action (silver ions) have been shown to delay chlorophyll loss (Wang, 1977; Aharoni *et al.*, 1985; Clarke *et al.*, 1994), whereas exogenous ethylene treatment enhances chlorophyll loss (Tian *et al.*, 1994).

The gene for the ethylene-forming enzyme in plants, 1-aminocyclopropane-1-carboxylic acid (ACC) oxidase was first isolated from tomato (*Lycopersicon esculentum* var. Ailsa Craig) by Hamilton *et al.* (1990). It was confirmed by down-regulating the gene with an inverted DNA sequence thought to contain the gene. This 'antisense' approach not only determined the presence of the gene in the DNA sequence but also provided a technique for effective gene silencing. The DNA fragment from this work has enabled the cloning of ACC oxidases in a number of crop species including *Brassica*

*oleracea* (Pogson *et al.*, 1995a). The other major enzyme in the ethylene biosynthetic pathway is 1-aminocyclopropane-1-carboxylic acid (ACC) synthase that synthesises ACC from S-adenosylmethionine (Yang and Hoffman, 1984) that is then oxidised by *ACC oxidase* to produce ethylene. The cDNA from this gene was first cloned by Sato and Theologis (1989) from zucchini fruits and has since been cloned from several other species.

Pogson and co-workers (1995a,b) used known cDNA probes from mustard and apple to isolate two *ACC oxidases* and an *ACC synthase* cDNA from *B. oleracea* L. cv Shogun. *ACC oxidase 1 (aco1)* and *ACC oxidase 2 (aco2)* shared nucleotide identity of 83% in putative translated regions and 48% in the 5' untranslated regions. Post-harvest expression studies were undertaken to establish the role of these genes in ethylene production and their role in senescence. *aco1* transcripts were found at low levels in the whole florets and increased markedly in abundance after harvest. *aco1* transcripts also increased in abundance in sepals after harvest. Transcripts corresponding to *aco2* were found exclusively within the reproductive structures. They were absent at harvest but started to increase in abundance within 2hr of harvest and accumulated to high levels. Pogson *et al.* (1995a) concluded that *aco1* was responsible for the basal level of ethylene required for plant physiological and developmental processes, whereas *aco2* was specifically induced by stress conditions as experienced during harvest. *ACC synthase (acs)*, often thought to be the rate-limiting enzyme in the biosynthesis of ethylene, showed no change in post-harvest transcript abundance in the florets, and was detected at similar levels in green and senescing leaves.

The main objective of this project is to test the hypothesis that post-harvest production of ethylene is one of the major factors involved in broccoli senescence. The ACC cDNAs isolated by Pogson *et al.* (1995a,b) were obtained to down-regulate the native broccoli ACC genes, by *in vivo* gene silencing as demonstrated by Hamilton *et al.* (1990). This approach may help to determine specific roles for *aco1*, *aco2* and *acs* in broccoli post-harvest senescence and extend product shelf-life. A control plasmid with  $\beta$ -glucuronidase (*gus*) is necessary to follow changes of ethylene production in transgenic plants without the ACC constructs.

Hamilton *et al.* (1990) showed that for effective gene silencing, high levels of mRNA transcripts are important. They demonstrated the effectiveness of the cauliflower mosaic virus (CaMV) 35S promoter in producing high levels of antisense ACC oxidase mRNA transcripts in tomato, which resulted in a reduction of ethylene production. The CaMV 35S promoter is active in the genome of a variety of monocotyledonous and dicotyledonous plants (Blaich, 1992). Benfey and Chua (1990) determined that the CaMV 35S promoter comprises a collection of sequences that individually direct a defined pattern of tissue specific and developmentally regulated gene expression which cumulatively result in constitutive gene expression. It is a suitable promoter for studying the down-regulation of the ACC genes in different tissues and stages of broccoli development, especially post-harvest. The nopaline synthase (*nos*) terminator (Bevan, 1983) has a polyadenylation signal. Polyadenylation of mRNAs is thought to confer greater stability to the mRNA and increase efficacy of nucleic acid interaction required for gene silencing.

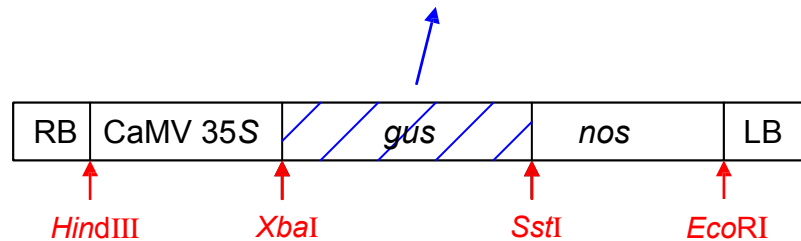
It is advantageous to produce marker-free plants that are phenotypically normal and do not contain superfluous bacterial DNA. A binary vector such as pSCV1.0 (Biogemma) contains a minimal amount of T-DNA between the borders without a selectable marker. There are eleven unique restriction sites within the T-DNA borders that can be used to clone genes of interest. Outside the borders the bacterial gentamicin/kanamycin and the pUC ampicillin ( $\beta$ -lactamase, *bla*) resistance genes are present. pSCV1.0 also contains co-existent origins of replication (Col E1 and RK2) that produce high copy numbers in both *E. coli* and *Agrobacterium*.

The aim for this part of the project is to clone the ACC cDNAs into the minimal T-DNA binary vector pSCV1.0 in both sense and antisense orientations between the CaMV 35S promoter and the *nos* terminator.

## 2.2 Materials and Methods

### 2.2.1 Cloning Strategy

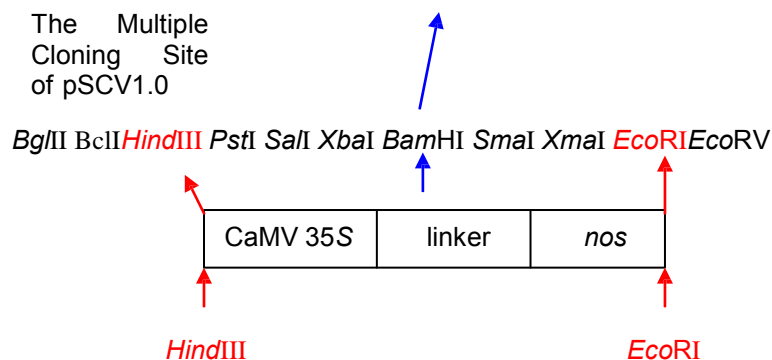
(a). The *gus* gene was removed from pBI121 with *Xba*I and *Sst*I restriction enzymes.



(b). The *gus* gene was replaced with an oligo-nucleotide (linker) which had been designed with suitable restriction endonuclease restriction sites.



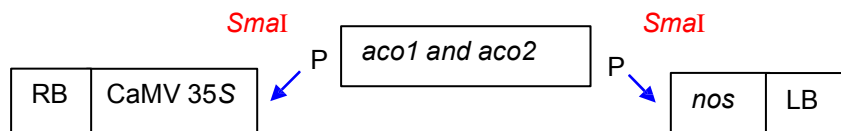
(c). The *Hind*III/*Eco*RI cassette was transferred into the multiple cloning site of the pSCV1.0 and renamed pJ1.0



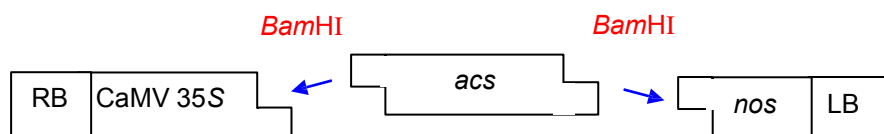
T-DNA region of pJ1.0 (All sites unique except those in bold)

RB	<i>Bgl</i> III, <i>Bcl</i> II, <i>Hind</i> III, <b><i>Sph</i>I</b> , <i>Pst</i> I	CaMV 35S	<i>ba</i> I, <i>Bam</i> HI, <i>Sal</i> I, <i>Sma</i> I, <b><i>Sst</i>I</b>	<i>nos</i>	<i>Eco</i> RI, <i>Eco</i> RV	LB
----	---	----------	--	------------	------------------------------	----

(d). *aco1* and *aco2* were PCR-amplified from pBluescript and the products were phosphorylated with the pMOS blue kit. pJ1.0 was digested with *Sma*I and the cut-ends were dephosphorylated. The cDNA clones were ligated into pJ1.0.



(e). *acs* was PCR-amplified from pBluescript with primers adding *Bam*HI sites to the ends. Both *acs* and pJ1.0 were digested with *Bam*HI and then ligated together.



(f). For the control plasmid, the *Hind*III/*Eco*RI fragment from pBI121 was ligated into the *Hind*III/*Eco*RI restriction sites of pSCV1.0.

## 2.2.2 Plasmids

### 2.2.2.1 The ACC oxidase and ACC synthase cDNAs

The *B. oleracea* ACC oxidase and ACC synthase cDNAs (Pogson *et al.*, 1995a,b) were obtained from Kevin Davies (Crop and Food Research,

Levin, New Zealand). The genes had been ligated into the *EcoRI* site of pBluescript SK, after attachment of *NotI*, *EcoRI* adapters, which had been checked by sequencing with the T3 and T7 promoter primers. The sequence analysis showed the adaptor sequence, and presence of the gene within the multiple cloning site of pBluescript. The *aco1* gene had been ligated in the sense orientation, whereas the *aco2* and *ACC synthase* sequences were in antisense orientation relative to the T7 promoter.

#### 2.2.2.2 Binary Vectors

The binary vector pSCV1.0 (Figure 2.2; Biogemma, Cambridge) was used as the backbone for the constructs. The binary vector pBI121 constructed by Jefferson *et al.* (1987) (Figure 2.1) and obtained from Dr J. Gittins, (HRI-East Malling, Kent) was used as a source of promoters and terminators as well as the  $\beta$ -glucuronidase (*gus*) gene for a control. pBI121 is derived from pBin19 (Bevan, 1984). It contains the CaMV 35S promoter fragment (Guilley *et al.* 1982), the  $\beta$ -glucuronidase gene (Jefferson *et al.*, 1987) and the *nos* terminator (Bevan *et al.*, 1983) within the T-DNA region. pBI121 also has the neomycin phosphotransferase (*nptII*) gene which detoxifies a number of aminoglycoside antibiotics, including neomycin, kanamycin and geneticin.

#### 2.2.2.3 Plasmid extraction

All plasmids were extracted with Qiagen miniprep (tip20) kits (Qiagen Ltd., Boundary Road, Crawley, West Sussex), which produced sufficient DNA for the next step of the cloning process.

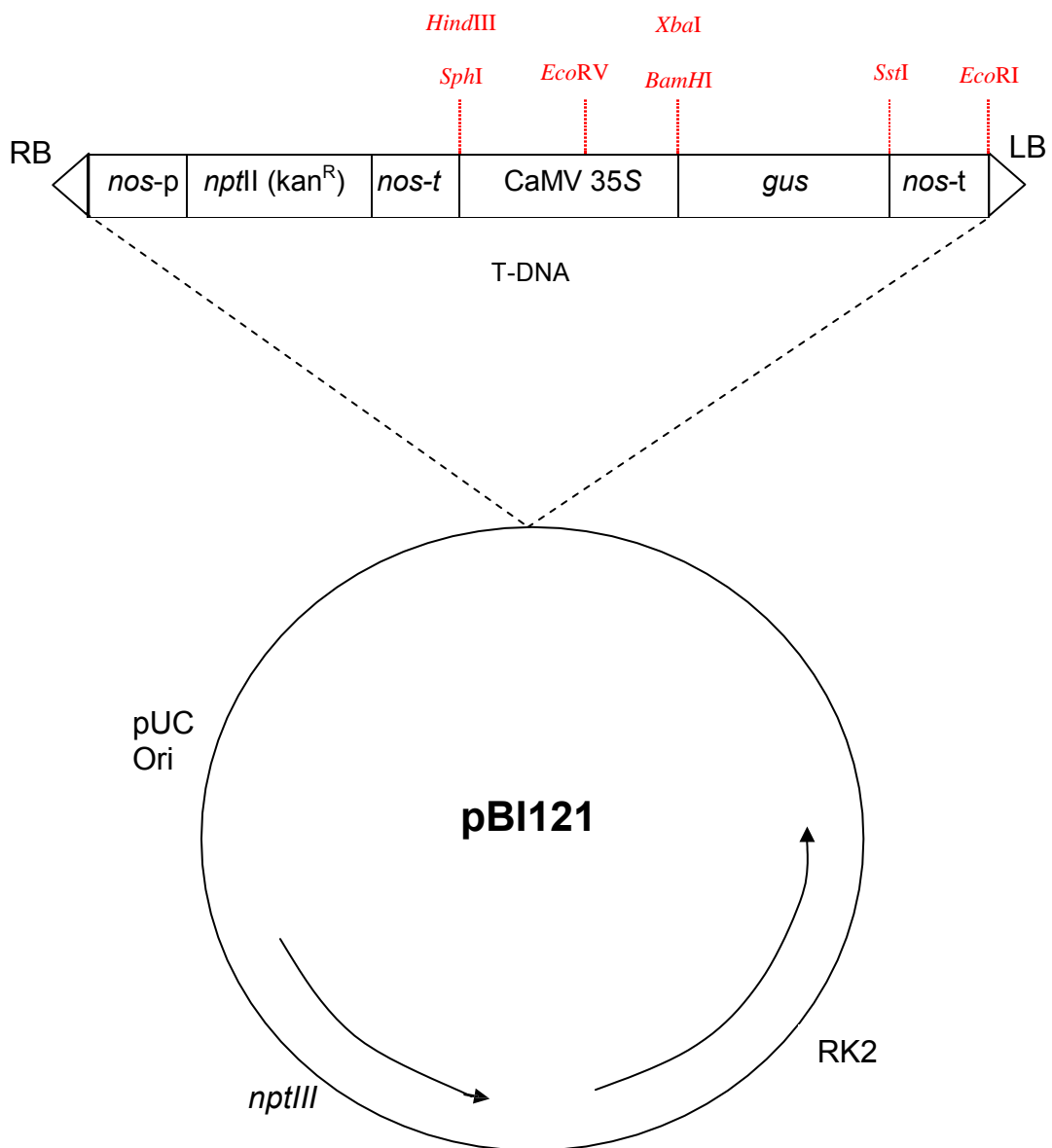


**Figure 2.1** Circular map of pBI121 (adapted from Frisch *et al.*, 1995 and Jefferson *et al.*, 1987) showing the T-DNA region with unique restriction endonuclease sites.

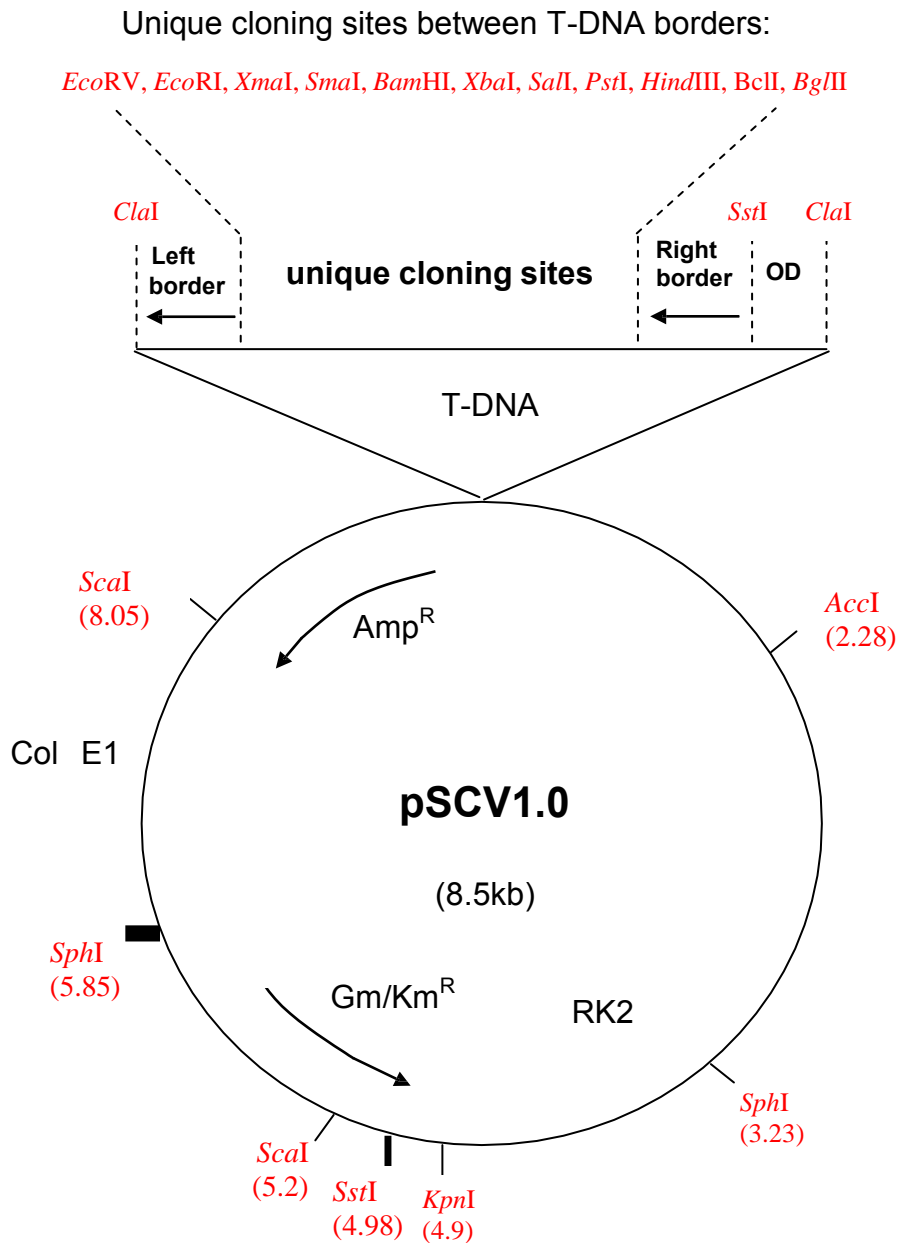


**Figure 2.2** Circular map of pSCV1.0

It shows the ampicillin, kanamycin/gentamycin bacterial resistance genes and origins of replication. Within the T-DNA borders, the eleven unique restriction endonuclease sites of the multiple cloning site are shown which can be used for cloning genes of interest.

### 2.2.3 Bacterial strains and media

All cloning steps were conducted in *E. coli* DH5 $\alpha$ , genotype: F<sup>-</sup>  $\phi$ 80d*lacZ* $\Delta$ M15  $\Delta$  (*lacZYA-argF*)U169 *deoR recA1 endA1 hsdR17*(r<sub>k</sub><sup>-</sup>, m<sub>k</sub><sup>+</sup>) *phoA supE44  $\lambda$ thi-1 gyrA96 relA1* (GIBCO-Life Technologies, Uxbridge, UK.) and cultured in LB media (see appendix). Transformed cells with either pBI121 or pSCV1.0 derivatives were selected for with 25mg/l kanamycin and those with pBluescript, 50mg/l ampicillin. *E. coli* cells were incubated at 37°C.

*Agrobacterium rhizogenes* strain LBA 9402 pRi1855::pMBRE36GFP was cultured either on YMB plates, or MGL (appendix) liquid broth at 25°C. The cells were selected for with tetracyclin, rifampicin and kanamycin for the cointegrate *Ri* plasmid, chromosomal DNA and binary plasmid, respectively.

### 2.2.4 Enzymes and DNA

All enzymes including restriction enzymes, DNA ligases, and *Taq* polymerases were purchased from GIBCO-Life Technologies, Uxbridge, U.K as were DNA ladders for gel electrophoresis. All oligonucleotides were synthesised by VH Bio Ltd., Gosforth, Newcastle upon tyne, UK (Table 2.1) and used in standard PCR conditions (Table 2.2).

**Table 2.1** Oligonucleotide sequences used in these experiments

Primer No.	Name	Sequence (5'- 3')	T <sub>m</sub> <sup>(a)</sup> (°C)
1	Oligo top	CTAGAGGATCCATGTTCGACCCGGGAGCT	72
2	Oligo bot	CCCGGGTTCGACATGGATCCT	67
3	35S (F)	ACGTTCCAACCACGTCTTCA	60
4	nos (R)	CCGATCTAGTAACATAGATGACAC	61
5	<i>aco1</i> (F)	TCAAACAACACTAGCTACTTCAAC	57
6	<i>aco1</i> (R)	TTTCTTAGAACAGTTATCATATTATT	54
7	<i>aco2</i> (F)	TCATATTTCCAATACAATTATTGC	54
8	<i>aco2</i> (R)	CTAACATCATCAACAACATTAAG	56
9	<i>acs</i> (F)	GCGGGATCCAATAACGATTAGAGAAATTATGGT	69
10	<i>acs</i> (R)	GCGGGATCCATCTCAACAGAACAAAACAAAC	67
11	<i>aco1</i> (I)	ACGTTCCAACCACGTCTTCA	60
12	<i>aco1</i> (II)	AGCTTCATCGCTTGCCTGTA	60
13	<i>aco1</i> (III)	CTTCTCGACGTTGTCCATCA	60
14	<i>aco1</i> (IV)	CCGATCTAGTAACATAGATGACAC	61
15	<i>aco2</i> (I)	GACATCTCCACTGACGTAAG	60
16	<i>aco2</i> (II)	CCACAGTCGAGACGTTCTAA	60
17	<i>aco2</i> (III)	TTCATGGCCGCTCGGTATTC	62
18	<i>aco2</i> (IV)	CCGATCTAGTAACATAGATGACAC	61
19	<i>acs</i> (I)	GACATCTCCACTGACGTAAG	60
20	<i>acs</i> (II)	AGAAGTGTTGGCAGAGTAGC	60
21	<i>acs</i> (III)	CTTCGCTACAGCTTGTCTGA	60
22	<i>acs</i> (IV)	CCGATCTAGTAACATAGATGACAC	61

(a) T<sub>m</sub> of the primers was calculated with the expression:

$$T_m = 81.5 + -16.6 + (41 \times (\#G + \#C/\text{length})) - (500/\text{length})$$

**Table 2.2** PCR reaction components.

To make a total 25 $\mu$ l for each reaction, 5 $\mu$ l of template DNA (100 $\mu$ mol/ $\mu$ l) and 5 $\mu$ l of primers (set at 4 $\mu$ mol/ $\mu$ l) were added. Primers and template DNA were suspended in autoclaved reverse osmosis water.

	x1 ( $\mu$ l)
10x Buffer	2.5
50mM MgCl <sub>2</sub>	0.75
dNTPs 25mM	0.2
H <sub>2</sub> O	11.42
BRL <i>Taq</i>	0.13
<b>Total</b>	<b>15</b>

The PCR program in Table 2.3 was used and annealing temperatures adjusted to 3°C below  $T_m$  of primer pairs (Table 2.1). This was performed on a Hybaid Omnigene PCR machine.

**Table 2.3** PCR program.

Stage 1 and 3 were cycled once. Stage 2 was cycled thirty five times.

<b>Stage 1.</b>	93°C/ 2 min	58°C/ 1 min	
<b>Stage 2.</b>	72°C/ 1 min	93°C/ 30 s	58°C/ 1 min
<b>Stage 3.</b>	72°C/ 10 min		

## 2.2.5 Cloning Strategy

### 2.2.5.1 Removing *gus* from pBI121

pBI121 was extracted with a Qiagen miniprep and 1 $\mu$ g was digested with *Xba*I and *Sst*I (5 units each) in the buffers specified in 20 $\mu$ l autoclaved reverse osmosis water for 2h at 37°C. The digest products were loaded, with bromophenol blue dye, onto a 0.7% (w/v) agarose gel containing 0.33 $\mu$ g/ $\mu$ l ethidium bromide. The Low DNA mass ladder (GIBCO-Life Technologies, Uxbridge, UK) was loaded alongside these samples. The gel was run for 50 minutes at 80 Volts, 0.1 amps in a BioRad gel tank. The digested pBI121 separated into 2 bands: one at 2Kbp, the *gus* gene; and the other 11Kbp, the remaining backbone. The 11Kbp fragment was cut out of the gel with a clean scalpel blade and placed into a 1.5ml microfuge tube. The DNA was purified with the Qiaex II kit (Qiagen Ltd., Boundary Road, Crawley, West Sussex), yielding 150ng of cut plasmid.

### 2.2.5.2 Replacing *gus* with synthetic linker

A synthetic DNA linker was created by annealing oligonucleotides 1 and 2. They were initially heated to 75°C in a water bath and left to cool for 2h. The linker contained 5 restriction endonuclease sites as shown below:



The linker was ligated into the *Xba*I/*Sst*I sites of the cut pBI121 plasmid. The digested pBI121 plasmid was 11Kbp and the synthetic linker

24bp in length and therefore, a 1:5 ratio by number would be 11000: 120 by weight. For the ligation, 45ng of plasmid and 0.45ng linker was used. The annealed synthetic linker was diluted to a concentration 0.1ng/ $\mu$ l. The digested plasmid was at a concentration 7.5ng/ $\mu$ l. The ligation reaction mixture consisted of: H<sub>2</sub>O 5.4 $\mu$ l; digested plasmid 6.0 $\mu$ l; linker 4.5 $\mu$ l; T4 ligase buffer 4.0 $\mu$ l and T4 DNA ligase 0.1 $\mu$ l, making a total 20 $\mu$ l. The ligation mixture was incubated at 22°C for two hours.

The transformation of ligated plasmid was carried out according to the protocol supplied with the DH5 $\alpha$  library efficient competent cells (GIBCO-Life Technologies). The cells transformed with the binary plasmid were selected with 25mg/l kanamycin on LB agar plates and grown overnight at 37°C. Single colonies were checked for presence of the synthetic linker insert with a colony PCR method taken from the pMOS*Blue* T-vector kit (Amersham International plc, Little Chalfont, Buckinghamshire, UK). This involved picking a white colony, approximately 1mm in diameter from the plate using a sterile cocktail stick. The tip was touched onto a master plate and then transferred to a 1.5ml tube containing 50 $\mu$ l sterile water. This was repeated for ten colonies. The tubes were placed in boiling water for 2 min to lyse the cells and denature genomic DNA and nucleases. The tubes were put on ice for a further 2 min for the plasmid DNA to renature and then centrifuged at 12000g for 1 minute to remove cell debris. In the PCR, the linker oligonucleotides (1 and 2) were used as primers, paired with primers designed from the CaMV 35S (3) and *nos* (4) sequences (Table 2.1). Colonies with positive PCR bands were grown overnight at 37°C in liquid LB and the plasmids were extracted with the Qiagen miniprep kit. Plasmid integrity was checked with restriction digests.

### 2.2.5.3 Transferring CaMV 35S-linker-nos cassette from pBI121 to pSCV1.0

*E. coli* DH5 $\alpha$  cells containing the pSCV1.0 plasmid were cultured overnight and plasmids extracted with the Qiagen miniprep tip20 kit. The pSCV1.0 and the pBI121 plasmid with the linker instead of *gus* were digested with *EcoRI* and *HindIII* with the specified buffers in 20 $\mu$ l sterile R.O. water at 37 $^{\circ}$  C for 2h. The digested products were run on a 0.7% (w/v) agarose gel at 80 volts for 50 minutes. The 1.1Kbp fragment from the adapted pBI121 plasmid and the 8.5 Kbp pSCV1.0 backbone were cut out of the gel with a clean scalpel and placed into 1.5 ml microfuge tubes. The DNA was re-extracted with the Qiaex II kit, supplied by Qiagen and quantified on an agarose gel in preparation for ligation. The *EcoRI/HindIII* fragment from pBI121 yielded a concentration of 1.5ng/ $\mu$ l, from an 18 $\mu$ l sample. The digested pSCV1.0 backbone yielded 75ng/ $\mu$ l, from a sample of 20 $\mu$ l. The size of pSCV1.0 was 8.5Kbp, whereas the *EcoRI/HindIII* fragment from the pBI121 plasmid was 1.1Kbp. Therefore, a 1:1 ratio by number would be 8.5:1.1 by weight and a 1:5 ratio 8.5:5.5. As the total quantity of fragment DNA was 27ng in 18 $\mu$ l, the amount of pSCV1.0 plasmid DNA required for a 1:5 ratio would be 42ng. As the concentration of pSCV1.0 was 75ng/ $\mu$ l, only 0.55 $\mu$ l of DNA was required for the ligation. The ligation reaction consisted of: 18 $\mu$ l *EcoRI/HindIII* fragment; 0.6 $\mu$ l *EcoRI/HindIII* pSCV1.0 digest; 4 $\mu$ l T4 DNA ligase buffer; 0.1 $\mu$ l T4 DNA ligase; total 22.7 $\mu$ l. The ligation was carried out at 22 $^{\circ}$ C overnight. DH5 $\alpha$  cells were transformed with the ligation mixture according to the GIBCO-Life Technologies protocol, and transformants were selected for on LB agar plates with 25mg/l kanamycin. Single colonies were checked with the PCR method described above with primer pairs of

oligonucleotides 1 and 4 and 3 and 2 (Table 2.1). Colonies giving bands were cultured in an overnight LB broth at 37°C. The plasmids were extracted with the Qiagen miniprep kit and checked by digestion with restriction endonucleases (Figure 2.4b) and called pJ1.0.

#### 2.2.5.4 Inserting the *Brassica oleracea ACC oxidase 1* and *2* cDNAs into pJ1.0 by blunt-ended cloning

The *ACC oxidase* genes were PCR amplified from pBluescript with primers 5-8 (Table 2.1). As the synthetic primers flank either end of the *ACC* cDNAs, bands of 1231bp for *aco1* and 1223 bp for *aco2* were expected (Figure 2.5). The PCR products were separated from the pBluescript template DNA on a 0.7% (w/v) agarose gel run for 30min at 100 volts. The PCR products were cut out of the gel with a clean scalpel and placed into a 1.5ml microfuge tube. The DNA was re-extracted from the agarose gel with the Qiaex II kit (Qiagen). This yielded 250ng/μl for each *ACC oxidase* cDNA clone.

Five micrograms of the pSCV1.0 35S-linker-*nos* plasmid was digested with *Sma*I as specified by GIBCO-Life Technologies for 2h at 30°C. As *Sma*I produces a blunt-ended fragment it was essential to dephosphorylate the cut ends to prevent the plasmid from closing up without insert during the ligation. After the digest, the incubation temperature was raised to 37°C and 1.59μl of calf intestinal alkaline phosphatase (CIP) was added. This figure was arrived at by a simple set of calculations. The molecular weight of the plasmid was roughly 9500bp X 660 (molecular weight of a pair of nucleotides) = 6270000 = 1gmole.

$$1\text{g} = \frac{1}{6270000} = 1.6 \times 10^{-7} \text{ moles}$$

$$1\mu\text{g} = \frac{1}{6270000 \times 10^6} = 1.6 \times 10^{-13}$$

$$1\mu\text{g} = \frac{1 \times 10^{12}}{6270000 \times 10^6} = 0.16 \text{ pmoles}$$

$$1\mu\text{g} = 0.32 \text{ pmole ends (2 ends per molecule)}$$

As there were 5 $\mu\text{g}$  of plasmid and 1 pmol ends requires 1 unit of enzyme, 1.6 units of enzyme (i.e. 1.6 $\mu\text{l}$  as 1u/ $\mu\text{l}$ ) were added and incubated for 1 h. The CIP was promptly inactivated at 75°C for ten minutes and DNA repurified with a phenol:chloroform extraction as below. The digested and dephosphorylated plasmid was made up to 100 $\mu\text{l}$  by adding 80 $\mu\text{l}$  R.O. water. An equal volume of phenol (100 $\mu\text{l}$ ) was added and the two were mixed by inverting the tube 5 times. The tube was spun in a microfuge at 11600g for ten seconds. The aqueous phase was removed and placed into another tube while the phenol was carefully discarded. Both phenol and chloroform were added to the aqueous phase in a 50:50 ratio and mixed and separated as above. Chloroform was added (100 $\mu\text{l}$ ) and again repeated as above. The aqueous phase was removed and to this 230 $\mu\text{l}$  ethanol was dispensed and centrifuged at 11600g for 20min. The supernatant was removed and the DNA pellet air dried for 5 min. The pellet was resuspended in 20 $\mu\text{l}$  sterile R.O. water. The DNA was quantified and the yield found to be 100ng/ $\mu\text{l}$ .

#### 2.2.5.5 pMOSBlue kit

To ligate the *ACC oxidase 1 and 2* PCR products into pJ1.0, the fragments were blunt-ended and phosphorylated. This was done using components from the pMOSBlue blunt-ended cloning kit (Amersham Life Science). The pSCV1.0 35S-linker-*nos* plasmid was 9.5Kbp and the cDNA insert 1.3Kbp. Therefore, a 1:2.5 ratio (9.5:3.25) would be 50ng plasmid and 17ng insert. This quantity of insert was added to the pMOSBlue reaction mixture as specified in the protocol and incubated for 40 min at 22°C. The reaction was promptly heat inactivated at 75°C for ten minutes and placed on ice for 2 min. For the ligation, 50ng of *Sma*I cut plasmid and 1µl T4 DNA ligase (4 Weiss units) were added and incubated overnight at 15°C. Transformation with DH5α cells and 1µl ligation reaction mixture was carried out according to the GIBCO-Life Technologies' protocol that comes with the cells and transformants selected using 25mg/l kanamycin in LB agar plates.

#### 2.2.5.6 Inserting *Brassica oleracea ACC synthase* cDNAs into pJ1.0

The *ACC synthase* gene was PCR amplified from pBluescript with primers 9 and 10 flanking both ends of the cDNA clone with *Bam*HI sites at the 5' ends. The synthetic primers produced a band 1746bp including the cDNA and *Bam*HI sites (Figure 2.5). The PCR products were separated from the pBluescript template DNA on a 0.7% (w/v) agarose gel run for 30min at 100 volts. The PCR products were cut out of the gel with a clean scalpel and placed into a 1.5ml microfuge tube. The DNA was re-extracted from the agarose gel with the Qiaex II kit (Qiagen) and yielded 300ng/µl for 20µl. The product was digested with *Bam*HI (GIBCO-Life Technologies) with the correct

buffer at 37°C for 2h. The restriction enzyme was inactivated at 80°C for 20min and then cooled on ice for 2min. Propan-2-ol (400µl) was added to the tube and spun in a microfuge at 11600g for 5 min to precipitate the fragment without the small pieces from the cut ends. The supernatant was removed and 0.5ml 70% ethanol was added. This was spun in a microfuge as before. The supernatant was removed and the DNA pellet air dried for 5 min. The pellet was resuspended in 20µl sterile R.O. water and adjusted to 200ng/µl.

Five micrograms of the pSCV1.0 35S-linker-*nos* plasmid was digested with *Bam*HI (GIBCO-Life Technologies) in the correct buffer at 37°C for 2h. It was dephosphorylated and repurified as described above with the *Sma*I cut plasmid. This yielded 100ng/µl.

The pSCV1.0 35S-linker-*nos* plasmid was 9.5Kbp and the cDNA insert 1.738Kbp. Therefore, a 1:5 ratio would be 9.5:8.7, or 50ng plasmid, 45ng insert. The ligation reaction mixture comprised of 0.5µl plasmid, 0.23µl insert, 4.0µl T4 DNA ligase buffer (GIBCO-Life Technologies), 0.1µl T4 DNA ligase (GIBCO-Life Technologies) and 15.2µl sterile R.O water. The ligation was carried out overnight at 22°C. The transformation was performed according to the protocol provided by GIBCO-Life Technologies, with the competent DH5α cells. Transformed cells were selected on 25mg/l kanamycin LB agar plates.

#### 2.2.5.7 Checking transformants for inserts

Twenty colonies from each of the *ACC oxidase 1 and 2* and *ACC synthase* plates were analysed with the colony PCR method described earlier. The same primer pairs as those used to amplify the cDNA from pBluescript were used to check presence of an insert. The DNA from the colonies with

positive bands on the gel was tested with four primer pairs to determine orientation. Figure 2.3 shows a schematic diagram of the orientation of the primer pairs depending on insertion of the cDNA. For example, if there has been a *aco1* cDNA inserted in antisense orientation, primers 3 and 4 will produce a 542bp DNA fragment, whereas primers 3 and 5 will not produce a fragment as in this orientation they are both forward primers (band sizes are shown in Table 2.4).

**Table 2.4** Predicted PCR product sizes for the insertion of ACC cDNAs in sense or antisense orientations into pJ1.0.

<b>Construct</b>	<b>Orientation</b>	<b>Primer Pairs</b>	<b>Predicted fragment size</b>
<i>aco1</i>	antisense	3+4	542
<i>aco1</i>	antisense	5+nos	462
<i>aco1</i>	sense	3+5	360
<i>aco1</i>	sense	4+nos	710
<i>aco2</i>	antisense	3+8	369
<i>aco2</i>	antisense	9+nos	676
<i>aco2</i>	sense	3+9	578
<i>aco2</i>	sense	9+nos	465
<i>acs</i>	antisense	3+12	471
<i>acs</i>	antisense	13+nos	628
<i>acs</i>	sense	3+13	530
<i>acs</i>	sense	12+nos	572

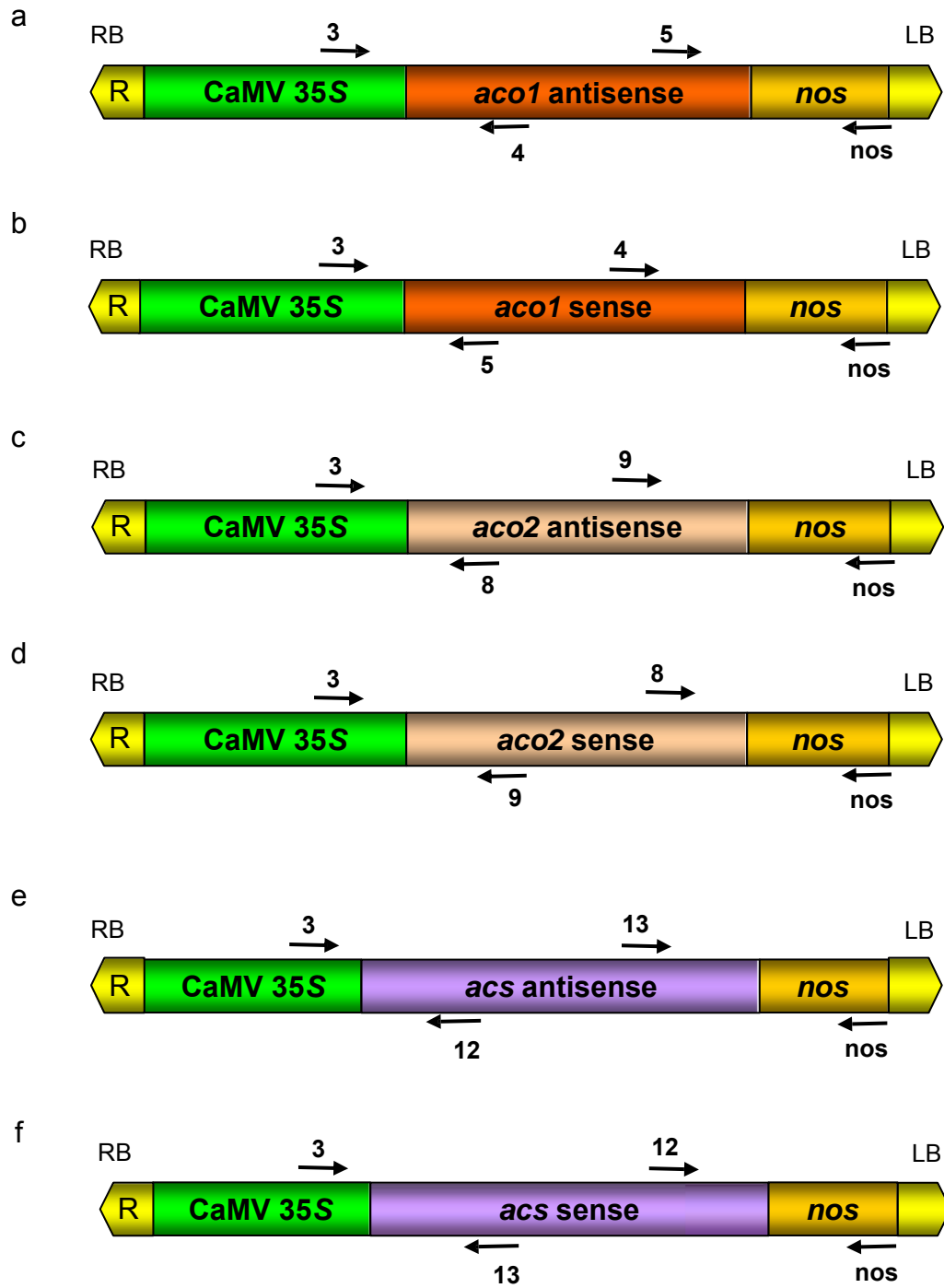


**Figure 2.3** Schematic diagram of primer pairings for cDNA inserts in antisense and sense orientations for *aco1*, *aco2* and *acs*.

The plasmids with positive bands were also extracted with the Qiagen miniprep tip20 kit and digested with *Bgl*/II (GIBCO-Life Technologies) to check orientation of insert and plasmid size (Figure 2.7a of results).

#### 2.2.5.8 Control Plasmid

A control plasmid was constructed with the pSCV1.0 backbone and pBI121 CaMV 35S-*gus-nos* gene cassette. DH5 $\alpha$  cells containing the plasmids were selected for with 25mg/l kanamycin and cultured overnight in liquid LB at 37°C in a shaking incubator. The plasmids were extracted with a Qiagen miniprep tip20 kit and 5 $\mu$ g restriction digested with *Eco*RI/*Hind*III (GIBCO-Life Technologies) with the specified buffers at 37°C for 2h. The digested products were run on a 0.7% (w/v) agarose gel at 80 volts for 50 minutes. The pSCV1.0 backbone (8.5Kbp) and the pBI121 CaMV 35S-*gus-nos* cassette (3Kbp) were cut out of the gel with a clean scalpel and placed into a 1.5ml microfuge tube. The DNA was re-extracted with the Qiaex II gel purification kit (Qiagen) and quantified. The CaMV 35S-*gus-nos* cassette yielded 10ng/ $\mu$ l (200ng/20 $\mu$ l) and pSCV1.0 backbone 150ng/ $\mu$ l (3 $\mu$ g/20 $\mu$ l). The size of the pSCV1.0 backbone was 8.5Kbp, and the gene cassette 3Kbp. For a 1:5 plasmid:insert ratio, 50ng backbone plasmid and 90ng gene cassette were used for the ligation. The ligation mixture comprised of: 9 $\mu$ l insert, 0.33 $\mu$ l backbone plasmid, 4 $\mu$ l T4 DNA ligase buffer, 0.1 $\mu$ l T4 DNA ligase and 6.57 $\mu$ l sterile R.O. water. The ligation mixture was incubated for 2h at 22°C. The transformation was performed according to the protocol provided by GIBCO-Life Technologies, with the competent DH5 $\alpha$  cells. Transformed cells were selected on 25mg/l kanamycin LB agar plates. Transformants were

checked with the colony PCR method described earlier with primers 11 and 13 (Table 2.1) and the plasmids were digested with *EcoRI* /*HindIII*.

#### 2.2.5.9 Producing and storing *E. coli* and *A. rhizogenes* stocks with the 7 constructs

The *E. coli* DH5 $\alpha$  cells with the constructs were cultured on liquid LB with 25mg/ml kanamycin and grown overnight at 37°C in a shaking incubator. They were grown to a density of approximately  $1 \times 10^9$  cells/ml. Sterile glycerol was mixed 50:50 with liquid LB. Into a sterile screw cap 1.5ml tube, 0.5ml DH5 $\alpha$  cells and 0.5ml glycerol/LB was added and gently mixed by inverting. These were frozen at -80°C and stored for future use.

Cells from *A. rhizogenes* strain LBA 9402 virulence plasmid pRi1855, cointegrate with pMBRE36 GFP were rendered competent using the technique from Mattanovich *et al.* (1989). Competent cells were transformed by electroporation (Mattanovich *et al.*, 1989) using a Biorad Gene Pulser. Transformants were selected for on YMB plates with 50mg/l kanamycin, 100mg/l rifampicin and 10mg/l tetracyclin and grown for 3 days at 25°C. They were stored in the same way as the DH5 $\alpha$  cells but with MGL instead of LB liquid broth.

### 2.3. Results

The backbone plasmid, pJ1.0 was constructed to be used as a cloning vector for the ACC cDNAs. It was based on pSCV1.0 with the addition of the CaMV 35S promoter and *nos* terminator, flanking a multiple cloning site linker. It is shown schematically in Figure 2.4 (a), and confirmed in Figure 2.4(b).

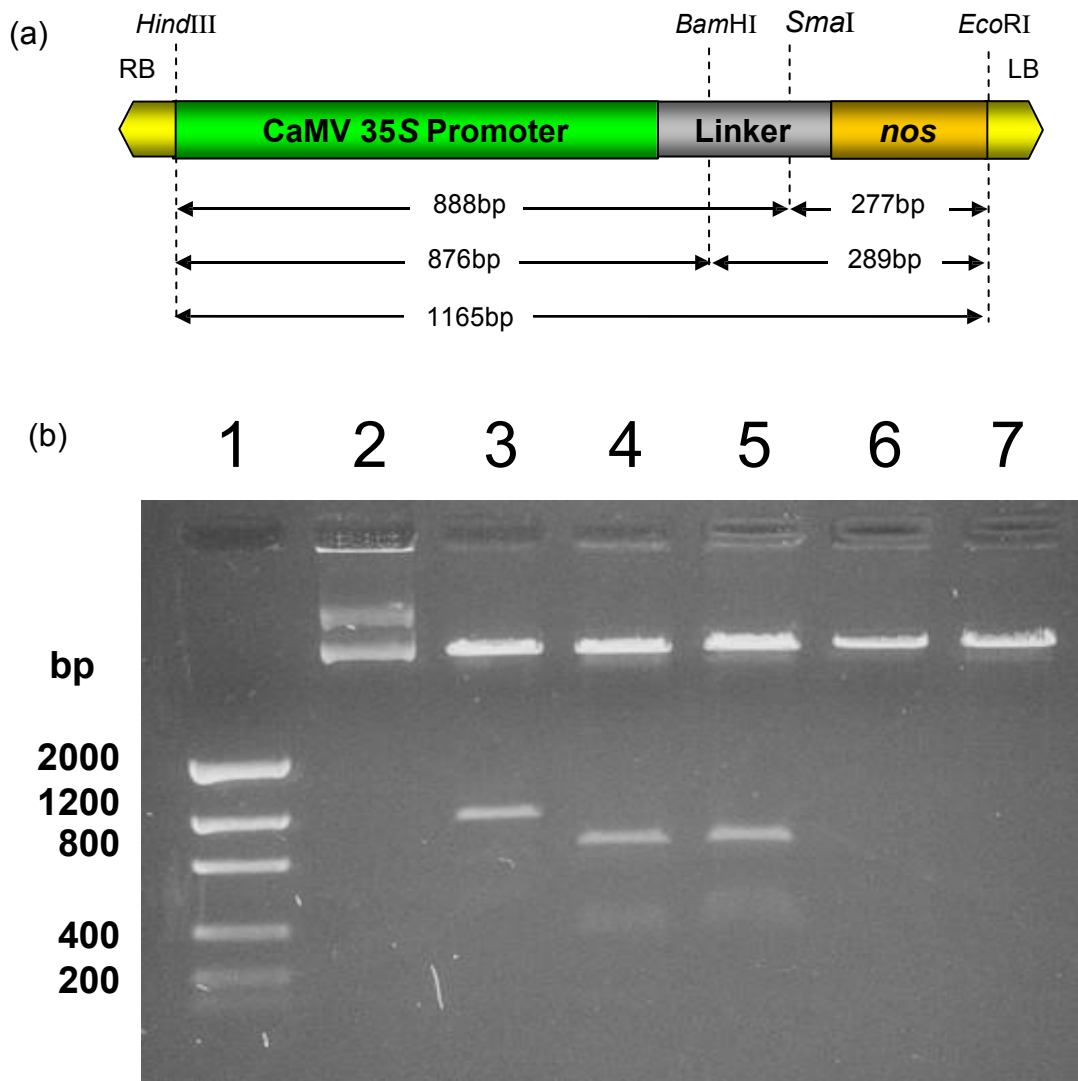


**Figure 2.4** (a) T-DNA region of pJ1.0 with restriction sites. (b) Restriction endonuclease digest confirming the integrity of the backbone plasmid, pJ1.0. The plasmid was digested with the restriction enzymes shown in Figure 2.4a. Lane 1, DNA Mass Ladder; Lane 2, uncut plasmid, Lane 3, *EcoRI/HindIII*; Lane 4, *EcoRI/HindIII/SmaI*; Lane 5, *EcoRI/HindIII/ BamHI*; Lane 6, *SmaI*; Lane 7, *BamHI*.

In Figure 2.4 (b), lane 3, the *EcoRI/HindIII* digest produced an 1165bp fragment. These sites are within the T-DNA borders and the fragment includes the CaMV 35S promoter, the linker, and the *nos* terminator. In lanes 4 and 5 the fragment including the promoter, linker and terminator is cut at the linker multiple cloning site by *SmaI* and *BamHI*, respectively. The band seen on the gel at 870bp is the 35S promoter. There should also be a *nos* terminator band (270bp), but there is not enough DNA for it to be visible. Although faint bands around 450bp are present these are unidentified, as the *nos* bands would run further. However, the difference in sizes of the bands in lanes 4 and 5 to the band in lane 3 is the size of the *nos* terminator.

The major bands in lanes 6 and 7 show linearised plasmids with just a single cut. They show that *SmaI* and *BamHI* sites within the linker must be unique within pJ1.0 and can be used to clone the ACC broccoli cDNAs.

Following cloning of ACC cDNA inserts into the pJ1.0 linker multiple cloning site, colony PCR was used to confirm the success of the procedure. The cDNA clones were originally amplified from pBluescript (SK) with specific primers. The same primers were used to check the transformed *E. coli* colonies produced from a ligation of vector and insert. A colony producing a positive band was then analysed with pairs of primers to determine the orientation of the insert.

In Figure 2.5, the *aco1* and *aco2* inserts were 1232/1237bp, respectively, and the ACC synthase 1700bp in size (lanes 2-4). The presence of these bands demonstrates the insertion of the *aco1*, *aco2* and *acs* cDNA clones. As the cDNAs were cloned non-directionally, they could insert in either sense or antisense orientation. Therefore, once it was clear an insert was

present, a second PCR was conducted to determine orientation. In order to avoid inaccuracies, the technique, detailed in the methods was based on a band/no band result. This worked very effectively for *aco1*. Lanes 5-8 show *aco1* antisense, and lanes 9-12 *aco1* sense.

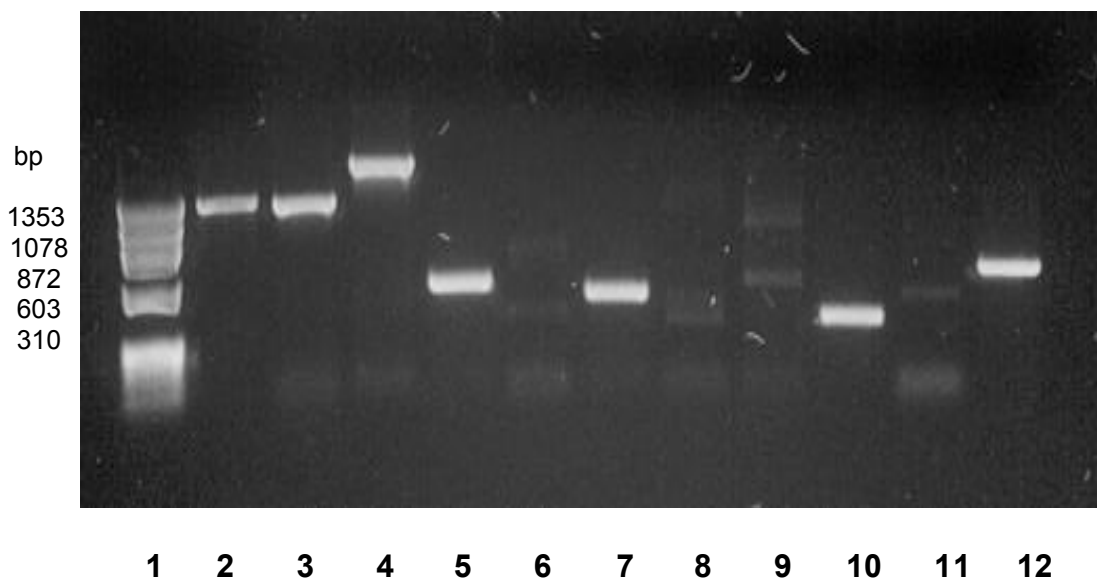


**Figure 2.5** PCR products to determine presence and orientation of insert (see Figure 2.3/Table 2.4). In lane 1,  $\phi$ x174/*Hae*III digest (marker); lane 2, *aco1* cDNA insert in pJ1.0; lane 3, *aco2* cDNA insert in pJ1.0; lane 4, *acs* cDNA insert in pJ1.0; lane 5, *aco1* A (primers 3+4); lane 6, *aco1* A (3+5); lane 7, *aco1* A (5+nos); lane 8, *aco1* A (4+nos); lane 9, *aco1* S (3+4); lane 10, *aco1* S (3+5); lane 11, *aco1* S (4+nos); lane 12, *aco1* S (5+nos).

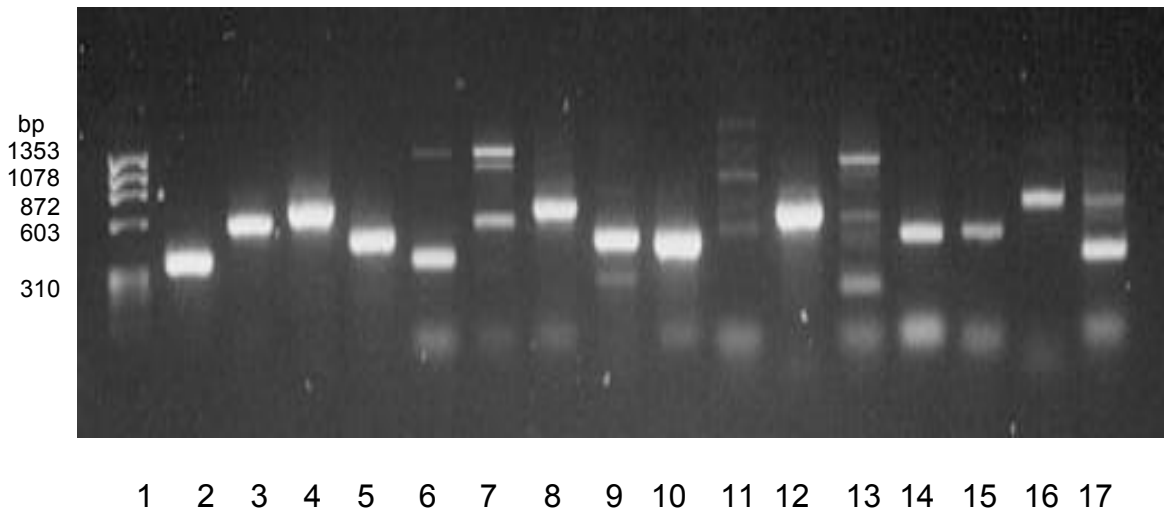


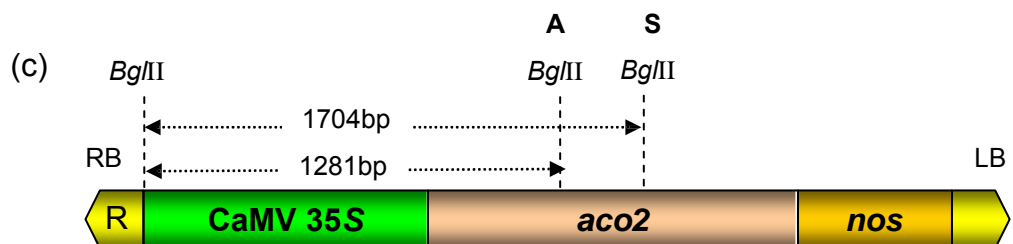
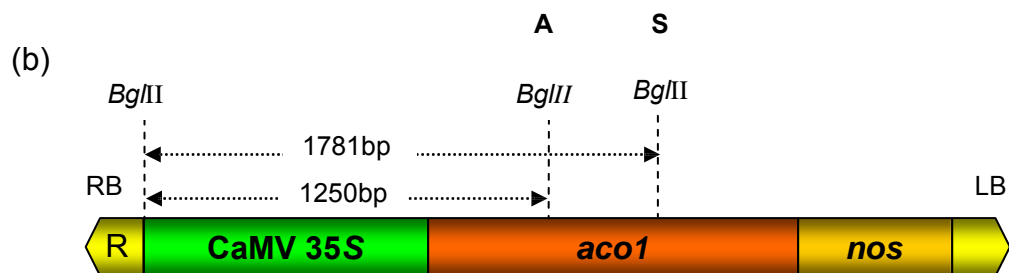
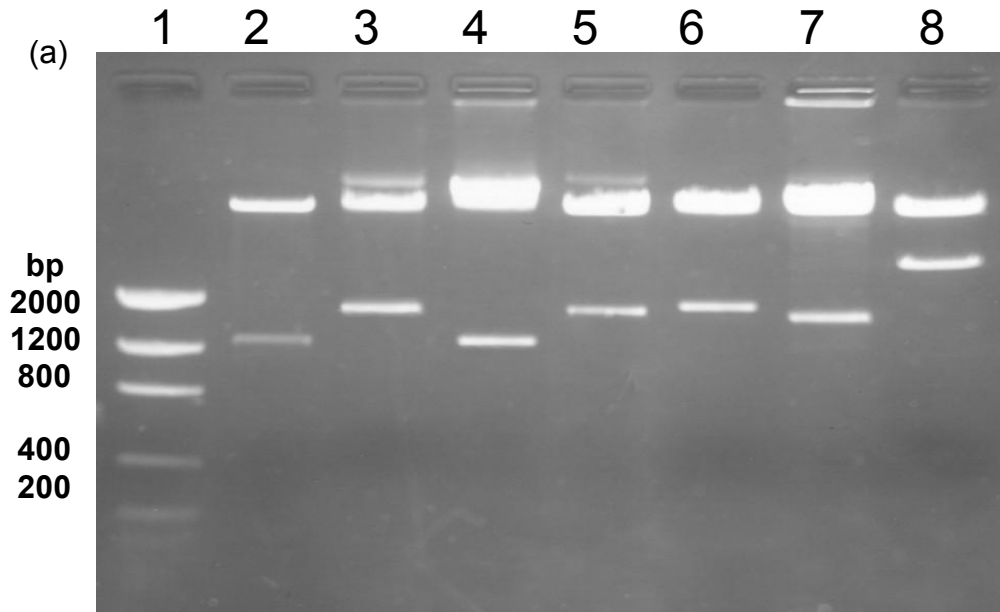
**Figure 2.6** PCR products to determine orientation of *aco2* and *acs* inserts.

In lane 1,  $\phi$ x174/*Hae*III digest markers; lane 2, *aco2* A (3+8); lane 3, *aco2* A (3+9); lane 4, *aco2* A (9+nos); lane 5, *aco2* A (8+nos); lane 6, *aco2* S (3+8); lane 7, *aco2* S (3+9); lane 8, *aco2* S (9+nos); lane 9, *aco2* S (8+nos); lane 10, *acs* A (3+12); lane 11, *acs* A (3+13); lane 12, *acs* A (13+nos); lane 13, *acs* A (12+nos); lane 14, *acs* S (3+12); lane 15, *acs* S (3+13); lane 16, *acs* S (13+nos); lane 17, *acs* S (12+nos).

In Figure 2.6, lanes 2 and 4 show the predicted bands for *aco2* antisense (as shown in Table 2.4). However, bands were also present in lanes 3 and 5. The predicted bands for *aco2* sense for these lanes was 578bp and 465bp and is therefore indistinguishable. It was the same for *aco2* sense, indicating that sequences elsewhere on the plasmid had been amplified non-specifically. This made it impossible to determine the orientation of *aco2* using these primers.

*ACC synthase* sense and antisense orientations are shown in lanes 10-17. *acs* antisense exhibited the band/no band result that was expected with lanes 10 and 12 showing bands of 471bp and 628bp, respectively. Although the *acs* sense primers produced bands similar to *acs* antisense,

primers 3 and 13 and, 12 and nos (lanes 15 and 17) did not. The actual results were not as straight forward as predicted but the insert could only be in one of two orientations. Therefore, these results were used relative to each other to determine that the inserts were in different orientations. Confirmation of orientation was completed with a series of restriction digests.



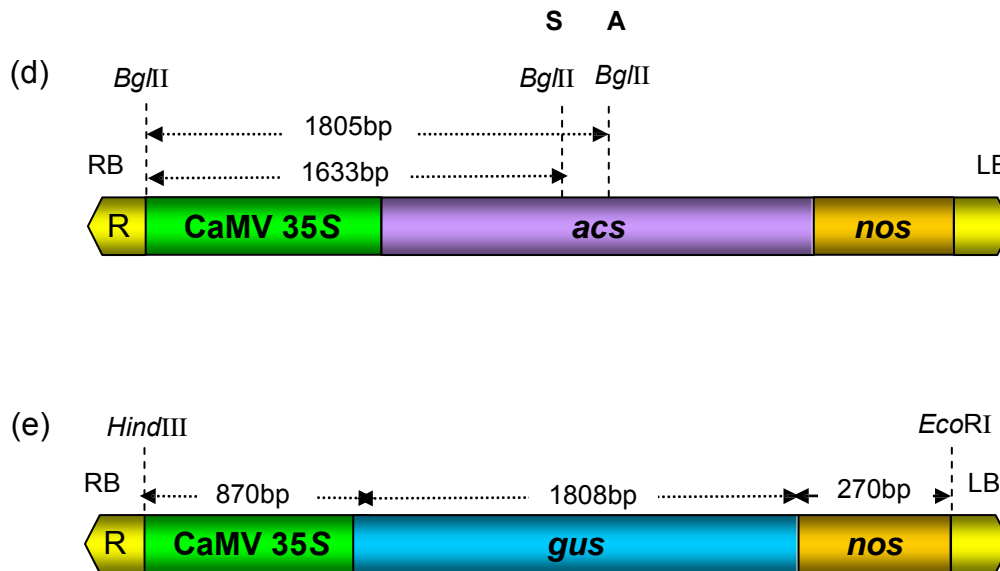


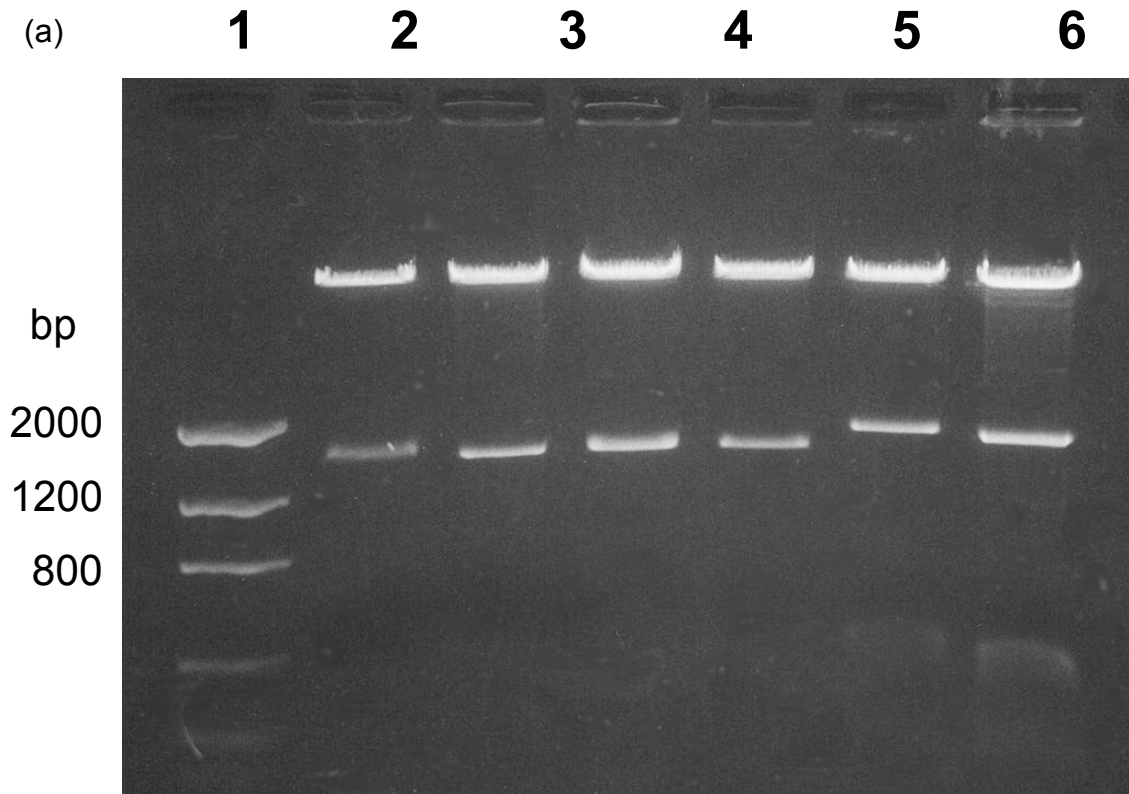
**Figure 2.7** Confirmation of cDNA inserts

(a) Restriction digest to confirm orientation of insert and presence of promoter. In lane 1, DNA Mass Ladder; lane 2, *aco1* antisense *Bgl*II; lane 3, *aco1* sense *Bgl*II; lane 4, *aco2* antisense *Bgl*II; lane 5, *aco2* sense *Bgl*II; lane 6, *acs* antisense *Bgl*II; lane 7, *acs* sense *Bgl*II; lane 8 pJGUS *Eco*RI/*Hind*III. (b,c and d) *aco1*, *aco2* and *acs* constructs depicting the size of band produced from *Bgl*II digests, depending on orientation of the insert. (e) pJGUS construct depicting the *Eco*RI/*Hind*III fragment produced in lane 8. RB=right border, LB=left border, A= antisense, S=sense.

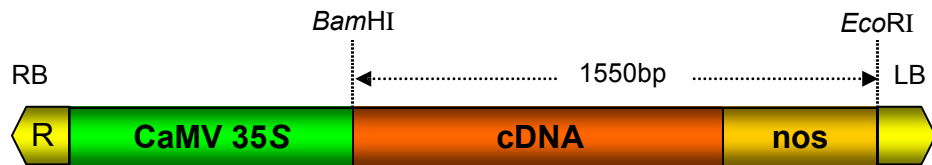
In pJ1.0 there is a single *Bgl*II site within the right border. There are also single *Bgl*II sites in the ACC cDNAs at asymmetrical positions along the DNA. Therefore, if an insert is present, the two sites produce a band size dependent on orientation. For example, in Figure 2.7 (a), lane 2 an *aco1* antisense insert must be present as the 1250bp fragment includes 870bp of the CaMV 35S promoter and 380bp of the *aco1* cDNA. If the insert was in the sense orientation as in lane 3, the band would be 1781bp including 870bp of the CaMV 35S promoter and 910bp of the cDNA. This is diagrammatically shown in Figure 2.7 (b). The same premise was used for *aco2* and *acs*. If *aco2* was in antisense orientation it would produce a band 1281bp (lane 4) and sense 1704bp (lane 5) as shown in Figure 2.7 (c). ACC synthase is slightly different in that the antisense band is larger (1805bp) than the sense

band (1633bp) due to restriction site position. This can be seen in Figure 2.7 (a) lanes 6 and 7 and Figure 2.7 (d). In Figure 2.7 (a) lane 8, the pJGUS control plasmid was digested with *EcoRI/HindIII*. The 2.9Kbp band shown includes the CaMV 35S promoter (870bp), the  $\beta$ -glucuronidase (1808bp) and the *nos* terminator (270bp). This is diagrammatically shown in Figure 2.7 (e). The *BglII* digests in lanes 2-7 also confirm the presence of the CaMV 35S promoter which had been cloned in an earlier step.

Having determined the presence of the CaMV 35S promoter and orientation of the ACC cDNA inserts in Figures 2.4 and 2.7, it seems necessary to confirm the presence of the *nos* terminator. Due to its small size, the *nos* band was expected to show little fluorescence and be difficult to see. However, the cumulative addition of the *nos* terminator to a larger fragment showed its presence. In Figure 2.8 (a), lanes 2-5 show *BamHI/EcoRI* digests for *aco1* and *aco2*. The digest produced 1570bp fragments, which are diagrammatically shown in Figure 2.8 (b). The *EcoRI* site is to the right of the *nos* terminator and the *BamHI* site to the left of the cDNA. The 1300bp cDNA and the 270bp *nos* terminator produce a 1570bp as can be observed in Figure 2.8 (a).



(b) *aco1* and *aco2*



(c) *acs*

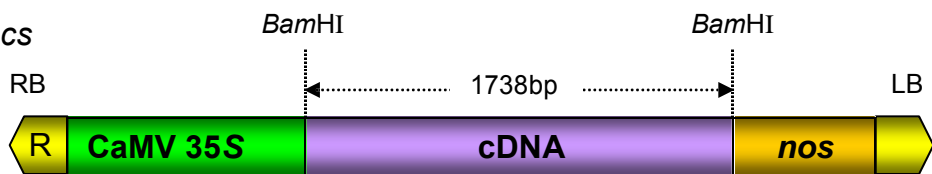


**Figure 2.8** Confirmation of cDNA inserts and *nos* terminator

(a) Restriction digest to confirm presence of insert and *nos* terminator. In lane 1, DNA Mass ladder; lane 2, *aco1* antisense *Bam*HI/*Eco*RI; lane 3, *aco1* sense *Bam*HI/*Eco*RI; lane 4, *aco2* antisense *Bam*HI/*Eco*RI; lane 5, *aco2* sense *Bam*HI/*Eco*RI; lane 6, Syn antisense *Bam*HI; Lane 7, *acs* sense *Bam*HI. (b) Schematic diagram of the fragment size that a *Bam*HI/*Eco*RI

restriction digest of *aco1* and *aco2* constructs would produce. (c) Schematic diagram of the fragment size that a *Bam*HI restriction digestion would produce from an *acs* construct with the insert.

Due to limitations with restriction sites, the *Bam*HI digest of *ACC synthase* in lanes 6 and 7 of Figure 2.8 (a,c) just show the presence of the cDNAs (1700bp) and that both *Bam*HI sites are intact from cloning.

Initially, the T-DNA region of pJ1.0 was sequenced to confirm the presence of the CaMV 35S promoter, *nos* terminator and the left and right borders. The primers used for this process were the oligonucleotides (1 and 2, Table 2.1) designed for the linker. The sequencing was carried out at Birmingham University 'Alta Biosciences'. The forward primer (1) sequenced the whole of the *nos* terminator and left border. The reverse primer (2) sequenced through 700bp of the 870bp CaMV 35S promoter. The sequencing confirmed the presence of the TATA box in the CaMV 35S promoter and the polyadenylation signal (AATAA) in the *nos* terminator. The *ACC* cDNAs *aco1*, *aco2* and *acs* were sequenced with the cloning primers (5, 6, 7, 8, 9 and 10). The insert sequences were aligned with the database sequences for the broccoli *aco1*, *aco2* and *acs* cDNAs by [www.ncbi.nlm.nih.gov/BLAST/](http://www.ncbi.nlm.nih.gov/BLAST/), confirming the results.

## 2.4. Discussion

The *Brassica oleracea* L. var. *italica* ACC oxidases 1 and 2 and ACC synthase cDNAs have been cloned into the minimal T-DNA vector pSCV1.0 between a CaMV 35S promoter and a *nos* terminator. To achieve this, a cloning strategy with a few steps that could be efficiently executed was devised. A backbone vector pJ1.0, was first constructed which could be used universally to clone in independent ACC cDNAs. As there were limitations with restriction sites, the  $\beta$ -glucuronidase (*gus*) gene from pBI121 was removed with *Xba*I and *Sst*I and replaced by a synthetic linker. The synthetic linker contained unique restriction sites in pSCV1.0 that could be used for cloning. The CaMV 35S promoter-linker-*nos* terminator cassette was transferred to the pSCV1.0 multiple cloning site as a *Hind*III/*Eco*RI inverted fragment relative to the left and right borders.

Originally, the ACC oxidase 1 and 2 and ACC synthase cDNAs had been ligated into the *Eco*RI site of pBluescript SK- after attachment of *Not*I adaptors. The *aco1* cDNA had been ligated in sense orientation, whereas the *aco2* and *acs* were in antisense orientation. There was a *Not*I restriction site in pSCV1.0 so it was not possible to use these adaptors for cloning. The cloning steps were also limited by restriction sites within the cDNAs. To circumvent these problems, the cDNAs were amplified by polymerase chain reaction (PCR) that provided ample quantities of DNA to complete the cloning steps and avoid the need for doing minipreps and digests that are labour intensive.

One of the objectives was to provide enough choice of restriction sites to facilitate the use of alternative promoters. Blunt-ended ligation into the

*Sma*I site of pJ1.0 would leave *Hind*III or *Pst*I with *Bam*HI for *aco1* and *aco2* and *Bcl*I with *Bam*HI for *acs*. The efficiency of blunt-ended cloning for *aco1* and *aco2* was about one colony in twenty with the insert. Enough colonies were found using the colony PCR method. Blunt-ended cloning did not work for *ACC synthase* (results not shown). *ACC synthase* is 1734bp, whereas *aco1* and *aco2* are 1237bp and 1233bp, respectively. The extra 500bp made this ligation too inefficient to proceed. The next progression in this strategy was to put *Bam*HI or *Sal*I sticky-ends onto the cDNA by adding extra bases to the cloning primers. The restriction enzyme *Sal*I was not very efficient at cutting pJ1.0. This meant that there were too many colonies which did not have the insert and impossible to find those with an insert. Instead, *Bam*HI ends were added to the cDNA by PCR and ligated to the *Bam*HI site of pJ1.0 at an efficiency of about 2 in 20 colonies. A consequence of this strategy was that unlike *ACC oxidase 1* and *2*, the promoter cannot be changed. However, it was successful in providing sense and antisense *ACC synthase* constructs.

In conclusion, an intermediate pJ1.0 backbone plasmid with the CaMV 35S promoter and *nos* terminator flanking a multiple cloning site has been successfully constructed and used for the cloning of *ACC oxidase 1* and *2* in sense and antisense orientations, *ACC synthase* in sense and antisense orientations, and a *gus* control. These constructs were introduced into *Agrobacterium rhizogenes* strain LBA 9402 for the transformation of *Brassica oleracea* L. var. *italica* to down-regulate genes involved in post-harvest ethylene production and extend the shelf-life of this floral vegetable.

# **3.0 Transformation of GDDH33 with *Agrobacterium rhizogenes***

### 3.1 Introduction

The soil bacteria *Agrobacterium rhizogenes* and *A. tumefaciens* are responsible for the development of hairy root and crown gall disease, respectively (Gelvin, 1990). They are able to insert DNA sequences (T-DNA or transferred DNA) via a natural system of genetic transformation, into the genome of mono- and di-cotyledonous plant cells. The determinants of both hairy root and crown gall disease are extra-chromosomal plasmids termed *Ri* (root inducing) and *Ti* (tumour inducing) harboured by the virulent bacteria (Gelvin, 1990). *Ri*- and *Ti*-plasmids are large (200 to greater than 800kbp) and contain two regions for tumourigenesis, the T-DNA and the *vir* (virulence) regions (Gelvin, 1990). The *vir* region contains genes involved in processing and transferring the T-DNA into the plant cell, and the T-DNA carries genes that induce neoplastic plant growth when expressed within the plant cell nucleus (Gelvin, 1990).

The natural capacity of *Agrobacterium* to genetically transform plant cells has been utilised to produce genetically modified plants in a range of species (Christou 1996). In brassica, *A. rhizogenes* and *A. tumefaciens* are widely used for plant transformation, both having advantages and limitations (reviewed by Poulsen, 1996 and Puddephat *et al.*, 1996). Transformation of *Brassica oleracea* L. var. *italica* with *A. rhizogenes* was easily distinguishable by the emergence of hairy roots (Tempe and Casse-Delbart, 1987). These hairy roots were clonal, arising from single cells (Tempe and Casse-Delbart, 1987), whereas Berthomieu *et al.* (1994) with *A. tumefaciens* produced a high frequency of undesirable chimeric plants. *A. tumefaciens* is often preferred by researchers (see Puddephat *et al.* 1996 for review) as it does not contain the root inducing loci (*rol* genes) on the *Ri* T<sub>L</sub>-DNA of *A. rhizogenes* that causes the hairy root syndrome in plants. This

phenotype typically exhibits wrinkled leaves, shortened internode lengths, non-geotropic roots, reduced apical dominance, altered flower morphology, and reduced seed production (Tepfer, 1990).

Transformation of *Brassica oleracea* with *Agrobacterium rhizogenes* and *tumefaciens* is achieved by inoculating explants in tissue culture (Poulsen, 1996). The inoculated cut plant surface stimulates the proliferation of untransformed adventitious roots, and these are phenotypically similar to transgenic 'hairy-roots'. It is important that the transgenic roots are distinguished from the adventitious roots, if they are to be isolated. Distinguishing between adventitious and *A. rhizogenes* transformed roots has been limited by poor selection efficiency achieved with antibiotic resistance genes (Hosoki and Kigo, 1994) whose presence also leads to abnormalities that are regarded as disadvantageous (Earle *et al.*, 1996). A standard approach is to use reporter genes that allow the visual detection of transgene expression without any need for a selectable marker. The *E. coli* derived  $\beta$ -glucuronidase gene (*gus*) (Jefferson *et al.*, 1987) is one of the most extensively used visual markers. It hydrolyses a wide variety of  $\beta$ -glucuronides that release bromo-chloro-indolyl compounds, staining the tissue blue. GUS is very stable, but the histochemical assay is destructive. The firefly luciferase enzyme, encoded by the *luc* gene, can be monitored *in vitro* (Ow *et al.*, 1986) but requires an exogenous substrate (luciferin) and emits light only at very low intensity (Ow *et al.*, 1986). The green fluorescent protein (GFP) from the jellyfish *Aequorea victoria* requires no exogenous substrate and emits visible light when excited by blue or UV light (Prasher, 1995). The use of the green fluorescent protein to detect transformed tissue has been reported (Molinier *et al.*, 2000; Blumenhal *et al.*, 1999 and Sheen *et al.*, 1995) to be a rapid, non-invasive

technique. The *gfp* gene has been incorporated into the T<sub>L</sub>-DNA of the virulence plasmid of *A. rhizogenes* strain LBA 9402 to produce the co-integrate vector pRi1855::GFP (see Figure 3.1).

The co-integrate strain possesses the *Ri* T<sub>L</sub>-DNA encoding genes necessary to produce transgenic hairy roots and the binary vector T-DNA carrying the genes of interest to be co-transferred during the transformation process. Co-transformation involves the stable integration of two species of T-DNA into the plant genome, achieved with high efficiency (>50%) by Christey and Sinclair (1992); Hosoki and Kigo (1994) and Puddephat *et al.* (2001) with vegetable brassica plants. Co-transformation efficiency has proven to be greater with co-integrate vectors (Fry *et al.*, 1987; Charest *et al.*, 1988) compared to binary vectors when the T-DNAs are located on separate plasmids. If the two T-DNA sequences integrate into the plant genome at physically unlinked loci it is possible to segregate the *Ri* T<sub>L</sub>-DNA from the gene of interest T-DNA. The *Ri* T<sub>L</sub>-DNA causes the 'hairy root' syndrome in plants, so it is important that it is segregated out. This may be achieved by either sexual crossing, self-pollinating or through microspore culture. Segregation frequencies of greater than 50% with one strain and two plasmids have been demonstrated by Daley *et al.* (1998) and Komari *et al.* (1996), with an *A. tumefaciens* protocol. More recently Puddephat *et al.* (2001) has produced transgenic marker-free brassica plants with an *A. rhizogenes* protocol.

The *Brassica oleracea* L. var. *italica* ACC oxidases 1 and 2 and ACC synthase cDNAs (Pogson *et al.*, 1995) and *gus* gene (Jefferson *et al.*, 1987) have been cloned into the minimal T-DNA vector pSCV1.0 (Biogemma) between a cauliflower mosaic virus (CaMV) 35S promoter and a nopaline synthase (*nos*)

terminator (chapter 2). They have been transferred into the *A. rhizogenes* co-integrate strain LBA 9402 pRi1855::GFP by electroporation (chapter 2).

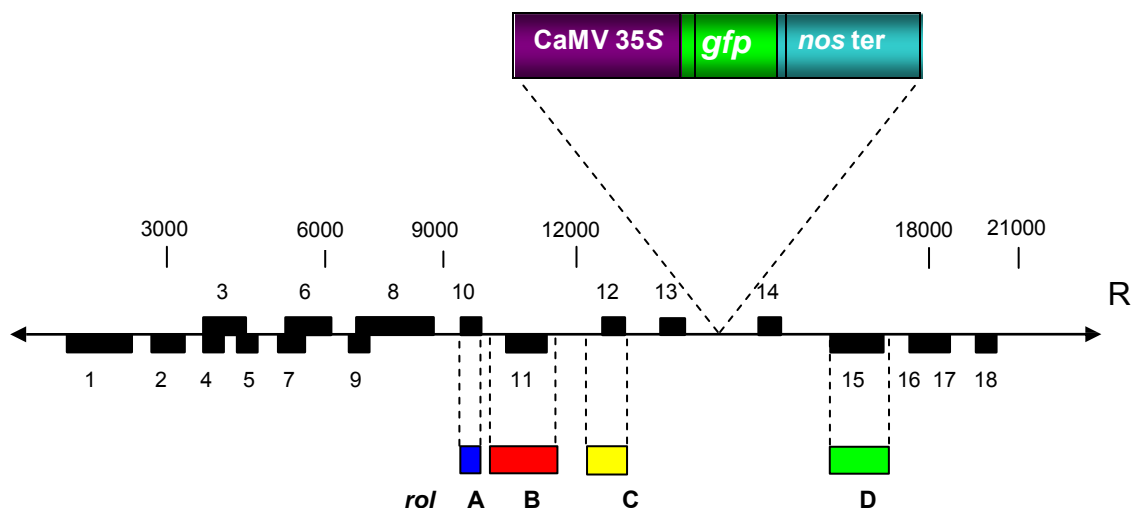


**Figure 3.1** The T<sub>L</sub>-DNA of the agropine *Ri* plasmid pRi1855::GFP.

It represents the relative location of each open reading frame (1-18) (Slightom *et al.*, 1985) and the insertion of the CaMV 35S-*gfp*-*nos* construct by homologous recombination (Ian Puddephat pers. comm. HRI-Wellesbourne). Recombination was achieved by amplifying E36 (a sequence between 13 and 14) by PCR and ligating into pBR322 with the pBIN m-*gfp*5-ER construct. Homology between E36 and the virulent plasmid facilitated recombination. The polarity of each ORF is given by the position of the solid boxes: boxes above the line indicate transcripts running left to right, and boxes below the line indicate transcripts running right to left.

GDDH33 is a doubled-haploid line derived from the calabrese cultivar Green Duke through anther culture. It has a homozygous genetic background, and is amenable to transformation and regeneration through *Agrobacterium rhizogenes* (H. Robinson, pers. comm. HRI-Wellesbourne) and is responsive to microspore culture (L. Harvey, pers. comm. HRI-Wellesbourne). It is therefore a suitable genotype for transformation and regeneration in these experiments.

The aim of this part of the project was to transform GDDH33 with *A. rhizogenes* co-integrate strain LBA 9402 pRi1855::GFP harbouring the binary vectors carrying the ACC constructs and *gus* reporter gene (Jefferson *et al.*, 1987) on the binary vector T-DNA. The target was to produce 20 independently transformed root clones for each construct and then if possible, to regenerate transgenic plants through tissue culture that could be tested for post-harvest production of ethylene, and chlorophyll levels. If the T-DNAs from the transformation events were physically unlinked, it would be possible to segregate the two sequences when the T<sub>0</sub> plants were self-pollinated to produce marker-free plants.

## 3.2 Materials and Methods

### 3.2.1 Plant material and culture conditions

Seeds from the *Brassica oleracea* L. var. *italica* doubled-haploid line GDDH33 were used in transformation experiments. They were surface sterilised by immersion in 1.7 % (w/v) sodium dichloroisocyanurate (BDH, UK) for 6 minutes followed by two rinses in sterile (purified) water. Seeds were then germinated for three days on moist filter paper in 9 cm Petri-dishes incubated at 22°C with 16 h light with a mix of 70 W white and 65/80 W gro-lux fluorescent tubes providing an irradiance of 80  $\mu\text{mol m}^{-2} \text{s}^{-1}$  at the culture level.

### 3.2.2 Plant transformation

The *Agrobacterium rhizogenes* co-integrate strain LBA 9402 pRi1855::GFP (Spano *et al.*, 1982, Puddephat *et al.*, 2001) was used. The root inducing plasmid pRi1855 carries the *gfp* reporter gene driven by the CaMV 35S promoter (see Figure 3.1). Seven binary plasmids were introduced into separate bacterial clones by electroporation (Mattanovich *et al.*, 1989). These binary plasmids were constructed from pSCV1.0, a minimal T-DNA vector (Biogemma) with the CaMV 35S promoter (Guilley *et al.*, 1982) and *nos* terminator derived from pBI121 (Bevan, 1984; Jefferson *et al.*, 1987) (chapter 2). cDNAs of aminocyclopropane carboxylic acid synthase and oxidase 1 and 2, isolated from *Brassica oleracea* by Pogson *et al.* (1995) had previously been ligated (chapter 2) between the promoter and terminator in both sense and antisense orientations, in relation to the promoter. The  $\beta$ -glucuronidase gene (*gus*) from Jefferson *et al.* (1987) had also been ligated into the pSCV1.0 T-DNA region. Prior to plant transformation experiments, LBA 9402 was sub-cultured on semi-solid YMB medium (see appendix). It was supplemented with

50 mg/l tetracyclin, 100 mg/l rifampicin and 50 mg/l kanamycin for selection of the cointegrate *Ri* plasmid, chromosomal DNA and binary plasmid, respectively and incubated at 25°C overnight.

From the overnight culture, three-four 10 $\mu$ l loops of *Agrobacterium* were used to inoculate 10 ml of MGL broth (see appendix). Broths were incubated for 16 hours at 25°C on a shaking platform (135-180g). *Agrobacterium* cells were pelleted by centrifugation at 11600g for 5 minutes. Cells were resuspended in liquid MS30 (see appendix) and supplemented with 1 mg/l 2,4-D to produce an optical density ( $A_{600nm}$ ) of 1.0 (+/- 0.1).

Explants for use in transformation experiments were excised from six-day-old seedlings, grown under aseptic conditions, by cutting the hypocotyl approximately 5 mm below the cotyledonary petioles. Explants were inverted and placed on 6ml MS30 medium supplemented with 200mg/l cefotaxime in 5cm deep-form Petri-dishes, with two explants per dish. A 2 $\mu$ l drop of re-suspended *Agrobacterium* was placed on the cut surface of the hypocotyl.

The general components of the experimental set-up involved preparing the *Agrobacterium*, excising the explants, inoculating the cut surface and labelling the Petri-dishes. This order varied in two different experimental approaches. In the first set of experiments (16), all of the explants were excised and then placed onto the medium before being inoculated. In the later experiments (5), batches of 50 explants were excised, placed onto the medium and then inoculated. Inoculated explants were incubated as previously described for germinating seedlings.

### 3.2.3 Identification of transformed 'hairy roots'

Transgenic root production was determined 21-35 days after inoculation. Explants were illuminated under long wave UV radiation (UVP BLAK-RAY lamp, model B-100 AP) to detect GFP fluorescence in roots. The numbers of explants producing excisable GFP roots (>1cm from root tip) were counted. For selected GFP fluorescent roots, root tip sections were excised and cultured on MS30 supplemented with 0.2mg/l naphthalene acetic acid (NAA) and 200mg/l cefotaxime to establish transgenic root clones. Root clones were transferred to fresh culture medium at 3-5 week intervals and cultured at 25°C in the dark.

### 3.2.4 GUS detection

Histochemical assays for the detection of  $\beta$ -glucuronidase activity were performed using buffers from Jefferson *et al.* (1987) (see appendix) on 2cm excised root tip sections.

### 3.2.5 PCR

A PCR protocol was designed to confirm the presence of T-DNAs in root clones. Under aseptic conditions, a root section (1cm from the growing tip) was excised by using fine forceps and placed onto a layer of Nescofilm (Osaka, Japan). A sterile cocktail stick was used to remove just the growing tip and 5mm root, which was placed into a 0.5ml microfuge tube with 50 $\mu$ l water. The tube was then heated at 99°C for 3 minutes, placed on ice for two minutes and then microfuged for 30 seconds at 11600g. Five microlitres of the supernatant was taken for each PCR.

Primers were designed (see Table 3.1) to produce fragments from: promoter/terminator of the *aco* and *acs* cDNAs, and internal primers on the *gus* gene to confirm insertion of the genes of interest in plant tissue; the *gfp* gene to detect the *Ri* plasmid; and the *Virulence (vir)* region on the *Ri* plasmid which is not transferred, to determine whether amplification is due to *Agrobacterium* contamination in the sample. The *aco1* and *aco2* primers were designed to amplify the 250bp 3' untranslated regions of the cDNA that share only 44% nucleotide identity, to be used as probes. The *acs* F and R primers amplify the whole cDNA region of *ACC synthase* to be used as a probe.

**Table 3.1** Oligonucleotide sequences used as primers for the verification of T-DNA insertion and making DNA probes for hybridisation.

Names	Primer sequence (5' - 3')*	$T_m$ (°C) <sup>(a)</sup>
3	ACG TTC CAA CCA CGT CTT CA	60
4	AGC TTC ATC GCT TGC CTG TA	60
5	CTT CTC GAC GTT GTC CAT CA	60
8	CCA CAG TCG AGA CGT TCT AA	60
9	TTC ATG GCC GCT CGG TAT TC	62
12	AGA AGT GTT GGC AGA GTA GC	60
13	CTT CGC TAC AGC TTG TCT GA	60
<i>nos</i> R	CCG ATC TAG TAA CAT AGA TGA CAC	61
<i>vir</i> F	ATG TCG CAA GGA CGT AAG CCG A	65
<i>vir</i> R	GGA GTC TTT CAG CAT GGA GCA A	63
<i>gus</i> F	GCG TGG TGA TGT GGA GTA TT	60
<i>gus</i> R	ACG CGG TGA TAC ATA TCC AG	60
<i>gfp</i> F	GGC CAA CAG TTG TCA CTA CT	60
<i>gfp</i> R	AAG AAG GAC CAT GTG GTC TC	60
<i>aco1</i> 3'UTR F	GAA GAA TTC TAA TGC AGT TAC AG	57
<i>aco1</i> 3'UTR R	CGC AAG CTT AGA ACA GTT ATC ATA	59
<i>aco2</i> 3'UTR F	GAA GAA TTC TGC AGC AAC CAC GGA TTT G	66
<i>aco2</i> 3'UTR R	GCG GAA GCT TTA AAA TTC ATA TTT CCA ATA C	62
<i>acs</i> cDNA F	AAT AAC GAT TAG AGA AAT TAT GGT	54
<i>acs</i> cDNA R	ATC TCA ACA GAA CAA AAA CAA AC	56

\*Primers designed in relation to the inserts being in sense orientation to the promoter.

(a)  $T_m$  of the primers was calculated with the expression:

$$T_m = 81.5 + -16.6 + (41 \times (\#G + \#C/\text{length})) - (500/\text{length})$$

**Table 3.2** PCR reaction components.

To make a total 25 $\mu$ l for each reaction, 5 $\mu$ l of template DNA (100 $\mu$ mol/ $\mu$ l) and 5 $\mu$ l of primers (set at 4 $\mu$ mol/ $\mu$ l) were added. Primers and template DNA were suspended in autoclaved R.O water.

	x1 ( $\mu$ l)
10x Buffer	2.5
dNTPs (25mM)	0.2
H <sub>2</sub> O	12.37
BRL <i>Taq</i>	0.13
<b>Total</b>	<b>25</b>

**Table 3.3** PCR program

The annealing temperature was adjusted to 3°C below the  $T_m$  of the primer pairs. This was performed on a Hybaid Omnigene PCR machine. Stage 1 and 3 were cycled once. Stage 2 was cycled thirty five times.

<b>Stage 1.</b>	1) 93°C/ 2 min	2) 53°C/ 1 min	
<b>Stage 2.</b>	1) 72°C/ 1 min	2) 93°C/ 30 sec	3) 53°C/ 1 min
<b>Stage 3.</b>	1) 72°C/ 10min.		

All oligonucleotides were synthesised by MWG-Biotech (MWG-BIOTECH AG Anzinger Str.7 D-85560 Ebersberg) (Table 3.1) and used in standard PCR conditions (Tables 3.2 and 3.3). PCR components including *Taq* polymerase, PCR buffer and dNTPs were obtained from GIBCO-Life Technologies, Uxbridge, UK.

### *3.2.6 Shoot Regeneration from established root clones selected by GFP fluorescence*

Six root explants with 15-20mm sections were excised from established root clones and cultured on MS30 medium, supplemented with 5mg/l NAA and 5mg/l benzylaminopurine (BA), and solidified with 6g/l agar in 5cm Petri-dishes. Cultures were incubated as previously described and root explants producing callus transferred to fresh regeneration medium at three-week intervals. Calli forming shoot initials were transferred to Gamborg's B5 medium (see appendix) with 20g/l sucrose supplemented with 0.3mg/l Indole-3-propionic acid (IPA) for shoot elongation. Single differentiated shoots with roots were transferred to 40ml of regulator-free, MS30 medium in magenta tubs (Sigma-Aldrich, Poole, Dorset, UK). All cultures were incubated as previously described, for 3 weeks. The rooted shoots were transferred to non-sterile compost (a 80:20 mix of Levington M2 and vermiculite) in 5cm modules. They were maintained in humidified plant propagators up to 7 days, progressively reducing the humidity before being transferred to 15cm pots. They were grown in glasshouse conditions set to maintain 22°C air conditioning with daylight extension to a minimum 14 hours photoperiod provided by high pressure sodium lamps.

### *3.2.7 DNA extraction*

Two grams (fresh weight) of the youngest leaves from post-headed transgenic and non-transgenic broccoli was immediately frozen in liquid nitrogen, before being freeze-dried at -80°C. The freeze-dried leaf material was ground into a fine powder with a mortar and pestle, and 0.5g was

transferred to a 50ml polypropylene centrifuge tube. To this 15ml Kirby mix (1% w/v sodium tri-isopropylphenyl sulphonate; 6% w/v sodium 4-amino salicylate; 2.5%v/v 2M Tris-HCl pH8 and 13.5ml R.O H<sub>2</sub>O) was mixed and shaken gently for 30min. 10ml phenol/chloroform was then added and shaken gently for 5min, before being centrifuged at 2677g for 10min at room temperature. The upper phase was removed and placed into a fresh 50ml tube with 0.1 volumes of 3M sodium acetate pH 6.0 and 0.6 volumes of propan-2-ol, and left for an hour. The tubes were then centrifuged at 2677g for 10min. Following this, the supernatant was poured off and the pellets were allowed to air dry for 30min. The pellets were resuspended in 2ml TE and 40µg/ml RNase and incubated at 37°C for 1 hour. They were then transferred to a 15ml polypropylene tube and mixed with 2ml phenol/chloroform for 5min. Following this, the tubes were centrifuged at 2677g for 10min. The upper phases were then transferred to fresh tubes and precipitated with 0.1 volumes of 3M sodium acetate pH 6.0 and 0.6 volumes of propan-2-ol, and left overnight. After precipitation, the tubes were centrifuged at 2677g for 10min, the supernatant poured off and pellet left to air dry for 1 hour. The pellets were resuspended in 120µl TE and left at room temperature for 1 hour.

### 3.2.8 *Endonuclease restriction digest of genomic DNA*

The genomic DNA was quantified on a 1% (w/v) agarose gel and ranged from 200ng/µl in the non-transformed control to 20ng/µl for 5/00 GUS 1. The restriction endonuclease *Sst*I was chosen as the constructs contain a single site between the cDNA and *nos* terminator. The digest comprised of 40µl genomic DNA; 20µl, reaction 2 buffer; 5µl *Sst*I enzyme; 10µl (10mg/ml)

spermidine; and 125 $\mu$ l H<sub>2</sub>O to make a final volume of 200 $\mu$ l. The reaction was left overnight at 37°C. The digestion components were then mixed with 200 $\mu$ l phenol, centrifuged at 11600g for 15sec and the aqueous phase removed. To this, 100 $\mu$ l phenol and 100 $\mu$ l chloroform were mixed and centrifuged as above. The aqueous phase was removed and mixed with 200 $\mu$ l phenol, centrifuged as above and the aqueous phase removed. This was placed in a 0.5ml microfuge tube with 600 $\mu$ l 100% ethanol and 100mM sodium acetate. The tubes were left for 1 hour, then centrifuged at 11600g for 30min. The pellet was air dried for 5 min and resuspended in 15 $\mu$ l H<sub>2</sub>O.

### 3.2.9 Southern Blot

Two 0.8% (w/v) agarose gels were poured and then loaded with the digestion products. The first gel was loaded in lanes 1-14 with: *Hind*III lambda ladder (GIBCO-Life Technologies); non-transformed GDDH33; 28/00 *aco1A* 3; 34/00 *aco1A* 1; 34/00 *aco1A* 4; 32/00 *aco1S* 3; 33/00 *aco1S* 4; 3/00 *aco2A* 2; 33/00 *aco2A* 3; 5/00 *aco2* S; 26/00 *aco2* S 1; 20ng pBIN m-*gfp5*-ER *Bcl*I digest; 20ng *aco2* construct *Bcl*I digest; *aco1* construct *Bcl*I digest. The second gel was loaded in lanes 1-13 with: *Hind*III lambda ladder (GIBCO-Life Technologies); non-transformed GDDH33; 7/00 *acsA* 12; 7/00 *acsA* 13; 9/00 *acsA* 1; 9/00 *acsA* 2; 7/00 *acsS* 7; 5/00 *gus* 1; 33/00 *gus* 3; 34/00 *gus* 2; 20ng pBIN m-*gfp5*-ER *Bcl*I digest; 20ng *gus* construct *Bcl*I digest; 20ng *acs* construct *Bcl*I digest. The gels were ran at 50 volts for 18h. They were stained in 0.33 $\mu$ g/ $\mu$ l ethidium bromide, photographed, and then de-stained in R.O water.

The blotting was performed by alkaline transfer onto Hybond N+ filters (Amersham) according to Sambrook *et al.* (1989).

### 3.2.10 Hybridisation between N+ filters and $\alpha^{32}\text{P}$ dCTP labelled DNA probes

The Hybond N+ filters were placed onto nylon mesh that had been wetted in 2x SSC (saline sodium citrate) wrapped tightly and placed in a Hybaid hybridisation bottle. Fifty millilitres of hybridisation buffer (0.5M Na phosphate pH 7.2; 70g/l sodium dodecyl sulphate [SDS]; 10mM EDTA, pH 8.0 and; 100 $\mu\text{g/ml}$  single stranded salmon sperm DNA) was added to the tubes at 65°C. The tubes were placed in a Hybaid rotisserie oven at 65°C and left to pre-hybridise for 3h. DNA probes were produced by PCR for regions of the *gus*, *gfp*, *aco1*, *aco2* and *acs* genes with primers shown in Table 3.1. The DNA probes were labelled with  $\alpha^{32}\text{P}$  dCTP according to the Rediprime II random prime labelling system kit (Amersham Pharmacia Biotech, Bucks. UK). The labelled DNA was separated from the other components by a sepharose column and counted with a scintillation counter. The 50mls of hybridisation buffer were replaced with 10mls fresh buffer, and 2 x 10<sup>7</sup> counts per minute labelled probe and left overnight at 65°C. The blots were washed at medium stringency with 2 x SSC and 1% SDS four times at 65°C. The filters were wrapped in Saranwrap (Dow Chemicals) and placed into x-ray cassettes with XAR5 film (Kodak) under a safelight. The cassettes were placed at -80°C for 2 nights, and then the film was developed.

### 3.2.11 Seeds

Seeds were obtained from T<sub>0</sub> plants by Linda Doyle at Horticulture Research International, Wellesbourne, containment glasshouses by selfing. Pollinations were carried out by hand at the unopened bud stage after isolation of inflorescences in cellophane bags, and seeds were harvested at maturity.

### 3.2.12 Statistical Analysis

Dr J. Lynn at Horticulture Research International, Wellesbourne, carried out the binomial regression analysis for the transformation results. Students T-Test was also used to compare sample means.

### 3.3 Results

#### 3.3.1 Constructs

The aim was to produce 20 independently-transformed GDDH33 root lines for each construct. The number of inoculations was therefore dependent on transformation efficiency. In total, 6566 GDDH33 seeds were chitted of which 4599 (72.1%) germinated and were inoculated with *A. rhizogenes* LBA 9402 pRi1855::GFP strain, harbouring the binary plasmids carrying the constructs. From 4599 inoculated explants, 150 produced GFP-fluorescent excisable roots, giving an overall transformation efficiency of  $3.63\% \pm 0.56$  (Table 3.4). Transformation efficiency of the *ACC synthase* antisense construct was significantly greater  $t(df) = 3.64(40)$ ,  $p < 0.001$ .

**Table 3.4** Transformation efficiency of LBA 9402 pRi1855::GFP carrying binary plasmids with the *B. oleracea* var. *italica* ACC cDNA constructs on GDDH33.

Construct	No. Inoculations	gfp <sup>+</sup> Roots	Efficiency (%)
<i>aco1A</i>	679	18	2.65
<i>aco1S</i>	685	18	2.63
<i>aco2A</i>	826	25	3.03
<i>aco2S</i>	622	20	3.22
<i>acsA</i>	294	21	7.14
<i>acsS</i>	474	18	3.80
<i>gus</i>	1019	30	2.94
<b>Total</b>	<b>4599</b>	<b>150</b>	<b>3.63 ± 0.56</b>

*aco1* = ACC oxidase 1; *aco2* = ACC oxidase 2; *acs* = ACC synthase; *gus* =  $\beta$ -glucuronidase. Suffix, A = antisense, S = sense

### 3.3.2 Inoculation treatment

The inoculation of explants with *A. rhizogenes* was divided into two separate treatments. In the first treatment, all of the explants were excised before inoculation and, in the second, batches of 50 explants were excised before inoculation. The second treatment produced significantly more explants with excisable GFP<sup>+ve</sup> roots than the first treatment  $t(df) = 6.33(39)$ ,  $p < 0.001$ . Individually, transformation efficiency was improved for all constructs in treatment 2, except *ACC synthase* sense which was non-significantly reduced  $t(df) = 0.07(39)$ ,  $p > 0.001$  (Figure 3.2). There was no treatment two for *ACC synthase* antisense as enough roots had been obtained in treatment one. The greatest difference occurred between treatments for the *gus* construct where transformation efficiency increased from 1.14-11.70%. This ten-fold increase in transformation efficiency in treatment two was not observed with the ACC constructs. It is assumed that the ACC constructs were having a negative impact on transformation efficiency. Thus, manipulation of *ACC oxidase* and ethylene biosynthesis appeared to have an influence on transformation efficiency.

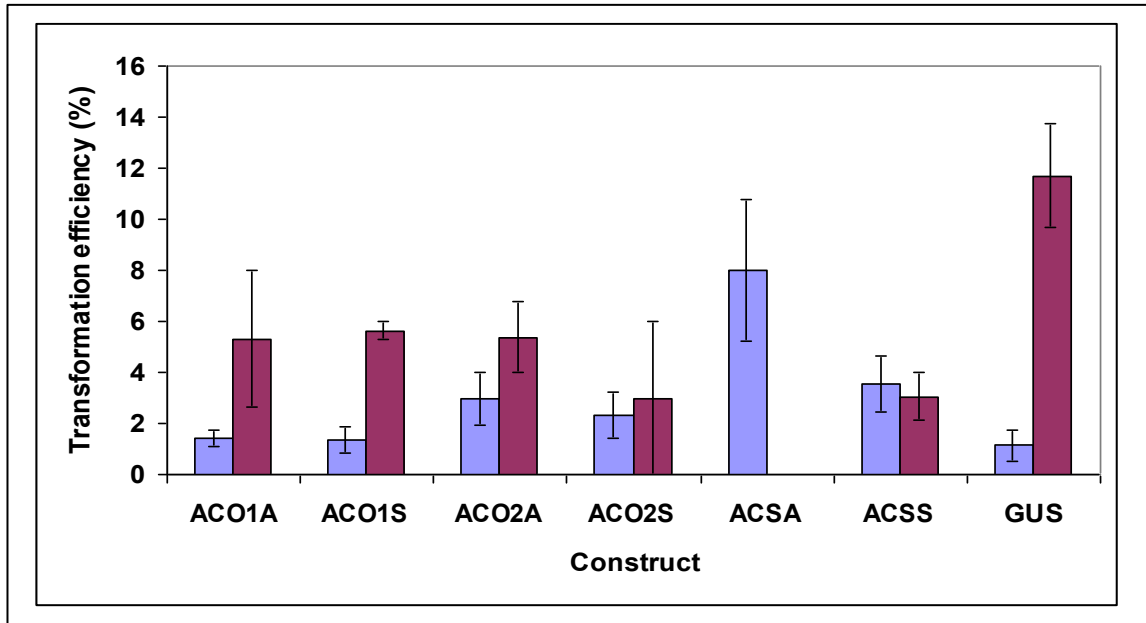


**Figure 3.2** The effect of treatment on construct transformation efficiency. The transformation efficiency of treatment 1 is shown by the blue bars and treatment 2, by the maroon bars. *aco1* = ACC oxidase 1; *aco2* = ACC oxidase 2; *acs* = ACC synthase; *gus* =  $\beta$ -glucuronidase. Suffix, A = antisense, S = sense

### 3.3.3 *gfp* reporter gene

The green fluorescent protein (GFP) was a very effective reporter of transgene expression in roots. Strong visual fluorescence was achieved simply by holding the root sample under the long-wave UV lamp (Figure 3.3) for 1-2 seconds. It was easy to distinguish between the bright 'lime-green fluorescing' GFP-expressing roots and the non-fluorescing roots that had not been transformed. This facilitated the removal and culture of only transgenic roots.

### 3.3.4 Co-transformation

The efficiency of co-integral insertion of the root-inducing T<sub>L</sub>-DNA and the T-DNA from the binary vectors was assessed using the *gus* construct. Transgenic hairy roots expressing the *gfp* reporter gene inoculated with *A. rhizogenes* carrying the *gus* construct were analysed histochemically for β-glucuronidase activity (Figure 3.4). Twenty-three out of twenty-seven roots tested showed GUS activity. All of these roots were tested by PCR for confirmation of the T-DNA inserts. The PCR demonstrated that all roots contained *gfp* inserts, and only one had no evidence for *gus* gene insertion. Therefore, only one from twenty-seven proved negative for the *gus* gene, and positive for *gfp* resulting in a 96% co-transformation efficiency.

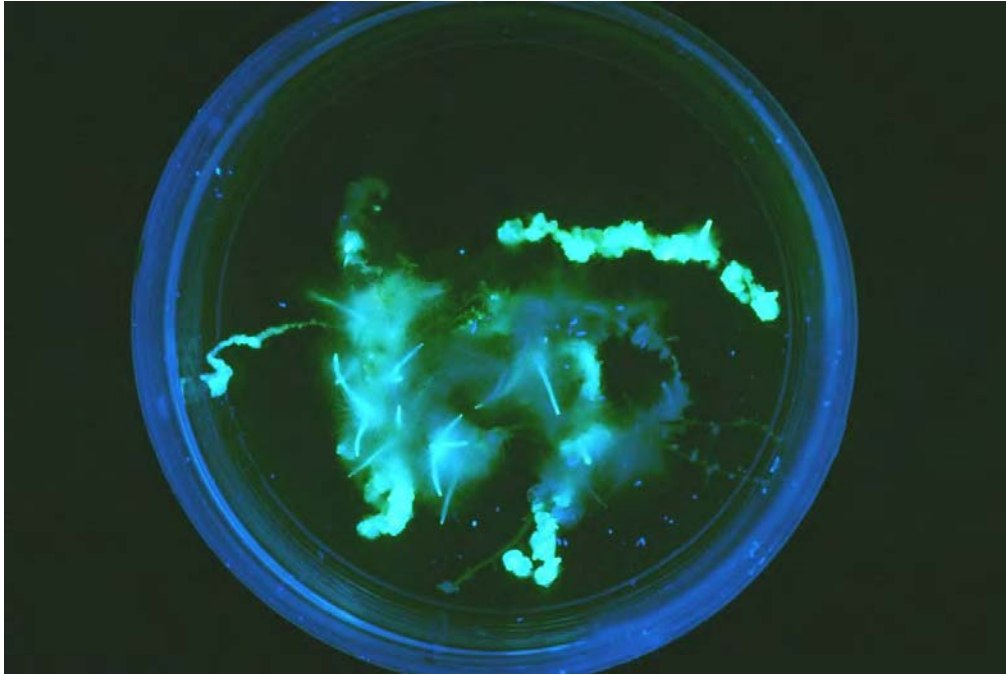


**Figure 3.3** Nine-week-old GFP fluorescing root/callus. The tissue was grown on MS30 supplemented with 5mg/l NAA and 5mg/l benzylaminopurine (BA), and solidified with 6g/l agar in 5cm Petri-dishes.



**Figure 3.4** Six-week-old GUS positive co-transformed root. The root was taken from the transformation event 32/00 6 (6<sup>th</sup> root from 32<sup>nd</sup> experiment in year 2000). It was grown on MS30 supplemented with 0.2mg/l naphthalene acetic acid (NAA) and 200mg/l cefotaxime. The 2cm excised root was incubated with buffers from Jefferson *et al.* (1987).

### 3.3.5 Regeneration

All lines producing shoots in tissue culture regenerated at least one whole plant in the glasshouse and the 18 regenerated lines produced a total number of 195 plants (Table 3.5). The sense constructs produced fewer lines (5) than the antisense (10), which was most clearly observed with the *ACC synthase* sense (1) and antisense (4). The regeneration of shoots from transgenic roots was a major limiting factor for producing transgenic plants. The overall efficiency of explants inoculated to the production of transgenic plants shows a mean of one explant in 200 (Table 3.5 and see Table 3.4 for transformations), outlining the difficulty of the whole tissue culture process.

**Table 3.5** Transgenic lines regenerated into whole plants

<b>Construct</b>	<b>No. lines producing shoots</b>	<b>Efficiency of root lines producing shoots (%)</b>	<b>Efficiency of lines producing shoots from inoculations (%)</b>
<b><i>aco1A</i></b>	3	16.67	0.44
<b><i>aco1S</i></b>	2	11.11	0.29
<b><i>aco2A</i></b>	3	12	0.36
<b><i>aco2S</i></b>	2	10	0.32
<b><i>acsA</i></b>	4	19.05	1.36
<b><i>acsS</i></b>	1	5.56	0.21
<b><i>gus</i></b>	3	10	0.29
<b>Total</b>	<b>18</b>	<b>12.05 ± 1.70</b>	<b>0.47 ± 0.15</b>

*aco1* = *ACC oxidase 1*; *aco2* = *ACC oxidase 2*; *acs* = *ACC synthase*; *gus* =  $\beta$ -*glucuronidase*. Suffix, A = antisense, S = sense

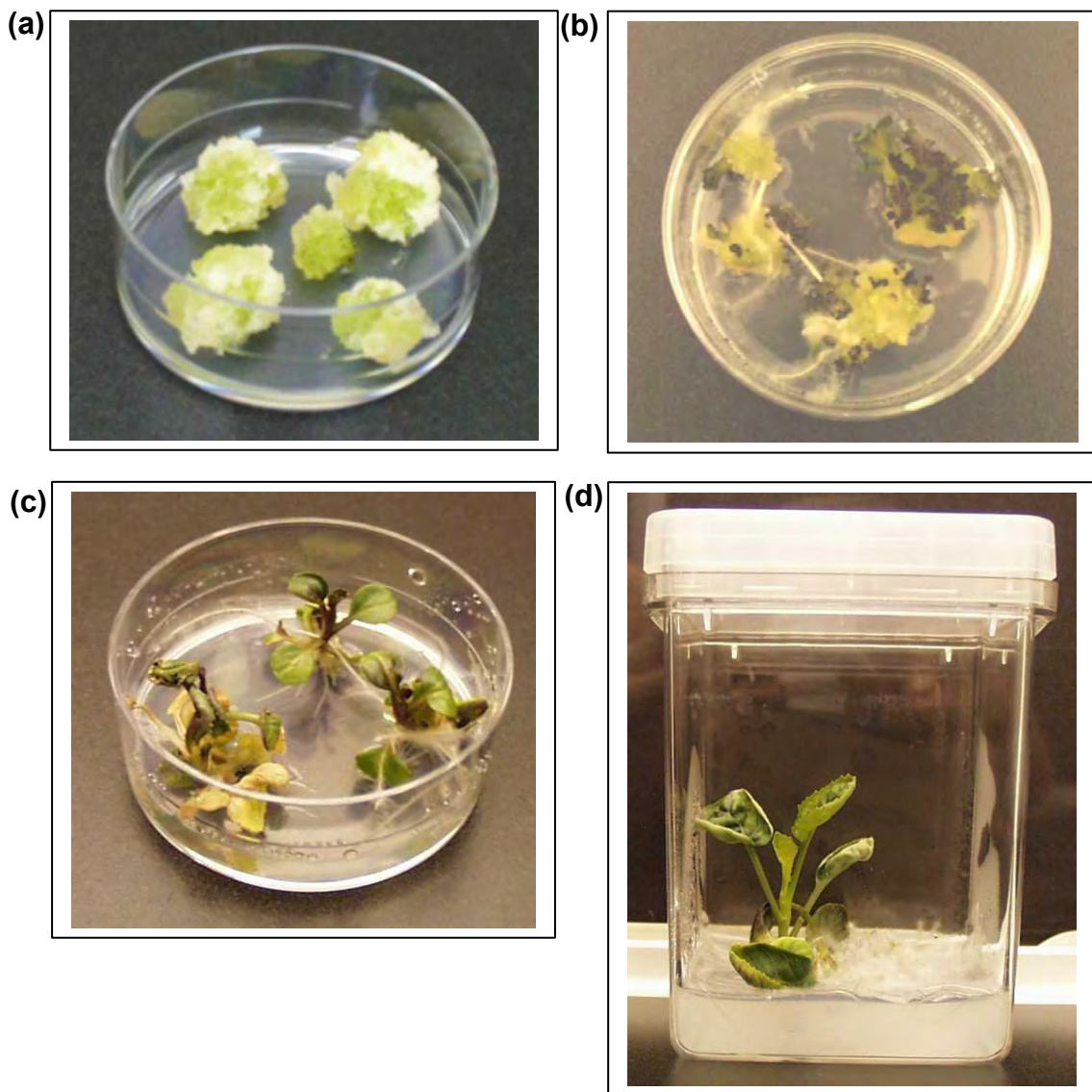


**Figure 3.5** The morphogenesis from root callus to plantlet. (a) Root callus; (b) Root callus producing shoots; (c) Single shoots from root callus (d) Small plantlet. Tissue in (a)-(c) is growing in 5cm Petri-dishes, and (d) in a magenta tub.

Root sections were placed onto a regeneration medium leading to a visible swelling and yellow colouration after 3 weeks. Root production was generally inhibited on this medium although it was not uncommon to have a root/callus tissue as shown in Figures 3.3 and 3.5(b). Tissue morphogenesis proceeded 6-12 weeks with further expansion and the production of chlorophyll pigments as shown in Figure 3.5(a). All of the root lines progressed into this callus phase but most deteriorated into brown, necrotic tissue after 12 weeks on the shoot inducing

medium. Only tissue from 18 out of 150 lines reached the next stage (Figure 3.5b) where calli produced anthocyanin pigments and developed into small shoots. Once the single shoots had been defined (3-6 weeks), they were transferred to a shoot elongation medium containing IPA (0.3mg/l) to develop and produce roots (Figure 3.5c). It was important to establish a root system on this medium, as not all of the lines were able to produce roots on hormone-free medium. Once the root systems had been established, the rooted shoots were transferred to hormone-free MS30 (Figure 3.5d), and grown for 6-9 weeks within magenta tubs. They were transplanted into trays containing compost in the glasshouse and moved into larger pots to be grown into whole T<sub>0</sub> plants.

The average time between the inoculation of the explant and the production of a mature broccoli head through regeneration was 389±16d, just under a year and a month. The lines transformed with the *gus* construct matured in 317±1.5d, significantly faster  $t(df) = 4.5(15)$ ,  $p < 0.001$  than those with the ACC constructs that took 404±16d. Interestingly, the *gus* lines actually took significantly longer  $t(df) = 5.9(15)$ ,  $p < 0.001$  to mature in the glasshouse with 168±14d, than the other lines with 106±8d. The overall difference arises because the ACC constructs had significantly reduced the efficiency of regenerating a transgenic hairy root into a plantlet,  $t(df) = 6.4(15)$ ,  $p < 0.001$ . It had taken 149±55d from inoculating to transferring the *gus* plantlets into the glasshouse, whereas it had taken 291±21d for the other lines.

### 3.3.6 Determining stable insertion of the T-DNAs into the plant genome

DNA was extracted from leaf material of lines regenerated from roots through tissue culture. Specific primers to the *gfp* gene were used to check for

the presence of the T<sub>L</sub>-DNA region of the *A. rhizogenes* virulence plasmid pRi1855::GFP, and for the insertion of the binary plasmid T-DNA containing the 7 constructs.

In Figure 3.6 (lanes 2-4), the lines inoculated with *A. rhizogenes* containing the *aco1* antisense constructs produced the 542bp band that would be expected if the target DNA was present. There are smears in lanes 5 and 6, and it is difficult to determine a 360bp band for the presence of *aco1* sense constructs. The *aco2* antisense lines in lanes 7 and 8 have produced the expected band of 369bp as with the two *aco2* sense lines in lanes 9 and 10 producing a 578bp band. Lanes 11-14 contain the lines derived from transformation with the *acs* antisense constructs. However, only 7/00*acsA* 12 and 9/00 *acsA* 1 have produced the 471bp fragment expected from amplification of the target DNA (transformation code= 7<sup>th</sup> experiment in the year 2000, *acs* antisense construct, and 12<sup>th</sup> explant with *gfp* fluorescing excisable root). The 7/00 *acsS* 7 line in lane 15 has produced the expected band of 530bp. Lanes 16-18 contain the 3 lines inoculated with the *gus* construct. There is only a distinctive band of 390bp in lane 18, 34/00 *gus* 2. This is the first time the PCR has not worked for all of the *gus* lines from this set of DNA.

A PCR was carried out on regenerated lines for the presence of the *gfp* gene as shown in Figure 3.7. Although there is a smear, it is clear that the 494bp band of the *gfp* gene has been amplified in all of the lines except 7/00 *acsS* 7 where it is difficult to ascertain.

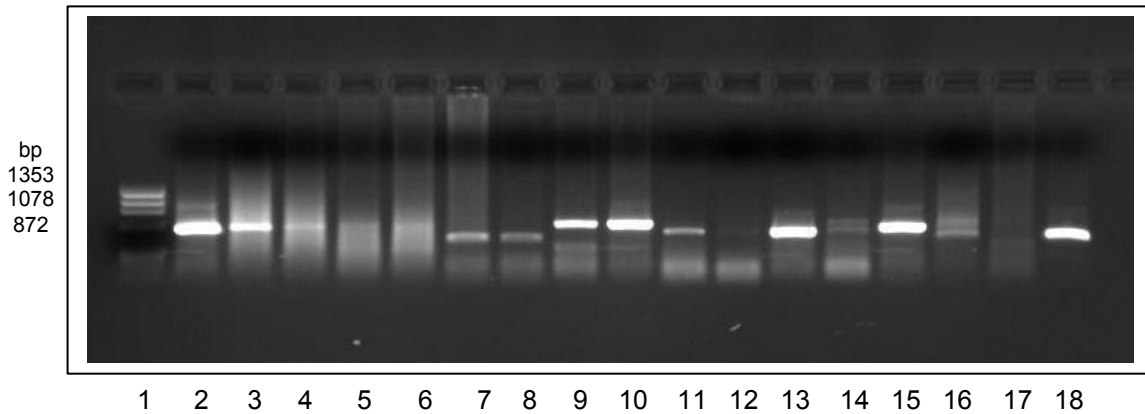


**Figure 3.6** PCR of genomic DNA from the transgenic plants to confirm insertion of the T-DNA constructs from the binary plasmid.

Lane 1,  $\phi$ X174RFDNA/*Hae*III fragments; lane 2, 28/00 *aco1A* 3 primers 3&4; lane 3, 34/00 *aco1A* 1 primers 3&4; lane 4, 34/00 *aco1A* 4 primers 3&4; lane 5, 32/00 *aco1* S 2 primers 3&5; lane 6, 33/00 *aco1S* 4 primers 3&5; lane 7, 3/00 *aco2A* 2 primers 3&8; lane 8, 33/00 *aco2* A 3 primers 3&8; lane 9, 5 *aco2S* 1 primers 3&9; lane 10, 26/00 *aco2S* 1 primers 3&9; lane 11, 7/00 *acsA* 12 primers 3&12; lane 12, 7/00 *acsA* 13 primers 3&12; lane 13, 9/00 *acsA* 1 primers 3&12; lane 14, 9/00 *acsA* 2 primers 3&12; lane 15, 7/00 *acsS* 7 primers 3&13; lane 16, 5/00 *gus* 1 primers *gus* F&R; lane 17, 33/00 *gus* 3 primers *gus* F&R; lane 18, 34/00 *gus* 2 primers *gus* F&R.

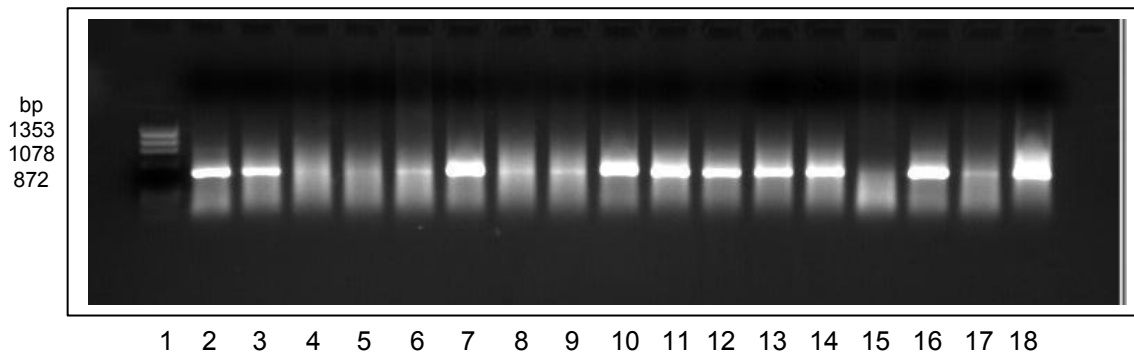


**Figure 3.7** PCR of the *gfp* gene from genomic DNA of the transgenic lines to confirm insertion of the T<sub>L</sub>-DNA region of the virulence plasmid.

All PCRs carried out with the GFP F&R primers. Lane 1,  $\phi$ X174RFDNA/*Hae*III fragments; lane 2, 28/00 *aco1A* 3; lane 3, 34/00 *aco1A* 1; lane 4, 34/00 *aco1A* 4; lane 5, 32/00 *aco1* S 2; lane 6, 33/00 *aco1S* 4; lane 7, 3/00 *aco2A* 2; lane 8, 33/00 *aco2* A 3; lane 9, 5 *aco2S* 1; lane 10, 26/00 *aco2S* 1; lane 11, 7/00 *acsA* 12; lane 12, 7/00 *acsA* 13; lane 13, 9/00 *acsA* 1; lane 14, 9/00 *acsA* 2; lane 15, 7/00 *acsS* 7; lane 16, 5/00 *gus* 1; lane 17, 33/00 *gus* 3; lane 18, 34/00 *gus* 2.

The PCR was a rapid tool to detect presence of the transgene but could not determine stable insertion and copy numbers of particular transgenes. The DNA extracted from the lines regenerated through tissue culture and that from non-transformed GDDH33 was digested with the *Sst*I endonuclease. It was ran on a 0.8% (w/v) agarose gel at 15V for 18h as shown in Figures 3.8 and 3.9 and blotted onto Hybond N+ filters (Amersham). The filters were then hybridised to specific probes, and the results are shown in Figures 3.10-3.15. Figures 3.8 and 3.9 show the quantity of DNA in each lane of the transgenic lines digested by *Sst*I as a reference for the autoradiographs in Figures 3.10-3.15.

Figure 3.10 shows the autoradiograph of the hybridisation between the *Brassica oleracea* var. *italica* *aco1* 250bp 3'UTR DNA probe and the DNA shown in Figure 3.8. Lane 14 shows the production of a large signal where there is hybridisation of the probe to the control DNA. There are no bands in lane 2, as the specific probe has not strongly hybridised to the non-transformed GDDH33 DNA even at medium stringency. The *aco1* antisense line in lane 3 has two distinct bands between the 6557 and 4361 markers. At the 2027 marker, there is a band with less intensity than the upper two. It occupies the same position as one of the distinctive DNA bands on Figure 3.8, and may have produced a signal due to weak binding and a high copy number. This lower band is possibly not the result of a T-DNA insert.

There are no clear distinctive bands in lanes 4-6. Lane 6 did not actually contain the DNA of 32/00 *aco1S* 3 as it had diffused from the well just after loading, as can be seen in Figure 3.8. This also occurred with 34/00 *aco1A* 1, although a small proportion remained within the well. There should

be enough DNA in lane 5 for 34/00 *aco1A* 4 for hybridisation with the *aco1* 3'UTR probe suggesting that this is a negative result. This is also possibly the case with 33/00 *aco1S* 4 in lane 7, but there is a positive band at 6557bp but due to the high background between the 23130 and 4361 markers is less defined.

As expected, there are no bands in lanes 8-10 containing the *aco2* lines 3/00 *aco2A* 2, 33/00 *aco2A* 3 and, 5/00 *aco2S* 1. This is not the case with 26/00 *aco2S* 1 in lane 11 that contains 8 visible bands. They appear to be genuine, but if compared to Figure 3.11, and the *aco2* 3'UTR probe, all of these bands are in common. There is a higher concentration of DNA from 26/00 *aco2S* 1 compared to the other lines that might relatively amplify a weak signal.

Figure 3.11 shows the autoradiograph of the hybridisation between the *Brassica oleracea* var. *italica* *aco2* 283bp 3'UTR DNA probe and the DNA shown in Figure 3.8. There are no bands in the non-transformed GDDH33 control DNA in lane 2. There are bands in lanes 5, 7, 8 and 11 at 2027bp corresponding to the visible DNA bands in Figure 3.11. These also occurred in Figure 3.10 and probably do not correspond to genuine *aco2* T-DNA inserts. There is a distinctive band in lane 7 between 23130 and 9416bp positioned within the largest fragments of DNA, but possibly not a genuine insert. There are no clear bands in lanes 9 and 10 containing the DNA of 33/00 *aco2A* 3 and 5/00 *aco2S* 1. In lane 11 with DNA from 26/00 *aco2S* 1, there are 10 distinctive bands. Eight of these correspond directly to the bands that hybridised to the *aco1* 3'UTR probe in Figure 3.10. The largest band, just

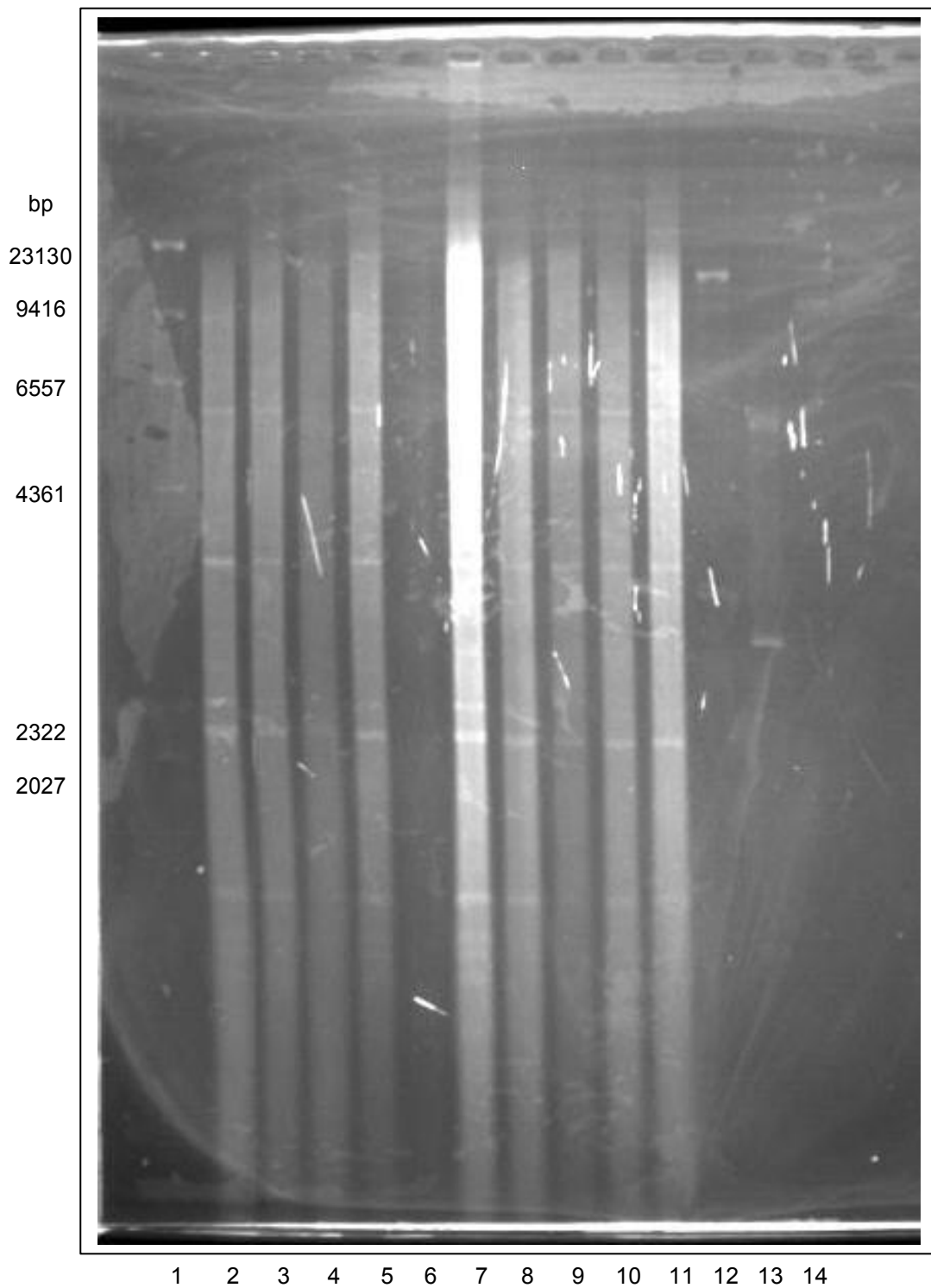
below the 6557bp marker and the fifth band down are not present in Figure 3.10 and probably represent the genuine bands for *aco2* T-DNA insertion.

Figure 3.12 shows the autoradiograph of the hybridisation between the *Brassica oleracea* var. *italica* *acs* full length cDNA probe and the DNA shown in Figure 3.9. In Figure 3.12, there are bands in all of the lanes between the 23130 and 9416bp markers. As this band is present in the non-transformed control it is probably not the result of a T-DNA insertion. There are 3 distinctive bands in lane 7 of 7/00 *acsS* 7 that are not present in the other lanes. There is one band greater than 4361bp, one that size, and one between 4361 and 2322bp that could be the result of 2-3 T-DNA insertions. There is no evidence for stable insertion of *acs* antisense T-DNAs from this experiment. The DNA from the *Sst*I endonuclease restriction of 9/00 *acsA* 1 and 9/00 *acsA* 2 had diffused from the wells of lanes 5 and 6 and therefore did not contain any DNA. There was DNA in lanes 3 and 4 for 7/00 *acsA* 12 and 7/00 *acsA* 13 that would be expected to have bands if the T-DNA insert was present.

Figure 3.13 shows the autoradiograph of the hybridisation between the *gus* 390bp DNA probe and the DNA shown in Figure 3.9. There are 9 strong bands between 6557 and 2027bp in lane 10 with the DNA from 34/00 *gus* 2. The *gus* probe has not hybridised to the other transgenic lines or the non-transformed control. It is possible that these are 9 genuine bands, although one band between 4361 and 2322bp produces a much stronger signal and may be the only genuine band. There was no 5/00 *gus* 1 DNA in lane 8 as it had diffused from the well. There was however, DNA in lane 9, but no bands could be a negative result.

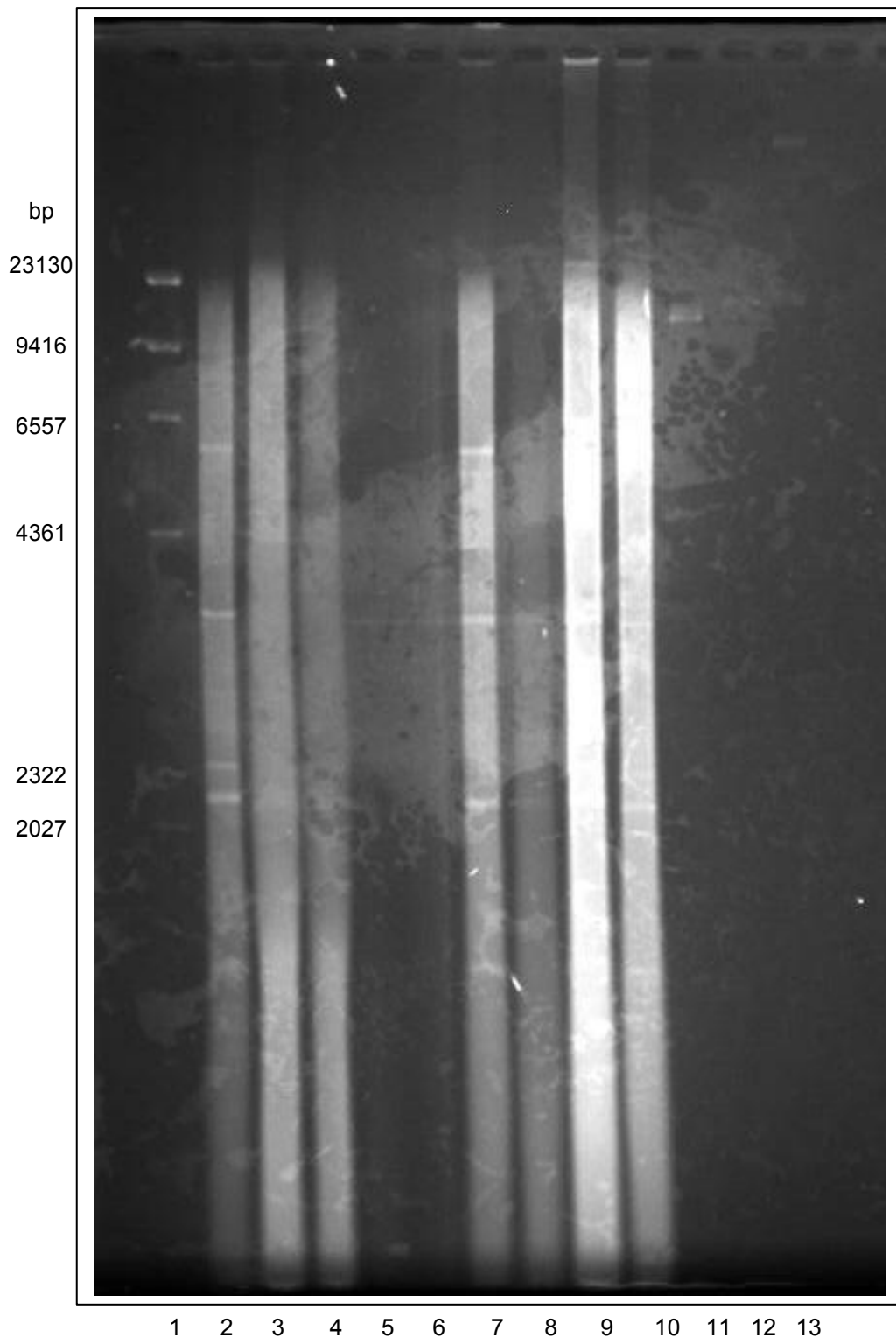
Figure 3.14 shows the autoradiograph of the hybridisation between the *gfp* 494bp DNA probe and the DNA shown in Figure 3.8. In lanes 2-11 (except 6 as no DNA), there are bands at 2322bp at the same position as the distinctive DNA bands in Figure 3.8. There is a band in the non-transformed control (lane 2) as well as the lines regenerated through tissue culture. The line 28/00 *aco1A* 3 in lane 3 has produced 4 distinctive bands between 23130 and 4361bp. In lane 4 with 34/00 *aco1A* 1, there is a band below 9416. There are no clear bands in lanes 5-7 for lines 34/00 *aco1A* 4, 32/00 *aco1S* 3 and 33/00 *aco1S* 4. In lane 8 for 3/00 *aco2A* 2, there are clearly 3 bands between the 9416 and 4361bp markers. There is not a band in lane 9, 33/00 *aco2A* 3, but there is a singular band at 9416bp in lane 10 of 5/00 *aco2S* 1. In the autoradiograph, there are clearly 5 distinctive bands in lane 11 for 26/00 *aco2S* 1, but is less obvious in the scanned image.

Figure 3.15 shows the autoradiograph of the hybridisation between the *gfp* 494bp DNA probe and the DNA shown in Figure 3.9. There is a band in the non-transformed control in lane 2 below the 4361bp marker consistent with the DNA band in Figure 3.9. This band is also present in the lanes with DNA from the regenerated lines. Lanes 3 and 4 containing DNA from 7/00 *acsA* 12 and 7/00 *acsA* 13 produced distinctive bands at 9416bp. There is no DNA in lanes 5 and 6 due to diffusion from the well. In lane 7 there are 3 bands for 7/00 *acsS* 7 and 10 bands in lane 10 with 34/00 *gus* 2 although there is one strong band between 9416 and 6557bp.



**Figure 3.8** Genomic DNA from *aco1* and *aco2* transgenic lines digested with *SstI* restriction endonuclease and run on a 0.8% (w/v) agarose gel at 50V for 18h.

Lane 1, Lambda *HindIII* fragments; lane 2, non-transformed GDDH33; lane 3, 28/00 *aco1A* 3; lane 4, 34/00 *aco1A* 1; lane 5, 34/00 *aco1A* 4; lane 6, 32/00 *aco1* S 2; lane 7, 33/00 *aco1S* 4; lane 8, 3/00 *aco2A* 2; lane 9, 33/00 *aco2A* 3; lane 10, 5 *aco2S* 1; lane 11, 26/00 *aco2S* 1; lane 12, pBIN m-*gfp5*-ER *BclI* digest; lane 13, *aco2* construct *BclI* digest; lane 14, *aco1* construct *BclI* digest.



**Figure 3.9** Genomic DNA from *acs* and GUS transgenic lines digested with *Sst*I restriction endonuclease and run on a 0.8% (w/v) agarose gel at 50V for 18h.

Lane 1, Lambda *Hind*III fragments; lane 2, non-transformed GDDH33; lane 3, 7/00 *acsA* 12; lane 4, 7/00 *acsA* 13; lane 5, 9/00 *acsA* 1; lane 6, 9/00 *acsA* 2; lane 7, 7/00 *acsS* 7; lane 8, 5/00 *gus* 1; lane 9, 33/00 *gus* 3; lane 10, 34/00 *gus* 2; lane 11, pBIN *m-gfp5-ER Bcl*I digest; lane 12, *gus* construct *Bcl*I digest; lane 13, *acs* construct *Bcl*I digest.

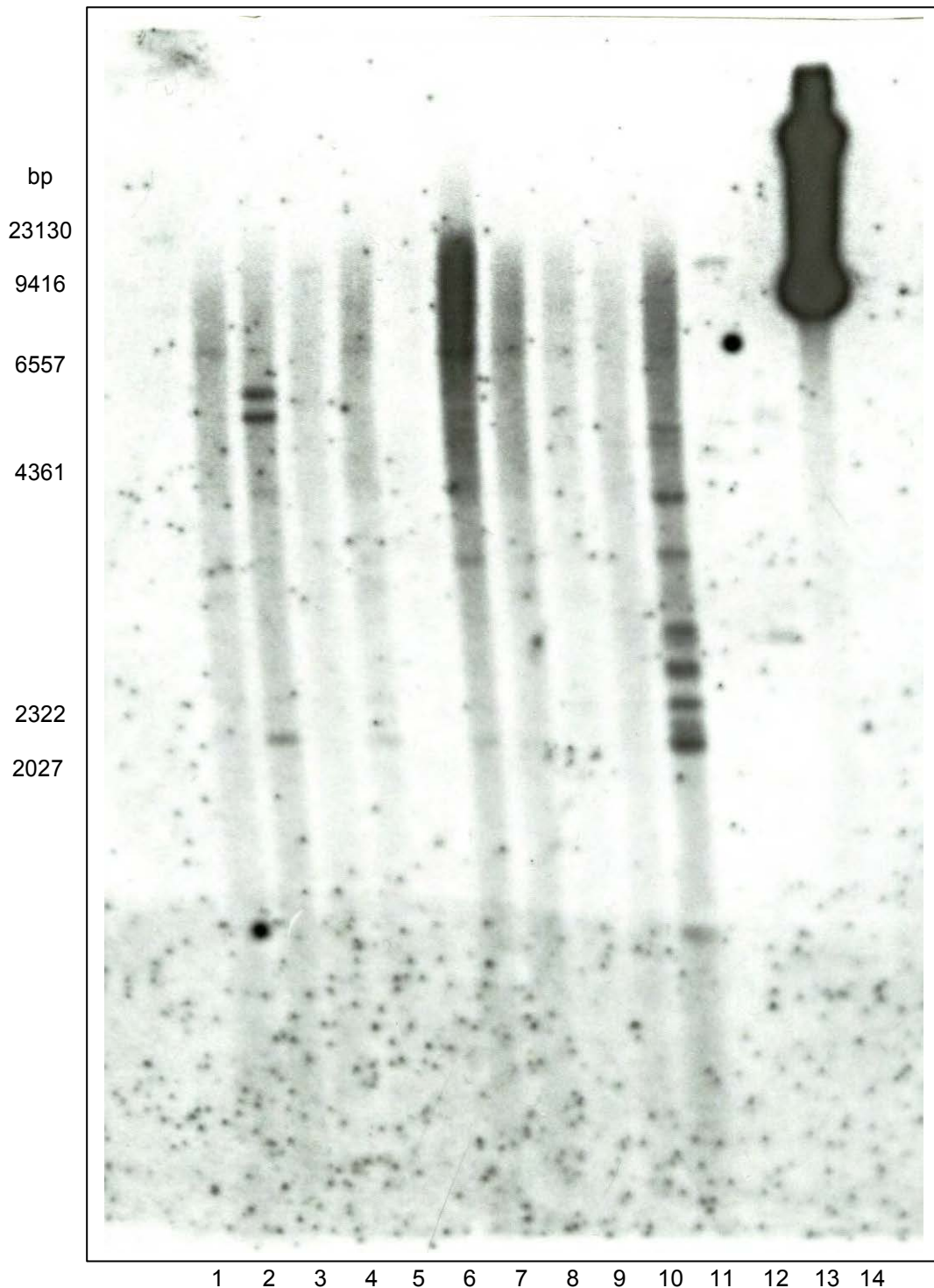


**Figure 3.10** Autoradiograph of the hybridisation between the *Brassica oleracea* L. var. *italica* *aco1* 283bp 3'UTR DNA probe and the digested genomic DNA of Figure 3.8.

Lane 1, Lambda *Hind*III fragments; lane 2, non-transformed GDDH33; lane 3, 28/00 *aco1A* 3; lane 4, 34/00 *aco1A* 1; lane 5, 34/00 *aco1A* 4; lane 6, 32/00 *aco1* S 2; lane 7, 33/00 *aco1S* 4; lane 8, 3/00 *aco2A* 2; lane 9, 33/00 *aco2A* 3; lane 10, 5 *aco2S* 1; lane 11, 26/00 *aco2S* 1; lane 12, pBIN *m-gfp5-ER Bcl*I digest; lane 13, *aco2* construct *Bcl*I digest; lane 14, *aco1* construct *Bcl*I digest.

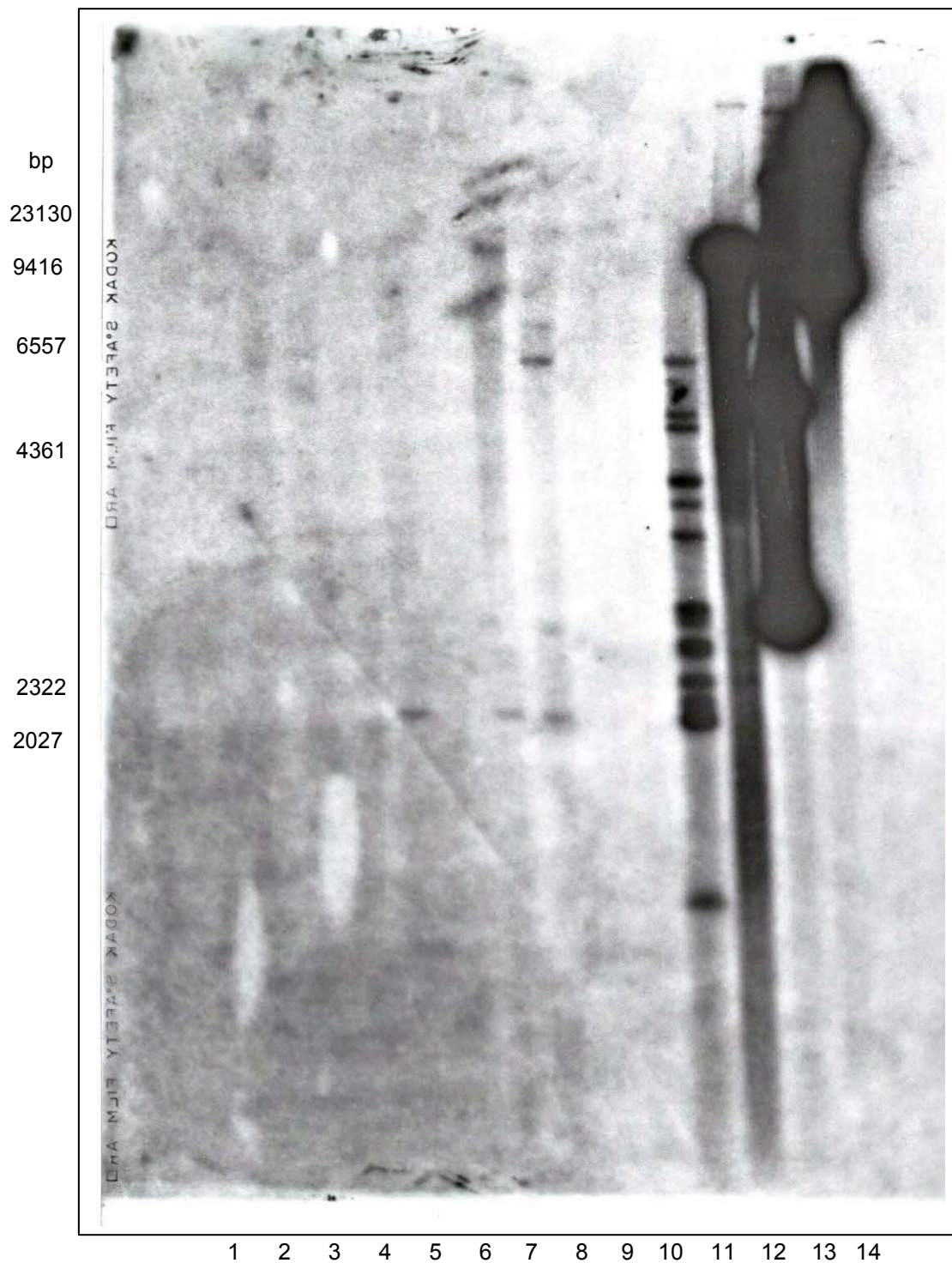


**Figure 3.11** Autoradiograph of the hybridisation between the *Brassica oleracea* L. var. *italica* *aco2* 252bp 3'UTR DNA probe and the digested genomic DNA of Figure 3.8.

Lane 1, Lambda *Hind*III fragments; lane 2, non-transformed GDDH33; lane 3, 28/00 *aco1A* 3; lane 4, 34/00 *aco1A* 1; lane 5, 34/00 *aco1A* 4; lane 6, 32/00 *aco1* S 2; lane 7, 33/00 *aco1S* 4; lane 8, 3/00 *aco2A* 2; lane 9, 33/00 *aco2A* 3; lane 10, 5 *aco2S* 1; lane 11, 26/00 *aco2S* 1; lane 12, pBIN *m-gfp5-ER* *Bcl*I digest; lane 13, *aco2* construct *Bcl*I digest; lane 14, *aco1* construct *Bcl*I digest.

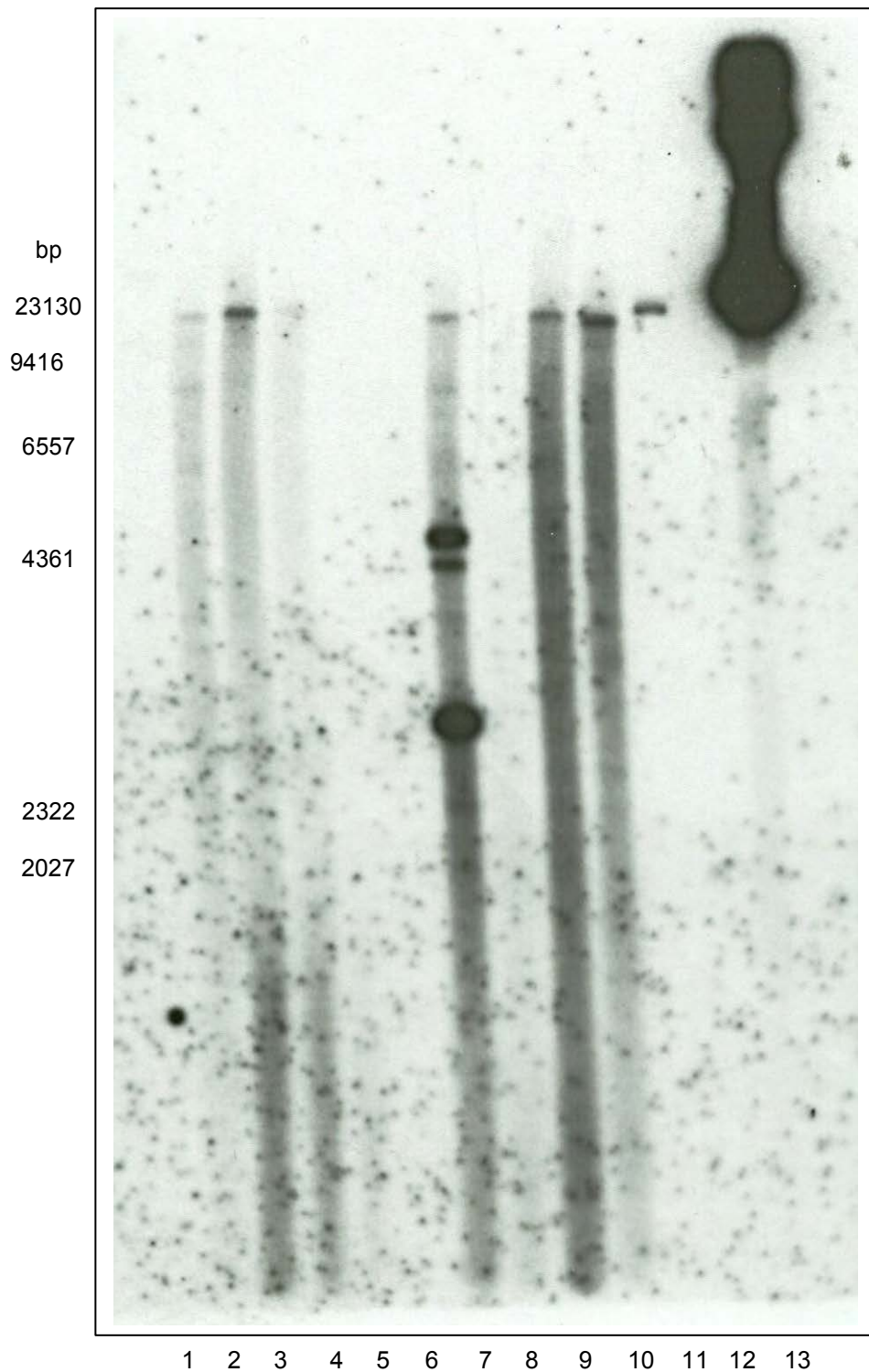


**Figure 3.12** Autoradiograph of the hybridisation between the *Brassica oleracea* L. var. *italica* *acs* full length cDNA probe and the digested genomic DNA of Figure 3.9.

Lane 1, Lambda *Hind*III fragments; lane 2, non-transformed GDDH33; lane 3, 7/00 *acsA* 12; lane 4, 7/00 *acsA* 13; lane 5, 9/00 *acsA* 1; lane 6, 9/00 *acsA* 2; lane 7, 7/00 *acsS* 7; lane 8, 5/00 *gus* 1; lane 9, 33/00 *gus* 3; lane 10, 34/00 *gus* 2; lane 11, pBIN *m-gfp5-ER Bcl*I digest; lane 12, *gus* construct *Bcl*I digest; lane 13, *acs* construct *Bcl*I digest.

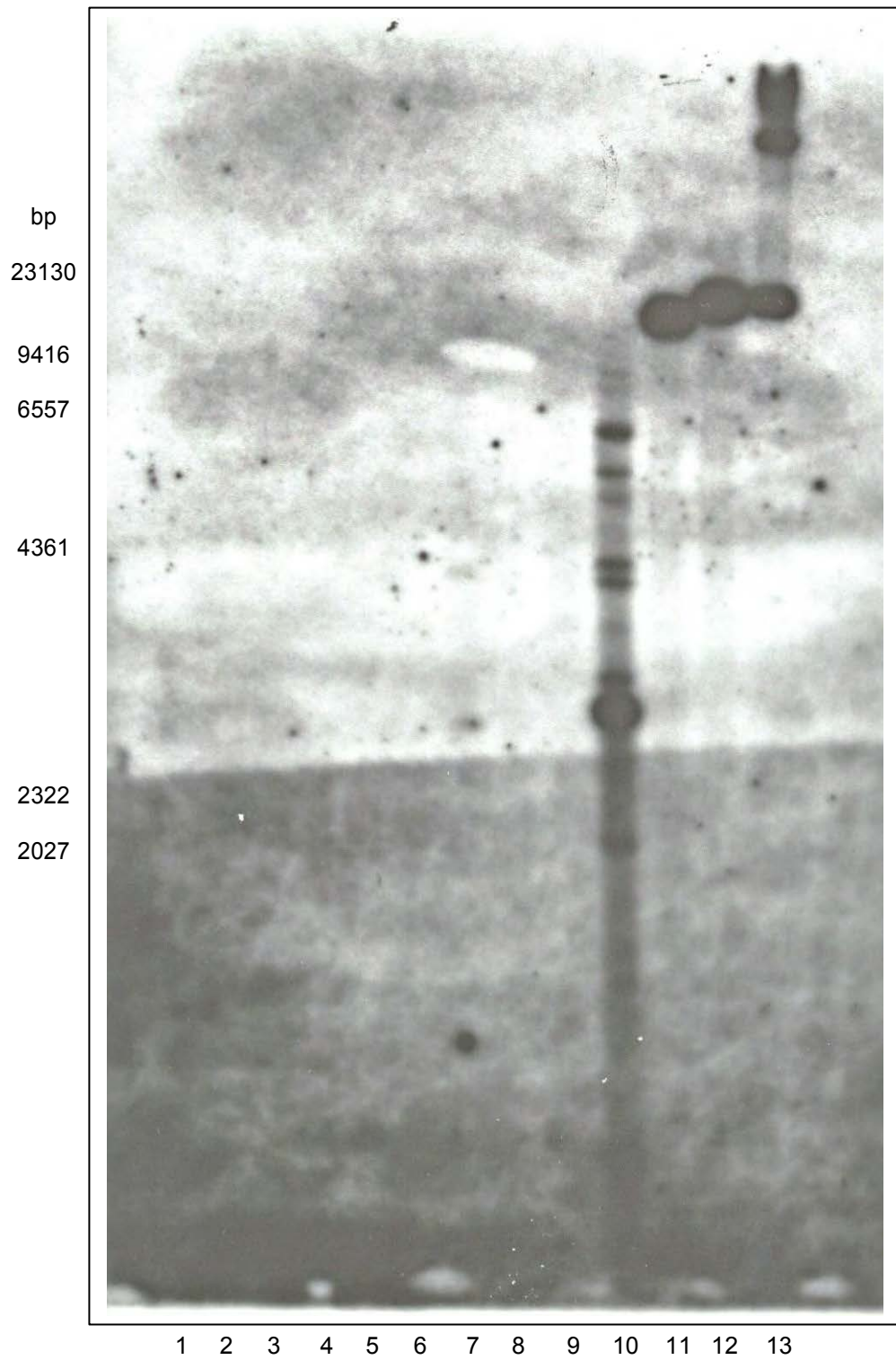


**Figure 3.13** Autoradiograph of the hybridisation between the 390bp *gus* DNA probe and the digested genomic DNA of Figure 3.9. Lane 1, Lambda *Hind*III fragments; lane 2, non-transformed GDDH33; lane 3, 7/00 *acsA* 12; lane 4, 7/00 *acsA* 13; lane 5, 9/00 *acsA* 1; lane 6, 9/00 *acsA* 2; lane 7, 7/00 *acsS* 7; lane 8, 5/00 *gus* 1; lane 9, 33/00 *gus* 3; lane 10, 34/00 *gus* 2; lane 11, pBIN *m-gfp5-ER Bcl*I digest; lane 12, *gus* construct *Bcl*I digest; lane 13, *acs* construct *Bcl*I digest.

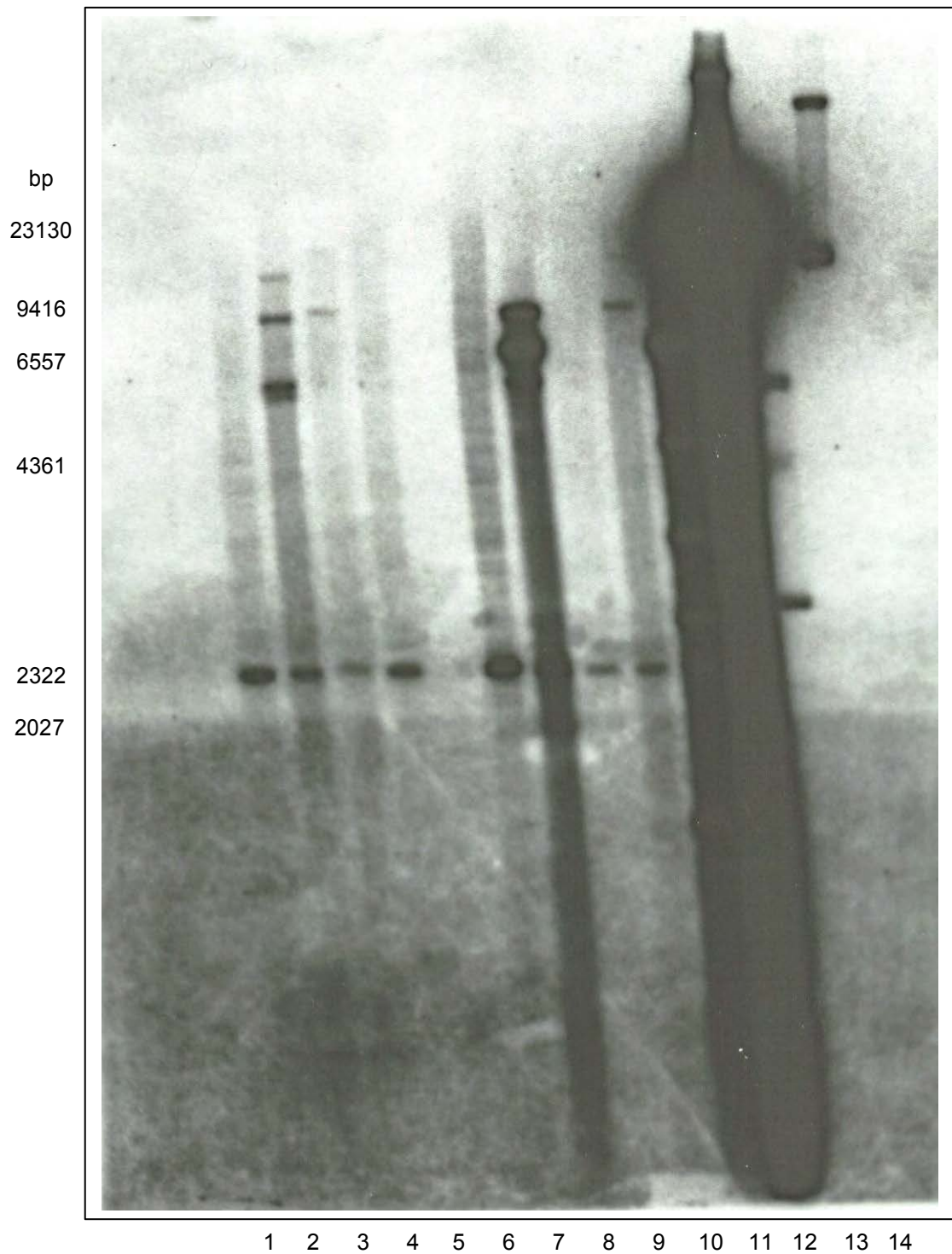


**Figure 3.14** Autoradiograph of the hybridisation between the 494bp GFP DNA probe and the digested genomic DNA of Figure 3.8. Lane 1, Lambda *Hind*III fragments; lane 2, non-transformed GDDH33; lane 3, 28/00 *aco1A* 3; lane 4, 34/00 *aco1A* 1; lane 5, 34/00 *aco1A* 4; lane 6, 32/00 *aco1 S* 2; lane 7, 33/00 *aco1S* 4; lane 8, 3/00 *aco2A* 2; lane 9, 33/00 *aco2 A* 3; lane 10, 5 *aco2S* 1; lane 11, 26/00 *aco2S* 1; lane 12, pBIN *m-gfp5-ER Bcl*I digest; lane 13, *aco2* construct *Bcl*I digest; lane 14, *aco1* construct *Bcl*I digest.

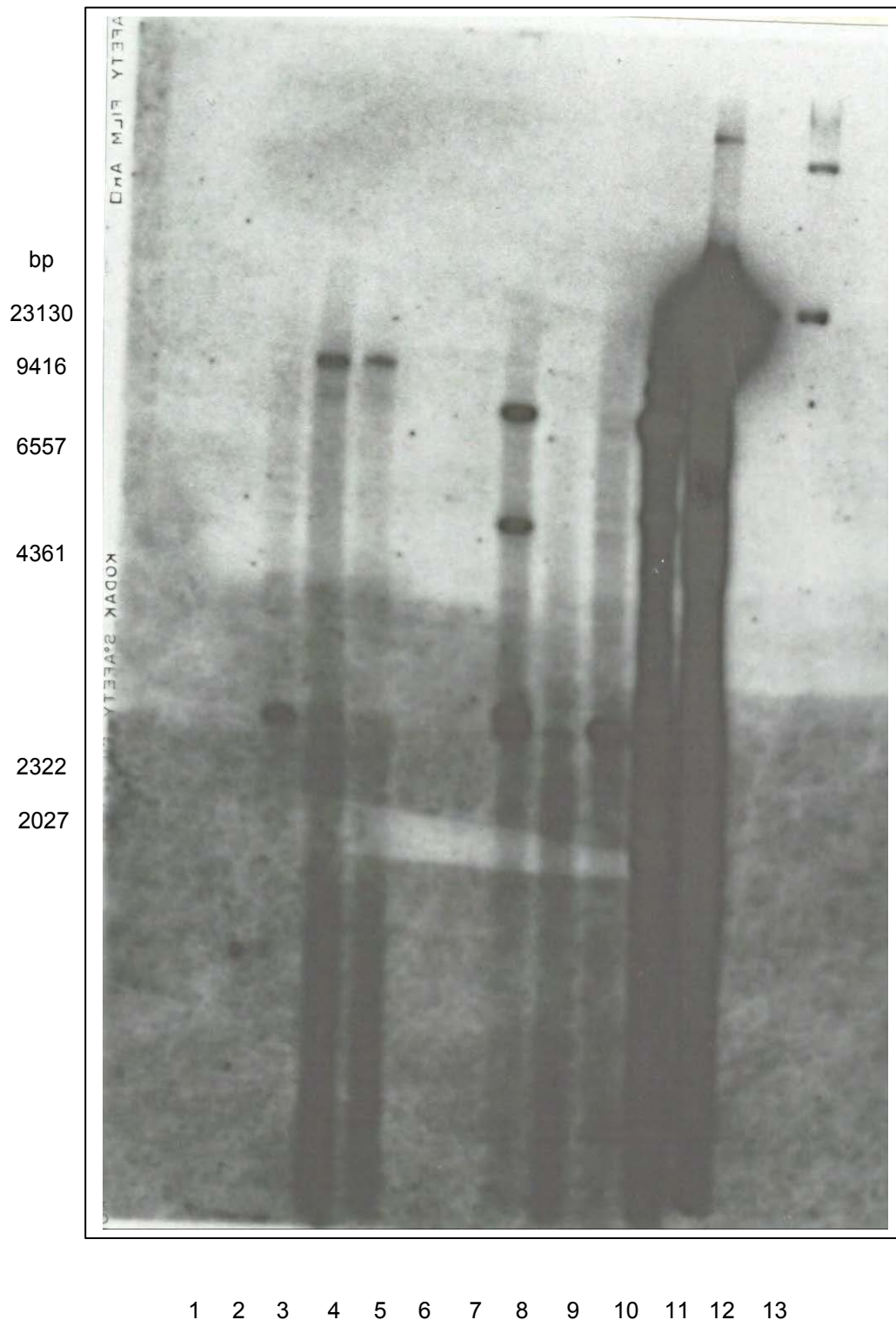


**Figure 3.15** Autoradiograph of the hybridisation between the 494bp GFP DNA probe and the digested genomic DNA of Figure 3.9. Lane 1, Lambda *Hind*III fragments; lane 2, non-transformed GDDH33; lane 3, 28/00 *aco1A* 3; lane 4, 34/00 *aco1A* 1; lane 5, 34/00 *aco1A* 4; lane 6, 32/00 *aco1* S 2; lane 7, 33/00 *aco1S* 4; lane 8, 3/00 *aco2A* 2; lane 9, 33/00 *aco2* A 3; lane 10, 5 *aco2S* 1; lane 11, 26/00 *aco2S* 1; lane 12, pBIN *m-gfp5-ER Bcl*I digest; lane 13, *aco2* construct *Bcl*I digest; lane 14, *aco1* construct *Bcl*I digest.

A summary of the data presented in Figures 3.6-3.15 is shown in Table 3.6. It is apparent that lines positive for construct and gfp by PCR are not always confirmed by the Southern analysis. The copy number for construct and that for the *Ri*-T-DNA insert ranges from 1-4 (or 11).

**Table 3.6** Summary of the PCR and autoradiograph data for confirming the presence of T-DNAs in lines regenerated through tissue culture.

Line	PCR Confirmation		Southern Analysis (Copy No.)	
	Construct	gfp	Construct	gfp
28/00 <i>aco1A 3</i>	√	√	2	4
34/00 <i>aco1A 1</i>	√	√	-	-
34/00 <i>aco1A 4</i>	√	√	-	-
32/00 <i>aco1S 3</i>	?	√	No DNA	No DNA
33/00 <i>aco1S 4</i>	?	√	1	-
3/00 <i>aco2A 2</i>	√	√	1	3
33/00 <i>aco2A 3</i>	√	√	-	-
5/00 <i>aco2S 1</i>	√	√	-	1
26/00 <i>aco2S 1</i>	√	√	2-10	1-7
7/00 <i>acsA 12</i>	√	√	-	1
7/00 <i>acsA 13</i>	?	√	-	1
9/00 <i>acsA 1</i>	√	√	No DNA	No DNA
9/00 <i>acsA 2</i>	?	√	No DNA	No DNA
7/00 <i>acsS 7</i>	√	√	3	3
5/00 <i>gus 1</i>	√	√	-	-
33/00 <i>gus 3</i>	√	√	-	-
34/00 <i>gus 2</i>	√	√	1-10	1-11

### 3.3.7 Transgenic plant phenotype

The morphology of regenerated transgenic plant lines varied from phenotypically normal to those with severe 'hairy root' syndrome. Four T<sub>0</sub> lines produced dwarfed plants (see Figure 3.16, a and c) with small, extremely wrinkled leaves; shortened internodes; and small heads with reduced chlorophyll. There were six T<sub>0</sub> lines exhibiting moderate phenotypes with wrinkled leaves and shortened internodes (Figure 3.16b), and eight (Figure 3.16c) that were phenotypically normal. It was possible to self-pollinate and take buds for microspore culture from the moderate/normal plants, but not from the plants with severe phenotype. Transgenic lines for these phenotypes were scored as shown in Table 3.7.

As shown by Table 3.7, there is no apparent correlation between the copy number of the *Ri*-T-DNA and the severity of the *rol* phenotype. There is not enough data to determine whether there is a pattern for selection of *Ri* phenotype within the constructs.



**Figure 3.16** Heading broccoli plants that have been regenerated from GFP fluorescing roots, through a tissue culture phase. They illustrate different severities of the hairy root phenotype. (a) Severe *rol* phenotype (9/00 *acsA* 1; (b) Moderate *rol* phenotype (9/00 *acsA* 2); (c) Weak *rol* phenotype (7/00 *acsA* 12; (d) The most severe *rol* phenotype (5/00 *aco2A* 1).

**Table 3.7** The effect of the *rol* genes on transgenic plant morphology.

<b>Line</b>	<b><i>gfp</i> Copy No.</b>	<b><i>rol</i> phenotype</b>
<b>28/00 <i>aco1A</i> 3</b>	<b>4</b>	<b>weak</b>
<b>34/00 <i>aco1A</i> 1</b>	<b>NK</b>	<b>weak</b>
<b>34/00 <i>aco1A</i> 4</b>	<b>NK</b>	<b>weak</b>
<b>32/00 <i>aco1S</i> 3</b>	<b>NK</b>	<b>weak</b>
<b>33/00 <i>aco1S</i> 4</b>	<b>NK</b>	<b>moderate</b>
<b>3/00 <i>aco2A</i> 2</b>	<b>3</b>	<b>moderate</b>
<b>5/00 <i>aco2A</i> 1</b>	<b>NK</b>	<b>severe</b>
<b>33/00 <i>aco2A</i> 3</b>	<b>NK</b>	<b>weak</b>
<b>5/00 <i>aco2S</i> 1</b>	<b>1</b>	<b>moderate</b>
<b>26/00 <i>aco2S</i> 1</b>	<b>1-7</b>	<b>weak</b>
<b>7/00 <i>acsA</i> 12</b>	<b>1</b>	<b>weak</b>
<b>7/00 <i>acsA</i> 13</b>	<b>1</b>	<b>moderate</b>
<b>9/00 <i>acsA</i> 1</b>	<b>NK</b>	<b>severe</b>
<b>9/00 <i>acsA</i> 2</b>	<b>NK</b>	<b>moderate</b>
<b>7/00 <i>acsS</i> 7</b>	<b>3</b>	<b>severe</b>
<b>5/00 <i>gus</i> 1</b>	<b>NK</b>	<b>severe</b>
<b>33/00 <i>gus</i> 3</b>	<b>NK</b>	<b>weak</b>
<b>34/00 <i>gus</i> 2</b>	<b>1-11</b>	<b>moderate</b>

NK=Not known

Plants transferred to the glasshouse from tissue culture were very susceptible to abiotic stresses such as water loss leading to desiccation, and biotic stresses through fungal pathogens and feeding insects. There was also a detrimental effect on the plants through the action of the *rol* genes. In Table 3.8, the contrast between the percentage of surviving plants with the normal phenotype (89) and the severe phenotype (31) is indicative of the negative impact of the *rol* genes.

**Table 3.8** The total numbers of transgenic plants produced from all constructs with the effect of the *rol* genes on mortality.

<i>rol</i> phenotype	No. plants transferred to glasshouse	No. plants to surviving heading	Percentage of plants surviving to heading
<b>Weak</b>	<b>106</b>	<b>94</b>	<b>89</b>
<b>Moderate</b>	<b>86</b>	<b>58</b>	<b>67</b>
<b>Severe</b>	<b>70</b>	<b>22</b>	<b>31</b>
<b>All phenotypes</b>	<b>262</b>	<b>174</b>	<b>66</b>

### 3.3.8 Seed production of the transgenic lines

The *rol* genes had a negative effect on seed production as shown in Table 3.9 as the lines with severe phenotypes did not produce any seeds. It also shows that the constructs had little effect on as seed production. Seeds were produced from lines with each construct except for *ACC synthase* sense, which only produced one line that had a severe *rol* phenotype.

**Table 3.9** The number of seeds recovered from transgenic lines with their particular *rol* phenotype

<b>Plant Line</b>	<b>No. of Seeds</b>	<b><i>rol</i> phenotype</b>
<b>03/00 <i>aco2</i> A 2</b>	<b>39</b>	<b>moderate</b>
<b>07/00 <i>acs</i> A 12</b>	<b>454</b>	<b>weak</b>
<b>09/00 <i>acs</i> A 2</b>	<b>2</b>	<b>moderate</b>
<b>26/00 <i>aco2</i> S 1</b>	<b>749</b>	<b>weak</b>
<b>28/00 <i>aco1</i> A 3</b>	<b>564</b>	<b>weak</b>
<b>32/00 <i>aco1</i> S 3</b>	<b>2048</b>	<b>weak</b>
<b>33/00 <i>aco1</i> S 4</b>	<b>42</b>	<b>moderate</b>
<b>33/00 <i>aco2</i> A 3</b>	<b>2075</b>	<b>weak</b>
<b>34/00 <i>aco1</i> A 1</b>	<b>16</b>	<b>weak</b>
<b>34/00 <i>aco1</i> A 4</b>	<b>20</b>	<b>weak</b>
<b>34/00 <i>gus 2</i></b>	<b>13</b>	<b>moderate</b>
<b>Total lines = 11</b>	<b>Total seeds = 6022</b>	<b>4 = moderate</b>
		<b>7 = weak</b>

The transgenic line 28/00 *aco1A* 3 produced 564 seeds, of which 69 were immediately sown. Sixty-seven of these germinated (97%), and were tested by PCR for presence of the *gfp* and *aco1A* T-DNA inserts. Figures 3.17 and 3.18 show the presence or absence of a band for the *gfp* and *aco1A* T-DNA inserts with primers 3 and 4 (for *aco1A*) and *gfp* F and R (for *gfp*).

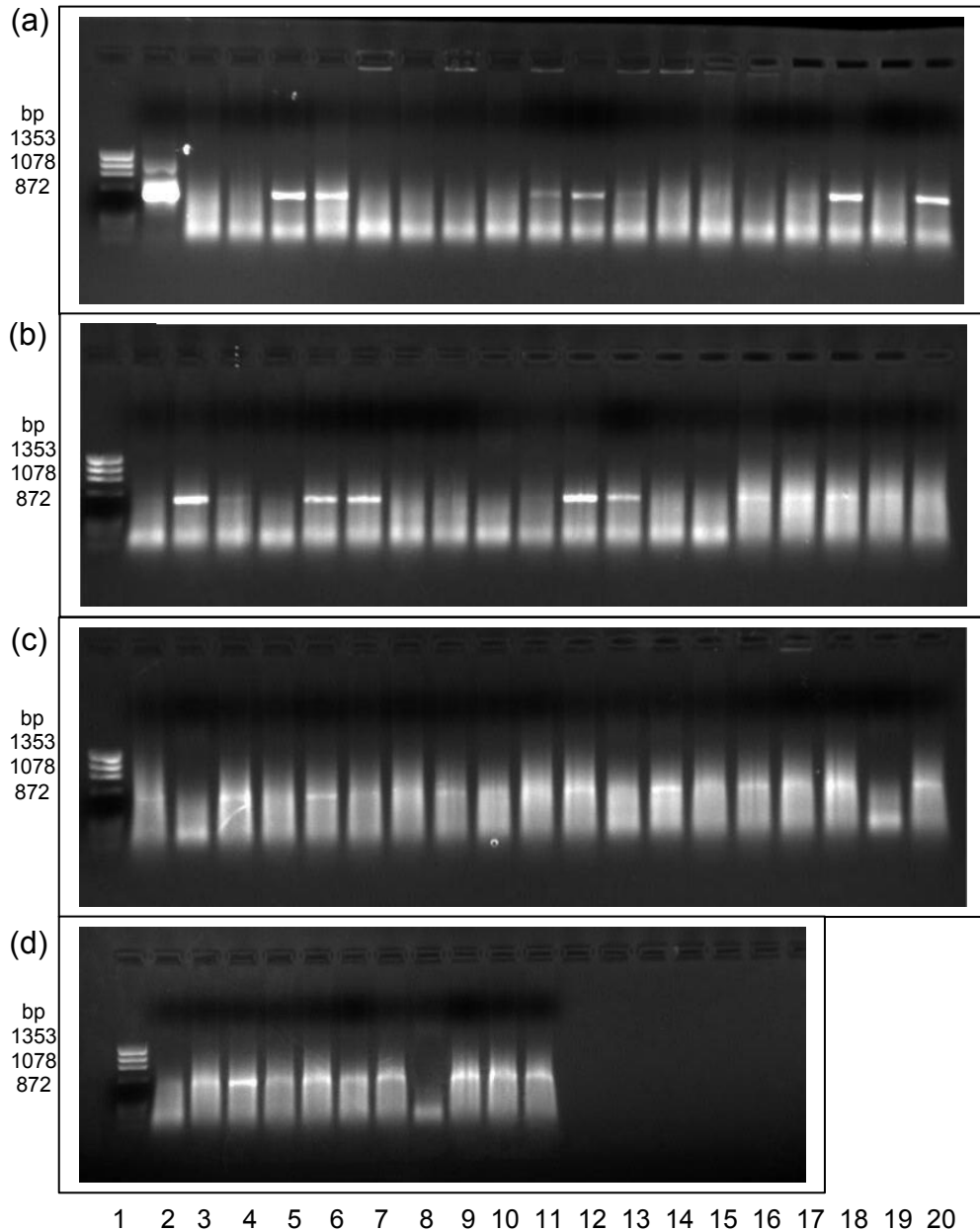


**Figure 3.17** Determination of *gfp* inserts by PCR of 67 28/00 *aco1A* 3 T<sub>1</sub> progeny grown from seed.

In lane 1 (a-d)  $\phi$ X174RF DNA/*Hae*III fragments. In (a) lane 2, *gfp*+ve control; lanes 3-20 contain seedlings 1-18. In (b), lanes 2-20 contain seedlings 19-37. In (c), lanes 2-20 contain 38-56. In (d), lanes 2-11 contain seedlings 57-67.

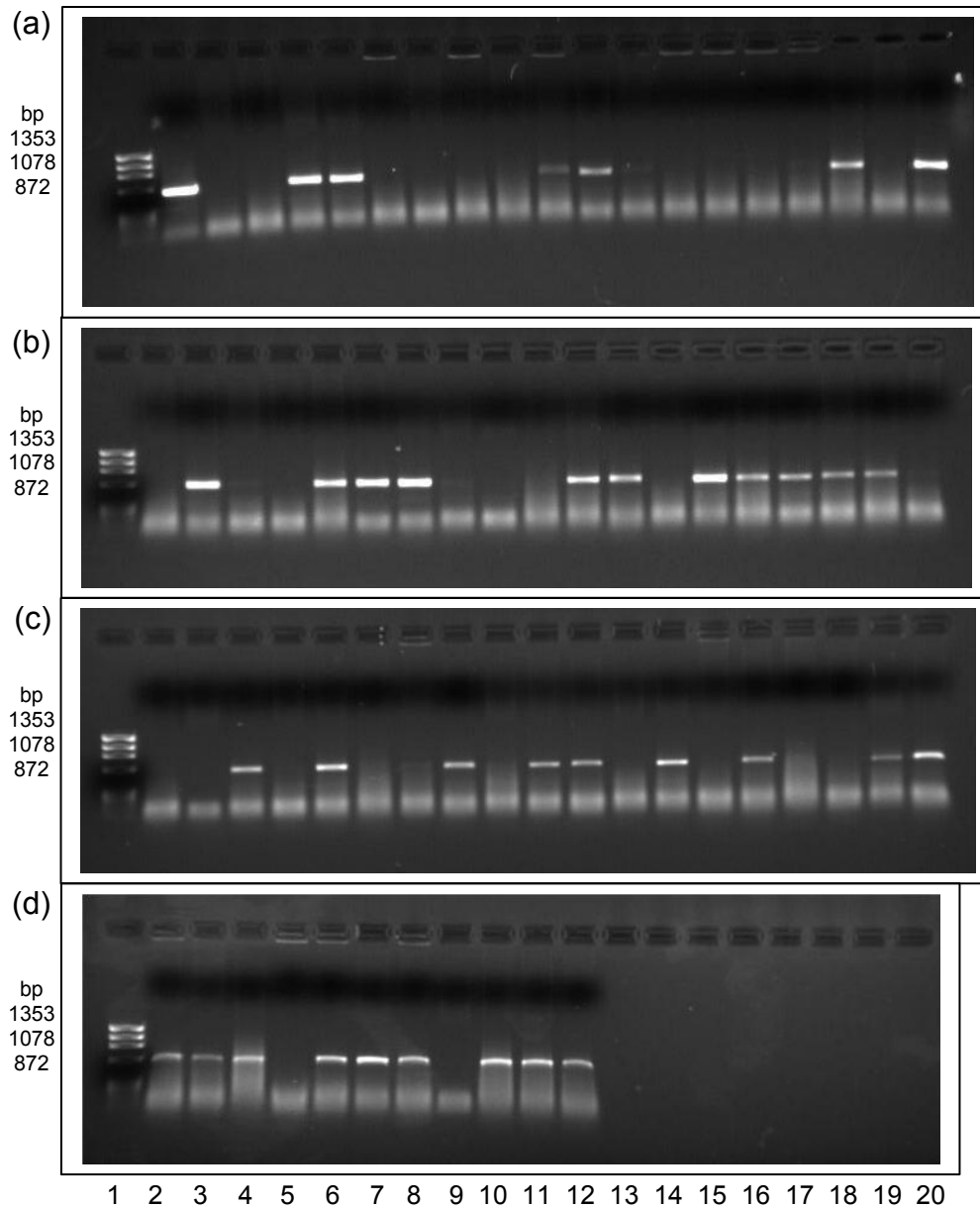


**Figure 3.18** Determination of *aco1A* inserts by PCR of 67 28/00 *aco1A* 3 T<sub>1</sub> progeny grown from seed.

In lane 1 (a-d)  $\phi$ X174RFDNA/*Hae*III fragments. In (a) lane 2, *aco1A*+ve control; lanes 3-20 contain seedlings 1-18. In (b), lanes 2-20 contain seedlings 19-37. In (c), lanes 2-20 contain 38-56. In (d), lanes 2-11 contain seedlings 57-67.

The data in Figures 3.17 and 3.18 is summarised in Table 3.10. It groups the seedlings into four categories depending on presence or absence of the *gfp* and *aco1A* T-DNA inserts. There are a high proportion of double-positives (57%) in Table 3.10 as the *gfp* and *aco1A* T-DNAs have co-segregated. There are half those numbers of double-negatives where none of the T-DNAs have been passed on. The smallest group with only 3% of the progeny are the marker-free plants with only the construct T-DNA.

**Table 3.10** Segregation of T-DNA inserts in the T<sub>(1)</sub> progeny of 28/00 *aco1A* 3

Segregation of T-DNA inserts	No. of plants
<i>gfp</i> <sup>+ve</sup> / <i>aco1A</i> <sup>+ve</sup>	38
<i>gfp</i> <sup>+ve</sup> / <i>aco1A</i> <sup>-ve</sup>	10
<i>gfp</i> <sup>-ve</sup> / <i>aco1A</i> <sup>+ve</sup>	2
<i>gfp</i> <sup>-ve</sup> / <i>aco1A</i> <sup>-ve</sup>	17
<b>Total</b>	<b>67</b>

### 3.4 Discussion

The overall transformation efficiency achieved by inoculating GDDH33 with the *A. rhizogenes* co-integrate strain LBA 9402 pRi1855::GFP was  $3.63 \pm 0.60\%$ . This refers to the proportion of explants that produced excisable (>1cm) GFP-fluorescing transgenic roots from those that were inoculated. This value is comparable to broccoli transformation efficiencies of Green Comet 3.1, Corvet 4.2, New River 6.7, and Vantage 2.1 achieved by Puddephat *et al.* (2001). It was not as great as the 20% efficiency achieved by Cogan *et al.* (2001) for GDDH33, although not all of the GFP-fluorescing roots would have been excisable by Cogan *et al.* (2001). It is also possible that GFP expression was reduced in some of the transgenic roots by co-suppression. Al-Kaff *et al.* (1998) silenced GUS expression in transgenic *Brassica napus* carrying the *gus* gene and a CaMV 35S promoter by infecting it with the CaMV. The homology of the promoter sequence was suggested to lead to the post-transcriptional silencing of the gene. The ACC constructs and the *gfp* gene both shared the CaMV 35S promoter, in the transformation experiments.

Manipulating either the explant and/or the bacterium to enhance virulence can increase transformation efficiency (Henzi *et al.*, 2000). In this work, transgenic root production was significantly improved by manipulation of the explant in treatment 2. In treatment 2, explants were inoculated after the excision of only 50 seedlings, whereas in treatment 1 this number could be up to 208. The shorter handling time in treatment 2, suggests that the newly excised tissue was more susceptible to *Agrobacterium*-mediated transformation. Braun (1954, 1978) found that tomato remained susceptible to tumourigenesis for up to two weeks after excision but these plants even when treated with acetosyringone never achieved

susceptibility equal to plants inoculated directly after wounding. Inoculating plants directly increased transformation efficiency in these experiments but it was still very low. For many plant species or cultivars/ecotypes, T-DNA integration is the most limiting factor for transformation protocols. This has been demonstrated by relatively efficient transient expression of reporter genes but poor stable transformation (Gelvin, 2000). It is therefore important to enhance the virulence of the bacterium, susceptibility of the plant, and the rate of stable T-DNA integration into the plant genome to optimise transformation efficiencies.

Transformation efficiency was observed to vary between the constructs used. Inoculation of GDDH33 with the *A. rhizogenes* strain carrying the *ACC synthase* antisense construct produced significantly greater numbers of explants with excisable transgenic roots ( $p < 0.001$ ). Most plants species contain multiple *ACC synthase* genes that can be quite divergent in DNA sequence, so it is possible that the function of the *ACC synthase* identical to the construct may have been silenced but replaced by another. Transformation efficiency increased 10-fold, with the inoculation of the *gus* construct in treatment 2, but not with the *ACC* constructs. The *gus* construct should not affect ethylene biosynthesis whereas it is possible with the *ACC* constructs. This suggests that regulation of this plant hormone is important for *Agrobacterium*-mediated transformation. Konings and Jackson (1979) working with tomato, rice and white mustard found that roots which elongated more rapidly, produced ethylene at the highest rate, and those species whose roots grew slowly produced only small amounts of the hormone. Chi *et al.* (1990) observed that silver nitrate (an inhibitor of ethylene perception) inhibited rooting, and AVG (an inhibitor of ethylene biosynthesis) inhibited root elongation in *Brassica juncea* plants. The *gus* control and the *ACC synthase*

antisense root lines produced rapidly growing roots. The constructs with poor transformation efficiencies produced roots with poor growth *in vitro* that often led to root mortality after a few subcultures.

Transgenic root growth was generally poor throughout all of the transformed GDDH33 lines. They did not show the characteristic plagiotropic growth as seen in other *Brassica* cultivars such as Shogun (Henzi *et al.*, 2000). Berthomieu and Jouanin (1992) similarly transformed a doubled haploid line of a rapid cycling cabbage (*Brassica oleracea* L. var. *capitata*) with *A. rhizogenes*. Nine roots were cultured of which four grew fast in hormone-free medium, but after two subcultures, significantly reduced their growth rate. The other five transformed roots grew very poorly and could not be significantly improved by using media with additional macro-elements or hormones. The lack of root growth is probably genotype-dependent, as other cultivars have proved very amenable to rapid growth in tissue culture (Henzi *et al.*, 2000).

The green fluorescent protein (GFP) was an excellent *in planta* reporter of transgene expression in *Brassica* hairy roots. It was a rapid, non-destructive technique that did not require exogenous substrates, thus making it more effective than the *gus* reporter gene (Jefferson *et al.*, 1987) and the *luc* gene (Ow *et al.*, 1986). Hairy roots expressing GFP were clearly distinguishable from those that had not been transformed, and were easily removed and cultured.

Inoculation with the *A. rhizogenes* co-integrate strain produced 96% co-transformed roots. This was higher than the 50% achieved by Komari *et al.* (1996) when rice and tobacco were co-cultivated with an *Agrobacterium* strain carrying a super binary plasmid with two different T-DNAs, and greater than that of Depicker *et al.* (1985) who reported co-transformation frequencies of 60-70% with tobacco

protoplasts. The success of co-transformation may be attributed to the co-integrate strain. It minimised the types of DNA being transferred to two: the root inducing T<sub>L</sub>-DNA and the gene of interest T-DNA, and the need for only one strain. Gelvin (1990) demonstrated the high efficiency of T-DNA transference by *Agrobacterium* through transient gene expression, so the limiting factor may have been *Ri* T<sub>L</sub>-DNA integration. When the 21Kbp *Ri* T<sub>L</sub>-DNA was integrated into the plant genome, 96% of the time the smaller 2-3Kbp binary vector T-DNA was also integrated. McCormac *et al.*, (2001) achieved 100% co-transformation of *Nicotiana tabacum* with the premise that the co-transformed T-DNA must be 2-fold smaller than the selected T-DNA region. If the two T-DNA sequences have integrated into the plant genome at physically unlinked sites it provides the opportunity to recover marker-free, phenotypically normal plants as shown by Puddephat *et al.* (2001).

Whole T<sub>0</sub> plants were regenerated from transgenic hairy root lines containing T-DNA constructs with the *B. oleracea ACC oxidase 1* and *2* and *ACC synthase* cDNAs in both sense and antisense orientations. Five lines had been transformed with sense constructs, 10 with antisense, and 3 with *gus*. It is difficult to draw conclusions about whether these constructs had any effect on root production without ethylene measurements. It is possible to argue that the promoters were actively producing mRNA transcripts as shown by the GFP and GUS assays, but impossible to determine whether this had any physiological effect. There is an overwhelming body of literature suggesting that ethylene is inhibitory to shoot formation, and that reducing it would enhance regeneration. Inhibitors of ethylene production (AVG) and ethylene action (silver ions) have been used to enhance shoot production of *Brassica oleracea* var. *italica/gemmifera* (Sethi *et al.*, 1990), *Zea mays* (Songstad *et al.*, 1988), and *Triticum aestivum*

(Purnhauser *et al.*, 1987) from callus. In *Helianthus annuus*, ethylene appeared to enhance callus formation but inhibited shoot production (Robinson and Adams, 1987). However, the role of ethylene in cultured plant cells and tissues remains unclear (reviewed by Kumar *et al.*, 1998).

Pua and Chi (1993) reintroduced the *ACC oxidase* of *B. juncea* in antisense orientation, producing lines that showed a greater capacity for shoot morphogenesis than the controls. This was not the case in the present experiments as actively growing tissue was the most important factor. Actively growing tissue was found in lines with the *gus* control and *ACC synthase* antisense constructs, which should be able to produce ethylene, but were more amenable to regeneration. Pua and Chi (1993) associated the presence of ethylene with culture browning, which is inhibitory to cell growth and/or differentiation. Culture browning is a major problem for tissue culture, but was necessarily related to ethylene in the current experiments, as this would have selected for lines that down-regulated ethylene and not those of the control or sense lines. This is not observed, so other factors may play a role in tissue browning.

It was demonstrated that the ACC constructs had affected regeneration by the time it took between inoculation of the explant and production of a mature broccoli head. The lines transformed with the *gus* construct, which would not manipulate ethylene, matured significantly faster ( $p < 0.001$ ), than the lines containing the ACC constructs. It suggests that ethylene is required for normal plant developmental growth.

Initially, explants were inoculated with *A. rhizogenes* strain LBA 9402 pRi1855::GFP (Spano *et al.*, 1982, Puddephat *et al.*, 2001) carrying the constructs

(chapter 2) on the binary plasmids. Transformants were selected for by 'hairy root' green fluorescence under long-wave UV light, and regenerated through tissue culture. The rate of co-transformation of the host genome by the T<sub>L</sub>-DNA and binary T-DNA was found to be 96% with the *gus* root lines. DNA was extracted from leaf material of regenerants and checked for the presence/absence of the *gfp* gene by PCR. As the *gfp* gene is located on the T<sub>L</sub>-DNA region it is used as a marker for identifying inserts containing the *rol* genes. The PCR confirmed that the target DNA sequence was present in the samples, although it may be argued that the DNA may have not integrated into the plant genome or have been present as a result *A. rhizogenes* contamination. The southern blots and hybridisation with specific DNA probes was carried out to determine copy number and stable integration of the T-DNAs into the plant host genome. The main limitation to this procedure was extracting DNA without co-purifying charged polysaccharides. The Kirby method was most effective, and although leaving traces of polysaccharides, was digested with the *Sst*I restriction endonuclease as shown in Figures 3.8 and 3.11. The impure DNA led to the diffusion of some of the samples from the wells of the gels after loading, and also made it difficult to equalise the amounts of DNA in each lane. However, data for *gfp* inserts was obtained for 8 of the lines, showing that copy number ranged from 1-4 inserts. The number of inserts did not appear to have any effect on the 'hairy root' phenotype shown by the T<sub>0</sub> regenerants (Table 3.7). For example, 28/00 *aco1A* 3 contained 4 *gfp* inserts and had a weak *rol* phenotype, whereas 5/00 *aco2S* 1 had a moderate phenotype with only 1 insert. The effects of insert number on phenotype suggest either position effects or possible silencing as the one copy of 5/00 *aco2S* 1 was more active than the 3 copies in 28/00 *aco1A* 3. There is no data for the regenerants with severe *rol* phenotype as the extraction did not produce very pure DNA.

The DNA extracted by the Kirby method was used to confirm presence of the construct binary T-DNA in the plant genomes. A PCR was carried out with sequence specific primers to the CaMV 35S promoter and cDNAs of the particular genes. All of the primer pairs worked except for *aco1S* that produced a smear. The negative results from 7/00 *acsA* 13 and 9/00 *acsA* 2 suggest no construct T-DNA insert, as the DNA had been amplified with the *gfp* primers. Only 6 lines produced positive bands for the constructs in the autoradiographs, and copy number ranged from 1-3. The results from the autoradiographs did not always match the PCR data as the Southern blots may have been improved with pure DNA at the same concentration. However, this has shown that T-DNA insert copy number appears to range between 1 and 3 in the plant genome of GDDH33.

The *A. rhizogenes*-mediated transformation produced 18 T<sub>0</sub> plants, all derived from single cells. It is important that each cell of the transformants contains the new construct for quantifying the impact of the transgenes on plant physiology, including the analysis of ethylene and chlorophyll. Berthomieu *et al.* (1994) produced a high frequency of chimeric plants with an *A. tumefaciens* protocol that would have been undesirable. The impact of the *rol* genes was severe in 4 of the 18 lines showing extremely wrinkled leaves, shortened internodes and smaller heads with reduced chlorophyll. These characteristics, termed the 'hairy root syndrome' by Tepfer (1990), have been attributed to certain loci following knockout experiments. Wrinkled leaves and reduced internodal distance are caused by *rolA* (Sinkar *et al.*, 1988); *rolB* produces flower heterostyly and abundant adventitious rooting (Cardarelli *et al.*, 1987); while *rolC* results in reduced apical dominance, altered leaf morphology and reduced seed production. It is not uncommon to produce a variable phenotype when regenerating from *A.*

*rhizogenes* transformed plants. Christey *et al.* (1999) produced a range of morphological differences with 20% normal phenotype, 40% moderate or slight hairy root phenotype and 40% with severe phenotype.

The negative effects of *rol* genes on plant mortality have not previously been reported. In these experiments, only 31% of the plants with severe hairy root phenotype grew to maturity. Eighty-nine percent of plants with a normal phenotype and 67% with a moderate phenotype survived. The plants with severe phenotype were also more susceptible to biotic and abiotic stresses in the glasshouse.

In total, there were approximately 6000 seeds recovered from 11 of the T<sub>0</sub> lines. This is a very high yield considering the heads were removed for ethylene and chlorophyll analysis (chapter 4) and floral organs had to grow from offshoots. It is not surprising that there were no seeds recovered from plants with severe *rol* phenotype as they had very small heads so even the offshoots were removed for the analysis. It is difficult to compare seed production from different lines as there were disparate plant numbers and varying degrees of decapitation. It does show that the constructs and T<sub>L</sub>-DNA were not too inhibitory on seed production. Sixty-seven progeny from 69 seeds of 28/00 *aco1A* 3 were tested for the presence or absence of the *gfp* and *aco1A* DNA sequences by PCR. The autoradiographs had shown that there were 4 T<sub>L</sub>-DNA and 2 construct T-DNA inserts. The largest group of segregants were the double-positives with 56% suggesting a possible linkage. The smallest group with 3% were the segregants that only contained an *aco1A* insert. These data suggest that the T<sub>L</sub>-DNA and the construct T-DNA that have co-transformed together are physically linked. It also shows, that given enough seeds it is possible to segregate out the unwanted marker genes to leave phenotypically

normal transgenic plants that contain desirable characteristics through this transformation protocol.

As the main aim of this part of the project was to transform GDDH33 and regenerate transgenic plants, there were aspects that could have been improved. If there had been more time available it would have been useful to improve the transformation efficiency by enhancing the virulence of the bacteria, or T-DNA integration. Researchers have used acetosyringone and mannopine along with feeder layers to improve virulence (Henzi *et al.*, 2000), but the main limiting factor appears to be T-DNA integration (Gelvin, 2000). If there had been more transgenic root available it would have been possible to take ethylene measurements, and determine the impact on growth and regeneration. It would have also been possible to add either substrates (ACC) or inhibitors of ethylene (silver ions/AVG) to the media to obtain the optimum combination for both root growth and regeneration. In future experiments, it might be worth using a broccoli post-harvest head-specific promoter that does not interfere with root physiology such as the senescence-related promoter used by Gan and Amasino (1995).

In these experiments, the *A. rhizogenes* co-integrate strain LBA 9402 pRi1855::GFP containing *B. oleracea* ACC oxidase 1 and 2 and ACC synthase in sense and antisense orientations transformed the doubled haploid calabrese line GDDH33 with an overall efficiency of  $3.6 \pm 0.6\%$ . Transformation efficiency was greater with constructs that did not manipulate ethylene, and improved by inoculating the cut surface soon after excision. The GFP reporter gene was an effective marker for transgene expression in hairy roots. It was used with the *gus* gene to produce 96% co-transformed roots. Reducing ethylene may have had an adverse effect on root growth but beneficial on shoot regeneration, although the

most important factor for regeneration was that the tissue was actively growing. Confirmation of transformation and stable integration of T-DNA inserts was achieved by PCR and Southern blots. The copy numbers of these two species of T-DNA ranged from 1-4 inserts, which did not relate to the extent of the severity of the *rol* phenotype. The *rol* genes had negative effects on 4 out of 18 T<sub>0</sub> plants reducing the size of plant and increasing mortality. It was possible to obtain viable seed from 11 of the T<sub>0</sub> plants and test some of them for segregation of T-DNAs. It showed that the T-DNAs were probably physically linked, but it was possible to produce marker-free, phenotypically normal plants with a desirable characteristic.

Given more time and root tissue, the efficiency of the processes may have been improved, but the main aim of producing transgenic plants containing the ACC cDNAs in sense and antisense orientations to be measured for post-harvest ethylene production was achieved.

# **4.0 Analysis of broccoli bud post-harvest ethylene production and chlorophyll levels**

#### 4.1 Introduction

Broccoli is one of the most successful 'new' crops in the United Kingdom. The crop value of home produced marketed broccoli has doubled from £18.9m to £44.9m in the last 10 years (DEFRA statistics, 2000), where there has been an overall decline of marketed *Brassicas*. Broccoli crops of the same variety treated in the same way after harvest vary in their post-harvest performance (D. Pink, pers. comm. HRI-Wellesbourne). This lack of predictability results in the major retailers specifying a product life of only two days from delivery to 'purchase before date', and a further two days 'best consumed by' in an attempt to ensure a 'quality' product for the consumer. This short post-harvest life results in significant waste for the retailer (a cost borne by the consumer) and consumers themselves.

Broccoli is a floral vegetable, harvested when the flowering heads are immature and growing rapidly (King and Morris, 1994a,b). Each broccoli floret is composed of male and female reproductive structures surrounded by immature petals and enclosed within chlorophyll containing sepals (Pogson *et al.*, 1995a). Post-harvest senescence is characterised by floret chlorophyll loss resulting in the yellowing of sepals (Wang, 1977). Sepal yellowing commences between 24 and 48h after harvest (20°C) and is essentially complete by 96h (Tian *et al.*, 1994). It is a relatively late event in the post-harvest senescence of broccoli preceded by major losses of sugars, organic acids and proteins (King and Morris, 1994).

Endogenous ethylene production is suggested to have an important role in the colour change of stored broccoli (Hyodo *et al.*, 1994; King and

Morris, 1994). Exogenous ethylene treatment has been shown to accelerate yellowing of broccoli (Aharoni *et al.*, 1985) and the effect has been attributed to stimulation of endogenous ethylene production (Makhlouf *et al.*, 1992) and increased tissue sensitivity to ethylene (Tian *et al.*, 1994). Furthermore, ethylene biosynthetic inhibitors such as aminoethoxyvinylglycine and inhibitors of ethylene action (silver ions and methylcyclopropene) delay chlorophyll loss (Wang, 1977; Ku and Wills, 1999).

In plants, ethylene production is induced during several developmental stages, including fruit ripening, seed germination, leaf and flower senescence, and abscission. It is also induced by external factors, such as wounding, anaerobiosis, viral infection, auxin treatment, chilling injury and drought (Abeles, 1973; Yang and Hoffman, 1984). Ethylene biosynthesis occurs via the enzymes ACC synthase and ACC oxidase, which catalyse the conversions of S-adenosylmethionine to 1-aminocyclopropane-1-carboxylic acid (ACC) and ACC to ethylene, respectively (see Figure 1.2) (Yang and Hoffman, 1984). In this pathway, the conversion of SAM to ACC is generally regarded as the rate-limiting step, although there is a large body of evidence indicating that regulation of ACC oxidase is also important (Yamamoto *et al.*, 1995; Barry *et al.*, 1996).

Detailed studies of the physiological changes occurring within individual broccoli florets after harvest suggest that the reproductive structures of the floral buds may exert some influence over chlorophyll loss. An increase in ACC oxidase activity and ethylene production occurs in the reproductive structures and removal of these significantly reduces the rate of sepal yellowing (Tian *et al.*, 1994). Senescence in carnations and orchid flowers is

associated with increased ethylene production arising from concomitant increases in both ACC synthase and ACC oxidase (Woodson *et al.*, 1992; O'Neil *et al.*, 1993). Tissues producing ethylene also become more sensitive to ethylene due to increased expression of ethylene receptors (Payton *et al.*, 1996).

Pogson *et al.* (1995a) isolated two cDNA clones, *ACC oxidase 1 (aco1)* and *ACC oxidase 2 (aco2)* from a *Brassica oleracea* L. var. *italica* cDNA library, derived from florets 48h post-harvest. The lengths of the *aco1* and *aco2* were 1237 and 1232bp, respectively. They shared nucleotide identity of 83% in their putative translated regions (86% amino acid identity) and 48% in the 3' untranslated regions. Transcripts were found at low levels in whole florets at the time of harvest and increased markedly in abundance after harvest. *aco1* transcript abundance also increased in sepals after harvest and in excised yellowing leaves. Transcripts corresponding to *aco2* were found exclusively within the reproductive structures and accumulated to high abundance post-harvest. Pogson *et al.* (1995b) also isolated an *ACC synthase (acs)* cDNA clone from *B. oleracea* with an apple cDNA probe. The transcript abundance of *ACC synthase* did not change in florets 0, 24, 48, 72h after harvest and was detected in similar abundance in green and senescing leaves. *ACC synthases* are known to belong to multigene families and there at least three different classes of *ACC synthase* in tomato (Rottman *et al.*, 1991). *ACC synthase* sequences are very divergent at the nucleotide level (Yang and Oetiker, 1998), and it is possible that the cDNA apple probe used by Pogson *et al.* (1995b) may not have hybridised to all of the cDNAs encoding for ACC synthase enzymes. At least two other ACC synthase

cDNAs have been identified (Gonzalez and Botella, 2001) in post-harvest broccoli, which share 38% and 42% nucleotide identity with the clone isolated by Pogson *et al.* (1995b).

Gene silencing with sense genes has been an important method for down-regulating the expression of endogenous plant genes (for review see Meyer and Saedler, 1996). However, the efficiency of silencing is unpredictable and the underlying mechanisms are unknown (Hamilton *et al.*, 1998). It is possible that sense constructs may up-regulate genes causing an over-expression of transcripts that can also reveal information about gene function. Hamilton *et al.* (1990) reduced ethylene synthesis in tomato fruit by 93%, by transformation with pTOM13 an *ACC oxidase* in antisense orientation in relation to a cauliflower mosaic virus (CaMV) 35S promoter. Henzi *et al.* (1999a, b) transformed *Brassica oleracea* L. var. *italica* with the same pTOM13 construct. There was generally greater production of ethylene in the flowers at 26h post-harvest in the transgenic lines than in the untransformed control and therefore, the construct did not reduce post-harvest ethylene production or chlorophyll loss. The tomato *ACC oxidase* only shared 70% nucleotide identity to the native *B. oleracea ACC oxidases*, which may not have been enough for effective gene-silencing.

The *B. oleracea* L. var. *italica ACC oxidase 1 and 2 and ACC synthase* cDNAs have been obtained from Pogson *et al.* (1995), and ligated between a CaMV 35S promoter and nopaline synthase (*nos*) terminator in sense and antisense orientations (chapter 2). Additionally, a  $\beta$ -glucuronidase gene (*gus*) (Jefferson *et al.*, 1987) was ligated between the same promoter and terminator for a control. Constructs were inserted into the T-DNA region of

pSCV1.0 (Biogemma) and introduced into the *Agrobacterium rhizogenes* co-integrate strain LBA 9402 pRi1855::GFP by electroporation (chapter 2).

Doubled haploid genotypes possess uniform genetic backgrounds, which are useful for breeding, gene mapping and quantifying an additional trait by plant transformation. In a field trial conducted at HRI, the post-harvest shelf-life of broccoli cultivars was assessed. The mean time for bud yellowing of GDDH33 was 46h 19min, 53h 23min for a doubled haploid line of Shogun and 81h 28min for Marathon F1 (D. Pink, pers. comm. HRI-Wellesbourne). As GDDH33 had the poorest shelf-life performance it was selected as a model to test the relation between post-harvest ethylene production and chlorophyll loss.

Explants of GDDH33 were inoculated with *Agrobacterium rhizogenes* co-integrate strain LBA 9402 pRi1855::GFP and transformants were selected to be regenerated into whole plants (see chapter 3). Seventeen lines were regenerated: 3 *aco1* antisense, 2 *aco1* sense, 2 *aco2* antisense, 2 *aco2* sense, 4 *acs* antisense and 1 *acs* sense and 3 *gus*.

The aim of the research was to a) determine the non/post-harvest physiological changes of ethylene and chlorophyll in the untransformed GDDH33 broccoli buds; b) test the post-harvest broccoli buds of T<sub>0</sub> plants for ethylene production and chlorophyll loss; c) to determine if there is a relationship between post-harvest ethylene production and chlorophyll loss in senescing buds; and d) to assess whether a transgenic method could produce broccoli florets that retain chlorophyll for a greater time and increase product shelf-life.

It was necessary to develop assays to measure ethylene and chlorophyll from broccoli florets. Previous studies have measured ethylene and chlorophyll from whole heads, florets and branchlets (King and Morris, 1994a,b; Pogson *et al.*, 1995a). Tian *et al.* (1994) used a more elegant approach by focusing on the floral buds. These were the organs responsible for post-harvest production of ethylene and experienced chlorophyll loss in the sepals.

## 4.2 Materials and Methods

### 4.2.1 Harvested broccoli heads

GDDH33 is a doubled-haploid line derived from the calabrese cultivar Green Duke through anther culture. It was grown from seed to head maturity in the glasshouses of HRI Wellesbourne (15°C min with forced air at 18°C, day length extension to 14h by high pressure sodium lamps) throughout the year in 15cm pots with non-sterile compost (a 80:20 mix of Levington M2 and vermiculite). Transgenic lines were produced by transformation of GDDH33 with *A. rhizogenes* co-integrate strain LBA 9402 pRi1855::GFP carrying *Brassica oleracea ACC oxidase 1* and *2* and *ACC synthase* cDNAs (Pogson *et al.*, 1995a,b) in sense and antisense orientations in relation to a CaMV 35S promoter and *nos* terminator and a *gus* gene construct (Jefferson *et al.*, 1987) on the binary vector T-DNA. Seventeen transgenic lines were regenerated for analysis (shown in Table 4.1). They had been regenerated from hairy roots, though a callus phase into plantlets. These were grown to maturity in air conditioned container glasshouse compartments set to maintain 22°C by forced air ventilation with a minimum 14 hours photoperiod at HRI Wellesbourne, throughout the year.

**Table 4.1** Transgenic lines regenerated by tissue culture

<b>Experiment No.</b>	<b>ACC cDNA*</b>	<b>Sense/ Antisense</b>	<b>Explant no. producing gfp root</b>
28/00	<i>aco1</i>	A	3
34/00	<i>aco1</i>	A	1
34/00	<i>aco1</i>	A	4
32/00	<i>aco1</i>	S	3
33/00	<i>aco1</i>	S	4
3/00	<i>aco2</i>	A	2
33/00	<i>aco2</i>	A	3
5/00	<i>aco2</i>	S	1
26/00	<i>aco2</i>	S	1
7/00	<i>acs</i>	A	12
7/00	<i>acs</i>	A	13
9/00	<i>acs</i>	A	1
9/00	<i>acs</i>	A	2
7/00	<i>acs</i>	S	7
5/00	<i>gus</i>	-	1
33/00	<i>gus</i>	-	3
34/00	<i>gus</i>	-	2

\**aco1* =ACC oxidase 1, *aco2*= ACC oxidase 2, *acs* = ACC synthase, *gus*=  $\beta$  glucuronidase

At maturity, whole heads were harvested in the morning at 9-10am, and transported to the laboratory within 20min. Heads were surface sterilised with 100ppm NaOCl as described by Rushing (1990) and placed into a 20°C incubator in the dark. At 0, 24, 48, 72 and 96h post-harvest, samples of 0.2g floral buds were removed from the broccoli heads with a scalpel. There were 12 different head replicates for each time sample, for the untransformed

GDDH33 and 3 replicates for the T<sub>0</sub> lines. At head maturity, bud samples were also taken directly from the untransformed control plants growing *in situ*. These samples were termed 'non-harvested' as the heads from which the buds were removed were still attached to the stem. Floral buds were removed from 12 intact broccoli heads with a scalpel at 0, 24, 48, 72 and 96h.

#### 4.2.2 Ethylene Measurements

A serial dilution of ethylene was prepared to calibrate gas chromatograph readings with ethylene concentrations. A 25ml flask was submerged in water to displace its air. It was filled with ethylene (BOC) to displace the water and fitted with a gas-tight subbaseal (Fisher). Three 1L volumetric flasks were filled with water, which was concurrently displaced with nitrogen (BOC) and the flasks sealed. A volume of nitrogen was removed and replaced with saturated ammonium sulphate (Sigma) to leave a final volume of 1L of nitrogen. A 1ml volume of ethylene was taken from the 25ml flask and added to the first volumetric flask with 1L nitrogen to make a 1:1000 dilution. This was mixed and left for 30 minutes. A 1ml sample was taken from this flask and added to the next to make a 1:1000 000 dilution. Twelve samples were taken from the 1ppm flask to calculate an average, for standardising ethylene measurements from the broccoli buds.

At each sample point, 0.2g (fresh weight) of floral buds from the broccoli heads were placed into a 25ml glass specimen bottle and fitted with a subbaseal (see Figure 4.1b). Sealed bottle, with buds, were placed in a 20°C incubator in the dark for 1h. Three 1ml gas samples were then taken with a gas-tight fixed-needle glass syringe and injected into a gas chromatograph

(GC, Analytical Instruments Model 93). The GC was fitted with a flame ionisation detector containing a 2.0mm diameter stainless steel column packed with Poropak Q (80-100 mesh) and a Spectra Physics integrator (see Figures 4.1a,c). The oven temperature was kept constant at 100°C while the column was kept at 60°C. In these conditions it took ethylene 1.3min to pass through the column. A value was recorded which could then be converted to an amount of ethylene using the calibration.

#### *4.2.3 Chlorophyll Measurements*

A system to measure chlorophyll levels was devised. An experiment was set up to test the speed of chlorophyll diffusion from broccoli buds into methanol. Three replicates of 0.2g broccoli buds were added to 5ml of methanol in 10ml round-bottomed tubes in the dark at 20°C (see Figure 4.4). Samples of 100µl were taken after 60min for each, up to 480min. A second experiment was set up to observe the effects of light on chlorophyll. Two broccoli bud samples of 0.2g per head were taken from 6 heads and placed in 5ml methanol, in 10ml round-bottomed tubes. One treatment was placed in the dark at 22°C, while the other was kept in the light (mix of 70 W white and 65/80 W gro-lux fluorescent tubes providing an irradiance of 80 µmol m<sup>-2</sup> s<sup>-1</sup>) at 22°C. Chlorophyll amounts were measured for all samples according to Hipkins and Baker (1986).

All chlorophyll measurements for untransformed and transgenic lines of GDDH33 were standardised. The 0.2g of floral broccoli buds from the ethylene measurements were transferred to a 10ml round-bottomed tube. Five millilitres of methanol (BDH analaR grade) were added to the buds and

left overnight at 20°C in the dark. A 1ml sample was added to a cuvette and measured using a single beam spectrophotometer, 10mm cell with absorbance at 645 and 663nm. The values were converted to microgram chlorophyll per gram fresh weight of broccoli buds (see Table 4.2).

**Table 4.2** The concentration of chlorophyll (Chl) in the cuvette was calculated using simultaneous equations, based on the absorbance readings at 645 and 663nm (Hipkins and Baker, 1986).

<b>Chl a</b>	<b>12.7 A<sub>663</sub> - 2.69 A<sub>645</sub></b>
<b>Chl b</b>	<b>22.9 A<sub>645</sub> - 4.68 A<sub>663</sub></b>
<b>Chl (total)</b>	<b>20.2 A<sub>645</sub> + 8.02 A<sub>663</sub></b>

#### 4.2.4 Measuring dry weight of broccoli buds

A 9cm diameter Whatman 1 filter paper was folded to fit into a 10cm diameter pyrex funnel. The 5ml of methanol and broccoli buds were decanted onto the filter paper. The tube was then filled with 10ml of water, which was also decanted onto the filter paper. Only the buds remained on the filter paper after this procedure. The filter paper was then placed in a 5cm by 5cm brown paper envelope and dried at 60°C for 2 days. Dried buds were weighed on a microbalance and values recorded. These values were used to calculate ethylene production nanolitre per gram dry weight of broccoli buds per hour.

#### 4.2.5 Data Analysis

Statistical analyses were carried out on the data. The comparison of sample means was performed with Students T-Test, and calculating the probability of regression with an Analysis of Variance (ANOVA) test.

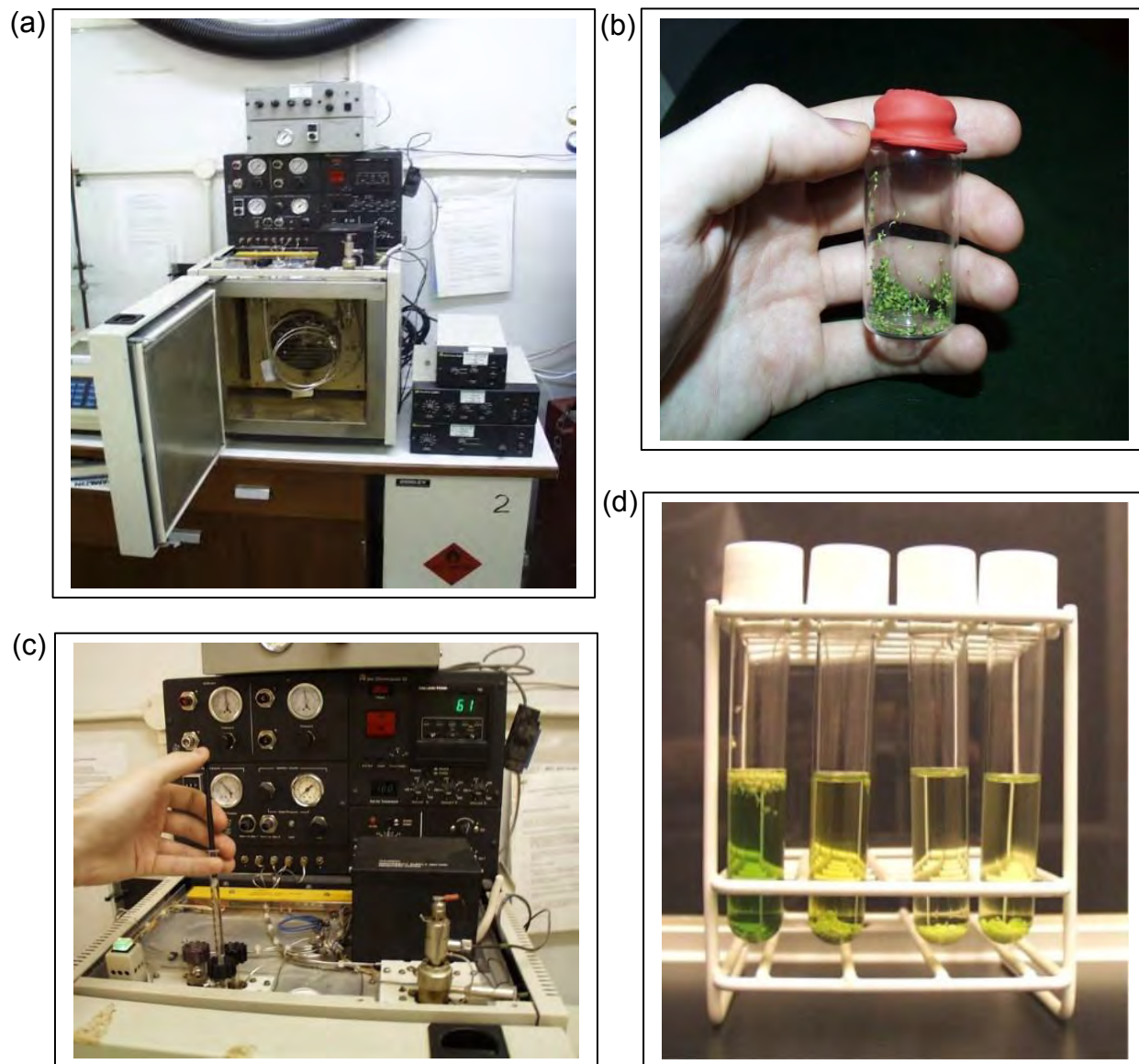


**Figure 4.1** (a) Gas chromatograph; (b) Glass container with broccoli buds evolving ethylene; (c) Injecting 1ml air sample taken from (b); (d) Chlorophyll diffusing from broccoli buds in 5mls methanol.

## 4.3 Results

### 4.3.1 Tissue to be assayed

The first experiments were designed to provide quantitative assays for measuring ethylene and chlorophyll from broccoli heads. Whole heads were the first tissue samples to be used but these gave inconsistent ethylene values, because the stalks were of different weights. The whole heads also gave off volatiles that were interfering with the column of the gas chromatograph, so that ethylene measurements were inconsistent between samples. It was decided to focus on broccoli buds for the ethylene and chlorophyll assays as these provided consistent ethylene results and could easily be used for chlorophyll assays.

### 4.3.2 Controls for standardising the analysis of ethylene and chlorophyll

#### 4.3.2.1 Calculating ethylene concentrations

The GC value for 1ppm ethylene was  $7419 \pm 93$ . The amount of ethylene produced (nl) for 1g (dry weight) of broccoli buds per hour is calculated from the expression: [mean ethylene value from 3 measurements/ ethylene value for 1ppm (7419)] x weight conversion factor (converts dry bud weight to 1g i.e 1/value) x volume of air in specimen tube (25mls).

At 20°C, the rate of diffusion of chlorophyll from broccoli buds in methanol was time dependent (see Figure 4.2). In this experiment, after 300 minutes the rate of diffusion began to level off as all of the chlorophyll had diffused into the methanol. The total quantity of chlorophyll per sample is an absolute value, and represents the amount in the broccoli buds at any given

time. As this could only be obtained by leaving the buds for at least 480min, it was decided to leave the broccoli buds overnight, in the dark.

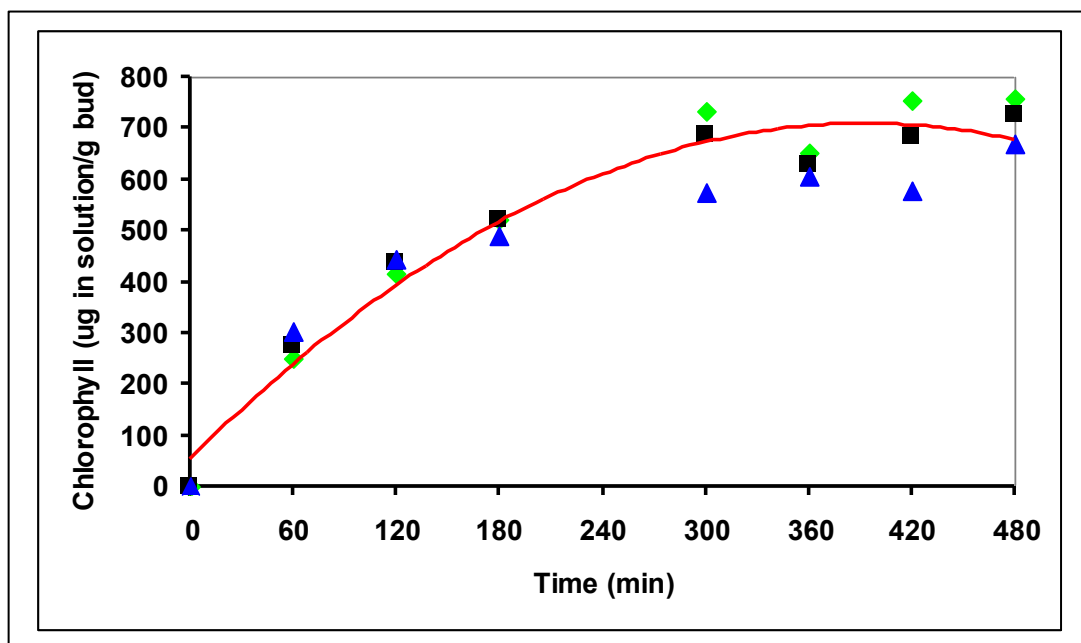


**Figure 4.2** The rate of diffusion of chlorophyll at 20°C in the dark, from 0.2g broccoli buds in 5ml methanol. Sample 1 (■) , sample 2 (▲), sample 3 (◆).

#### 4.3.2.2 Analysis of pre/post harvest ethylene production and chlorophyll levels in broccoli buds of non-transformed GDDH33

In Figure 4.3, the basal amount of ethylene produced by non-harvested GDDH33 broccoli buds was  $44 \pm 1$ nl/g bud/h. After harvesting, an increase in ethylene production was observed. There was little physiological change at 0h between harvested ( $61 \pm 1$ nl/g bud/h) and non-harvested buds ( $44 \pm 1$ nl/g bud/h). The major difference occurred at 24h, when the harvested buds produced  $176 \pm 18$ nl/g bud/h ethylene, significantly more than the non-harvested buds with  $44 \pm 1$ nl/g bud/h [ $t(df)= 7(24) p<0.005$ ]. This peak is clearly a response to harvest, and stays high for 48h ( $116 \pm 13$ nl/g bud/h) before declining to the basal amount at 72h and 96h.

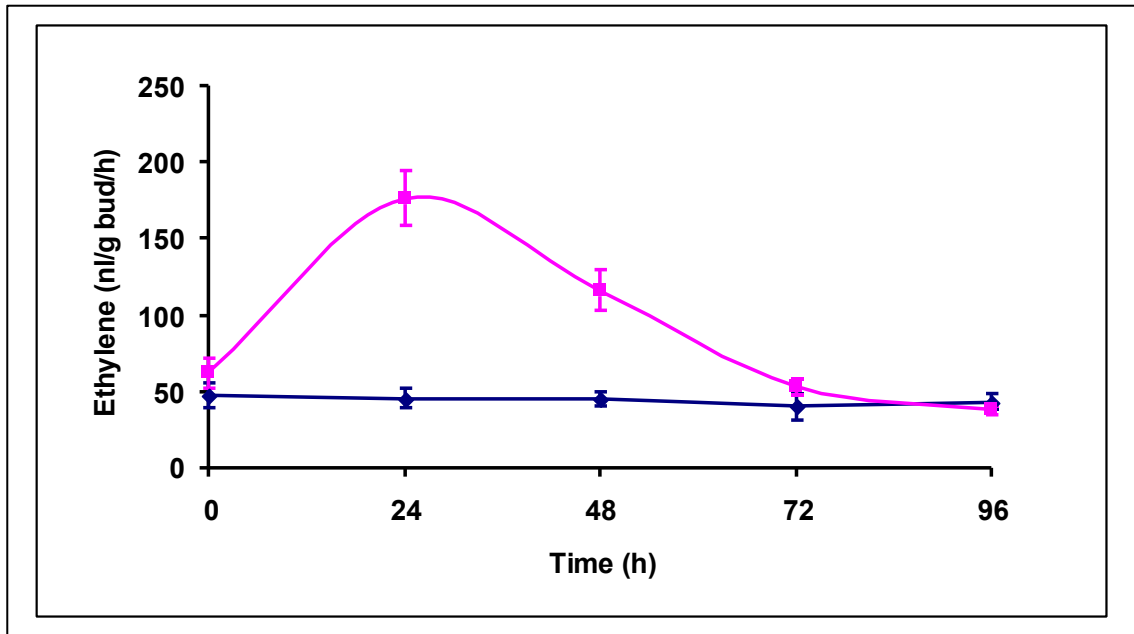


**Figure 4.3** Ethylene production by harvested/non-harvested untransformed GDDH33 broccoli buds. Harvested buds (■), and non-harvested (◆), n=1x12.

In Figure 4.4, the non-harvested broccoli buds had no detectable change in chlorophyll levels over this period of time with an overall mean of  $651 \pm 50 \mu\text{g/g bud}$ . The loss of chlorophyll in the harvested buds is a direct physiological response to the removal of the head. As with Figure 4.3, there was insufficient time for there to be much of a difference between non-harvested and harvested buds at 0h. The major reductions of chlorophyll levels occurred between 0h and 72h. Chlorophyll loss occurred very rapidly, initially at 24h, 26% was lost compared to 0h, and by 96h over 80% chlorophyll was lost.

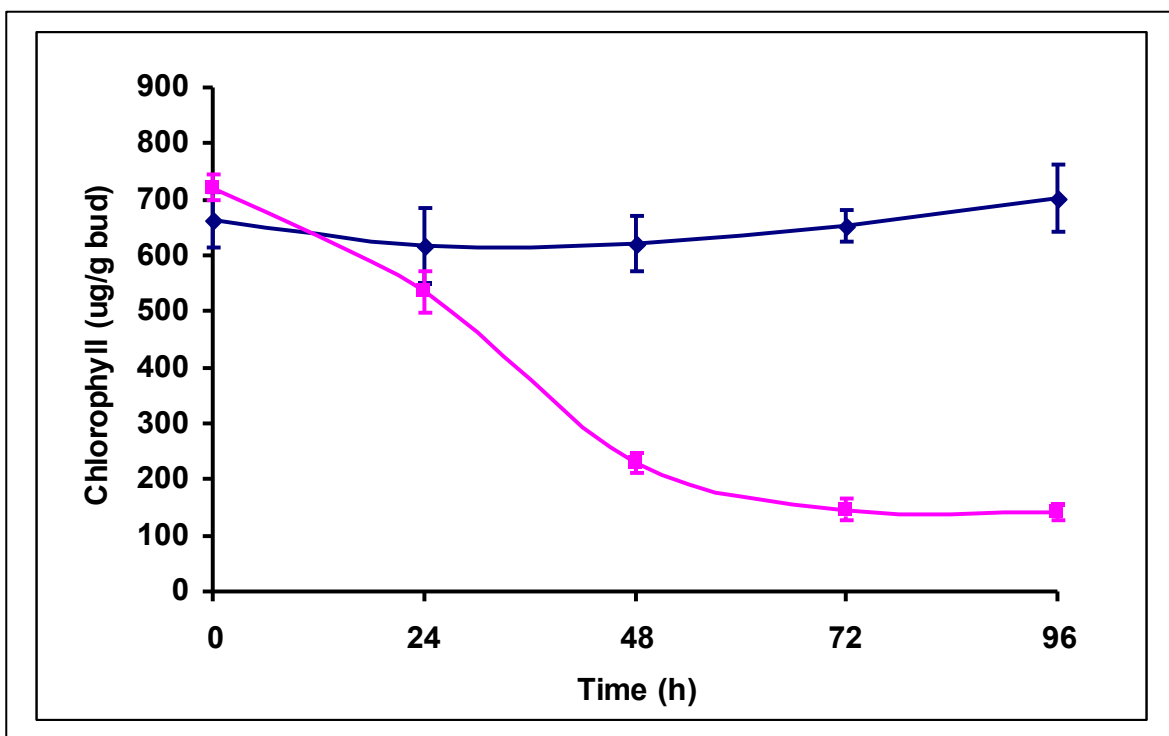


**Figure 4.4** Chlorophyll levels of harvested/non-harvested untransformed GDDH33 broccoli buds. Harvested buds (■), non-harvested (◆), n=1x12.

#### 4.3.3 Analysis of post-harvest ethylene production and chlorophyll levels of non-transformed GDDH33 and the transgenic lines

Tables 4.3 and 4.4 contain the underlying data for the Figures 4.5-4.14 as reference in the rest of this section. The data for 'construct lines' has been grouped together (for each particular construct) as all of the lines have performed similarly, except for *ACC synthase* antisense. The 'total' ethylene production is defined better as an 'ethylene production index' as it is not the total amount of ethylene that the broccoli buds have produced post-harvest, but the sum of the recorded values over 96h. The percentage of chlorophyll loss in Table 4.4 is the difference between the value at 96h and that at 0h, expressed as a percentage.

**Table 4.3** Ethylene levels of GDDH33 buds post-harvest as nanolitres per gram bud (dry weight) per hour.

The means and SEs for each time point were calculated with numbers of lines (n) and numbers of replicates. For the constructs these were: untransformed GDDH33 n=1x12; and transformed with *gus*, n=3x3; *aco1* antisense, n=3x3; *aco1* sense, n=2x3; *aco2* antisense, n=2x3; *aco2* sense, n=2x3; *acs* antisense, n=4x3; and *acs* sense, n=1x3.

Constructs	Means						S.E.s				
	Time (h)						Time (h)				
	0	24	48	72	96	Total	0	24	48	72	96
Un-t	61.9	176.1	116.0	52.9	37.7	444.7	10.5	18.1	22.4	7.7	16.4
<i>gus</i>	56.9	114.6	99.7	42.9	52.3	366.4	9.6	26.1	25.4	19.2	11.0
<i>aco1A</i>	35.8	31.9	59.2	46.7	48.3	221.9	6.8	9.0	15.0	9.8	12.4
<i>aco1S</i>	23.4	59.3	49.8	30.3	31.0	193.7	3.7	12.3	12.0	10.4	12.0
<i>aco2A</i>	10.6	44.9	32.2	47.4	9.8	144.8	5.0	19.3	6.5	12.0	4.8
<i>aco2S</i>	52.6	49.1	39.9	54.0	65.7	261.3	8.0	8.1	5.4	11.5	13.5
<i>acsA</i>	59.0	79.9	74.8	92.1	48.9	354.8	10.9	20.1	11.3	15.4	8.6
<i>acsS</i>	245.6	7.3	79.4	77.1	30.9	440.3	65.2	4.7	39.7	16.6	30.9

**Table 4.4** Chlorophyll values of GDDH33 buds post-harvest as micrograms per gram bud (fresh weight).

The means and SEs for each time point were calculated with numbers of lines (n) and numbers of replicates. For the constructs these were: untransformed GDDH33 n=1x12; and transformed with *gus*, n=3x3; *aco1* antisense, n=3x3; *aco1* sense, n=2x3; *aco2* antisense, n=2x3; *aco2* sense, n=2x3; *acs* antisense, n=4x3; and *acs* sense, n=1x3.

Constructs	Means						S.E.s				
	Time (h)						Time (h)				
	0	24	48	72	96	%loss	0	24	48	72	96
Un-t	721.5	535.8	229.3	145.7	140.9	80.5	21.4	36.5	19.3	18.9	14.4
<i>gus</i>	409.7	387.9	338.7	164.4	159.1	61.2	48.7	44.1	38.7	48.9	34.2
<i>aco1A</i>	292.3	307.4	290.8	212.7	175.8	39.9	18.6	17.9	21.6	32.5	32.6
<i>aco1S</i>	355.8	379.8	379.2	305.1	361.7	-1.7	19.9	27.3	42.5	54.8	86.9
<i>aco2A</i>	365.8	399.1	273.5	293.3	299.7	18.1	52.2	35.6	26.4	20.6	45.8
<i>aco2S</i>	279.3	277.4	210.6	202.6	146.8	47.4	32.5	27.8	27.9	43.1	37.6
<i>acsA</i>	268.1	276.5	178.8	142.4	91.2	66.0	38.42	40.9	18.9	31.5	21.5
<i>acsS</i>	200.4	247.1	294.8	164.5	161.6	19.3	28.6	20.4	109.2	60.1	121.1

Figure 4.5 includes the post-harvest data of Figures 4.3 and 4.4 in one graph. It demonstrates the post-harvest elevation of ethylene production with rapid chlorophyll loss in untransformed GDDH33.

The *gus* control plants showed the impact of transformation on ethylene and chlorophyll levels in GDDH33 broccoli buds. The transformed plants in Figure 4.6 have reduced ethylene and chlorophyll levels in comparison to the untransformed control. The ethylene peak at 24h in Figure 4.5 of 176nl/g bud/h is reduced to 116nl/g bud/h in the transformed plants, but this is not significant [ $t(df) = 2(22)$ ,  $p > 0.005$ ], and the other values are comparable. The transformed plants produced 18% less 'total' ethylene over the time period compared to the untransformed control, as a result of the reduced peak. At 0h, there is a 43% reduction of chlorophyll from 721 $\mu$ g/g bud in the untransformed to 409 $\mu$ g/g bud in the transformed plants. However, the rate of chlorophyll loss in the transformed plant is also reduced and occurs mostly between 48 and 72h, after the ethylene peak. After 48h, there has only been 18% chlorophyll loss in the transformed plant, whereas there has been 68% in the untransformed. It is clear that the effects of transformation and regeneration have reduced ethylene production and the starting amount of chlorophyll, and also reduced chlorophyll loss.

In Figure 4.6, the effect of the transformation and regeneration reduced total ethylene production of GDDH33 buds by 18%. In Figure 4.7, the plants transformed with *aco1* antisense construct produced 50% less 'total' ethylene than the untransformed control and 32% less than the *gus* controls. At 24h, where the untransformed buds produced 176nl/h ethylene, the plants transformed with *aco1* antisense produced only 32nl/h, an 82% reduction and

significantly less [t(df)= 6(17), p<0.005], than the *gus* control. *aco1* antisense constructs reduced ethylene to the basal levels required for normal physiology shown in Figure 4.3. Chlorophyll loss started to occur at 48h, but over the whole time period lost only 40%, significantly less than the untransformed control [t(df)= 4(20), p<0.005], but not significantly less than 62% in the *gus* control. It is clear both the untransformed and *gus* controls started with more chlorophyll, and therefore had more to lose. However, the *aco1* antisense plants had more chlorophyll at 96h than both, so must have retained a much greater proportion.

Transformation of GDDH33 with the *aco1* sense constructs reduced ethylene and prevented chlorophyll loss (Figure 4.8), over this time period. Ethylene evolved from the broccoli buds produced the same shape curve as the controls with a peak at 24h. The *aco1* sense lines produced significantly less ethylene at 24h than the untransformed control [t(df)= 4(19), p<0.005]. This peak was 49% of the *gus* control, but was not significantly different [t(df)= 1.67(13), p>0.005].

The quantity of chlorophyll in *aco1* sense lines ( $355 \pm 20\mu\text{g/g bud}$ ) at 0h is similar to the *gus* control ( $409 \pm 48\mu\text{g/g bud}$ ). However, by 96h chlorophyll loss of buds in the *gus* line is significantly greater [t(df)= 2.55(19), p<0.005] than in the *aco1* sense line where there is no chlorophyll loss.

The curves in Figure 4.9 are similar to those of Figures 4.6 and 4.8. Ethylene has been significantly reduced by *aco2* antisense constructs in comparison to the untransformed control significant [t(df)= 4(18), p<0.005] to non-harvest basal levels. Between 0h and 96h, chlorophyll loss has been significantly reduced from 61% in the *gus* controls to only 18% with the *aco2*

antisense lines [t(df)= 2.99(13), p<0.005]. Again it shows that by manipulating ACO enzymes through mRNA transcript suppression, post-harvest ethylene production and chlorophyll loss have been reduced.

In Figure 4.10, the *aco2* sense constructs also reduced post-harvest production of ethylene to basal levels. At 24h there was significantly less ethylene production than the untransformed control [t(df)= 2.29(17), p<0.005]. There was greater chlorophyll loss (48%) from these buds than the other ACO lines at 96h but, this was still significantly less than the untransformed control [t(df)= 2.89(7), p<0.005] and less than the *gus* control plants (61%).

In Figure 4.11, the *ACC synthase* antisense constructs did not down-regulate post-harvest ethylene production as much as the ACO constructs. Total ethylene production was much higher (354nl/g bud/h), similar to the *gus* control plants (366nl/g bud/h). However, the ethylene peak from the *gus* plants occurred between 24-48h, producing 114 and 99nl/g bud/h ethylene, respectively. In the *ACC synthase* antisense lines the values at these time points are 79 and 74nl/g bud/h, respectively, and the peak has been shifted to 72h. It is difficult to observe this with Figure 4.11, so Figure 4.12 has been included. There was 66% chlorophyll loss over the time period, which is slightly higher than the *gus* control (61%) and not significantly less than the untransformed control [t(df)= 1.33(12), p<0.005].

All nine lines transformed with the *aco1* and *aco2* sense and antisense constructs produced relatively similar ethylene curves post-harvest. There was more variation between lines transformed with *acs* antisense. The mean values in Figure 4.11 do not take into account such variation, so Figure 4.12 has been provided to illustrate this disparity. In Figure 4.12, 9/00 *acsA* 1 has

produced a similar post-harvest ethylene curve to the untransformed GDDH33 and *gus* controls. Either *acs* is not important in post-harvest ethylene, or the construct has not down-regulated the native gene. The latter seems more plausible, as the peak of ethylene production has shifted from 24h (126nl/g bud/h) in 9/00 *acsA* 1 to 72h (143nl/g bud/h) in 7/00 *acsA* 12. If 9/00 *acsA* 1 has not been manipulated by the *acs* antisense construct, then 7/00 *acsA* 12 must have been to produce such a different curve. It follows that the peak at 24h, present in the controls and 9/00 *acsA* 1 of Figure 4.12, must be dependent on *acs* and production of ACC, as this is absent in 7/00 *acsA* 12.

The line transformed with the *ACC synthase* sense construct in Figure 4.13 produced the most distinctive post-harvest ethylene curve out of all of the lines. Ethylene production at harvest (0h) is very high (245nl/g bud/h). In Figures 4.3 and 4.4 there was very little physiological change between the non-harvested/harvested buds at 0h. As there is a very high amount of ethylene production at 0h, it suggests that ethylene is being produced at very high levels in growing broccoli buds of the *ACC synthase* sense line. However, between 0 and 24h there is a very rapid post-harvest decline in ethylene production. These are the highest and lowest ethylene values of all 18 lines, and occur over a very short time. The peak recorded at 24h for the untransformed and *gus* controls has been reduced by 96 and 94%, respectively, suggesting that *ACC synthase* plays a role in the post-harvest ethylene peak. Similar to *ACC synthase* antisense, there is recovery between 24 and 96h.

There has been a large decrease in ethylene production at 24h and post-harvest chlorophyll levels actually increased between 0-48h from 200 to

294 $\mu$ g/g bud (see Table 4.4). The overall post-harvest chlorophyll loss was not significantly less than the *gus* control [t(df)= 1.44(12), p<0.005] as this occurred parallel to the recovery of ethylene production 48-72h where the broccoli buds produced 79.38 and 77.09 nl/g bud/h ethylene, respectively.

In Figure 4.14, there is a positive correlation between the 'total' ethylene production and chlorophyll loss of post-harvest broccoli buds. As ethylene production increases, chlorophyll loss increases. The significance of the regression was tested with the F-distribution by comparing the ratio of the regression and the residual mean squares. The percentage chlorophyll loss response variate had a significant dependence [F(df)= 0.0015(7)] on the total ethylene production variate. Total amount of ethylene production appears to be the most important factor for chlorophyll loss. The untransformed GDDH33 is characterised by a large peak (176nl/ g bud/h) at 24h. Its rate of chlorophyll loss was not significantly different to the *ACC synthase* antisense lines, which peaked at 72h. If the timing of the ethylene peak was important, this would not be the case. The transgenic lines that have reduced ethylene have also reduced chlorophyll loss throughout the time period. It is clear in Figure 4.14 that reducing total ethylene production to less than 200nl/g bud/h is beneficial, to decrease chlorophyll loss to only 20%. The 'total' amount of basal ethylene production from non-harvested buds was 200nl/g bud/h from 0-96h. Therefore, if post-harvest ethylene production is not greater than the basal level, chlorophyll loss is significantly reduced. There was 80% chlorophyll loss in the untransformed control with over double the amount of ethylene production by 96h at 20°C.

In Figure 4.15, the post-harvest senescence of GDDH33 broccoli heads from 0h-96h is shown visually. At 72h, bud yellowing can be observed in the untransformed control, where there has already been 68% chlorophyll loss. Chlorophyll loss through bud yellowing can be seen more clearly at 96h where there has been 80% chlorophyll loss. There is no visible yellowing of the head transformed with 3/00 *aco2A 2* antisense constructs. However, GDDH33 produces very small heads that are more susceptible to water loss, and flaccidity cannot be prevented. It appears in the 3/00 *aco2A 2* line that the buds at 96h are larger than at 0h. If this is the case, the buds in the 3/00 *aco2A 2* must have kept growing post-harvest.

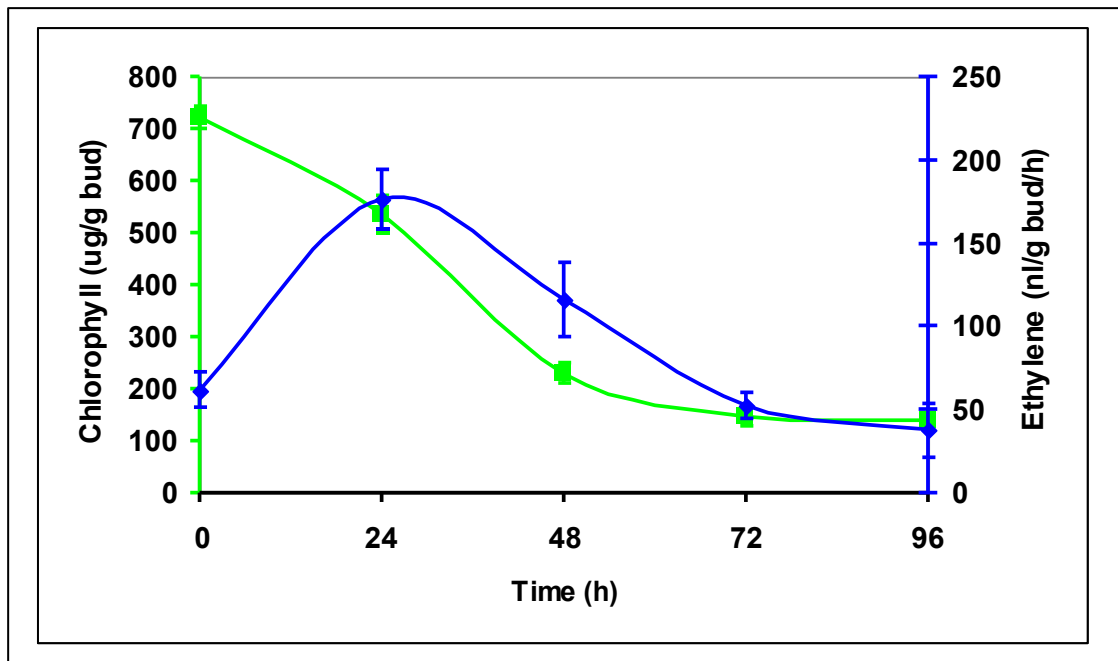


**Figure 4.5** Post-harvest ethylene production and chlorophyll levels of buds from untransformed GDDH33. Chlorophyll levels (■), ethylene production (◆), n=1x12.

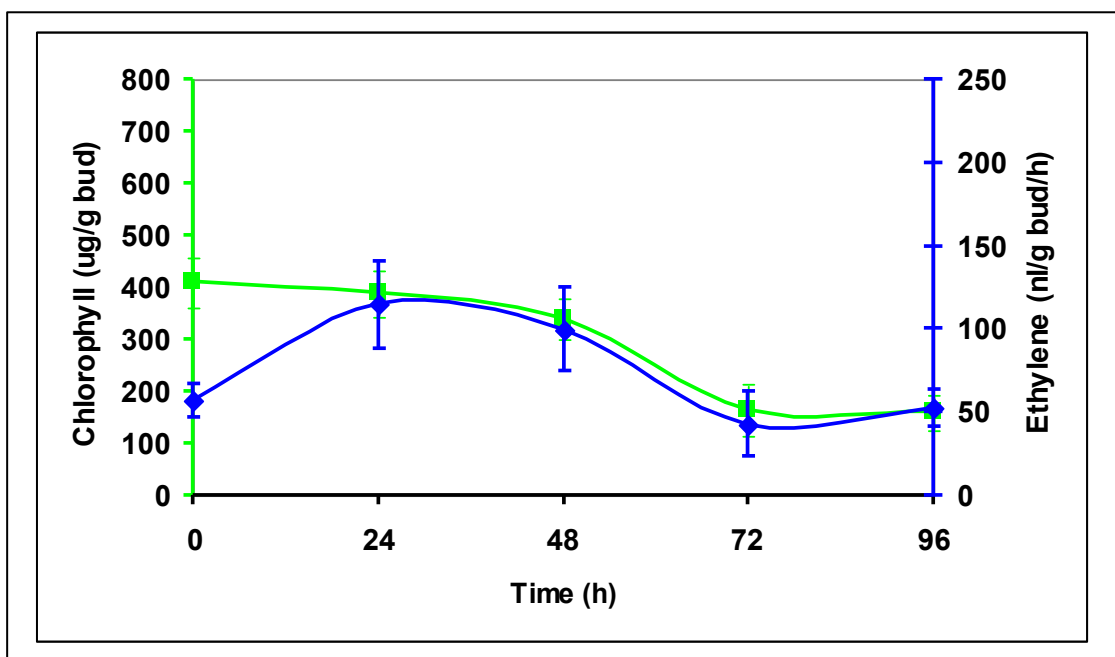


**Figure 4.6** Post-harvest ethylene production and chlorophyll levels of buds from GDDH33 transformed with *gus* control constructs. Chlorophyll levels (◆), ethylene production (■), n=3x3.

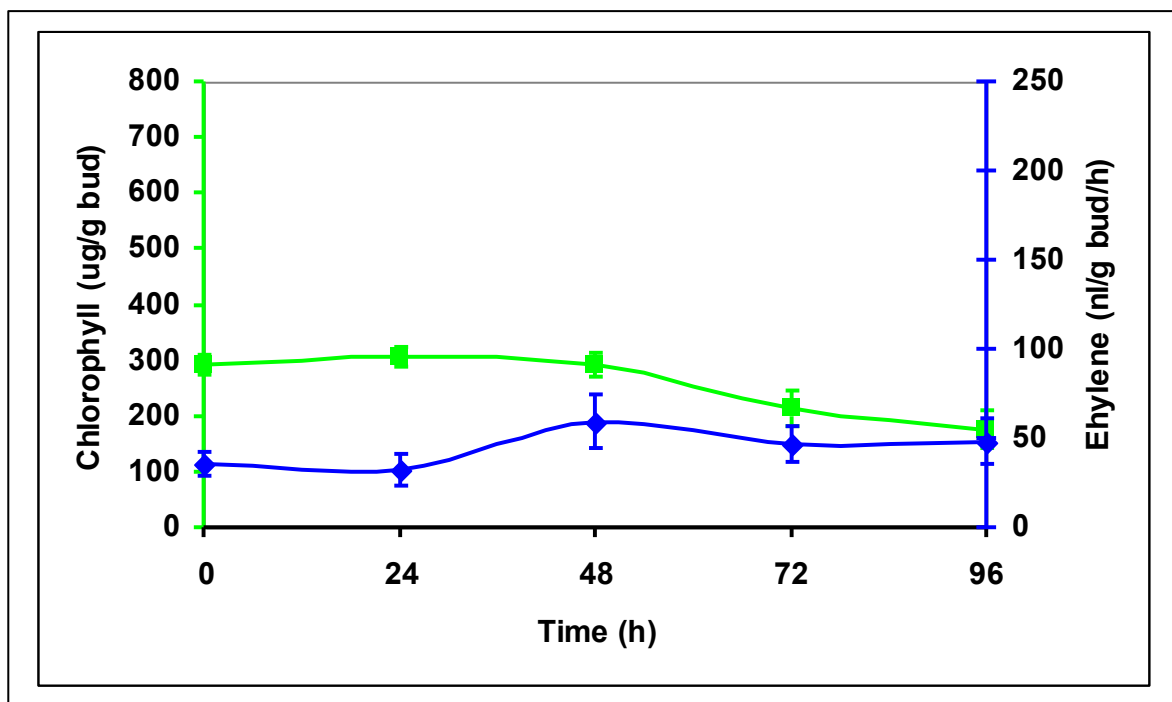


**Figure 4.7** Post-harvest ethylene production and chlorophyll levels of buds from GDDH33 transformed with *ACC oxidase 1* antisense constructs. Chlorophyll levels (■), ethylene production (◆), n=3x3.

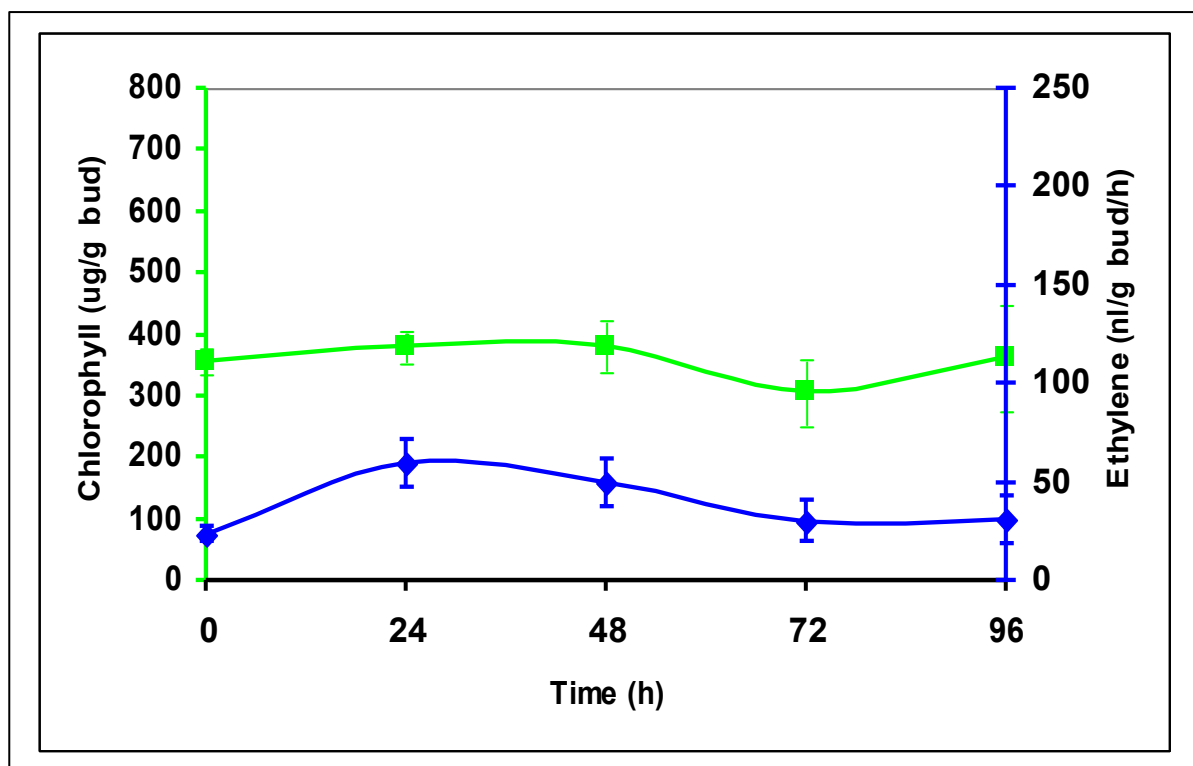


**Figure 4.8** Post-harvest ethylene production and chlorophyll levels of buds from GDDH33 transformed with *ACC oxidase 1* sense constructs. Chlorophyll levels (■), ethylene production (◆), n=2x3.

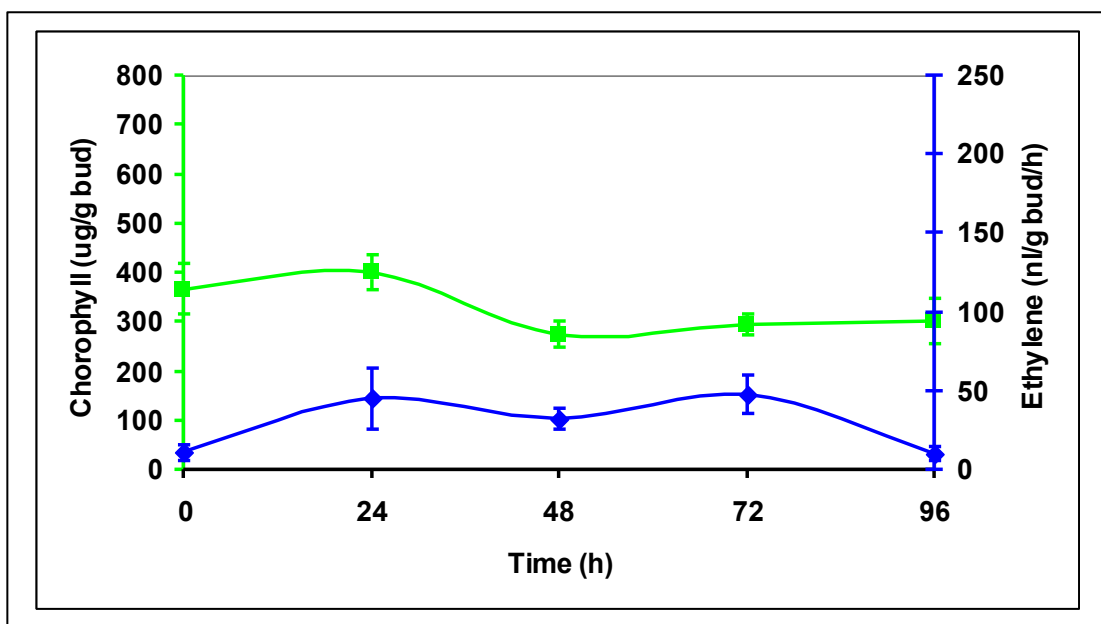


**Figure 4.9** Post-harvest ethylene production and chlorophyll levels of buds from GDDH33 transformed with *ACC oxidase 2* antisense constructs. Chlorophyll levels (■), ethylene production (◆), n=2x3.

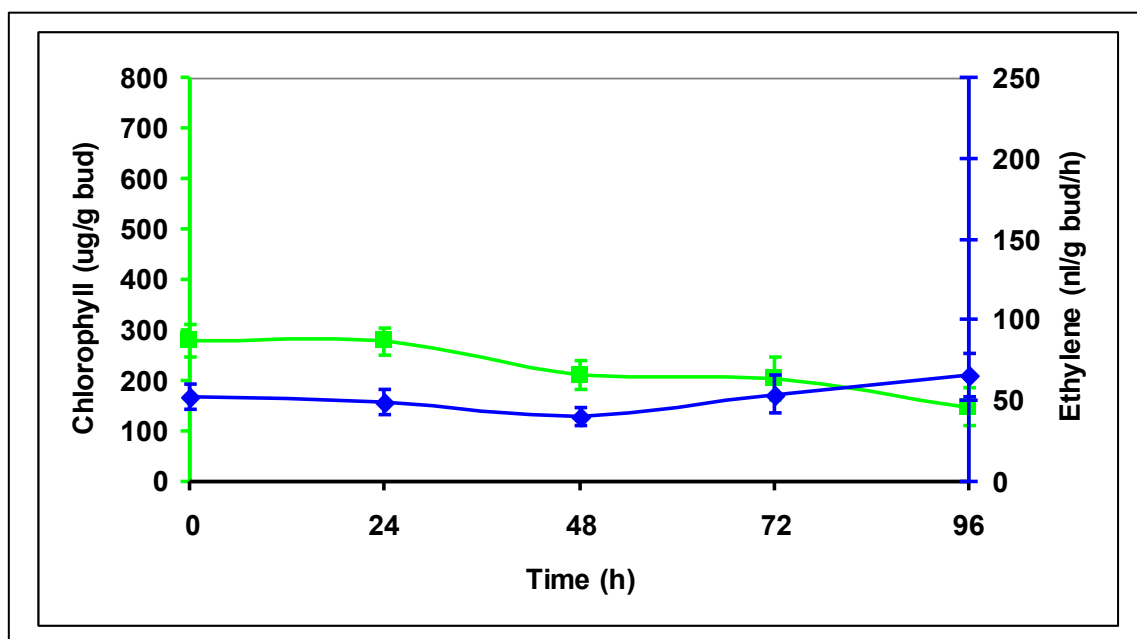


**Figure 4.10** Post-harvest ethylene production and chlorophyll levels of buds from GDDH33 transformed with *ACC oxidase 2* sense constructs. Chlorophyll levels (■), ethylene production (◆), n=2x3.

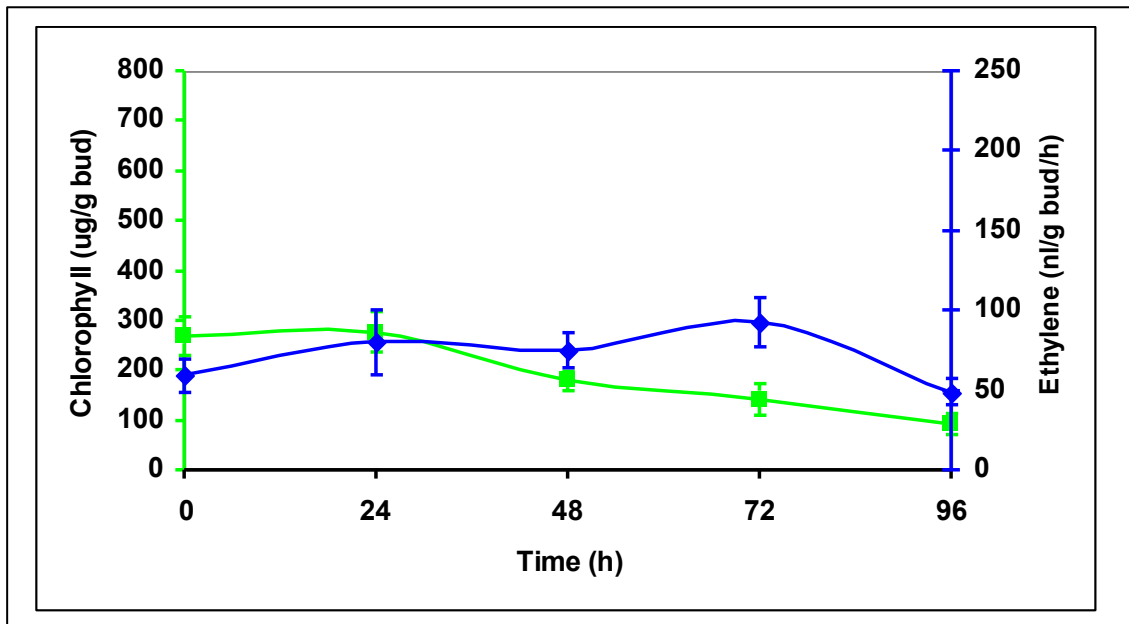


**Figure 4.11** Post-harvest ethylene production and chlorophyll levels of buds from GDDH33 transformed with *ACC synthase* antisense constructs. Chlorophyll levels (■), ethylene production (◆), n=4x3.

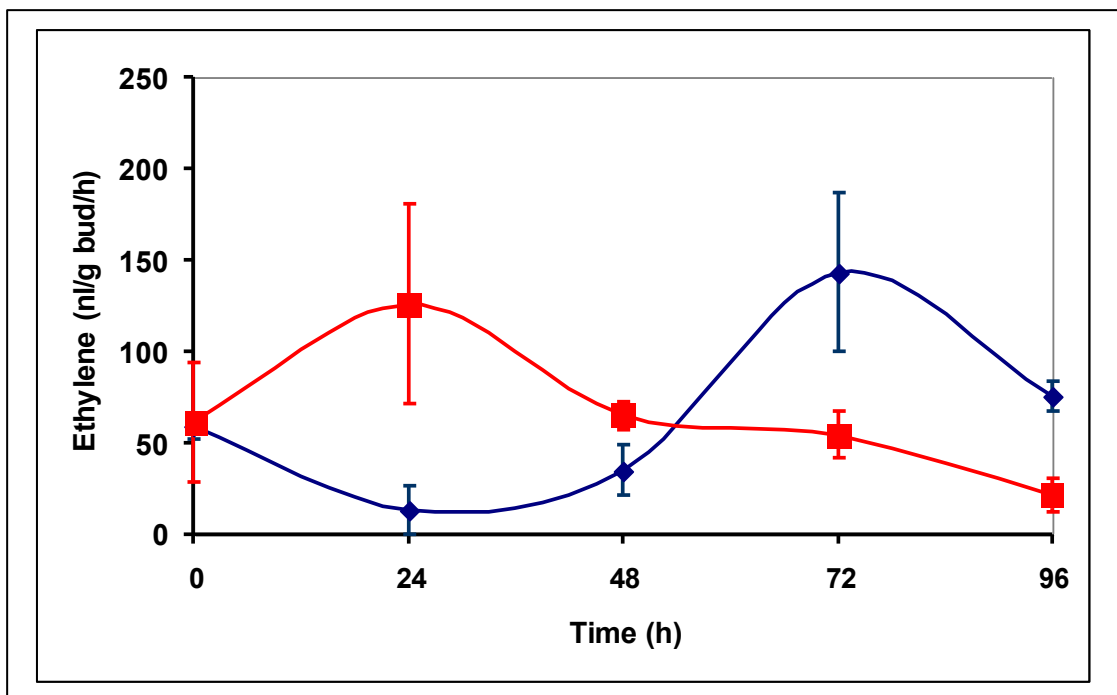


**Figure 4.12** Post-harvest ethylene production of buds from two lines of GDDH33 transformed with *ACC synthase* antisense constructs. These are 9/00 *acsA* 1 (■), and 7/00 *acsA* 12 (◆), n=3.

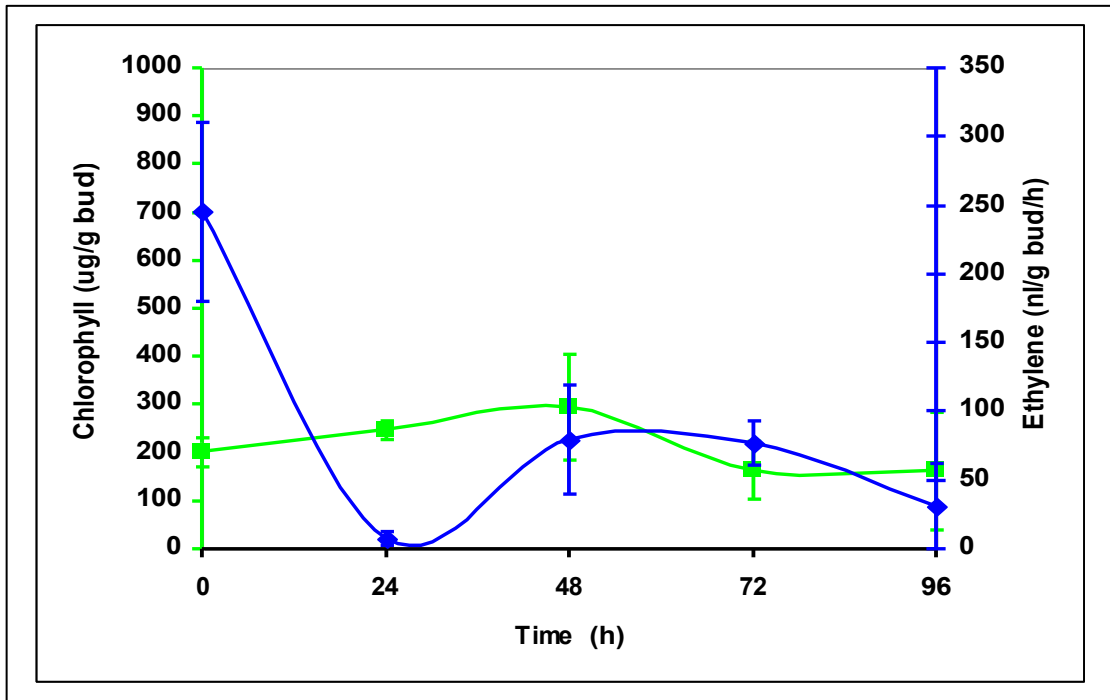


**Figure 4.13** Post-harvest ethylene production and chlorophyll levels of buds from GDDH33 transformed with *ACC synthase* sense construct. Chlorophyll levels (■), ethylene production (◆), n=1x3.

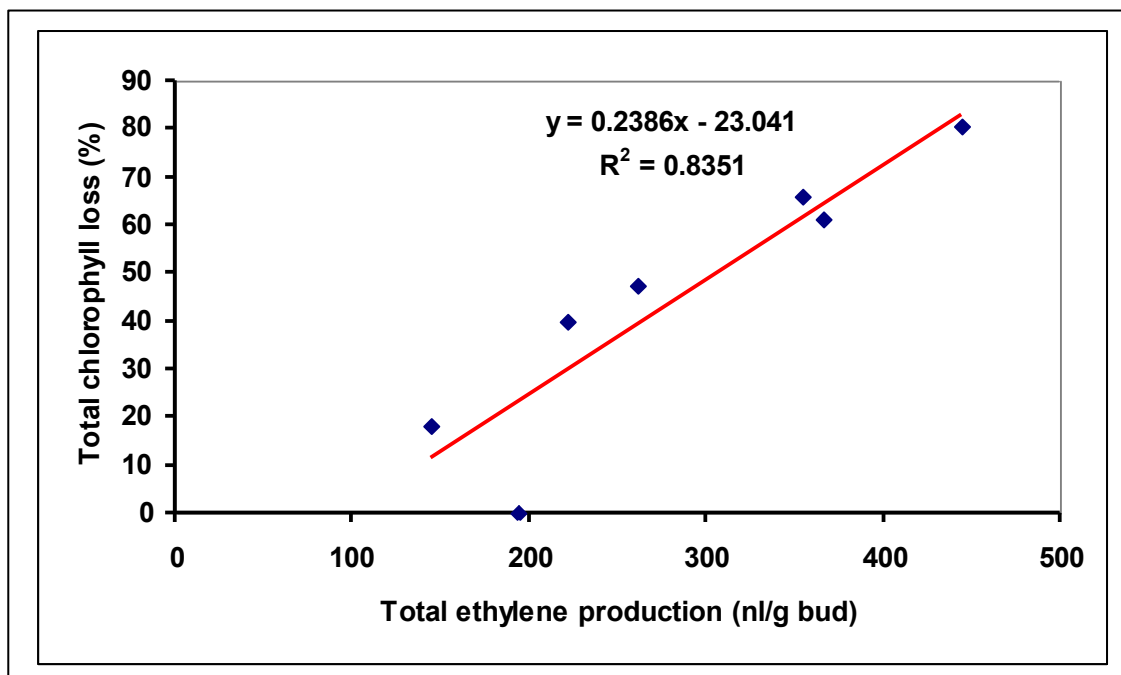
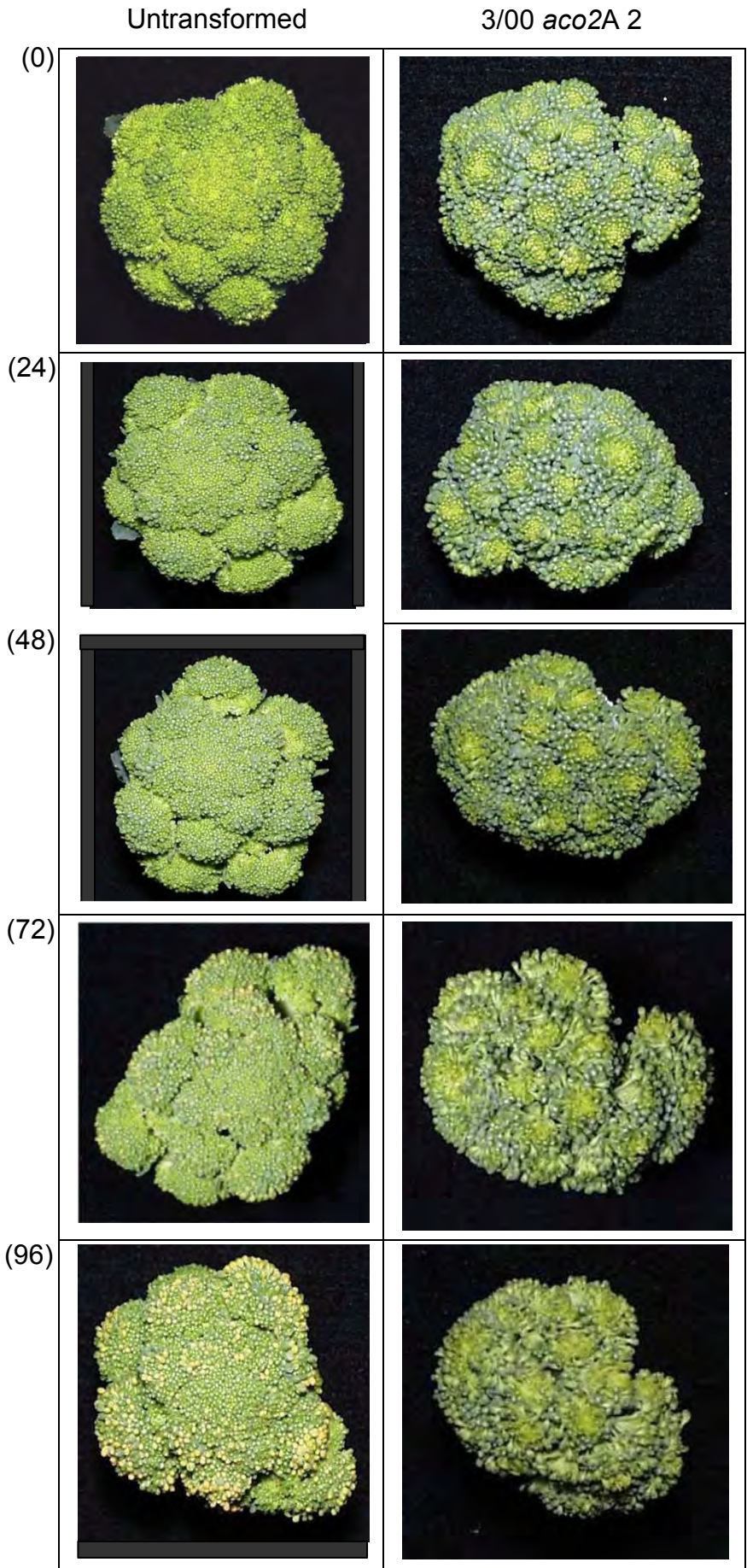


**Figure 4.14** Relationship between post-harvest ethylene production and chlorophyll loss of buds from transformed and untransformed GDDH33. The markers (◆) represent all of the lines in Figures 4.5-4.13. The ACC sense line has been omitted as the chlorophyll levels increased for the first three ethylene values, and cannot be characterised by chlorophyll loss. Total ethylene production is the amount from each time point added together. The percentage chlorophyll loss is the difference between the starting chlorophyll value at 0h to that at 96h.

**Figure 4.15** Broccoli heads post-harvest. Untransformed GDDH33 (left) and transformed 3/00 *aco2A* 2 antisense (right). From top to bottom: 0, 24, 48, 72 and 96h post-harvest broccoli heads.



#### 4.4 Discussion

Broccoli buds were chosen for assaying ethylene and chlorophyll, as they were the main organs responsible for post-harvest ethylene production and experienced chlorophyll loss in the sepals (Tian *et al.*, 1994). They had a number of advantages over whole heads and florets that were more cumbersome to handle and produced volatiles that interfered with the ethylene assay by gas chromatography. Chlorophyll extraction was achieved by diffusion into methanol overnight, in the dark. These assays provided simple and accurate means for testing ethylene and chlorophyll levels in mature broccoli heads.

It was important to establish ethylene production from 'non-harvested' buds as a control for 'harvested buds'. It was clear from the results in Figures 4.3 and 4.4 that as expected, values at 0h post-harvest were very similar to the non-harvested buds growing *in situ*. There must have been insufficient time for a physiological response to harvesting to have taken place. The basal amount of ethylene produced by non-harvested GDDH33 broccoli buds was 44nl/g bud/h. Basal ethylene is regulated through *ACC synthase* and *aco1* (Pogson *et al.*, 1995) to maintain normal broccoli head physiology in actively growing plants. Harvesting the head altered the physiology resulting in a significant increase of ethylene ( $p < 0.005$ ) from 44 to 176nl/g bud/h at 24h. Pogson *et al.* (1995) found that the abundance of *aco2* transcripts increased dramatically 24h after harvest, especially in the reproductive organs of the floral buds. The post-harvest peak of ethylene is probably related to the increase of *aco2* transcripts in these organs, but this would also require a substantial amount of ACC substrate from ACC Synthase. Tian *et al.* (1994)

and Kasai *et al.* (1996) observed the same post-harvest ethylene curves as the GDDH33 control with 'Green Beauty', 'Shogun', 'Green Belt' and 'Green Valiant' broccoli cultivars. There was an increase of ethylene after harvest, peaking at 24h before declining in these cultivars. The actual values recorded by Tian *et al.* (1994) and Kasai *et al.* (1996) are lower compared to those in this study since whole florets were used, of which the buds produce the majority of the ethylene. The post-harvest bud chlorophyll levels also declined in GDDH33 at the same rate and to the same point as the cultivars used by Tian *et al.* (1994) and Kasai *et al.* (1996). Chlorophyll loss was probably related to being harvested, as chlorophyll levels in the non-harvested control did not decline.

The change in post-harvest broccoli bud ethylene production is associated with the up-regulation of *aco2* transcripts within the male and female reproductive organs (Pogson *et al.*, 1995a). This tissue-specific expression suggests a role for ethylene in reproduction. In *Brassica napus*, ethylene production occurs first at 20 days after pollination (DAP), while a second greater peak occurs at 35DAP (Rays *et al.*, 2000). In flowers whose senescence is pollination-dependent or pollination accelerated, pollination is accompanied by a rapid increase of endogenous ethylene (Hadfield and Bennett, 1997). The initial pollination induces expression of an *ACC synthase* gene in the stigma, which produces ACC that may be oxidised directly to ethylene or potentially translocated to distal floral organs to be oxidised into ethylene. Flower organ senescence serves to remobilise nutrients from the petals and sepals to the developing ovary (Lawton *et al.*, 1989; 1990). It appears that harvesting forces the immature broccoli buds into premature

senescence. The probable role for *aco2* is to facilitate remobilisation of nutrients from surrounding tissues to support the developing ovaries after pollination. However, *aco2* induced by stress after harvest assists the breakdown of macromolecules into respirable substrate which includes major losses of sugars, organic acids and proteins (King and Morris, 1994).

The ethylene peak at 24h of 176nl/g bud/h in the untransformed control was reduced to 116nl/g bud/h in the *gus* control lines. Although this not a significant difference ( $p>0.005$ ) it shows that factors to do with the transformation and regeneration reduces ethylene production. Henzi *et al.* (1999a,b) produced broccoli plants transformed with *A. rhizogenes* that had slightly reduced ethylene production compared to the non-transgenic controls. Henzi *et al.* (1999a,b) attributed this reduction of ethylene to the *ro/C* locus. Martin-Tanguy *et al.* (1993) noted a reduction in ethylene production during floral development in tobacco plants transformed with *ro/C* (ORF 12 from the *Ri T<sub>L</sub>*-DNA of *Agrobacterium rhizogenes*), driven by the CaMV 35S virus promoter. It is possible that the *rol* genes also caused a reduction of chlorophyll at 0h between the untransformed 721 $\mu$ g/g bud and 409 $\mu$ g/g bud in the transformed plants. However, the rate of chlorophyll loss in the transformed plants was also reduced.

The transgenic lines containing the *aco1* antisense construct produced only 32nl/g bud/h of ethylene at 24h, significantly less than the untransformed and transformed *gus* control plants ( $p<0.005$ ). It shows that the ACO cDNAs isolated by Pogson *et al.* (1995a,b) are important in the post-harvest peak of ethylene of *Brassica oleracea*. It demonstrates that they can effectively be down-regulated by antisense constructs transferred through plant

transformation. Accompanying the reduction of ethylene was a loss of chlorophyll that was significantly reduced ( $p < 0.005$ ) compared to the untransformed control.

Transgenic lines transformed with the *aco1* sense construct also reduced post-harvest production of ethylene to basal levels. The *aco1* sense lines significantly reduced ethylene production compared to the untransformed control ( $p < 0.005$ ), and did not experience any chlorophyll loss over the 96h. These lines show that gene silencing may be achieved with both antisense and sense constructs, and that the CaMV 35S promoter was suitable to achieve this.

The reduction of post-harvest production of ethylene was achieved with as much success with the *aco2* constructs as with *aco1*. This suggests that there has been cross-hybridisation between the transcripts of both genes and constructs to reduce total amount of ethylene to a basal level. The cDNAs of *aco1* and *aco2* share 83% nucleotide identity in their putative translated regions (Pogson *et al.*, 1995a). *aco2* antisense significantly reduced post-harvest ethylene compared to the untransformed control ( $p < 0.005$ ), and significantly reduced chlorophyll loss compared to the transformed *gus* control ( $p < 0.005$ ). The *aco2* sense constructs also manipulated post-harvest production of ethylene to basal levels, and reduced chlorophyll loss significantly ( $p < 0.005$ ) compared to the untransformed control. Reduction of endogenous ethylene to extend shelf-life has not been achieved before with transformation of broccoli. Experiments with methylcyclopropane an inhibitor of ethylene action, have shown that storage life of broccoli treated and stored at 20°C may be extended (Ku and Wills, 1999).

The *ACC synthase* antisense constructs did not decrease total post-harvest ethylene production as much as the *ACO* constructs. The *acs* constructs shifted the ethylene peak from 24h to 72h (Figure 4.12). The native *ACC synthase* is probably normally active 0 - 24h post-harvest as this function has been lost. It shows that the *ACC synthase* cDNA obtained from Pogson *et al.* (1995) could play a major role in the post-harvest peak of ethylene in broccoli. It also suggests that there may be another(s) *ACC synthase(s)* active between 48 and 72h with a different nucleotide sequence that has not been silenced. Although there is evidence for the regulation of *ACC synthase* at the post-translational level (Jones and Woodson, 1999; Felix *et al.*, 1991, 1994; Spanu *et al.*, 1994), expression studies indicate that ACC Synthase activity is most often the result of the increased accumulation of *ACC synthase* mRNA transcripts (Kende, 1993; Zarembinski and Theologis, 1994). However, Pogson *et al.* (1995b) states that there is no change in expression of this gene post-harvest, and that the protein might become post-translationally activated. Kasai *et al.* (1998) found that the post-harvest increase of ethylene in senescing broccoli was suppressed by cycloheximide (an inhibitor of translation), suggesting that it results from the *de novo* synthesis of the ACC Synthase enzyme. It would be surprising if transcripts of this gene were not increased post-harvest as in wounded, ripening tomato (*Lycopersicon esculentum*), the ACC synthase protein decays rapidly *in vivo* with a half-life of 58 minutes (Kim and Yang, 1992).

The transgenic line transformed with the *ACC synthase* sense construct provided more evidence that the *acs* isolated by Pogson *et al.* (1995b) appears to play a role in the post-harvest peak of ethylene. Post-

harvest ethylene production at 0h was very high at 245nl/g bud/h, suggesting high levels in the growing buds. By 24h, this was reduced to only 7nl/g bud/h. Such a dramatic decrease in ethylene production must either be due to silencing of the transcripts or inhibition of the ACO or ACS enzymes. If the CaMV 35S promoter has constitutively produced transcripts in the other constructs throughout the time period to reduce ethylene production, it is possible that *acs* sense transcripts are still produced. It may be hypothesised that the native *ACC synthase* is up-regulated post-harvest and together with the construct produces transcripts above a threshold, leading to co-suppression of the transcript. As the protein has a high turn over rate (Kim and Yang, 1992), there would be little ACC substrate for the ACC oxidases to oxidise to produce ethylene.

ACC synthase is probably the rate-limiting enzyme in broccoli bud ethylene production. In the *acs* sense lines, the growing buds produced 245nl/g bud/h ethylene, whereas the buds in the untransformed control produced only 44nl/g bud/h. If the functional *acs* sense construct has produced more mRNA transcript, and more ACC synthase enzyme, without silencing, this would produce more ACC. If this is the case, the native ACO present was not limiting the production of ethylene in growing buds with 44nl/g bud/h, as with more ACC, ACO could catalyse the production of 245nl/g bud/h. It follows that increasing ACC oxidase activity post-harvest would have little effect if there was not an increase in the ACC pool, which would probably be mediated through ACC Synthase(s). Either an up-regulation of the native *acs* transcript or post-translational activation of ACS enzyme might increase the ACC pool. It is possible to propose a model where the rate-limiting step in

the biosynthesis of ethylene in *Brassica oleracea* var. *L. italica* is controlled by ACC synthases. ACC synthases appear to play a role in controlling post-harvest production of ethylene in broccoli buds. It is possible that ACS also controls normal basal levels of ethylene through ACC production that is oxidised by ACC oxidases into ethylene. After harvest, the stress could induce the up-regulation of at least two *acs* (0-48h and 24-96h) and *aco1/aco2* in the reproductive structures, resulting in an increase in biosynthesis of ethylene.

All of the lines were used to plot 'total' ethylene production with the percentage of chlorophyll loss over the time period. There was a positive correlation between ethylene production and chlorophyll loss of post-harvest broccoli buds at 20°C. As ethylene increased, chlorophyll loss increased. This linear correlation was described by the equation  $y = 0.2386x - 23.041$ , where  $y$  = chlorophyll loss and  $x$ , the 'total' production of ethylene. It was confirmed by comparing the ratio of the regression and the residual mean squares with the F-distribution ( $p < 0.005$ ). 'Total' post-harvest production of ethylene appeared to be an important factor for chlorophyll loss. When the peak varied between 24 and 72h in different lines, chlorophyll loss was dependent on 'total' amount of ethylene, not the timing of maximum production. The transgenic lines that have down-regulated production of ethylene have also reduced chlorophyll loss suggesting that chlorophyll loss had a dependence on ethylene. It was clear that reducing post-harvest ethylene production to the basal level produced in non-harvested buds, prevented chlorophyll loss. Although ethylene production and post-harvest decay have been significantly positively correlated in melon fruits (Zheng and Wolff, 2000), this has not yet been determined in broccoli. Chlorophyll loss is an important factor because

yellowing is the last stage of senescence preceded by the breakdown of sugars, organic acids and proteins (King and Morris, 1994). It demonstrates that the shelf-life of a very perishable vegetable may be increased at least up to 3 days at 20°C by reducing post-harvest ethylene. This should be of benefit to retailers and consumers preserving the nutritional quality of the product for a longer time period.

In the experiments described here, the data were collected from primary transformants, which means that they are effectively heterozygous for the constructs. In chapter 3, seeds were harvested from 11 of the T<sub>0</sub> lines, and 67 seeds were sown from the 28/00 *aco1A* 3 line. It showed that the T<sub>L</sub>-DNA, carrying the *rol* genes may be removed by segregation. As the *rolC* locus appears to reduce endogenous ethylene production (Martin-Tanguy *et al.*, 1993) it would therefore be more useful to analyse the T<sub>1</sub> generation for the effects of the constructs on ethylene production and bud chlorophyll loss. The T<sub>1</sub> generation may also be homozygous for construct T-DNA inserts and this may show more extreme effects. It also allows the opportunity for crossing the T<sub>x</sub> lines containing different constructs, such as an *acs* antisense line with an *aco1/aco2* antisense. A T<sub>x</sub> line with stacked genes may produce even less ethylene post-harvest, and possibly produce a phenotype with a longer shelf-life. There is a possibility that construct copy number and, the effect of their position within the genome may lead to differences of mRNA expression. There was no evidence in chapter 3 that copy number of the T<sub>L</sub>-DNA related to the severity hairy root phenotype, and the T<sub>0</sub> line with greatest reduction of post-harvest ethylene production (3/00 *aco2A* 2) appeared only to have one insert. It is possible that the 'position effect' of construct within the

plant genome had a greater influence over mRNA expression, and effects on the plant phenotype.

This research has showed that there was a relationship between post-harvest production of ethylene and chlorophyll loss in broccoli heads. *aco1*, *aco2* and *acs* appear to play major roles in the post-harvest production of ethylene, although there may be more, equally important genes. The native genes are probably up-regulated following the stress caused by harvesting, forcing the buds into premature senescence that would usually be required to support the developing ovary after pollination. An assay was set up to measure ethylene and chlorophyll levels using broccoli buds that proved to be reliable and efficient. The whole process shows that genes can be targeted and via a transformation system be down- or up-regulated to study characteristics *in vivo*, to either understand the genetic control behind physiological responses or introduce beneficial traits to complement breeding programmes. In this case, utilising the *aco1*, *aco2* and *acs* cDNAs isolated from *Brassica oleracea* L. var. *italica* by Pogson *et al.* (1995a,b) has helped understand the genetic control behind the senescence of broccoli buds and may enable the manipulation of the post-harvest physiology of broccoli.

## **5.0 Identifying *Brassica oleracea***

### ***ACC oxidases***

## 5.1 Introduction

Ethylene biosynthesis occurs via the enzymes ACC Synthase (ACS) and ACC Oxidase (ACO), which catalyse the conversions of S-adenosylmethionine (SAM) to 1-aminocyclopropane-1-carboxylic acid (ACC) and ACC to ethylene, respectively (Kende, 1993). In broccoli, ethylene appears to play an important role in sepal yellowing after harvest, since chlorophyll loss is associated with an increase in ethylene production (Tian *et al.*, 1994). The post-harvest increase of ethylene synthesis is associated with an increase of *ACC oxidase 1* and *ACC oxidase 2* mRNA transcripts in the broccoli florets (Pogson *et al.*, 1995a).

*ACC oxidases* have been isolated and characterised from multigene families from three species including tomato (3 genes), petunia (4 genes) and melon (3 genes) (Barry *et al.*, 1996; Tang *et al.*, 1993; Lasserre *et al.*, 1996). *ACC oxidases* show very different expression patterns in various tissues at different stages of development and in response to specific stimuli (Barry *et al.*, 1996). Pogson *et al.* (1995a) isolated two cDNAs encoding *ACC oxidases*, *aco1* (1237bp) and *aco2* (1232bp), from broccoli. *aco1* and *aco2* share 83% nucleotide identity in their putative translated regions, 48% in the untranslated regions, and share 86% amino acid identity (Pogson *et al.*, 1995a). Southern analysis of the *aco1* and *aco2* at high stringency gave distinct hybridisation patterns, confirming that they encoded by different genes (Pogson *et al.*, 1995a). Low stringency analysis revealed only one additional hybridising band not accounted for by either *aco1* or *aco2*, indicating that broccoli may contain at least one other closely related gene (Pogson *et al.*, 1995). *aco1* and *aco2* appear to be important genes in the post-harvest senescence of broccoli as

their protein products catalyse the last step in the ethylene biosynthetic pathway. If ACO1 and ACO2 do play a major role in post-harvest senescence of broccoli it would be useful to understand regulation of the gene family, and characterise different alleles as these may produce phenotypes with reduced post-harvest ethylene production. Allelic variation could be determined by genetic markers and assist efforts to lengthen post-harvest shelf-life of broccoli.

*Brassica oleracea* is considered a diploid species ( $2n=18$ ) along with *B. nigra* ( $2n=16$ ) and *B. rapa* ( $2n=20$ ). Pairwise combinations of the diploid species *B. rapa* (*syn. Campestris*)(AA), *B. nigra* (BB) and *B. oleracea* (CC) have resulted in the amphidiploid species *B. juncea* (AABB), *B. napus* (AACC) and *B. carinata* (BBCC) (U. 1935). Many genetic maps have been assembled for *Brassica* species (reviewed by Paterson *et al.*, 2000). Sebastian *et al.*, (2000) constructed an integrated AFLP and RFLP *Brassica oleracea* linkage map from F<sub>1</sub> crosses of *Brassica oleracea* doubled haploid populations: Chinese Kale X Calabrese (*var. alboglabra* X *var. italica*) and cauliflower X Brussels sprouts (*var. botrytis* X *var. gemmifera*) (Sebastian *et al.*, 2000). Integration of the map was based on 105 common loci including RFLPs and AFLPs to provide a consensus map of 547 markers mapping to nine linkage groups. It is thought that the integrated *B. oleracea* genetic map will facilitate the mapping of loci across the populations (Sebastian *et al.*, 2000).

Bacterial artificial chromosomes (BACs) are large genomic DNA clones, ranging from 100 to 200kb, used for map based cloning (Jackson *et al.*, 1999). A BAC library has been constructed for *Brassica oleracea* from the

doubled haploid *alboglabra*12 (G. King, pers. comm. HRI-Wellesbourne), and can be used for cloning genes.

The aim of this section was to: a) confirm whether *aco1* and *aco2* are different genes, and if so how many copies are there of each gene in the *Brassica oleracea* genome; b) try to determine whether there are any other *aco* genes in the *Brassica oleracea* genome; c) locate their genetic map positions with the integrated linkage map from (Sebastion *et al.*, 2000) and; d) to determine how similar the *Brassica oleracea* var. *italica* *aco* genes are to other *Brassica aco* genes.

## 5.2 Materials and Methods

### 5.2.1 PCR

Primers were designed to produce fragments from *B. oleracea aco1* and *aco2* cDNAs and genes (see Table 5.1). All oligonucleotides were synthesised by MWG-Biotech (MWG-BIOTECH AG Anzinger Str.7 D-85560 Ebersberg) (Table 5.1) and used in standard PCR conditions (Tables 5.2 and 5.3). PCR components including *Taq* polymerase, PCR buffer and dNTPs were obtained from GIBCO-Life Technologies, Uxbridge, UK.

**Table 5.1** Oligonucleotide sequences used for primers to determine gene polymorphisms and produce DNA probes .

Primer Name	Sequence (5'- 3')	$T_m$ (a) (°C)
2	GCT TTG GTC GAC GAT GCT TG	62
3	AGT CTC TAC GGC TGC TGT TG	62
4	CGT CTC GAC TGT GGC CAC CG	68
5	TAG GAC AAG CTG GAT AGT TGC T	61
6	CTC ACA CTG ATG CAG GAG GC	65
7	CCT GAT ATG TCT GAT GAA TAC CG	61
8	CCT CAG CAA GAT TCT CCA ATC	61
9	TGG TCG ACG ATG CTT GTC A	60
10	GTC CAT AAG ATC ATA TGG TAT TCC	59
<i>aco1</i> 3'UTR F	GAA GAA TTC TAA TGC AGT TAC AG	57
<i>aco1</i> 3'UTR R	CGC AAG CTT AGA ACA GTT ATC ATA T	59
<i>aco2</i> 3'UTR F	GAA GAA TTC TGC AGC AAC CAC CGA TTT G	66
<i>aco2</i> 3'UTR R	GCG GAA GCT TTA AAA TTC ATA TTT CCA ATA C	62
<i>aco2</i> R	TCA TAT TTC CAA TAC AAT TAT TGC	54
<i>aco2</i> F	CTA ACA TCA TCA ACA ACA TTA AG	56

(a)  $T_m$  of the primers was calculated using the expression:

$$T_m = 81.5 + -16.6 + (41 \times (\#G + \#C/\text{length})) - (500/\text{length})$$

**Table 5.2** PCR reaction components.

To make a total 25 $\mu$ l for each reaction, 5 $\mu$ l of template DNA (100 $\rho$ mol/ $\mu$ l) and 5 $\mu$ l of primers (set at 4 $\rho$ mol/ $\mu$ l) were added. Primers and template DNA were suspended in autoclaved R.O water.

	x1 ( $\mu$ l)
10x Buffer	2.5
50mM MgCl <sub>2</sub>	0.75
dNTPs 25mM	0.2
H <sub>2</sub> O	11.42
<i>Taq</i>	0.13
<b>Total</b>	<b>15</b>

The PCR program in Table 5.3 was used and the annealing temperature adjusted 3°C below the  $T_m$  of primer pairs (Table 5.1). The PCR reactions were performed on a Hybaid Omnigene PCR machine.

**Table 5.3** PCR program.

Stages 1 and 3 were cycled once. Stage 2 was cycled thirty five times.

<b>Stage 1.</b>	1) 93°C/ 2 min	2) 53° C/ 1 min	
<b>Stage 2.</b>	1) 72°C/ 1 min	2) 93° C/ 30 sec	3) 53° C/ 1 min
<b>Stage 3.</b>	1) 72° C/ 10min.		

The location of the primers (Table 5.1) on the *ACC oxidase 1* and *ACC oxidase 2* cDNAs are shown Figures 5.1 and 5.2. Figures 5.1 and 5.2 are included as a reference for sequences that are amplified by PCR.

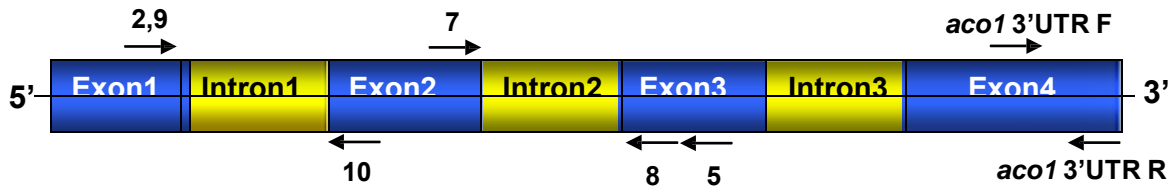


**Figure 5.1** Schematic diagram of the predicted *Brassica oleracea* L. var. *italica* ACC oxidase 1 gene.

The arrows and numbers represent forward and reverse primer locations (see Table 5.1).

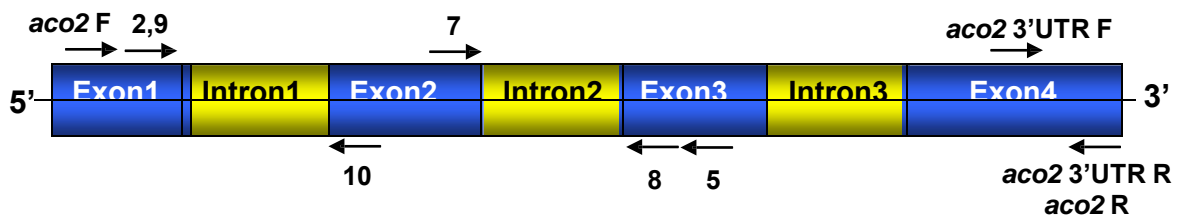


**Figure 5.2** Schematic diagram of the predicted *Brassica oleracea* L. var. *italica* ACC oxidase 2 gene.

The arrows and numbers represent forward and reverse primer locations (see Table 5.1).

### 5.2.2 Bacterial Artificial Chromosomes (BACs)

*E. coli* carrying the *Brassica oleracea* physical map BACs were cultured in 10mls LB with 10 $\mu$ l (50mg/ml) chloramphenicol, in sterile 50ml centrifuge tubes, overnight at 37°C. Three millilitres of cells were added to 1.5ml microfuge tubes, centrifuged at 11600g for 1min, and the supernatant discarded. 0.3ml Qiagen P2 lysis buffer was added to the pellet and left for 5min at room temperature, then 0.3ml of pre-chilled Qiagen P3 neutralisation buffer was added and left for 5min on ice (Qiagen Ltd., Boundary Road, Crawley, West Sussex). The tubes were centrifuged at 11600g for 10min, and the 450 $\mu$ l supernatant was added to 1125 $\mu$ l 100% ethanol (analaR grade,

BDH) and 32 $\mu$ l 5M sodium acetate. The tubes were centrifuged at 11600g for 30min, and the supernatant was removed allowing the pellet to air dry for 5min at room temperature. The pellet was resuspended in 100 $\mu$ l sterile, purified H<sub>2</sub>O. The DNA was quantified on a 1% (w/v) agarose gel.

An *Eco*RI endonuclease restriction digest was carried out at 37°C overnight with the BAC DNA in the following reaction: 17 $\mu$ l DNA (85ng); 2 $\mu$ l reaction buffer 3; 0.5 $\mu$ l *Eco*RI enzyme (GIBCO-Life Technologies); 1 $\mu$ l spermidine (10mg/ml); 0.1 $\mu$ l RNase (10mg/ml), to make a final volume of 20.6 $\mu$ l.

### 5.2.3 Southern Blots and filters

The restriction endonuclease digestion products from section 5.2.2 were loaded onto a 0.8% (w/v) agarose gel and separated by gel electrophoresis for 15h at 50V. They were stained in 0.33 $\mu$ g/ $\mu$ l ethidium bromide, photographed, and then de-stained in R.O. water. The blotting was performed by alkaline lysis onto Hybond N+ filters (Amersham) according to Sambrook *et al.* (1989).

The *Brassica oleracea* BAC library (BoB) filters, and the AG and NG mapping filters were obtained from Graham King (HRI-Wellesbourne). The mapping filters are derived from the integrated map of *B. oleracea* based on the segregation data of F<sub>1</sub>-derived doubled-haploid mapping populations (Sebastion *et al.*, 2000).

#### 5.2.4 Hybridisation between N+ filters and $\alpha^{32}\text{P}$ dCTP labelled DNA probes

The Hybond N+ filters were placed onto nylon mesh that had been wetted in 2x SSC (saline sodium citrate), wrapped up tightly and placed in a Hybaid hybridisation bottle. Fifty millilitres of hybridisation buffer (0.5M Na phosphate pH 7.2; 7.0% sodium dodecyl sulphate [SDS]; 10mM EDTA, pH 8.0 and; 100 $\mu\text{g}/\text{ml}$  single stranded salmon sperm DNA) was added to the tubes at 55°C. The tubes were placed in a Hybaid rotisserie oven at 55°C and left to pre-hybridise for 3h. DNA probes were produced by PCR with primers *aco1* 3'UTR F, *aco1* 3'UTR R, *aco2* 3'UTR F, *aco2* 3'UTR R, *aco2* R, *aco2* F, set at the conditions of Tables 5.2 and 5.1, and purified with the QIAquick PCR Purification Kit (Qiagen Ltd., Boundary Road, Crawley, West Sussex). The DNA probes were labelled with  $\alpha^{32}\text{P}$  dCTP according to the rediprime II random prime labelling system kit (Amersham Pharmacia Biotech, Bucks. UK). The labelled DNA was separated from the other components by a sepharose column and counted with a scintillation counter. The 50mls of hybridisation buffer were replaced with 10mls fresh buffer, and 2 x 10<sup>7</sup> cpm (in 2x10<sup>6</sup>/ml) labelled probe and left overnight at 55°C. The blots were washed at low stringency with 10 x SSC and 1% SDS four times at 55°C. The filters were wrapped in Saranwrap (Dow Chemicals) and placed into X-ray cassettes with XAR5 film (Kodak) under a safelight. The cassettes were placed at -80°C for 48h, and then the film was developed.

#### 5.2.5 Genetic Mapping

The *B. oleracea* mapping filters obtained from Graham King (HRI-Wellesbourne) were hybridised to the  $\alpha^{32}\text{P}$  dCTP labelled *aco1* 3'UTR and

*aco2* 3'UTR DNA probes. These experiments produced autoradiographs that were scored by James Higgins for segregation of progeny from the parents. The data was analysed in conjunction Dr Graham Teakle (HRI-Wellesbourne) with the computer software JOINMAP 2.0 (Stam *et al.*, 1995), to calculate a map position.

#### 5.2.6 Cloning and sequencing PCR fragments

DNA fragments were amplified by PCR from BACs 3(10 J 22), 4(11 K 12), 12(43 P 13), 20(62 O 07), with primers 2 and 5 (Table 5.1). DNA products from 3 reactions of 4 BACs (12) were ligated into the pCRII-TOPO cloning vector, with the TOPO TA cloning kit (Invitrogen). The transformation of the ligated plasmid was carried out according to the protocol supplied with the DH5 $\alpha$  library efficient competent cells (*E. coli* DH5 $\alpha$ , genotype: F $^{-}$   $\phi$ 80d/*lacZ* $\Delta$ M15  $\Delta$  (*lacZYA-argF*)U169 *deoR recA1 endA1 hsdR17*(r $_{k}^{-}$ , m $_{k}^{+}$ ) *phoA supE44*  $\lambda$ *thi-1 gyrA96 relA1*) (GIBCO-Life Technologies, Uxbridge, UK.). Cells were cultured in LB media and selected for with 25mg/l kanamycin. Single colonies were checked for presence of the insert with a colony PCR method taken from the pMOS*Blue* T-vector kit (Amersham International plc, Little Chalfont, Buckinghamshire, UK), using primers 2 and 5. The plasmids from positive colonies were extracted with Qiagen miniprep (tip20) kits (Qiagen Ltd., Boundary Road, Crawley, West Sussex) and the PCR fragment inserts were sequenced at Birmingham University.

DNA was extracted from agarose gels with the QiaexII kit (Qiagen, Boudary Court, Crawley, W. Sussex) and sequenced by SEQLAB, Gottingen.

### *5.2.7 Analyses of sequences*

Nucleotide sequences were identified and compared with BLAST searches (<http://www.ncbi.nlm.nih.gov/blast/>), and the similarities and possible phylogeny determined by MegAlign computer software of DNASTar (Lasergene).

## 5.3 Results

### 5.3.1 Identifying *Brassica oleracea* BACs containing ACC oxidase genes

#### 5.3.1.1 Isolating BACs containing ACC oxidases

In Figure 5.3 (a,b) the autoradiographs show 'hits' where the *B. oleracea* var. *italica* full length ACC oxidase 2 cDNA probe has hybridised to *E. coli* colonies carrying BACs with homologous regions of DNA. The hybridisation was carried out at 55°C, and washed at low stringency, so the *aco2* cDNA sequence should hybridise to both *aco1* and *aco2* and any other closely related genes, and not be washed off. The BAC codes for the 'hits' are shown in Table 5.4.

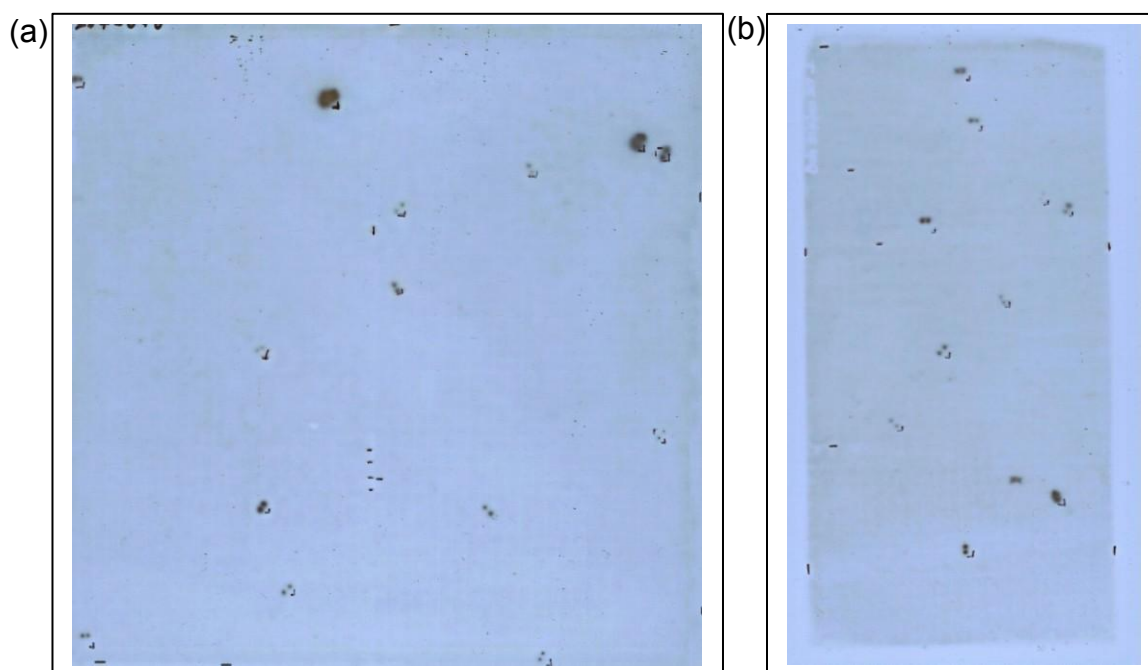


**Figure 5.3** Autoradiograph showing hybridisation between the *Brassica oleracea* BAC library filter 1, (a) and filter 2, (b) and the *Brassica oleracea* var. *italica* ACC oxidase 2 full length cDNA (Pogson *et al.*, 1995a).

**Table 5.4** The codes of the *B. oleracea* BAC colonies that hybridised to the *B. oleracea* ACC oxidase 2 full length cDNA probe.

Hit No.	Bob BAC code	Hit No.	Bob BAC code
1	02 D 02	12	43 P 13
2	10 I 20	13	46 E 09
3	10 J 22	14	50 C 13
4	11 K 12	15	50 O 10
5	12 N 02	16	51 M 19
6	23 I 16	17	51 N 21
7	29 D 02	18	60 E 16
8	29 O 22	19	61 I 11
9	34 O 03	20	62 O 07
10	35 E 16	21	62 I 13
11	37 K 18	22	65 I 13

### 5.3.1.2 Identifying ACC oxidases from BACs isolated

In Figure 5.4, the *aco1* 3' UTR probe hybridised to BAC hit numbers 11, 12, 13 and 15. In Figure 5.5, the *aco2* 3' UTR probe hybridised to BAC colonies 9, 10, 16, 20, and 22. There appears to be specific binding of the *aco1/aco2* probes to the *aco1/aco2* genes and no cross-hybridisation. The 283bp *aco1* and 252bp *aco2* 3'UTR probes share only 44% nucleotide identity, spread evenly along the sequences. There was specific hybridisation of the *aco1* probe to BAC colonies 11, 12 and 15 (Figure 5.4) and the *aco2* probe to BAC 20 (Figure 5.5). If single bands suggest single gene copies, these data suggest that BACs 11, 12, 15 contain one single *aco1* gene and BAC 20 contains one single *aco2* gene. This leaves 18 BACs unaccounted for which contain sequences that originally hybridised to the whole length *B. oleracea aco2* cDNA sequence.

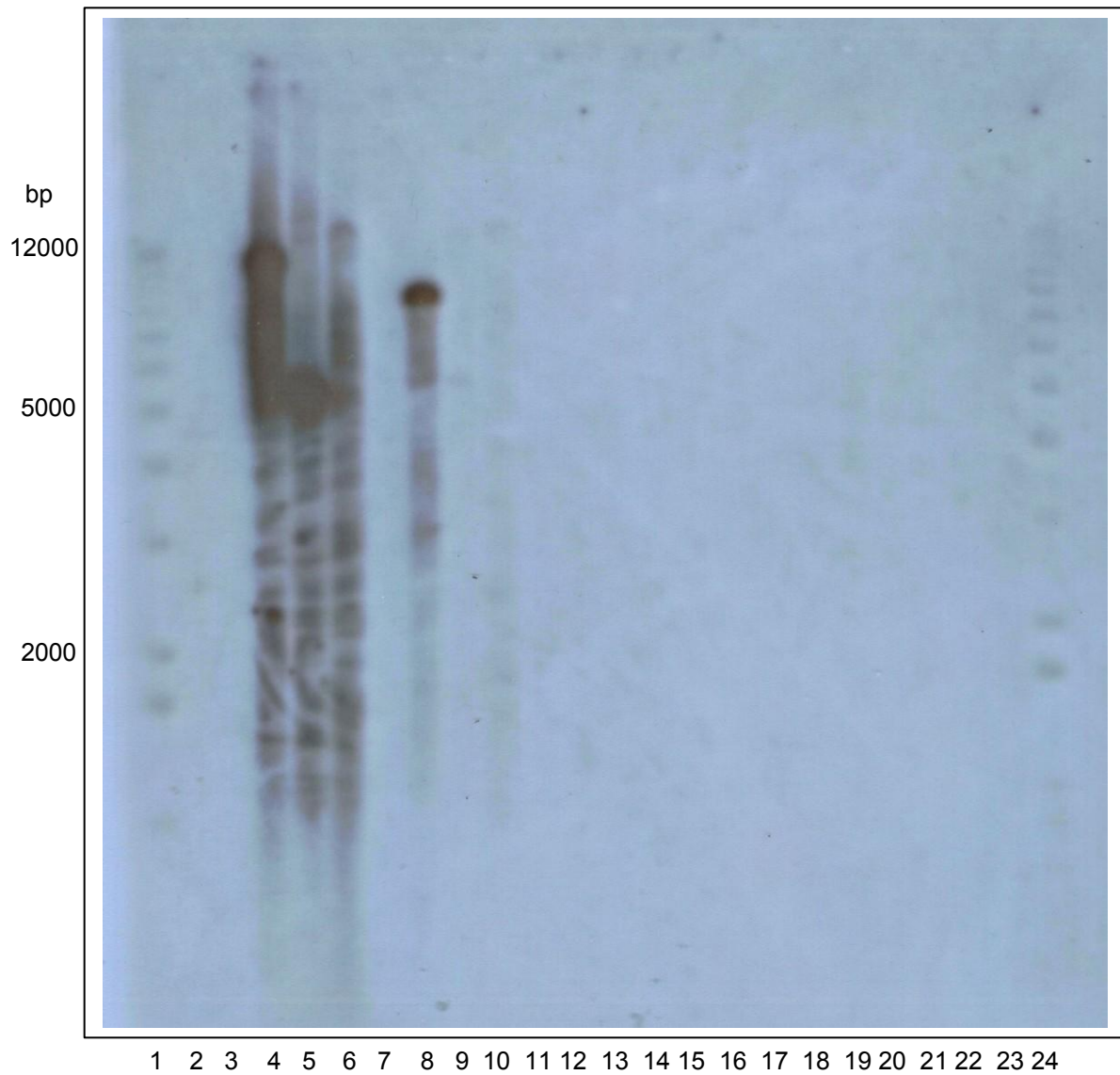


**Figure 5.4** Autoradiograph showing hybridisation between the *B. oleracea* ACC oxidase 1 cDNA (Pogson *et al.*, 1995a) 3' UTR 283bp probe and the EcoRI RFLP BAC filter.

In lanes 1 and 24, the 1kb Plus DNA Ladder (GIBCO-Life Tehnologies) and in lanes 2-23 BAC clone hit numbers left-right: 1, 5, 11, 12, 13, 14, 15, 19, 21, 2, 3, 4, 6, 7, 8, 9, 10, 16, 17, 18, 20, 22 (see Table 5.4).

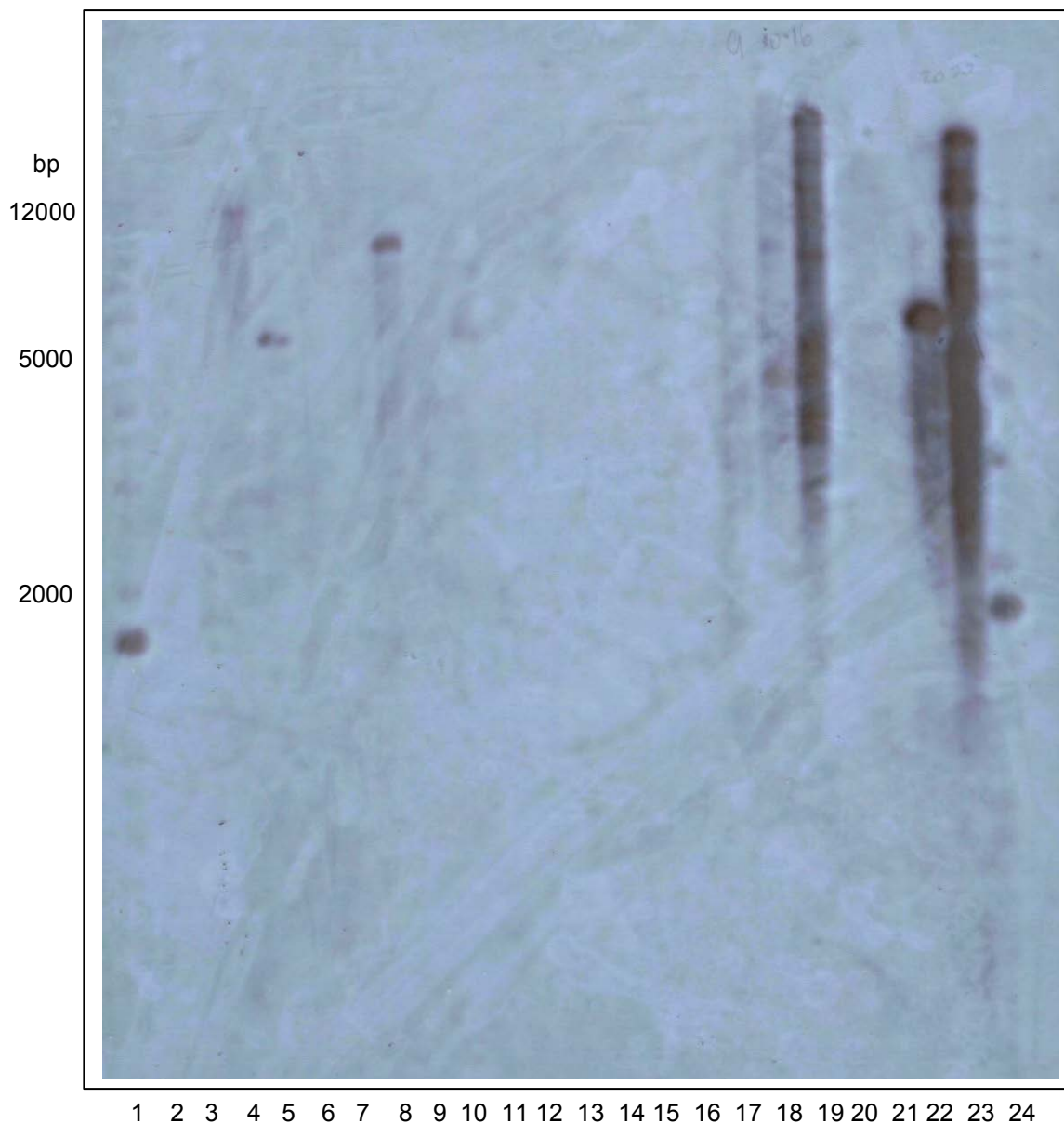


**Figure 5.5** Autoradiograph hybridisation between the *B. oleracea* ACC oxidase 2 cDNA (Pogson *et al.*, 1995a) 3' UTR 252bp probe and the *Eco*RI RFLP BAC filter.

In lanes 1 and 24, the 1kb Plus DNA Ladder (GIBCO-Life Tehnologies) and in lanes 2-23 BAC clone hit numbers left-right: 1, 5, 11, 12, 13, 14, 15, 19, 21, 2, 3, 4, 6, 7, 8, 9, 10, 16, 17, 18, 20, 22 (see Table 5.4).

In Figure 5.6, the *aco1* specific primers amplified the same size fragment (1300-1400bp) from all 22 BACs. The BAC sequences must have had high homology to the primers for amplification and producing the same size fragment suggests that all of the BACs contain *ACC oxidase* sequences. The positive control from the cDNA (889bp) was smaller than the product from the BACs that were 1300-1400bp. This suggests that all of the BACs contain *ACC oxidases* with introns that amount to 400-500bp in the region between primers 2 and 5. These data suggest that either all BACs contain an *aco1* sequence or that these primers do not distinguish between *aco1* and *aco2* sequences (or any other closely related sequences).

The *aco2* specific primers (2 and 4) amplified fragments in Figure 5.6, from only 5 BAC hits, 9, 10, 16, 20 and 22. These were the same BAC clones that the *aco2* 3' UTR probe hybridised to on the *EcoRI* BAC RFLP filter. It appears that these colonies contain *aco2* genes, thus leaving 17 BACs that need characterising.

PCR products from the amplification of BAC hit numbers 3, 4, 12 and 20 with primers 2 and 5 were ligated into a vector for sequencing. Three individual colonies from each transformation were chosen for sequencing in forward (primer 2) and reverse (primer 5) orientations. Sequencing BACs 3 and 4 produced two separate sequences that aligned to both *aco1* and *aco2* cDNA sequences in a BLAST search (<http://www.ncbi.nlm.nih.gov/blast/>). BAC 12 contained a single *aco1* sequence, and BAC 20 contained an *aco2* sequence, when entered into a BLAST search (<http://www.ncbi.nlm.nih.gov/blast/>). The aligned consensus sequences of *aco1* and *aco2* are shown in Figures 5.7 and 5.8. It is clear in Figures 5.7 and

5.8 that *aco1* and *aco2* are different genes. Intron 1 in *aco1* is much smaller (97bp) than the *aco2* intron 1 (248bp) and they share only 18% nucleotide identity. The intron 2 of *aco1* is much larger (312bp), than that of *aco2* (108bp) and they share only 21% nucleotide identity. There is no homology shared between introns of *Brassica oleracea aco1* and *aco2*.

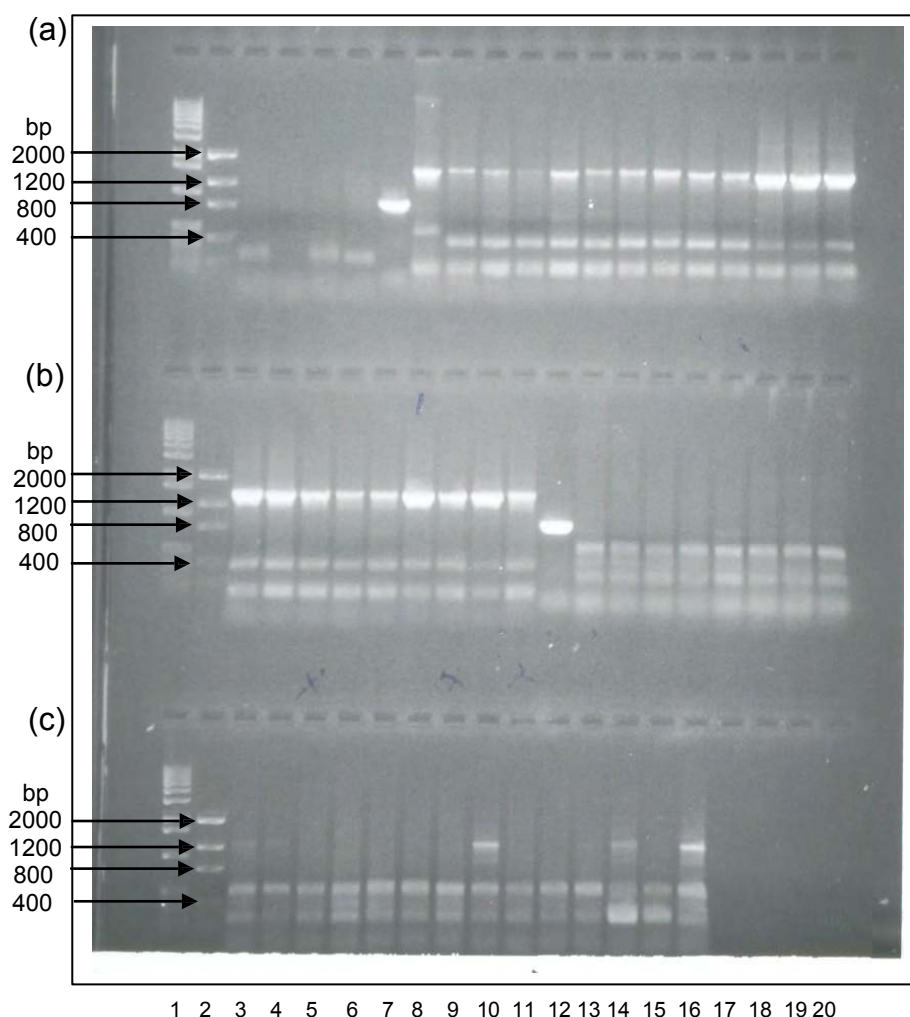


**Figure 5.6** Electrophoretogram showing the products of a PCR between the BAC DNA and *aco1* specific primers (2 and 3) and *aco2* specific primers (2 and 4).

Lanes 1 and 2 contain the Step ladder and Low DNA Mass ladder, respectively (GIBCO-Life Technologies). The 7th lane in row (a) is the positive control from the cDNA of *aco1*. Lanes 8 –20 (a), and 3-11 (b) are the PCR products from primers 2 and 3 on all of the BACs. The 12th lane (b) is the positive control from the cDNA of *aco2* for primers 2 and 4. Lanes 13-20 (b) and 3-15 (c) are the PCR products from primers 2 and 4 from the BAC hits 1-22.

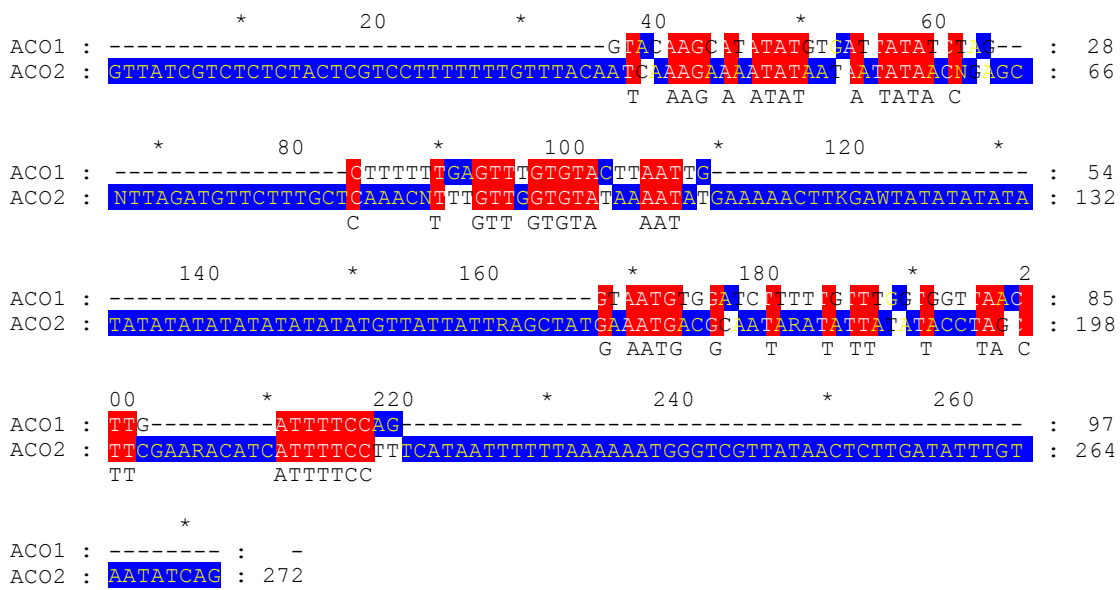


**Figure 5.7** *Brassica oleracea* ACC oxidases 1 and 2 intron 1 aligned to determine possible homology. Red boxes with white letters= consensus; Blue boxes with yellow letters= no consensus. A= adenine, T=thymine, C=cytosine, G= guanine.

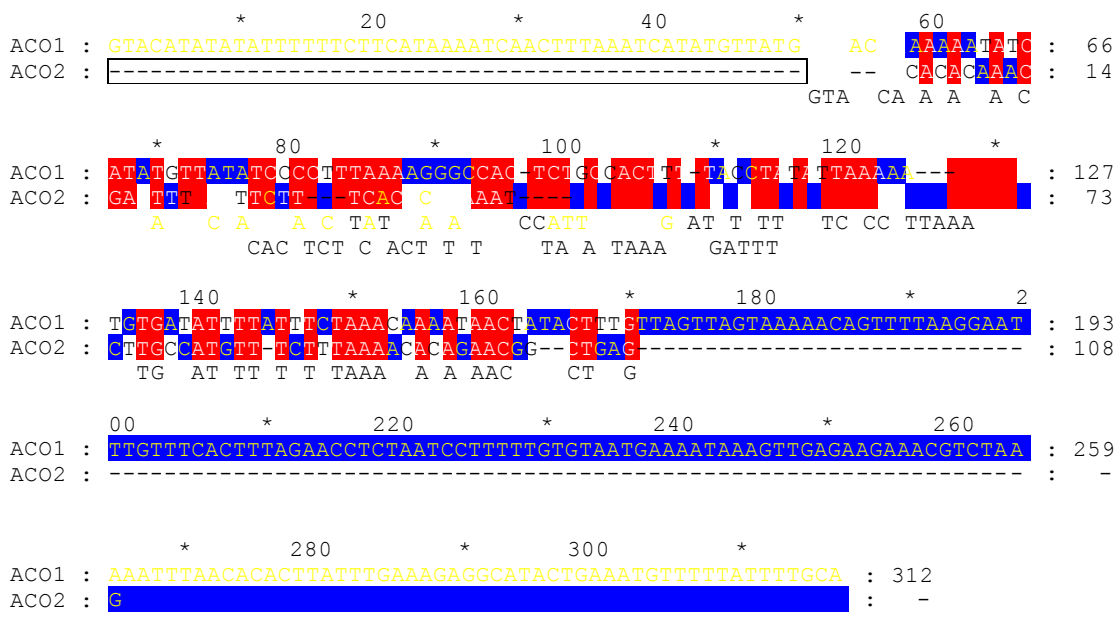


**Figure 5.8** *Brassica oleracea* ACC oxidases 1 and 2 intron 2 aligned to determine possible homology. Red boxes with white letters= consensus; Blue boxes with yellow letters= no consensus. A= adenine, T=thymine, C=cytosine, G= guanine.

Primers were designed to amplify intron 1 (9 and 10) and intron 2 (5 and 7) for both *aco1* and *aco2* (see Figures 5.1 and 5.2). Primers 5 and 7 should amplify a 500bp DNA fragment by PCR with an *aco1* template and a 280bp fragment with *aco2*. Primers 9 and 10 should amplify a 130bp DNA fragment with an *aco1* template and a 300bp with *aco2*. These fragments could be separated on a 1% (w/v) agarose gel by electrophoresis to show polymorphism between *aco1* and *aco2*. In Figure 5.9, the BACs that had been sequenced (3, 4, 12 and 20) were tested with primers 9 and 10, and 2 and 5 for evidence of *aco1* or *aco2* introns. Intron 2 was amplified with primers 5 and 7 and produced the lower 280bp fragment from *aco2* and the larger (500bp) fragment of *aco1*. The PCR showed that BACs 3 and 4 contained both *aco1* and *aco2*, whereas BAC 12 contained only *aco1* and BAC 20, only *aco2* sequences.

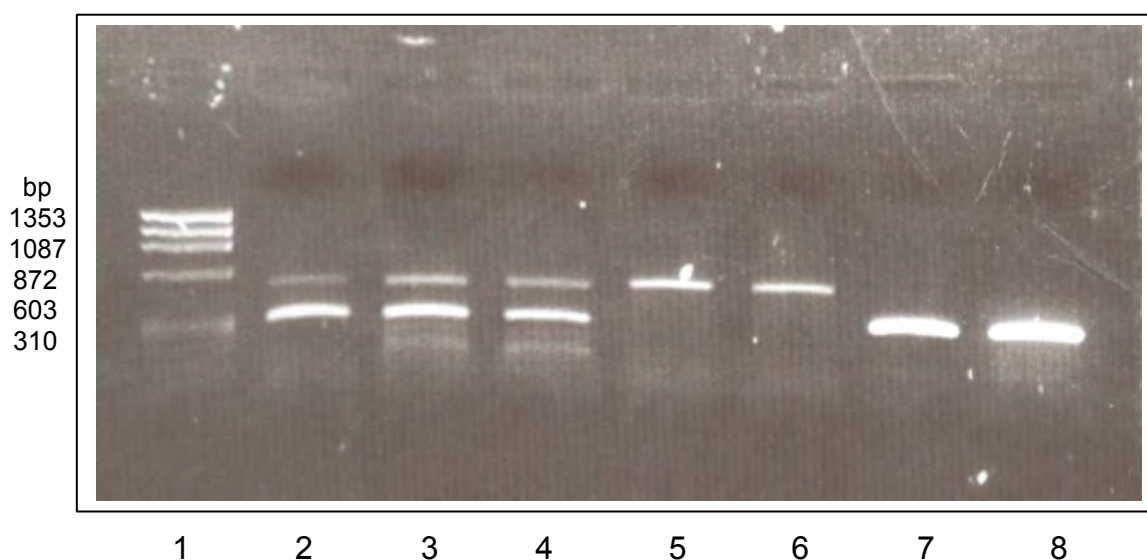


**Figure 5.9** Electrophoretogram showing the PCR products from primers 5 and 7 on BAC's 3, 4, 12 and 20.

Lane 1,  $\phi$ X174 RF DNA/*Hae*III fragments; lane 2, BAC 3; lanes 3 and 4 BAC 4; lanes 5 and 6; BAC 12; lanes 7 and 8, BAC 20.

In Figure 5.10, primers 5 and 7, and primers 9 and 10 were used to amplify fragments from all of the BACs. BAC 12 has evidence for only having an *aco1* gene. The other 21 BACs have evidence for having both *aco1* and *aco2*. The PCR fragments A-D in Figure 5.10 were extracted from the gel and sequenced. They were the same sequences as the *aco1* and *aco2* introns 1 and 2.

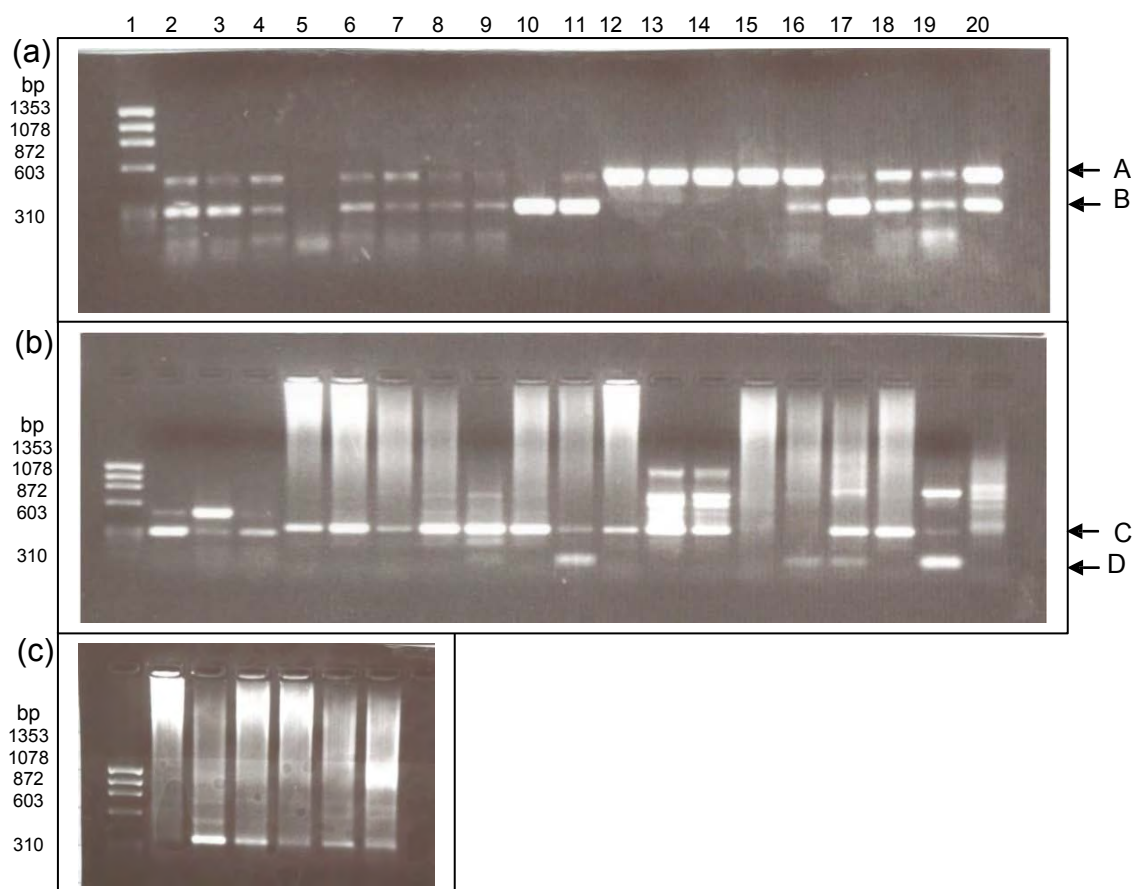


**Figure 5.10** Electrophoretogram showing PCR products from all BACs with primers 5 and 7, and, 9 and 10. Lane 1 for rows (a-c) is the DNA ladder of  $\phi$ X174 RF DNA/ *Hae*III fragments. In row (a), lanes 2-20 show PCR products from primers 5 and 7 and BACs 1-19. In row (b), lanes 2-4 show PCR products from primers 5 and 7 and BACs 20-22. Lanes 5-20 show PCR products from primers 9 and 10 with BACs 1-16. In row (c), lanes 2-7 show PCR products from primers 9 and 10 with BACs 17-22. Arrows: A= *aco1* intron 2; B=*aco2* intron 2; C= *aco2* intron 1; D=*aco1* intron1.

Figure 5.11 shows the autoradiograph produced from the hybridisation between the BAC *Eco*RI RFLP filter and the *aco1* intron 2 probe, amplified by PCR from BAC 12 with primers 5 and 7. The intron probe hybridised to the same locations as the *aco1* 3' UTR probe in Figure 5.4. The hybridisation to BACs 11 and 12 at 12000 and 5000bp, respectively, suggest that the *B. oleracea aco1* gene is located on these two BACs. It also suggests that originally, the full length cDNA *aco2* probe hybridised to this sequence at 55°C, with low stringency washings.

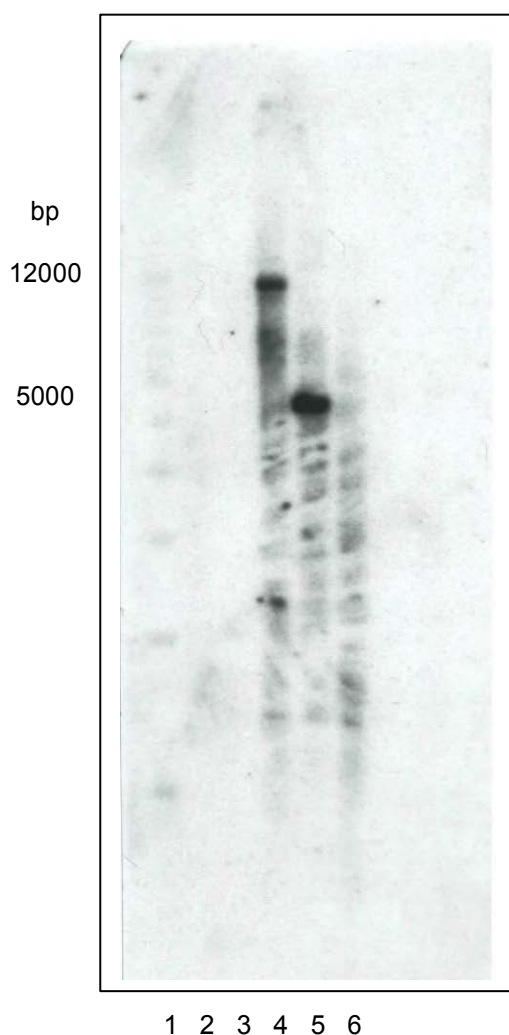


**Figure 5.11** Autoradiograph showing the hybridisation between the *Brassica oleracea* BAC *Eco*RI RFLP filter and the *Brassica oleracea aco1* intron 2 probe.

In lane 1 the 1kb Plus DNA Ladder (GIBCO-Life Tehnologies) and in lanes 2-6 BAC clone hit numbers left-right: 1, 5, 11, 12, 13.

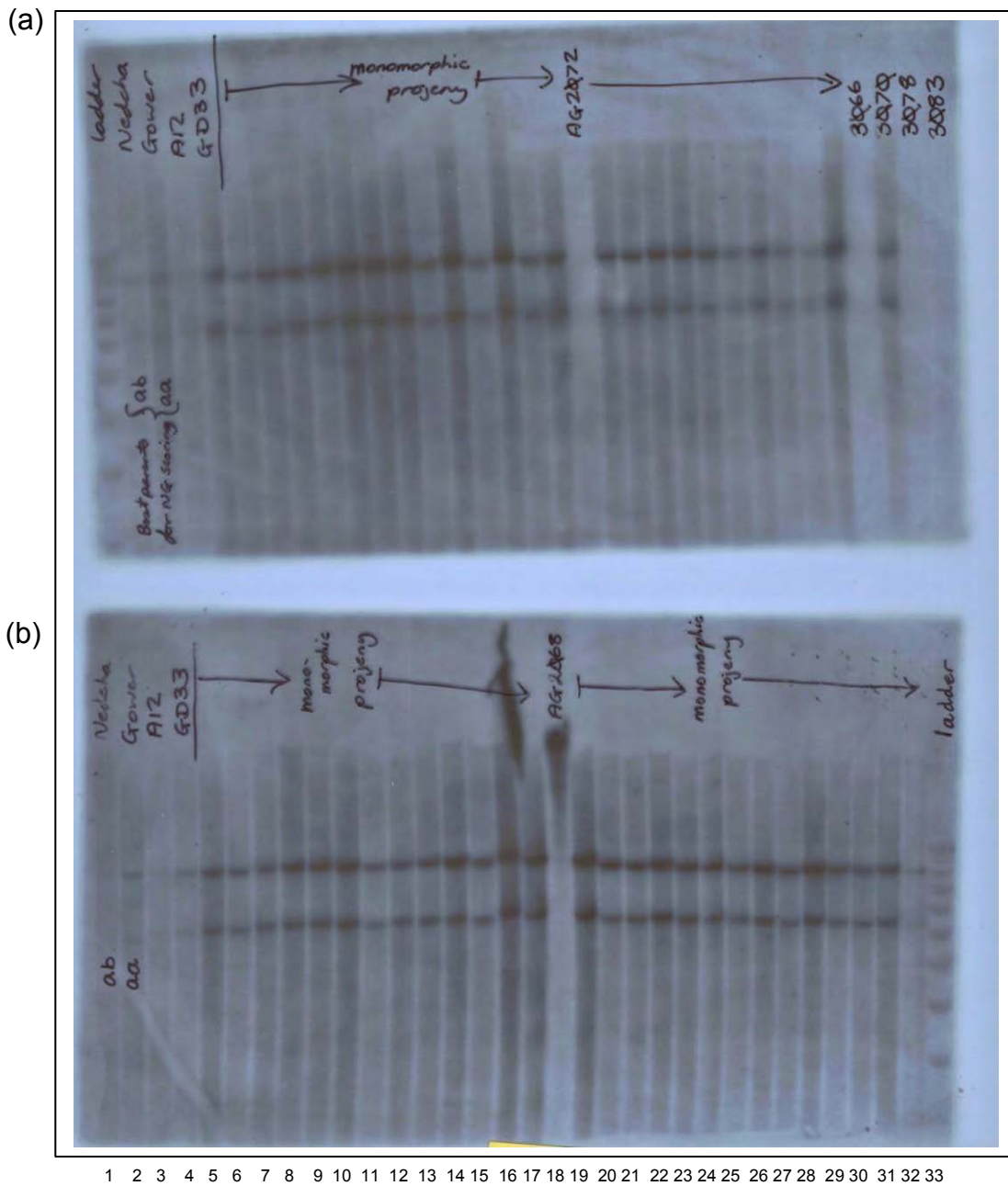
### 5.3.2 Genetic Mapping of *Brassica oleracea aco1* and *aco2* genes

Figure 5.12, shows the autoradiograph produced from the hybridisation between the *aco1* 3'UTR probe and the *EcoRI* digested DNA from the cross between A12 and GD33 (AG population). There are clearly 2 major bands, suggesting that there are two copies of the *aco1* gene that have hybridised to the probe. However, the lines have the same binding pattern so there is no polymorphism to score for segregation of the progeny.

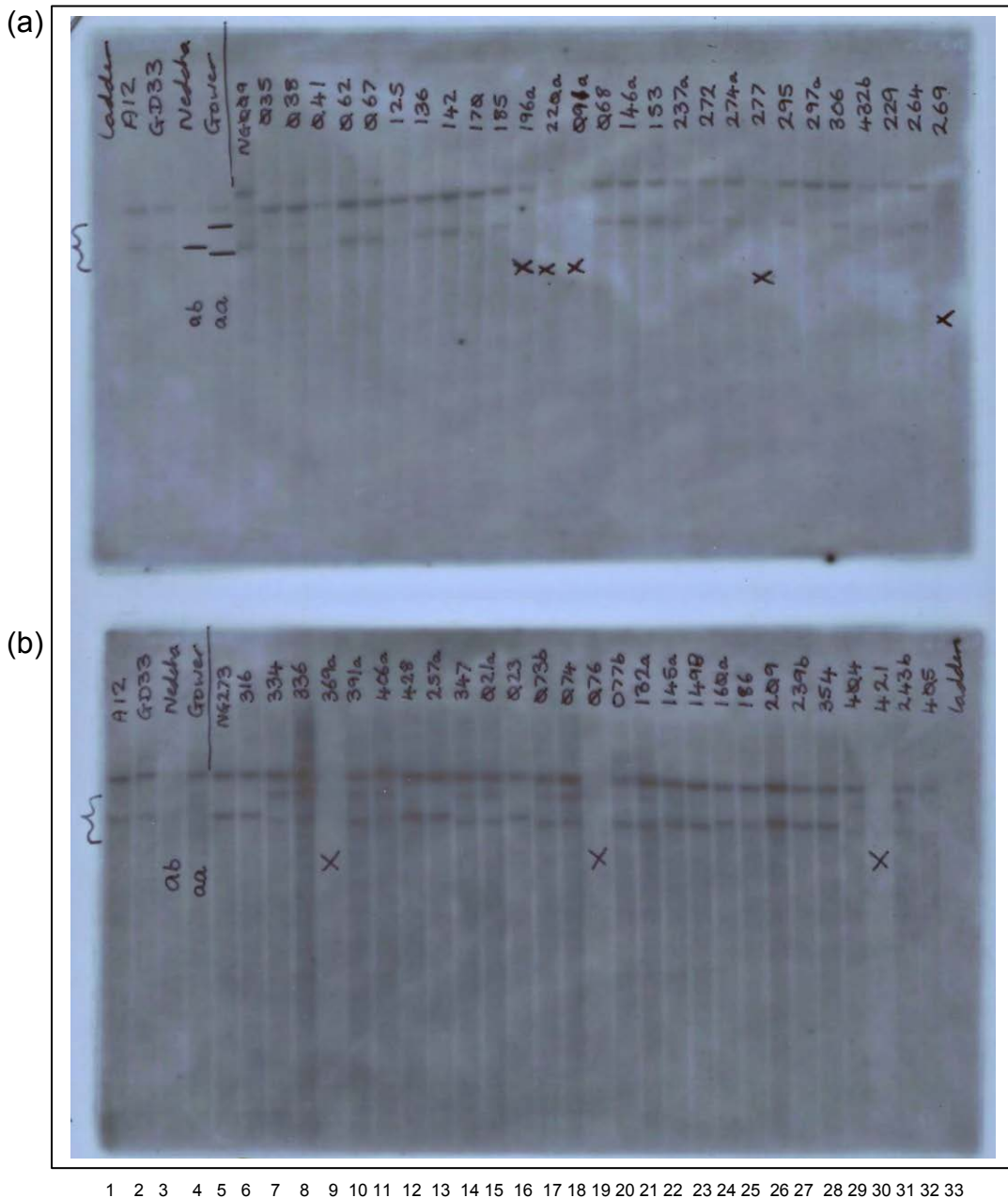
Figure 5.13, shows the autoradiograph produced from the hybridisation between the *aco1* 3'UTR probe and the *EcoRI* digested DNA from the cross between Nedcha and Gower (NG population). In this population there were also two major bands containing sequences with high homology to the *aco1* 3'UTR probe. There was segregation of the progeny in the DH lines of the NG population so it was possible to score the autoradiograph.

Figure 5.14, shows the autoradiograph produced from the hybridisation between the *aco2* 3'UTR probe and the *EcoRI* digested DNA from the cross between A12 and GD33 (AG population). There were two major bands where the probe had hybridised to, and segregation of the progeny that could be scored.

Figure 5.15, shows the autoradiograph produced from the hybridisation between the *aco2* 3'UTR probe and the *EcoRI* digested DNA from the cross between Nedcha and Gower (NG population). There were also two major bands in this population containing sequences with high homology to the *aco2* 3'UTR probe and segregation of the progeny.



**Figure 5.12** Autoradiograph showing the hybridisation between the *B. oleracea* ACC oxidase1 cDNA 3' UTR 283bp probe and the AG mapping filter. In row (a) the parents (Alboglabra12 and GD33) are in lanes 3-5 and, in row (b) the parents (Alboglabra12 and GD33) are in lanes 3 and 4. In row (a), lanes 6-33, and in row (b) lanes 5-32 contain the progeny of the cross.



**Figure 5.13** Autoradiograph showing the hybridisation between the *B. oleracea* ACC oxidase1 cDNA 3' UTR 283bp probe and the NG mapping filter. In row (a) the parents (Nedcha and Gower) are in lanes 3-5 and, in row (b) the parents (Nedcha and Gower) are in lanes 3 and 4. In row (a), lanes 6-33, and in row (b) lanes 5-32 contain the progeny of the cross.

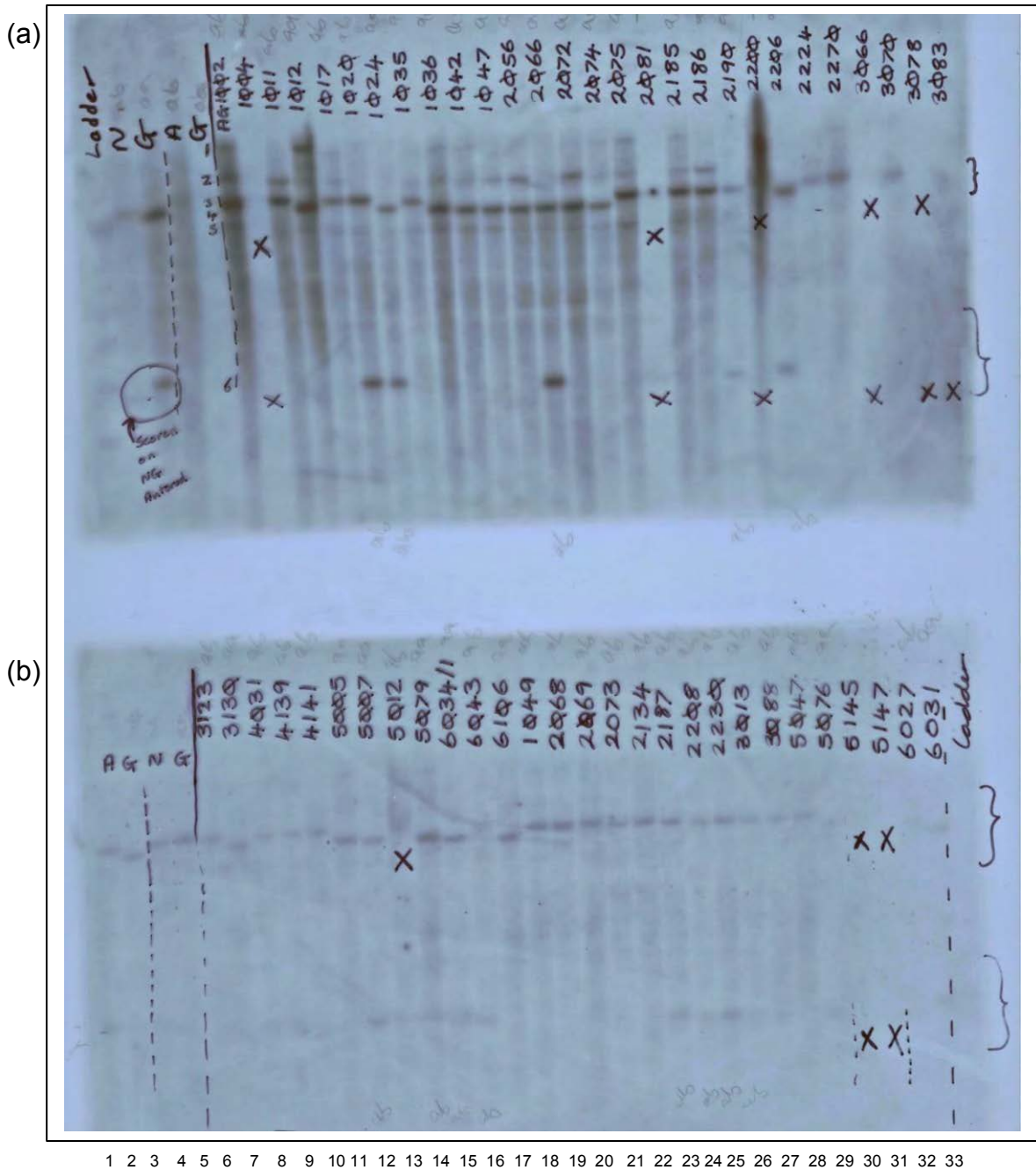


**Figure 5.14** Autoradiograph showing the hybridisation between the *B. oleracea* ACC oxidase2 cDNA 3' UTR 252bp probe and the AG mapping filter. In row (a) the parents (Alboglabra12 and GD33) are in lanes 3-5 and, in row (b) the parents (Alboglabra12 and GD33) are in lanes 3 and 4. In row (a), lanes 6-33, and in row (b) lanes 5-32 contain the progeny of the cross.

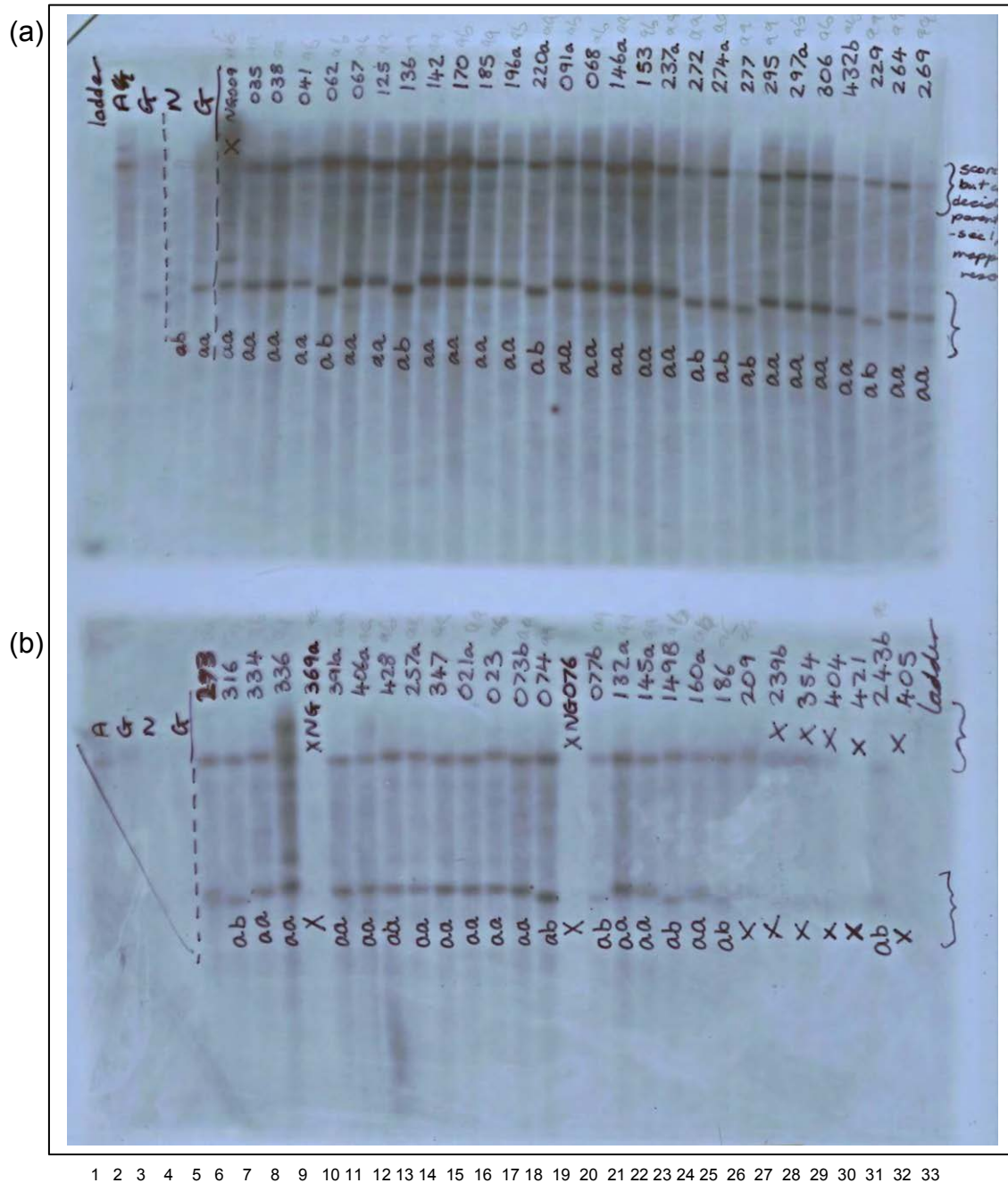


**Figure 5.15** Autoradiograph showing the hybridisation between the *B. oleracea* ACC oxidase2 cDNA 3' UTR 252bp probe and the NG mapping filter.

In row (a) the parents (Nedcha and Gower) are in lanes 3-5 and, in row (b) the parents (Nedcha and Gower) are in lanes 3 and 4. In row (a), lanes 6-33, and in row (b) lanes 5-32 contain the progeny of the cross.

The autoradiographs in Figures 5.12-5.15 were scored for segregation of *aco1* and *aco2* in the progeny from the parent crosses. The data was entered into a spreadsheet and analysed in conjunction with Dr Graham Teakle at HRI-Wellesbourne, with the computer software JOINMAP 2.0 (Stam *et al.*, 1995). JOINMAP 2.0 (Stam *et al.*, 1995) predicted linkage of *aco1* and *aco2* genes in *Brassica oleracea* as shown in Figure 5.15. Of the predicted 2 genes x 2 loci, only one locus from each gene was calculated due to the lack of polymorphism of the *EcoRI* mapping filters.

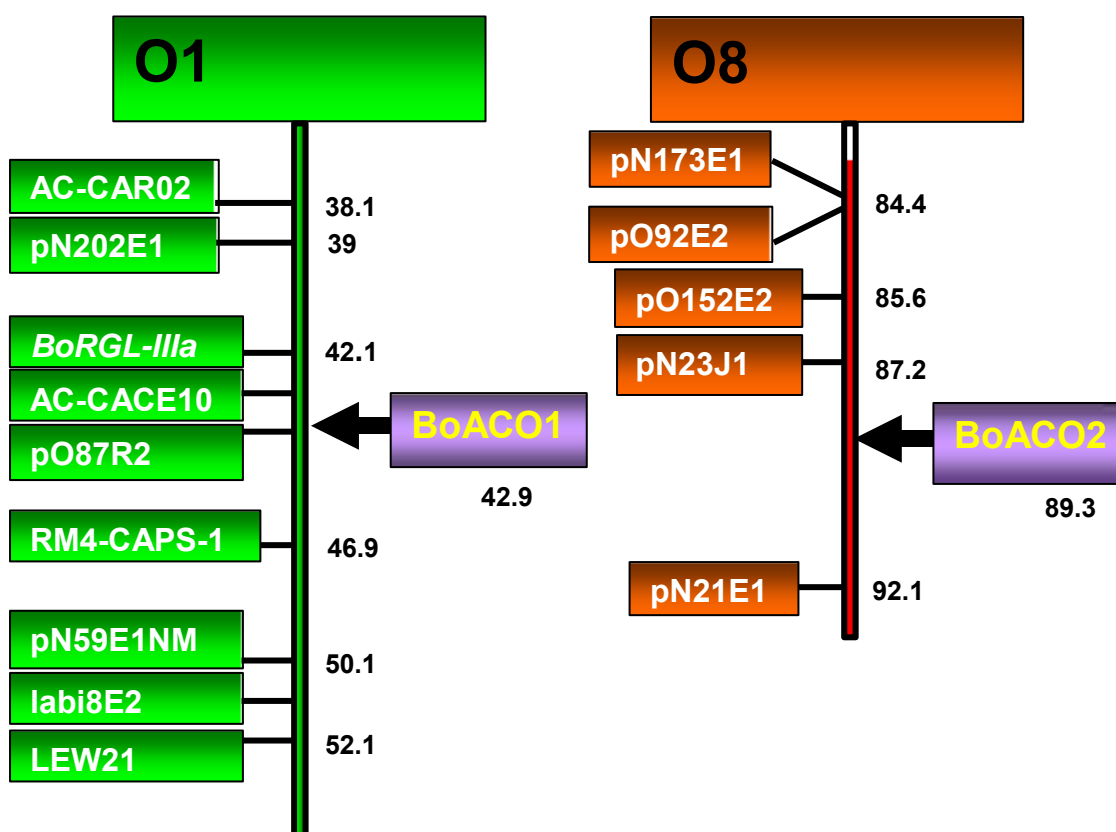


**Figure 5.16** The linkage map positions of *aco1* and *aco2* in *Brassica oleracea* for the loci that could be scored by *EcoRI* RFLP polymorphism. Genetic markers are shown on the left-hand side and map distances (cM) on the right-hand side of the linkage groups.

### 5.3.3 Analysis of nucleotide sequences of closely related genes to *Brassica oleracea aco1* and *aco2*

The *B. oleracea* ACO1 cDNA sequence is very similar to the *Brassica juncea* ACO mRNA (96.7% nucleotide identity) (emb/z11750/BJEFEMR). It is also very similar to the *Brassica napus* (gene bank ref: gb/L27664/BNAACCOX1) mRNA sequence with 70.8% and *Brassica rapa* 70% nucleotide identity. The *Brassica napus* ACC oxidase is the only sequence to have homology with the *B. oleracea aco1* intron 1, but most *Brassica aco* sequences have been obtained from cDNAs and do not show the introns.

The cDNA sequence of *B. oleracea aco2* is most like the *Brassica rapa aco* mRNA with 80.9% nucleotide identity. It is also very similar to the *B. napus* sequence (gb/L27664/BNAACCOX1) with 77% identity. The *B. napus* Introns 1 and 2 of this sequence share 93% identity with the *aco2* introns sequenced in these experiments. There is also high similarity between the *B. oleracea aco2* and the *aco* cDNA from *B. juncea* with a nucleotide identity of 70.1 %.

These sequence analyses show high conservation of *aco1* and *aco2* within the Brassica family.

## 5.4 Discussion

The aims of this chapter were to determine how many *aco* genes exist, their copy number and where they mapped to in the *Brassica oleracea* genome. The first stage was to identify *aco* sequences, and the second to map these sequences.

The full length *B. oleracea* var. *italica* *aco2* cDNA sequence (Pogson *et al.*, 1995) was hybridised to the *Brassica oleracea* BAC (BoB) library and washed at low stringency. This produced twenty-two BAC colonies that hybridised to the cDNA probe. The BAC *EcoRI* RFLP filter was concurrently hybridised to the *aco1* 3'UTR and *aco2* 3'UTR sequence specific probes. The *aco1* 3'UTR probe hybridised to BAC hit numbers 11, 12, 13 and 15 and the *aco2* 3'UTR probe hybridised to BAC hit numbers 9, 10, 16, 20 and 22. However, specific primers for *aco1* amplified fragments from all of the BACs. Specific primers for *aco2* only amplified fragments from the BACs that the *aco2* 3'UTR probe had hybridised to. It was difficult to interpret this data, so four out of the 22 BACs were sequenced between primers 2 and 5 of the *ACC oxidase* sequence. Exon sequences were aligned with the either *aco1* or *aco2* cDNA sequences from Pogson *et al.* (1995a). The exon sequences of BAC 12 matched only *aco1* and BAC 20 only *aco2*. BACs 3 and 4, which had not hybridised to either of the 3'UTR probes, appeared to have both *aco1* and *aco2* sequences. Sequences matched up to either *aco1* or *aco2*, so BACs that hybridised to the full length *aco2* cDNA probe, but not to the 3'UTR probes may contain *aco1* and/or *aco2* genes.

The sequences for introns 1 and 2 from *B. oleracea* *aco1* and *aco2* were obtained. They showed that *aco1* and *aco2* were two different genes,

and they did not share homology between the introns. The *aco1* intron 1 (312bp) sequence was amplified and hybridised to the BAC *EcoRI* RFLP filter. The *aco1* intron 1 sequence hybridised to the same places as the *aco1* 3'UTR probe, suggesting that they were hybridising to the same fragment. The polymorphism between intron sizes was used to determine the identities of BAC sequences that had originally hybridised to the *B. oleracea aco2* full length cDNA probe. The results appeared to show that all of the BACs contained an *aco1* and *aco2* gene, except BAC 12, which only had evidence for an *aco1* gene, and BAC 20 that appeared to have an *aco2*.

The *aco1* 3'UTR and *aco2* 3'UTR probes were used to identify map positions on the *Brassica oleracea* integrated map (Sebastion *et al.*, 2000). There was sufficient segregation of the progeny from the parents in the doubled haploid lines to calculate a map position for *aco1* on linkage group 1 (42.9cM) and for *aco2* on linkage group 8 (89.3cM). There were two dominant bands in Figures 5.12-5.15, suggesting two copies for both *aco1* and *aco2*, although there was not enough segregation within the progeny to map both these loci.

The conclusions that can be drawn from these data are that *aco1* and *aco2* are individual genes with two copies. This is in accordance with Pogson *et al.* (1995a), and examples of small *aco* gene families including tomato (3 genes), petunia (4 genes) and melon (3 genes) (Barry *et al.*, 1996; Tang *et al.*, 1993; Lasserre *et al.*, 1996). There is no evidence for an third ACC oxidase, and *aco1* and *aco2* may be physically linked in the genome. There appears to be high sequence conservation between the two *Brassica oleracea* var. *italica* cDNA exons, and divergence between the introns. There also

appears to be high conservation of the nucleotide sequences of the *ACC oxidases* within the *Brassica* genus, and it is not surprising that the *Brassica napus* (AACC) *aco* gene introns shared 93% nucleotide identity with *B. oleracea* (CC).

Genetic and protein conservation suggest an important role for these genes, such as post-pollination ethylene bursts and enhancing responses to stress (Rays *et al.*, 2000; Abeles, 1973). This work has shown that there is nucleotide sequence divergence between the introns of *B. oleracea aco1* and *aco2* genes, but not in the exons. There are clearly two copies of the genes, but are these regulated in the same way, and are they both active? It would be useful to isolate the promoters and carry out expression studies of these genes to determine allelic variation. Alleles that produce less post-harvest ethylene could be selected for to possibly extend broccoli shelf-life.

# 6.0 General Discussion

## 6.1 Assessing the strategies

### 6.1.1. Constructs

The *Brassica oleracea* L. var. *italica* ACC oxidases 1 and 2 and ACC synthase cDNAs were ligated into the minimal T-DNA vector pSCV1.0 between a CaMV 35S promoter and a *nos* terminator. It was essential to produce constructs containing *aco1*, *aco2* and *acs* in sense and antisense orientations to understand their role in post-harvest ethylene production. Both antisense and sense constructs have been shown to down-regulate genes (Meyer and Saedler, 1996) and sense constructs may even up-regulate the genes. It would not have been possible to transform broccoli with ACC cDNAs or to analyse ethylene production in relation to chlorophyll loss without the constructs. There were a number of factors limiting the cloning strategy, most notably the large number of restriction sites within the cDNA clones and cloning vector, using a minimal T-DNA vector and leaving the vector with restriction sites to change the promoter at some later date. The most efficient way to achieve this was by amplifying the sequences by PCR and blunt-ended ligating them into the pJ1.0 backbone vector. Although this approach was successful for *aco1* and *aco2*, it did not work for ACC synthase. *Bam*HI sites were added to the primers before PCR and then the product digested and ligated into the pJ1.0 vector. It was advantageous to have compatible ends so the cDNA insert could be ligated into the vector in either antisense or sense orientation. A *gus* control construct was produced to determine the impact of the transformation effects on the T<sub>0</sub> plants, and confirm activity of the CaMV 35S promoter. It took longer to produce seven, marker-free constructs, but these aspects became useful down-stream. In chapter 3,

marker-free plants were produced from the progeny of 28/00 *aco1A* 3 by selecting out the unwanted *rol* genes of the *Ri* T<sub>L</sub>-DNAs. A marker-free strategy would be essential to produce commercial transgenic plants, as these would not be permitted to contain superfluous sequences such as antibiotic markers. Unfortunately, there was not enough time to grow the T<sub>1</sub> generation and assay for the post-harvest production of ethylene and chlorophyll levels. The *ACC synthase* sense line in chapter 4 gave information that would not have been obtained from antisense constructs. It showed that ACC synthase appears to be the rate-limiting enzyme in the biosynthesis of ethylene as the buds at 0h produced 245nl/g bud/h ethylene, 5-fold more than the normal basal level. If the construct was actively producing mRNA transcripts that were being translated into protein enzymes, it is possible that more ACC substrate was produced for the ACO to catalyse into ethylene. It was also important to produce constructs with the native *ACC oxidase* and *ACC synthase* cDNAs isolated by Pogson *et al.* (1995a,b) from *Brassica oleracea* L. var. *italica*. Henzi *et al.* (1999b) had obtained the pTOM13 construct (Hamilton *et al.*, 1990) containing a tomato *ACC oxidase* between the CaMV 35S promoter and its terminator. The *Brassica oleracea* L. var. *italica* *aco1* and *aco2* shared 71% and 70% nucleotide identity with the tomato *ACC oxidase*. However, Henzi *et al.* (1999b) did not achieve sufficient reduction of ethylene and even increased the ethylene peak at 26h in most of the lines.

### 6.1.2 Transformation and regeneration

A transformation protocol was chosen to utilise the natural capacity of *Agrobacterium rhizogenes* to transfer T-DNA into the recipient plant genome. The overall transformation efficiency was very low (3.3%), but this could be improved by inoculating the cut surface soon after excision. Transformation was highest for the *gus* construct with 11.7%, suggesting that the ACC constructs may have had a detrimental effect on the transformation efficiency. There is no evidence that transformation with another method such as biolistics, protoplast transformation or *Agrobacterium tumefaciens* would produce higher frequencies (Puddephat *et al.*, 1996). Ninety six percent of the roots transformed with the *A. rhizogenes* strain LBA 9402 carrying the co-integrate vector pRi1855::GFP, had been co-transformed with the T<sub>L</sub>-DNA and binary T-DNA, containing the *gus* constructs. The aim to produce 20 independently-transformed GDDH33 root lines for each construct was achieved. Cells transformed by *A. rhizogenes* were easily distinguishable by the emergence of 'green fluorescing' hairy roots. Hairy roots are clonal, arising from single cells (Tempe and Casse-Delbart, 1987) and do not create chimeric plants. The transformed roots were easily identified and transferred to media for maintenance and regeneration. The other transformation techniques do not transfer the *Ri* T-DNA containing the *rol* genes and therefore have advantages over *A. rhizogenes*-mediated transformation. The *Ri* T-DNA produces a phenotype that exhibits wrinkled leaves, shortened internode lengths, non-geotropic roots, reduced apical dominance, altered flower morphology, and reduced seed production (Tepfer, 1990). Severe *rol* phenotype was present in 4 out 18 of the regenerated T<sub>0</sub>

lines. This did not appear to be related to copy number and relative severity was probably a 'position effect'. No seeds were harvested from T<sub>0</sub> lines with severe *rol* phenotype as the majority of the floral buds had been removed for ethylene and chlorophyll samples. Seeds were obtained from 11 of the lines with moderate/weak *rol* phenotype as these produced larger heads with greater numbers of floral buds. The results in chapter 5 showed that the impact of the *rol* genes reduced both the post-harvest production of ethylene and chlorophyll loss from broccoli buds. However, it was possible to analyse these plants when compared to the *gus* control lines.

In the T<sub>1</sub> generation, it will be possible to segregate out the unwanted *rol* genes and produce homozygous lines for the construct T-DNA. T<sub>1</sub> lines from different constructs and transformation events could be crossed to produce lines with stacked genes that may possess a more extreme phenotype, and produce broccoli heads with a longer post-harvest shelf-life.

Regeneration was clearly the main limiting factor in this process as from 150 transgenic roots, only 18 regenerated into mature whole plants, and this took on average a year and a month. It had taken 149±55d from inoculating to transferring the *gus* plantlets into the glasshouse, whereas it had taken 291±21d for the other lines.

The doubled-haploid cultivar GDDH33 was chosen for transformation as it has a homozygous genetic background, is amenable to transformation through *Agrobacterium rhizogenes* (H. Robinson, pers. comm. HRI-Wellesbourne) and is responsive to microspore culture (L. Harvey, Pers. comm. HRI-Wellesbourne), and also had a short post-harvest head shelf-life. It was amenable to transformation through *A. rhizogenes* but produced roots

with very poor growth, which often died after a few subcultures. This was clearly a genotypic effect as earlier experiments with cultivars Shogun and Packman (results not shown) had produced rapidly growing roots. The regenerated plants from GDDH33 produced very small heads, limiting sampling to just ethylene and chlorophyll measurements. It was not possible to measure the biochemical activity of ACC Oxidase or ACC Synthase *in vivo* due to lack of material.

### 6.1.3 Ethylene and chlorophyll

The strategy for analysing T<sub>0</sub> plants was to measure ethylene production and chlorophyll levels on broccoli buds, the organs that were most affected by post-harvest senescence. It could be used to test the hypothesis that endogenous ethylene plays a major role on sepal chlorophyll loss, and whether it was possible to extend shelf-life. There was not enough material to test for the biological activity of ACC Oxidase and ACC Synthase, or to quantify amounts of proteins, carbohydrates or organic acids. There was not enough time to analyse mRNA expression levels, as this also would have been useful.

There was a positive correlation between ethylene production and chlorophyll loss of post-harvest broccoli buds at 20°C. As 'total' ethylene increased, chlorophyll loss increased. This linear correlation was described by the equation  $y = 0.2386x - 23.041$ , where  $y$  = chlorophyll loss and  $x$ , the total production of ethylene. It was confirmed by comparing the ratio of the regression and the residual mean squares with the F-distribution ( $F = 0.0015$ ).

All of the *ACC oxidase* constructs (*aco1* and *aco2*, sense and antisense) significantly ( $p < 0.005$ ) reduced post-harvest production of ethylene at 24h and significantly ( $p < 0.005$ ) delayed chlorophyll loss, compared to the untransformed control. The *ACC synthase* constructs significantly reduced post-harvest ethylene production at 24h, but did not inhibit a large peak at 72h, and did not significantly reduce chlorophyll loss.

The 'total' post-harvest endogenous ethylene production and chlorophyll loss in the sepals was described by a possible linear relationship. The relationship also shows that down-regulating the native *ACC oxidases* may delay chlorophyll loss. Delaying chlorophyll loss could have a major impact on retailers as heads producing less ethylene could be stored at 20°C for longer, and less would go to waste. It could also benefit the consumers, as the freshness of the head would last longer after purchase.

#### 6.1.4 *The aco1 and aco2 genes*

In chapter 5, it was shown that there were two copies of *aco1* and *aco2*, and apparently no other similar *aco* genes. One of the *aco1* loci was mapped on linkage group 1 and one of the *aco2* loci was mapped to linkage group 8. In both chapters 3 and 5 there were difficulties in achieving consistent results with the hybridisations due to DNA quantity and purity, specificity of the probe and hybridisation conditions. In chapter 3, at 65°C with medium stringency washings, the 3'UTR *aco1* and *aco2* probes did not hybridise to the native GDDH33 genes. In chapter 5, at 55°C hybridisation and low stringency washings, the same probes hybridised to the map filters and the BAC *EcoRI* RFLP filters. In both sets of experiments there were

examples where the probes had not hybridised but there was other evidence of the correct sequences (PCR, GFP assay, sequencing).

## 6.2 A role for ethylene

The plant hormone ethylene plays a major role in plant development. In these experiments it appeared that ethylene increased respiration and plant growth/senescence. The transformation rate and root growth was considerably lower in the lines transformed with the ACC constructs compared to those transformed with the *gus* constructs. The lines with the *gus* constructs significantly regenerated faster ( $p < 0.001$ ) than those with the ACC constructs. However, the lines with the *gus* constructs also senesced faster than the lines with the ACC constructs.

Endogenous ethylene production in the plant appears to be regulated by a multigene family of *ACC synthases* (>1) and two *ACC oxidases*. A model was put forward in chapter 4, suggesting that the basal amount of ethylene produced by the plant is controlled by ACC synthases by producing the ACC substrate that is oxidised into ethylene by ACO1. It is hypothesised that after pollination there are two bursts of ethylene, regulated by two ACC synthases and oxidised by ACO1 and ACO2 in the stamen and carpel structures. This serves to recycle nutrients for the growing embryo by up-regulating genes through a phosphorylation pathway that catabolise macromolecules to be respired for energy. The post-harvest stress on the head, possibly through lack of photosynthate to the buds appears to up-regulate the *aco1* and *aco2* and *ACC synthase 1* and *2(?)*, which forces the head into premature senescence.

## 6.3 Future work

### 6.3.1 Fully understand the role and expression of the *aco* and *acs* genes

Introns 1 and 2 of *B. oleracea* ACC oxidases 1 and 2 were sequenced (chapter 5). ACC oxidases 1 and 2 are two distinct genes, each with two loci. Pogson *et al.* (1995a) carried out post-harvest *aco* mRNA expression studies but little is known of their specific regulation during seed germination, hypocotyl growth, pollination, stress responses or general maintenance. Only one ACC synthase has been isolated from *Brassica oleracea* L var. *italica*. ACC synthases are known to belong to multigene families (Rottman *et al.*, 1991) and are the rate limiting enzymes in the biosynthesis of ethylene (Yang and Hoffman, 1994). There are at least three different classes of ACC synthase in tomato, which could be used to probe either cDNA or BAC libraries of *B. oleracea* and isolate and sequence the genes (Yang and Oetiker, 1998). ACC synthase cDNA clones could then be used as probes for measuring mRNA at different physiological stages or isolating the promoters and fusing different sections to reporter genes such as *gus* (Jefferson *et al.*, 1987) to determine tissue specific expression.

### 6.3.2 Biochemical aspect

The biochemical activity of ACC synthase and ACC oxidase in pre/post harvest broccoli and after pollination could be measured. The substrates for ACC sSynthase, S-adenosylmethionine (SAM) and ACC oxidase aminocyclopropane carboxylic acid (ACC) could be added to media at different amounts with broccoli buds and ethylene production measured. The biochemical activity of the ACC enzymes could be quantified by determining

the maximum rate of ethylene production. There could be assays for proteins, carbohydrates and organic acids (according to King and Morris, 1994), to confirm the extended quality by retaining nutritious macromolecules.

### 6.3.3 Improved silencing of *aco* and *acs* in broccoli

There is a strong body of evidence that the most effective method for gene silencing is to introduce tandem inverted DNA repeats into the plant genome. The mRNA transcripts are thought to hybridise creating double-stranded RNA molecules (Muskens *et al.*, 2000; Cogoni and Macino, 2000; Levin *et al.*, 2000). These double-stranded RNAs are thought either to affect RNA stability, transcription and/or translation directly, or to generate a signal for gene silencing and defence against viruses (Terry and Rouze, 2000).

Constructs with inverted repeats of *ACC oxidase 1* or *2* and *ACC synthase* could be very effective at down-regulating the expression of these genes. The constructs would have to be targeted at post-harvest expression or they might have detrimental effects on plant physiology, such as growth and seed production. A post-harvest specific promoter, preferably one that has not been patented, would be most suitable. Either the *B. oleracea ACC oxidase 2* or *ACC synthase* promoters would probably be effective, but the sequence that up-regulates the genes after pollination would have to be removed to avoid seed yield loss. Such a construct would not interfere with any essential requirements, except possibly pathogen attack. A transformation system with *A. rhizogenes* could be used to produce marker-free, phenotypically normal plants.

#### 6.3.4 Conventional breeding

In melon (*Cucumis melo* L. *melo*) RFLP polymorphisms have been linked to the length of shelf-life (Zheng and Wolff, 2000). Markers for longer shelf-lives were associated with low ethylene and markers for shorter shelf-lives with high ethylene production. It is possible that markers linked to ethylene production could be used in broccoli to select for lines which produce lower amounts of ethylene and that would possess longer shelf-lives. This approach would be more acceptable to the consumers, and possible if there exists variation between the *ACC oxidase* and *ACC synthase* promoters of different *Brassica oleracea* L var. *italica* cultivars.

At HRI-Wellesbourne, there is currently a project to generate a doubled-haploid mapping population of crosses between the long shelf-life Mar34 and short shelf-life GD33, for a QTL analysis on bud yellowing and loss of turgor.

#### 6.3.5 Other ways to improve shelf-life

Application of ethylene biosynthesis inhibitors such as aminoethoxyvinylglycine (Wang, 1977) and ethylene action including silver ions (Aharoni *et al.*, 1985) have been shown to delay chlorophyll loss of broccoli sepals, but are not registered for use on broccoli. Ku and Wills (1999) have shown that methylcyclopropene, an inhibitor of ethylene action could be used to achieve such an end, although this would require continuous exposure to the gas in sealed storage.

Cytokinins have been shown to prolong shelf-life of broccoli by reducing chlorophyll loss. This was first demonstrated by Batal *et al.* (1981) by

dipping broccoli heads in 6-benzyladenine and supported by Rushing (1990) and Clarke *et al.* (1994). Gan and Amasino (1995) isolated a senescence-associated-gene promoter from *Arabidopsis* and fused it to an *isopentyltransferase* gene (*ipt*). The gene product from *ipt* catalyses the rate limiting step in cytokinin biosynthesis. Gan and Amasino (1995) transformed tobacco and retarded leaf senescence. Chen *et al.* (2001) have recently obtained this construct from Gan and Amasino (1995) and transformed broccoli with *Agrobacterium tumefaciens*. They found that bud yellowing was retarded by >50% over 4 days of post-harvest storage at 25°C. This procedure could be optimised to produce broccoli with greater shelf-life.

This project has shown that the technology exists to successfully transform crop plants with traits beneficial for the retailer and consumer. It is essential to understand the genetics and biochemistry behind plant physiology for the improvement of crop plants, which may be achieved by classical breeding and molecular techniques.

# 7.0 Appendices

## 7.1 Media

The following media are made up to a litre with R.O. water, and 6g/l agar added when appropriate.

### LB (pH 7.0)

Component	(g/l)
yeast extract	10
sodium chloride	10
tryptone	10

### YMB (pH 7.0)

Component	(g/l)
mannitol	10
yeast extract	0.4
sodium chloride	0.1
magnesium sulphate	0.2
di-potassium hydrogen orthophosphate	0.5

### MGL (pH 7.0)

Component	(g/l)
mannitol	5
yeast extract	2.5
bactotryptone	5
sodium chloride	5
sodium-glutamate	1.16
di-potassium hydrogen orthophosphate	0.25
magnesium sulphate	0.1
biotin	0.001

**MS30 (pH 5.7)**

Component	(g/l)
Murashige and Skoog medium	1
sucrose	30

**Regeneration Medium (pH 5.7)**

Component	(g/l)
Murashige and Skoog medium	1
sucrose	30
benzyl adenine	0.005
naphthalene acetic acid	0.005

**Rooting and shoot medium (pH 5.7)**

Component	(g/l)
Gamborg's B5 medium	1
sucrose	20
indole-3-propionic acid	0.0003

**Antibiotics** (All antibiotics were filter sterilised before use).

Antibiotic	Solution
cefotaxime	1g Claforan/10mls H <sub>2</sub> O
kanamycin	0.5g/10mls H <sub>2</sub> O
ampicillin	1g/10mls H <sub>2</sub> O
tetracyclin	1g/10mls H <sub>2</sub> O
chloramphenicol	1g/10mls H <sub>2</sub> O
rifampicin	0.5g/10mls methanol

## **Histochemical GUS assay (Jefferson *et al.*, 1987)**

### **Assay buffer (X-Gluc)**

2mM X-Gluc in 50mM NaHPO<sub>4</sub> buffer, pH7.0  
Add 0.1% Triton X-100

### **Stock Solutions**

A. Disodium hydrogen orthophosphate (200mM)

B. Sodium dihydrogen orthophosphate (200mM)

Buffer preparation and use

1. Mix 61mls of stock A with 39mls stock B, to make buffer C.
2. Dissolve 10mg X-Gluc in 2.5ml buffer C.
3. Add 200 $\mu$ l for each root sample.

## 7.2 DNA Sequences

### pJ1.0 T-DNA region (5'-3')

#### Right Border

TTACAACGGTATATATCCTGCCA GGAGATCTGATC

#### CaMV 35S Promoter

AAGCTTGCAT GCCTGCAGGT CCCCAGATTA GCCTTTTCAA TTTCAGAAAG AATGCTAACC  
CACAGATGGT TAGAGAGGCT TACGCAGCAG GTCTCATCAA GACGATCTAC CCGAGCAATA  
ATCTCCAGGA AATCAAATAC CTTCCCAAGA AGGTTAAAGA TGCAGTCAA AGATTCAGGA  
CTAACTGCAT CAAGAACACA GAGAAAGATA TATTTCTCAA GATCAGAAAGT ACTATTCCAG  
TATGGACGAT TCAAGGCTTG CTTCAAAAC CAAGGCAAGT AATAGAGATT GGAGTCTCTA  
AAAAGGTAGT TCCCAGTAA TCAAAGGCCA TGGAGTCAA GATTCAAATA GAGGACCTAA  
CAGAACTCGC CGTAAAGACT GGCGAACAGT TCATACAGAG TCTCTTACGA CTCAATGACA  
AGAAGAAAAT CTTCTGCAAC ATGGTGGAGC ACGACACACT TGTCTACTCC AAAAATATCA  
AAGATACAGT CTCAGAAGAC CAAAGGGCAA TTGAGACTTT TCAACAAAGG GTAATATCCG  
GAAACCTCCT CGGATTCCAT TGCCAGCTA TCTGTCACTT TATTGTGAAG ATAGTGGAAA  
AGGAAGGTGG CTCCTACAAA TGCCATCATT GCGATAAAGG AAAGGCCATC GTTGAAGATG  
CCTCTGCCGA CAGTGGTCCC AAAGATGGAC CCCACCCAC GAGGAGCATC GTGGAAAAAG  
AAGACGTTCC AACACGTCT TCAAAGCAAG TGGATTGATG TGATATCTCC ACTGACGTAA  
GGGATGACGC ACAATCCAC TATCCTTCGC AAGACCCTC CTCTATATAA GGAAGTTCAT  
TTCATTTGGA GAGAACACGG GGGACT

#### Linker

CTAGAGGATCCATGTCGACCCGGGAGCT

#### *nos* terminator

CGAATTTCCCGA TCGTTCAAAC ATTTGGCAAT AAAGTTTCTT AAGATTGAAT CCTGTTGCCG  
GTCTTGCGAT GATTATCATA TAATTTCTGT TGAATTACGT TAAGCATGTA ATAATTAACA  
TGTAATGCAT GACGTTATTT ATGAGATGGG TTTTATGAT TAGAGTCCCG CAATTATACA  
TTTAATACGC GATAGAAAAC AAAATATAGC GCGCAAATA GGATAAATTA TCGCGCGCGG  
TGTCATCTAT GTTACTAGAT CGGGAA

#### Left Border

TTCGATA TCATTTACAATTGAATATATCCTGCCGCATCG

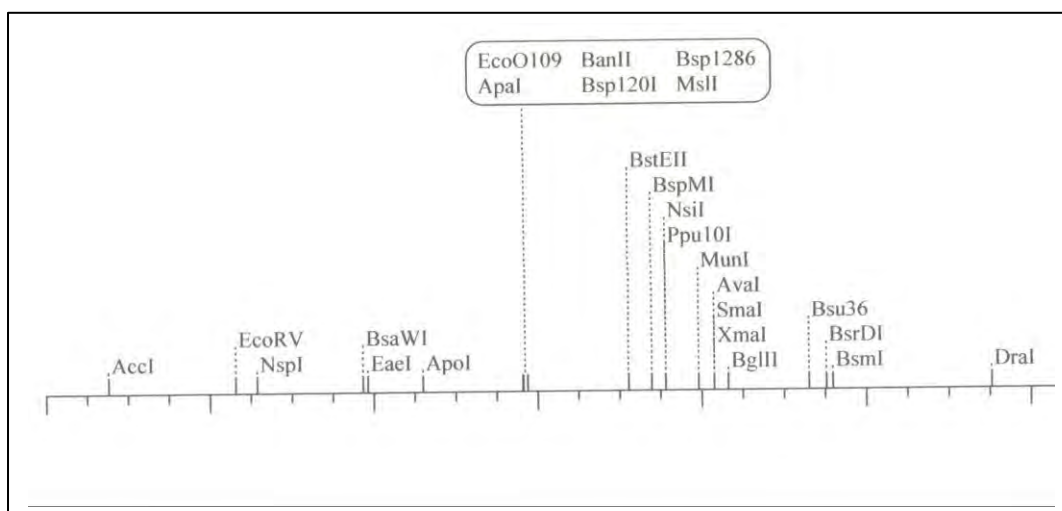
### ACC oxidase 1: cDNA sequence (5'- 3') (Pogson *et al.*, 1995a)

```

1   atcaaaacaac tagctacttc aaccaataac tttcaaagaa gagagagaga tggagaagaa
61  cattaagttt ccagttgtag acttgtccaa gctcattggt gaagagagag accaaacat
121 ggcttttgatc aacgatgctt gtgagaattg gggcttcttt gagatagtga accatggttt
181 accacatgat  ttgatggaca acgtcgagaa gatgacaaaag gaacattaca agatatcaat
241 ggaacaaaag  ttcaacgaca tgctcaaatc aaaaggtttg gaaaatcttg agagagaagt
301 tgaggatggt  gattgggaaa gcacttttcta ccttcgcat  ctccctcagt ccaatctcta
361 cgacattcct  gatatgtctg atgaataccg gacggccatg aaagattttg ggaagagatt
421 ggagaatcct  gctgaggatt tgttggatct attgtgtgag aatttagggg tagagaaagg
481 gtacttgaag  aaagtttttc atggaacaaa aggtccaacc tttgggacta aggtgagcaa
541 ctatccagct  tgtcctaagc cagagatgat caaaggctct agggcccaca ctgatgcagg
601 aggcatcacc  ttgtttgttc aagatgacaa ggtcagtggg ctccagcttc ttaaagatgg
661 tgactggatt  gatgttcctc cactcaacca ctctattgtc atcaatcttg gtgaccaact
721 tgaggtgata  accaacggca ggtacaagag tgtgatgcat cgtgtggtga ctcagaaaga
781 aggaaacaga  atgtcaattg catcttttcta caaccgggga agcgatgctg agatctctcc
841 agcttcatcg  cttgcctgta aagaaaccga gtaccaaatg tttgtttttg atgactacat
901 gaagctctat  gctgggggtca agtttcagcc taaggagcca cggttcgagg caatgaagaa
961 tgctaatgca  gttacagaat tgaacccaac agcagccgta gagactttct aaaaacaag
1021 tggagtttga  gcgaaagcaa agaaacaaaa atgtgttttg tgttgtgtgt ttacgtcaat
1081 aagttaaaga  ctgatattat tgttgatata attaagatgt ctggtggtta attgttggtc
1141 aatgggtgtg  ttaaagtgtg ggggtgtttat ttatgtttat ggaagatgat aataataata
1201 aaaataaata  atatgataac tgttctaaga aaaaaaa

```

### ACC oxidase 1: Restriction endonuclease map



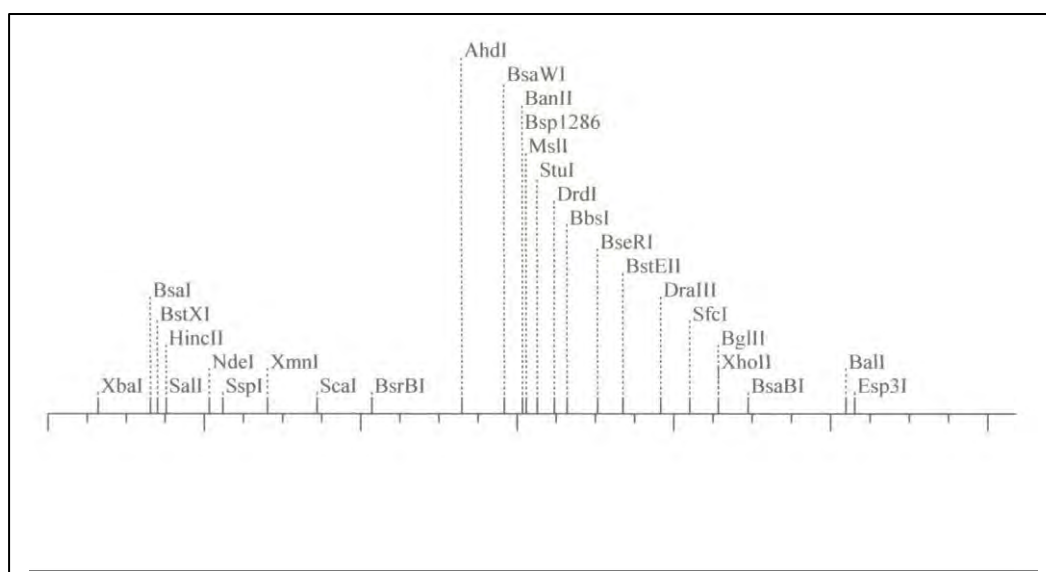
## ACC oxidase 2: cDNA sequence (5' - 3') (Pogson *et al.*, 1995a)

```

1   actaacatca tcaacaacat taagttgcc a gtttaaagcg attcataagt ttacatagag
61  agggctctaga gtaatggaga aaaacattaa gtttcctggt gtagacttgt ctaagctaaa
121 tgggtgaagag agagacccaaa ccatggcttt ggtcgacgat gcttgtcaaa actggggcct
181 ctttgagctg ctaaaccatg gaataccata tgatcttatg gacaatattg agaggatgac
241 aaaggaacac tacaaaaaat ttatggaaca aaagttcaaa gaaatgcttc gttccaaaaa
301 tttagatact ctggagactg aagttgagaa tgttgattgg gaaagtactt tcttccttca
361 ccatcttcct cagactaatc tctacgacat cccggatatg tcagatgaat accgagcggc
421 catgaaggac tttgggaaga ggctagagaa cctagcggaa gaactgttgg atttggttgg
481 tgagaatcta gggttggaga aagggactt gaagaagggtg tttagtggga caaagggctc
541 aacttttggg acaaaggtta gcaactatcc accatgtcct aaaccggaga tgatcaaagg
601 gcttagggct cacacggatg caggaggcct catattgcta tttcaagacg ataaggtcag
661 tggctctcag cttctcaaag atgggtgttg ggttgatgtc cctcctctca aacactccat
721 tgtcatcaat cttggtgacc aacttgagggt gataaccaac gggaagtaca agagcataat
781 gcaccgtgtg atgacacaaa aagaaggaaa caggatgtct atagcgtcgt tctacaacc
841 tggaagtgat gcgagatct ctcccgcacc atctctagtg gagaaagact ctgatgaata
901 tccgagtttt gtgtttgatg actacatgaa gctatatgct ggagtcaagt ttcagcccaa
961 ggagccacgt tttgaggcga tgaagaatgt tgcagcaacc accgatttga acccgggtgg
1021 cacagtcgag acgttctaaa tggatgtggg attcttctat gaaggcaaga aagatggggg
1081 ttgatatgtg tgtggtgggt aataatgtaa aataagtatt gaagttaatg ttatagtaga
1141 atcaagaact aagttgtgat cacttatgaa tctagtgtgg ttaagtgtgg gagtgtttat
1201 gcaataattg tattggaaat atgaatttta aag

```

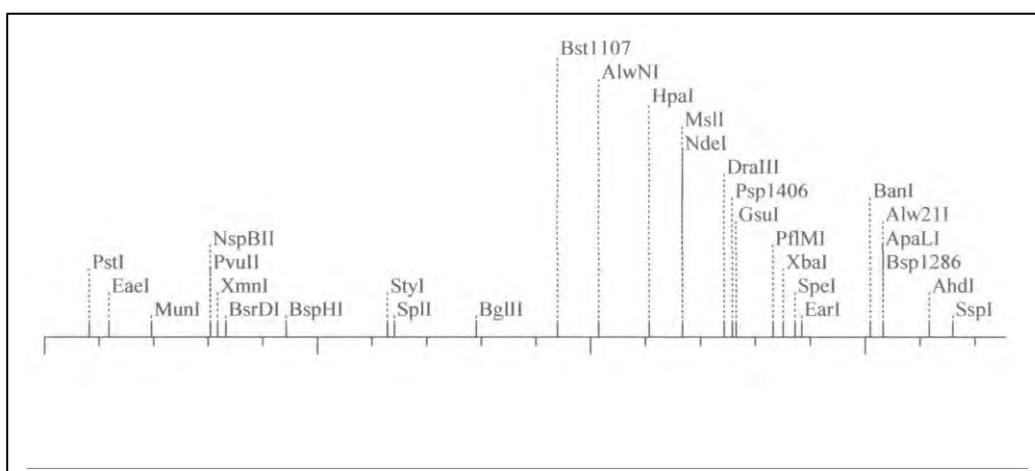
## ACC oxidase 2: Restriction endonuclease map



## ACC synthase: cDNA sequence (5' - 3') (Pogson *et al.*, 1995b)

```
1 atctcaacag aacaaaaaca aaccacaactt attaaaaccc cttttgaaga aacaaaaatg
61 gtagctttga ctgcagagaa gcaagaccag aacctactgt cgagaatggc cgccggtgac
121 ggacacggcg agaaatcagc ttatttccgat ggctggaaag cttatgaaga aaaccattt
181 cacccaattg atagaccgga tggagttatt cagatgggtc tcgctgaaaa tcagctttgt
241 ggagatttga tgcgtaaagt ggttttagaa cccccggaag cttcgatttg cacagctgaa
301 ggtgtgaatc agttcagcga cattgcgatt tttcaggatt atcatggctt gcctgaattc
361 agacaagctg tagcgaagtt tatggagaag acaagaaaca acaaagtgaa gtttgatcct
421 gaccggatcg tcatgagcgg cggcgcaacc ggagcgcacg agacggttgc tttctgttta
481 gccaatcccg gcgacggttt cttggttccg actccttatt atccagggtt tgatagagat
541 ttgagatgga gaaccggagt gaatcttgta cgggttactt gtcatagctc caacgggtt
601 aagatcacgg cggaagcctt ggacgctgcg tacgaaaacg cgcgtgtatc gaacattccg
661 gttaagggtt tactcataac caatccttcc aaccgctcgg gtacgacggt agaccgggat
721 tgcttgaaat ctttggttaa gttcaccaat gacaaagggg ttcaccttat tgctgatgag
781 atctatgcag caactacttt tgggtaatcc gagtttatca gcgtcgcaga agtaattgac
841 gagatccccg attgcaacac cgatttgatc catattgtct atagtttatc aaaagatag
901 ggtctgcccg gtttaagagt cggtatagta tactcttaca atgaccgggt ggttcaaatt
961 gccaggaaaa tgtcgagttt cggtttggtt tcgtctcaaa cgcagcatct gatcgccaaa
1021atgttatccg acgaagactt tgtagacgaa ttcacccgca agagcaaact acggttggtc
1081gaaagacacg cagagttaac caccggttta gacggtttaa gcattgggtg gttaaaggcc
1141ggagccgggtt tgttcatatg gatggattta agaaaccttt tgaagacggc tacattcgac
1201tcggagatgg agctgtggcg tgtgatcgtc cacaagggtg agctgaacgt ttctccaggc
1261ggttcgtgcc actgccacga accgggatgg tttagagtat gttttgcgaa catggactac
1321cagacaatgg agaccgctct agagaggatc agagtgttca ctagtcaaac tgaagaggag
1381agtctgatac tgactaaacc gatggctaag aaaaagaagt gttggcagag tagcctccgg
1441ttaagcttta aggacacgag acggttcgag gagggtctct tctctcctca ttcaccggtg
1501ccaccttctc cgcttgctcg tgcacagata taagaccggt tcagtttttg actagaccaa
1561gctgtcgtaa attgaaagat aaaaattatt taacattgat tgtgacattt tgtctaatta
1621aatgtatagc tactactgtc aagttgaata tttttataat gtatctcttg taagtttaac
1681cagttgaata atataatatg agaaaccata atttctctaa tcgttattaa aaaa
```

## ACC synthase: Restriction endonuclease map



## 8.0 References

- Abeles, F.B. (1973) Ethylene in Plant biology. New York: Academic. pp. 302
- Aharoni, N., Philosoph-Hadas, S., Barkai-Golan, R. (1985) Modified atmospheres to delay senescence and decay of Broccoli. In SM Blankenship, ed, Controlled Atmospheres for Storage and Transport of Perishable Agricultural Commodities, Horticulture Report 126. Department of Horticultural Science, Raleigh, NC, pp 167-177
- Al-Kaff, N.S., Covey, S.N., Kreike, M.M., Page, A.M., Pinder, R., Dale, P.J. (1998) Transcriptional and posttranscriptional plant gene silencing in response to a pathogen. *Science*, **279**: 2113-2115
- Aronson, A.I., Shai, Y. (2001) Why *Bacillus thuringiensis* insecticidal toxins are so effective: unique features of their mode of action. *FEMS Microbiology Letters*, **195**: 1-8
- Ayub, R., Guis, M., BenAmor, M., Gillot, L., Roustan, J.P., Latche, A., Bouzayen, M., Pech, J.C. (1996) Expression of ACC oxidase antisense gene inhibits ripening of cantaloupe melon fruits. *Nature Biotechnology*, **14**: 862-866
- Barry, C.S., Blume, B., Bouzayen, M., Cooper, W., Hamilton, A.J., Grierson, D. (1996) Differential expression of the 1-aminocyclopropane-1-carboxylate oxidase gene family of tomato. *Plant Journal*, **9**: 525-535
- Batal, K.M., Heaton, E.K., Beuchat, L.R., Granberry, D.M. (1981) Effects of N-6-benzyladenine and storage temperatures on shelf-life and quality of raw and cooked broccoli (*Brassica oleracea* L var *italica*). *Hortscience*, **16**: 284-284
- Benfy, P.N., Chua, N.-H. (1990) The cauliflower mosaic virus 35S promoter: Combinational regulation of transcription in plants. *Science*, **250**: 959-966
- Berthomieu, P., Beclin, C., Charlot, F., Dore C., Jouanin L. (1994) Routine transformation of rapid cycling cabbage (*Brassica oleracea*)-molecular evidence for regeneration of chimeras. *Plant Science*, **96**: 223-235
- Bevan, M. (1984) Binary *Agrobacterium* vectors for plant transformation. *Nucleic Acids Research*, **12**: 8711-8721
- Bevan, M., Barnes, W.M., Chilton, M-D. (1983) Structure and transcription of the *nopaline synthase* gene region of the T-DNA. *Nucleic Acids Research*, **11**: 369-385
- Blaich, R. (1992) Function of genetic material: activity of genes in transgenic plants. *Progress in Botany*, **53**: 207-220
- Blumenthal, A., Kuznetzova, L., Edelbaum, O., Raskin, V., Levy, M., Sela, I. (1999) Measurement of green fluorescence protein in plants: quantification, correlation to expression, rapid screening and differential gene expression. *Plant Science*, **142**: 93-99

Bolitho, K.M., LayYee, M., Knighton, M.L., Ross, G.S. (1997) Antisense apple ACC-oxidase RNA reduces ethylene production in transgenic tomato fruit. *Plant Science*, **122**: 91-99

Braun, A. (1954) The physiology of plant tumors. *Annual Review of Plant Physiology*, **5**: 133-162

Braun, A. (1978) Plant tumours. *Biochimica Et Biophysica Acta*, **51**: 167-191

Brennan, P.S., Shewfelt, R.L. (1989) Effect of cooling delay at harvest on broccoli quality during postharvest storage. *Journal of Food Quality*, **12**: 13-22

Bryant, J.A. (1988) *Plants Today*, **1**: 23-28

Buchanan-Wollaston, V. (1997) The molecular biology of leaf senescence. *Journal of Experimental Botany*, **48**: 181-199

Burg, S.P. (1962) The physiology of ethylene formation. *Annual Review of Plant Physiology*, **13**: 265-302

Buttner, M., Singh, K.B. (1997) *Arabidopsis thaliana* ethylene-responsive element binding protein (AtEBP), an ethylene inducible, GCC box DNA-binding protein interacts with an ocs element binding protein. *Proceedings of National Academy of Science USA*, **94**: 5961-5966

Cardarelli, M., Mariotti, D., Pomponi, M., Spano, L., Capone, I., Constantino, P. (1987) *Agrobacterium rhizogenes* T-DNA genes capable of inducing hairy root phenotype. *Molecular and General Genetics*, **209**: 475-480

Chalfie, M., Tu, Y., Euskirchen, G., Ward, W.W., Prasher, D.C. (1994) Green fluorescent protein as a marker gene for gene expression. *Science*, **263**: 802-805

Charest, P.J., Holbrook, L.A., Gabard, J., Iyer, V.N., Miki, B.L. (1988) *Agrobacterium*-mediated transformation of thin cell layer explants from *Brassica napus* L. *Theoretical and Applied Genetics*, **75**: 438-445

Chen, L.F.O., Hwang, J.Y., Charng, Y.Y., Sun, C.W., Yang, S.F. (2001) Transformation of broccoli (*Brassica oleracea* var. *italica*) with isopentenyltransferase gene via *Agrobacterium tumefaciens* for post-harvest yellowing retardation *Molecular Breeding*, **7**: 243-257

Chi, G.L., Barfield, D.G., Sim, G.E., Pua, E.C. (1990) Effect of AgNO<sub>3</sub> and amino-ethoxyvinylglycine on in vitro shoot and root organogenesis from seedling explants of recalcitrant brassica genotypes *Plant Cell Reports*, **9**: 195-198

Chrispeels, M.J., Sadava, D.E. (1994) *Plants, Genes and Agriculture*. Jones & Bartlett Pub.

Christey, M.C., Braun, R.H., Reader, J.K. (1999) Field performance of transgenic brassicas (*Brassica oleracea* and *B. rapa*) transformed with *Agrobacterium rhizogenes*. *SABRAO Journal of Breeding and Genetics*, **31**:93-108

Christey, M.C., Sinclair, B.K. (1992) Regeneration of transgenic kale (*Brassica oleracea* var *acephala*), rape (*Brassica napus*) and turnip (*Brassica campestris* var *rapifera*) plants via *Agrobacterium rhizogenes* mediated transformation. *Plant Science*, **87**: 161-169

Christou, P. (1996) Transformation technology. *Trends In Plant Science*, **1**: 423-431

Clarke, S.F., Jameson, P.E., Downs, C.G. (1994). The influence of 6-benzylaminopurine on post-harvest senescence of floral tissues of broccoli (*Brassica oleracea* var. *italica*). *Plant Growth Regulation*, **14**: 21-27

Cogan, N.O.I., Harvey, E., Robinson, H.T., Lynn, J., Pink, D.A.C., Newbury, H.J., Puddephat, I.J. (2001) The effects of anther culture and plant genetic background on *Agrobacterium rhizogenes*-mediated transformation of commercial cultivars and derived double haploid *Brassica oleracea*. *Plant Cell Reports*, **20**:755-762

Cogoni, C., Macino, G. (2000) Post-transcriptional gene silencing across kingdoms *Current Opinion in Genetics & Development*, **10**: 638-643

Cordes, S., Deikmann, J., Margossian, L.J., Fischer, R.L. (1989) Interaction of a DNA binding factor with the 5 flanking region of an ethylene-responsive fruit ripening gene from tomato. *EMBO Journal*, **7**: 3315-3320

Crisp, P., Gray, A.R., Angell, S.M., Salter, P.J., Akehurst, J., Sutherland, R.A. (1986). The effect of spacing on the breeding of broccoli from an expanded genetic base. *Journal of Horticultural Science*, **61**: 205

Daley, M., Knauf, V.C., Summerfelt, K.R., Turner, J.C. (1998) Co-transformation with one *Agrobacterium tumefaciens* strain containing two binary plasmids as a method for producing marker-free transgenic plants. *Plant Cell Reports*, **17**: 489-496

David C., Tempe, J. (1988) Genetic transformation of cauliflower (*Brassica oleracea* L. var. *botrytis*) by *Agrobacterium rhizogenes*. *Plant Cell Reports*, **7**: 88-91

DEFRA (2000) Basic Horticultural Statistics for the United Kingdom, Calendar and Crop Years 1989/90-1999/00

de Framond, A.J., Back, E.W., Chilton, W.S., Kayes, L., Chilton, M-D. (1986) Two unlinked T-DNAs can transform the same tobacco plant cell and segregate in the F1 generation. *Molecular and General Genetics*, **202**: 125-131

- Delagrave, S., Hawtin, R.E., Silva, C.M., Yang, M.M., Youvan, D.C. (1995) Red-shifted excitation mutants of the green fluorescent protein. *Bio/Technology*, **13**: 151-154
- Depicker, A., Herman, L., Jacobs, A., Schell, J., Van Montagu, M. (1985) Frequencies of simultaneous transformation with different T-DNAs and their relevance to the *Agrobacterium*/plant cell interaction. *Molecular and General Genetics*, **201**: 477-484
- Draper, J., Scott, R., Armitage, P., Walden, R. (1988) Plant genetic transformation and gene expression: A laboratory manual. Blackwell Scientific pub. Oxford.
- Earle, E.D., Metz T.D., Roush R.T., Shelton A.M. (1996) Advances in transformation technology for vegetable brassica. *Acta Horticulturae*, **407**: 161-168
- Felix, G., Grosskopf , D.G., Regenass, M., Basse, C.W., Boller, T. (1991) Elicitor-induced ethylene biosynthesis in tomato cells - characterization and use as a bioassay for elicitor action. *Plant Physiology*, **97**: 19-25
- Filichkin, S.A., Gelvin, S.B. (1993) Formation of a putative relaxation intermediate during T-DNA processing directed by the *Agrobacterium tumefaciens* VirD1, D2 endonuclease. *Molecular Microbiology*, **8**: 915-926
- Fray, R.G., Grierson, D. (1993). Molecular genetics of tomato fruit ripening. *Trends in Genetics*, **9**: 438-443
- Frisch, D.A., Harris-Haller, L.W., Yokubaitis, N.T., Thomas, T.L., Hardin, S.H., Hall, T.C. (1995). Complete sequence of the binary vector Bin 19. *Plant Molecular Biology*, **27**:405-409
- Fry, J., Barnason, A., Horsch, R.B (1987) Transformation of *Brassica napus* with *Agrobacterium tumefaciens* based vectors. *Plant Cell Reports*, **6**: 321-325
- Gan, S.S., Amasino, R.M. (1995) Inhibition of leaf senescence by autoregulated production of cytokinin *Science*, **270** (5244): 1986-1988
- Gelvin, S.B. (1990). Crown Gall Disease and Hairy Root Disease. *Plant Physiology*, **92**: 281-285
- Gelvin, S. B. (2000). *Agrobacterium* and plant genes involved in T-DNA transfer and integration. *Annual Review of Plant Physiology*, **51**: 223-256
- Gonzalez, N.M and Botella, J.R (2001) Characterization of three ACC synthase gene family members during post-harvest-induced senescence in broccoli (Unpublished).
- Gray, A.R. (1982). Taxonomy and evolution of broccoli (*Brassica oleracea* var

*italica*). *Economic Botany*, **36**: 397

Gray, A.R. (1993). Broccoli *Brassica oleracea* L. (*italica* group). In: Genetic improvement of vegetable crops. Eds. Kalloo, G., Bergh, B.O. pp 61-86.

Gray, J., Picton, S., Shabbeer, J., Schuch, W., Grierson, D. (1992) Molecular-biology of fruit ripening and its manipulation with antisense genes. *Plant Molecular Biology*, **19**: 69-87

Grierson, D. (1996). Silent genes and everlasting fruits and vegetables? *Nature Biotechnology*, **14**: 828-829

Guilley, H., Dudley, R.K., Jonard, G., Balazs, E., Richards, K.E. (1982). Transcription of cauliflower mosaic-virus DNA - Detection of promoter sequences, and characterization of transcripts. *Cell*, **30**: 763-773

Guis, M., Botondi, R., BenAmor, M., Ayub, R., Bouzayen, M., Pech, J.C., Latche, A. (1997) Ripening-associated biochemical traits of Cantaloupe Charentais melons expressing an antisense ACC oxidase transgene. *Journal of American Society of Horticultural Science*, **122**: 748-751

Hadfield, K.A., Bennett, A.B. (1997) Programmed senescence of plant organs. *Cell Death and Differentiation*, **4**: 662-670

Hamilton, A.J., Brown, S., Han, Y.H., Ishizuka, M., Lowe, A., Solis, A.G.A., Grierson, D. (1998) A transgene with repeated DNA causes high frequency, post-transcriptional suppression of ACC-oxidase gene expression in tomato. *Plant Journal*, **15**: 737-746

Hamilton, A.J., Lycett, G.W., Grierson, D. (1990). Antisense gene that inhibits synthesis of the hormone ethylene in transgenic plants. *Nature*, **346**: 284-287

Hao, D.Y., OhmeTakagi, M., Sarai, A. (1998) Unique mode of GCC box recognition by the DNA-binding domain of ethylene-responsive element-binding factor (ERF domain) in plants. *Journal of Biological Chemistry*, **273**: 26857-26861

Haseloff J, Siemering KR, Prasher DC, Hodge S (1997) Removal of a cryptic intron and subcellular localization of green fluorescent protein are required to mark transgenic Arabidopsis plants brightly. *Proceedings of the National Academy of Sciences USA*, **94**: 2122-2127

Heim, R., Cubitt, A.B., Tsien, R.Y. (1995) Improved green fluorescence. *Nature*, **373**: 663-664

Heim, R., Prasher, D.C., Tsien, R.Y. (1994) Wavelength mutations and posttranslational autoxidation of green fluorescent protein. *Proceedings of the National Academy of Sciences USA*, **91**: 12501-12504

Helm, J. (1963) Morphologisch-taxonomische Gleiderung der Kultursippen

von *Brassica oleracea*. *Kulturpflanze*, **11**: 92-210

Henzi, M.X., Christey, M.C., McNeil, D.L. (2000) Factors that influence *Agrobacterium rhizogenes*-mediated transformation of broccoli (*Brassica oleracea* L. var. *italica*). *Plant Cell Reports*, **19**: 994-999

Henzi, M.X., Christey, M.C., McNeil, D.L., Davies, K.M. (1999a) *Agrobacterium rhizogenes*-mediated transformation of broccoli (*Brassica oleracea* L var. *italica*) with an antisense 1-aminocyclopropane-1-carboxylic acid oxidase gene. *Plant Science*, **143**: 55-62

Henzi, M.X., McNeil, D.L., Christey, M.C., Lill, R.E. (1999b) A tomato antisense 1-aminocyclopropane-1-carboxylic acid oxidase gene causes reduced ethylene production in transgenic broccoli. *Australian Journal of Plant Physiology*, **26**: 179-183

Hipkins, M.F., Baker, N.R. (1986) Spectroscopy. In Photosynthesis energy transduction Ed Hipkins, M.F., Baker, N.R. IRL press Oxford

Hodgkin, T. (1995). Cabbages, Kales, etc. *Brassica oleracea* (Cruciferae). In: Smartt J. Simmonds NW (eds) Evolution of Crop Plants. pp 76-82. Longman

Hoekema, A., Hirsch, P.R., Hooykaass, P.J.J., Schilperoot, R.A. (1983). A binary vector strategy based on separation of vir- and T-region of *Agrobacterium tumefaciens* Ti-plasmid. *Nature*, **303**: 179-180

Hooykaas, P.J.J., Beijersbergen, A.G.M (1994) The virulence system of *Agrobacterium tumefaciens*. *Annual Review of Phytopathology*, **32**: 157-179

Hosoki, T., Kigo, T. (1994) Transformation of brussels sprouts (*Brassica oleracea* var. *gemmifera* Zenk.) by *Agrobacterium rhizogenes* harbouring a reporter  $\beta$ -glucuronidase gene. *Journal of Japanese Society of Horticultural Science*, **63**: 589-592

Hosoki, T., Kigo, T, Shiraishi, K. (1991) Transformation and regeneration of broccoli (*Brassica oleracea* var. *italica*) mediated by *Agrobacterium rhizogenes*. *Journal of Japanese Society of Horticultural Science*, **60**: 71-75

Hyodo, H., Morozumi, S., Kato, C., Tanaka, K., Terai, H. (1994) Ethylene production and ACC oxidase activity in broccoli flower buds and the effect of endogenous ethylene on their senescence. *Acta Horticulturae*, **394**: 191-198

Jackson, S.A., Fenggao, D., Jiang, J. (1999) Digital mapping of bacterial artificial chromosomes by fluorescence *in situ* hybridisation. *The Plant Journal*, **17**: 581-587

James, C. Global review of commercialized transgenic crops: 2000. ISAAA Briefs No. 21

Jefferson, R.A., Burgess, S.M., Hirsh, D. (1986) Beta-glucuronidase from

*Escherichia coli* as a gene-fusion marker. *Proceedings of the National Academy of Sciences USA*, **83**: 8447-8451

Jefferson, R.A., Kavanagh, T.A., Bevan, M.W. (1987). GUS fusions:  $\beta$ -glucuronidase as a sensitive and versatile gene fusion marker in higher plants. *The EMBO Journal*, **6**:3901-3907

Jin, S., Prusti, R.K., Roitsch, T., Ankenbauer, R.G., Nester, E.W. (1990a) Phosphorylation of the VirG protein of *Agrobacterium tumefaciens* by the autophosphorylated VirA protein: essential role in biological activity of VirG. *Journal of Bacteriology*, **172**: 4945-4950

Jin, S., Roitsch, T., Ankenbauer, R.G., Gordon, M.P., Nester, E.W. (1990b) The VirA protein of *Agrobacterium tumefaciens* is autophosphorylated and is essential for *vir* gene regulation. *Journal of Bacteriology*, **172**: 525-530

John, I., Drake, R., Farrell, A., Cooper, W., Lee, P., Horton, P., Grierson, D. (1995) Delayed leaf senescence in ethylene-deficient ACC-oxidase antisense tomato plants: molecular and physiological analysis. *The Plant Journal*, **7**: 483-490

Jones, M.L., Woodson, W.R. (1999) Differential expression of three members of the 1-aminocyclopropane-1-carboxylate synthase gene family in carnation. *Plant Physiology*, **119**: 755-764

Kasai, Y., Hyodo, H., Ikoma, Y., Yano, M. (1998) Characterization of 1-aminocyclopropane-1-carboxylate (ACC) oxidase in broccoli florets and from *Escherichia coli* cells transformed with cDNA of broccoli ACC oxidase. *Botanical Bulletin Of Academia Sinica*, **39**: 225-230

Kasai, Y., Kato, M., Hyodo, H. (1996). Ethylene biosynthesis and its involvement in senescence of broccoli florets. *Journal of Japanese Society of Horticultural Science*, **65**: 185-191

Kato, M., Hyodo, H. (1999) Purification and characterization of ACC oxidase and increase in its activity during ripening of pear fruit. *Journal of Japanese Society of Horticultural Science*, **68**: 551-557

Kende, H. (1989) Enzymes of ethylene biosynthesis. *Plant Physiology*, **91**: 1-4

Kende, H. (1993) Ethylene Biosynthesis. *Annual Review of Plant Physiology and Plant Molecular Biology*, **44**: 283-307

Kim, W.T., Yang, S.F. (1992) Turnover of 1-aminocyclopropane-1-carboxylic acid synthase protein in wounded tomato fruit tissue. *Plant Physiology*, **100**: 1126-1131

King, G.A., Morris, S.C. (1994a). Early compositional changes during postharvest senescence of broccoli. *Journal of American Society of Horticultural Science*, **119**: 1000-1005

King, G.A., Morris, S.C. (1994b). Physiological-changes of broccoli during early postharvest senescence and through the preharvest-postharvest continuum. *Journal of American Society of Horticultural Science*, **119**: 270-275

Knoester, M., Linthorst, H.J.M., Bol, J.F., Van Loon, L.C. (1997) Modulation of stress-inducible ethylene biosynthesis by sense and antisense gene expression in tobacco. *Plant Science*, **126**:173-183

Komari, T., Hiei, Y., Saito, Y., Murai, N., Kumashiro, T. (1996) Vectors carrying two separate T-DNAs for co-transformation of higher plants mediated by *Agrobacterium tumefaciens* and segregation of transformants free from selection markers. *The Plant Journal*, **10**: 165-174

Konings, H., Jackson, M.B. (1979) A relationship between rates of ethylene production by roots and the promoting or inhibiting effects of exogenous ethylene and water on root elongation. *Zeitschrift Fur Pflanzenphysiologie*, Bd. 92. S. 385-397

Ku, V.V.V., Wills, R.B.H. (1999) Effect of 1-methylcyclopropene on the storage life of broccoli. *Postharvest Biology and Technology*, **17**: 127-132

Kumar, P.P., Lakshmanan, P., Thorpe, T. (1998) Review Regulation of morphogenesis in plant tissue culture by ethylene. *In vitro Cellular and Developmental Biology-Plant*, **34**: 94-103

Lasserre, E., Bouquin, T., Hernandez, J.A., Bull, J., Pech, J.C., Balague, C. (1996) Structure and expression of three genes encoding ACC oxidase homologs from melon (*Cucumis melo* L.). *Molecular and General Genetics*, **251**: 81-90

Lawton, K.A., Huang, B., Goldsbrough, P.B., Woodson, W.R. (1989) Molecular-cloning and characterization of senescence-related genes from carnation flower petals. *Plant Physiology*, **90**: 690-696

Lawton, K.A., Raghothama, K.G., Goldsbrough, P.B., Woodson, W.R. (1990) Regulation of senescence-related gene-expression in carnation flower petals by ethylene. *Plant Physiology*, **93**: 1370-1375

Levin, J.Z., de Framond, A.J., Tuttle, A., Bauer, M.W., Heifetz, P.B. (2000) Methods of double-stranded RNA-mediated gene inactivation in *Arabidopsis* and their use to define an essential gene in methionine biosynthesis. *Plant Molecular Biology*, **44**: 759-775

Liang, X.W., Abel, S., Keller, J.A., Shen, N.F., Theologis, A. (1992) The 1-aminocyclopropane-1-carboxylate synthase gene family of *Arabidopsis thaliana*. *Proceedings of the National Academy of Science USA*, **89**: 11046-11050

Lieberman, M., Hardenburg, R.E. (1954) Effect of modified atmospheres on

respiration and yellowing of broccoli at 75 degrees F. *Proceedings of the American Society of Horticultural Science*, **63**: 409-414

LopezGomez, R., Campbell, A., Dong, J.G., Yang, S.F., GomezLim, M.A. (1997) Ethylene biosynthesis in banana fruit: Isolation of a genomic clone to ACC oxidase and expression studies. *Plant Science*, **123**: 123-131

Makhlouf, J., Willemot, C., Arul, J., Castaigne, F., Emond, J.P. (1989) Regulation of ethylene biosynthesis in broccoli flower buds in controlled atmospheres. *Journal of the American Society of Horticultural Science*, **114**: 955-958

Martintanguy, J., Corbineau, F., Burtin, D., Benhayyim, G., Tepfer, D. (1993) Genetic-transformation with a derivative of *rolC* from *Agrobacterium-rhizogenes* and treatment with alpha-aminoisobutyric-acid produce similar phenotypes and reduce ethylene production and the accumulation of water-insoluble polyamine-hydroxycinnamic acid conjugates in tobacco flowers. *Plant Science*, **93**: 63-76

Mattanovich, D., Ruker, F., Machadom A.D., Laimer, M., Regner, F., Steinkellner, H., Himmler, G., Katinger, H. (1989) Efficient transformation of *Agrobacterium* spp by electroporation. *Nucleic Acids Research*, **17**: 6747-6747

MbenguieAMbenguie, D., Chahine, H., Gomez, R.M., Gouble, B., Reich, M., Audergon, J.M., Souty, M., Albagnac, G., FilsLycaon, B. (1999) Molecular cloning and expression of a cDNA encoding 1- aminocyclopropane-1-carboxylate (ACC) oxidase from apricot fruit (*Prunus armeniaca*). *Physiologia Plantarum*, **105**: 294-303

McCormac, A.C., Fowler, M.R., Chen, D-F., Elliot, M.C. (2001) Efficient co-transformation of *Nicotiana tabacum* by two independent T-DNAs, the effect of T-DNA size and implications for genetic separation. *Transgenic Research*, **10**: 143-155

McGarvey, D.J., Sirevag, R., Christoffersen, R.E. (1992) Ripening-related gene from avocado fruit - ethylene-inducible expression of the messenger-RNA and polypeptide. *Plant Physiology*, **98**: 554-559

McGrath, R.B., Ecker, J.R. (1998). Ethylene signalling in Arabidopsis: Events from the membrane to nucleus. *Plant Physiology and Biochemistry*, **36**: 103-113

McKeon, T.A., Fernandez-Maculet, J.C., Yang, S.F. (1995) Biosynthesis and metabolism of ethylene. pp. 118-139. In: P.J. Davies (ed). *Plant hormones*. Kluwer Academic publishers, Dordrecht

Meyer, P., Saedler, H. (1996) Homology-dependent gene silencing in plants. *Annual Review of Plant Physiology And Plant Molecular Biology*, **47**: 23-48

Molinier, J., Himber, C., Hahne, G. (2000) Use of green fluorescent protein for the detection of transformed shoots and homozygous offspring. *Plant Cell Reports*, **19**:219-223

Morgan, P.W., Drew, M.C. (1997) Ethylene and plant responses to stress. *Physiologia Plantarum*, **100**: 620-630

Murashige, T., Skoog F. (1962) A revised medium for rapid growth and bioassays with tobacco tissue culture. *Physiologia Plantarum*, **15**: 473-497

Muskens, M.W.M, Vissers, A.P.A., Mol, J.N.M., Kooter, J.M. (2000) Role of inverted DNA repeats in transcriptional and post-transcriptional gene silencing. *Plant Molecular Biology*, **43**: 243-260

Nichols, R. (1977) Sites of ethylene production in the pollinated and unpollinated senescing carnation (*Dianthus caryophyllus*) inflorescence. *Planta*, **135**: 155-159

Oeller, P.W., Wong, L.M., Taylor, L.P., Pike, D.A., Theologis, A. (1991). Reversible inhibition of tomato fruit senescence by antisense RNA. *Science*, **254**: 437-439

Oetiker, J.H., Olson, D.C., Shiu, O.Y., Yang, S.F. (1997) Differential induction of seven 1-aminocyclopropane-1-carboxylate synthase genes by elicitor in suspension cultures of tomato (*Lycopersicon esculentum*). *Plant Molecular Biology*, **34**: 275-286

Olson, D.C., White, J.A., Edelman, L., Harkins, R.N., Kende, H. (1991) Differential expression of two genes from 1-aminocyclopropane-1-carboxylate synthase in tomato fruits. *Proceedings of the National Academy of Sciences USA*, **88**: 5340-5344

O'Neil, S.D., Nadeau, J.A., Zhang, X.S., Bui, A.Q., Halevy, A.H. (1993) Interorgan regulation of ethylene biosynthetic genes by pollination. *The Plant Cell*, **5**: 419-432

Ow, D.W., Wood, K.V., DeLuca, M., Wet J.R de., Helinski, D.R., Howell, S.H. (1986) Transient and stable expression of the firefly luciferase gene in plant cell and transgenic plants. *Science*, **234**: 856-859

Paterson, A.H., Bowers, J.E., Burrow, M.D., Draye, X., Elsik, C.G., Jiang, C.X., Katsar, C.S., Lan, T.H., Lin, Y.R., Ming, R., Wright, R.J. (2000) Comparative genomics of plant chromosomes. *Plant Cell*, **12**: 1523-1539

Payton, S., Fray, R.G., Brown, S., Grierson, D. (1996) Ethylene receptor expression is regulated during fruit ripening, flower senescence and abscission. *Plant Molecular Biology*, **31**: 1227-1231

Picton, S., Gray, J.E., Grierson, D. (1995) The manipulation of tomato fruit ripening by expression of antisense RNA in transgenic plants. *Euphytica*, **85**:

Pierpoint, W.S. (1995) Targets for the introduction of pest and disease resistance crops by genetic engineering. IACR- Long Ashton Research Station. April 1995

Pogson, B.J., Downs, C.G., Davies, K.M. (1995a). Differential expression of two 1-aminocyclopropane-1-carboxylic acid oxidase genes in broccoli after harvest. *Plant Physiology*, **108**: 651-657

Pogson, B.J., Downs, C.G., Davies, K.M., Morris, S.C. (1995b). Nucleotide sequence of a cDNA clone encoding 1-aminocyclopropane-1-carboxylic acid synthase from broccoli. *Plant Physiology*, **108**: 857-858

Pogson, B.J., Morris, S.C. (1997). Consequences of cool storage of broccoli on physiological and biochemical changes and subsequent senescence at 20°C. *Journal of the American Society of Horticultural Science*, **122**: 553-558

Poulsen, G.B. (1996). Genetic transformation of *Brassica*. *Plant Breeding*, **115**: 209-255

Prasher, D.C. (1995) Using GFP to see the light. *Trends in Genetics*, **11**: 320-323

Pua, E.C., Chi, G.L. (1993) *De Novo* shoot morphogenesis and plant growth of mustard (*Brassica juncea*) in vitro in relation to ethylene. *Physiologia Plantarum*, **88**: 467-474

Pua, E.C., Sim, G.E., Chye, M.L. (1992) Isolation and sequence analysis of a cDNA clone encoding ethylene forming enzyme in *Brassica juncea* (L.) Czern & Coss. *Plant Molecular Biology*, **19**: 541-544

Puddephat, I.J., Riggs, T.J., Fenning, T.M. (1996). Transformation of *Brassica oleracea* L.: A critical review. *Molecular Breeding*, **2**: 185-210

Puddephat, I.J., Robinson, H.T., Fenning, T.M., Barbara, D.J., Morton, A., Pink, D.A.C. (2001) Recovery of phenotypically normal transgenic plants of *Brassica oleracea* upon *Agrobacterium rhizogenes*-mediated co-transformation and selection of transformed hairy roots by GUS assay. *Molecular Breeding*, **7**: 229-242

Purnhauser, L., Medgyesy, M., Czeko, P.J., Marton, L. (1987) Stimulation of shoot regeneration in *Triticum aestivum* and *Nicotiana plumbaginifolia* Viv. tissue culture using the ethylene inhibitor AgNO<sub>3</sub>. *Plant Cell Reports*, **6**: 1-4

Rays, D.B., Reid, D.M., Yeung, E.C., Pharis, R.P. (2000) Role of ethylene in cotyledon development of microspore-derived embryos of *Brassica napus*. *Journal of Experimental Botany*, **51**: 1851-1859

Robinson, K.E.P., Adams, D.O. (1987) The role of ethylene in the

regeneration of *Helianthus annuus* (sunflower) plants from callus. *Physiologia Plantarum*, **71**: 151-156

Rottmann, W.H., Peter, G.F., Oeller, P.W., Keller, J.A., Shen, N.F., Nagy, B.P., Taylor, L.P., Campbell, A.D., Theologis, A. (1991) 1-aminocyclopropane-1-carboxylate synthase in tomato is encoded by a multigene family whose transcription is induced during fruit and floral senescence. *Journal of Molecular Biology*, **222**: 937-961

Rushing, J.W. (1990) Cytokinins affect respiration, ethylene production, and chlorophyll retention of packaged broccoli florets. *Horticultural Science*, **25**: 88-90

Sambrook, J., Fritsch, E.F., Maniatis, T. (1989) *Molecular Cloning: A Laboratory Manual*. 2nd. Edition. Cold Spring Harbor Laboratory Press, Plainview, New York.

Sato, T., Theologis, A. (1989). Cloning the mRNA encoding 1-aminocyclopropane-1-carboxylate synthase, the key enzyme for ethylene biosynthesis in plants. *Proceedings of the National Academy of Sciences USA*, **86**: 6621-6625

SatoNara, K., Yuhashi, K., Higashi, K., Hosoya, K., Kubota, M., Ezura, H. (1999) Stage- and tissue-specific expression of ethylene receptor homolog genes during fruit development in muskmelon. *Plant Physiology*, **120**: 321-329

Schmulling, T., Schell, J., Spena, A. (1988) Single genes from *Agrobacterium rhizogenes* influence plant development. *The EMBO Journal*, **7**: 2621-2629

Sebastian, R.L., Howell, E.C., King, G.J., Marshall, D.F., Kearsey, M.J. (2000) An integrated AFLP and RFLP Brassica oleracea linkage map from two morphologically distinct doubled-haploid mapping populations. *Theoretical Applied Genetics*, **100**: 75-81

Senior, I., Holford, P., Cooley, R.N., Newbury, H.J. (1995) Transformation of *Antirrhinum majus* using *Agrobacterium rhizogenes*. *Journal of Experimental Botany*, **46**: 1233-1239

Sethi, U., Basu, A., Guha-Mukherjee, S. (1990) Control of cell proliferation and differentiation by modulators of ethylene biosynthesis and action in *Brassica hypocotyl* explants. *Plant Science*, **69**: 225-229

Sheen, J., Hwang, S., Niwa, Y., Kobayashi, H., Galbraith, D.W. (1995) Green-fluorescent protein as a new vital marker in plant cells. *The Plant Journal*, **8**: 777-784

Sinkar, V.P., Pythoud, F., White, F.F., Nester, E.W., Gordon, M.P. (1988) *rolA* locus of the *Ri* plasmid directs developmental abnormalities in transgenic tobacco plants. *Genes and Development*, **2**: 688-697

- Slater, A., Maunder, M.J., Edwards, K., Schuch, W., Grierson, D. (1985) Isolation and characterisation of cDNA clones for tomato polygalacturonase and other ripening-related proteins. *Plant Molecular Biology*, **5**: 37-147
- Slightom, J.L., Durand-Tardif, M., Jouanin, L., Tepfer, D. (1986). Nucleotide sequence analysis of T<sub>L</sub>-DNA of *Agrobacterium rhizogenes* agropine type plasmid. *Journal of Biological Chemistry*, **261**: 108-121
- Song, K., Osborn, T.C., Williams, P.H. (1988) Brassica taxonomy based on nuclear restriction fragment length polymorphisms (RFLPs), 3. Genome relationships in Brassica and related genera and the origin of *B. oleracea* and *B. rapa* (syn. *Campestris*). *Theoretical and Applied Genetics*, **79**: 497
- Songstad, D.D., Duncan, D.R., Widholm, J.M. (1988) Effect of 1-aminocyclopropane-1-carboxylic acid, silver nitrate, and norbornadiene on plant regeneration from maize callus cultures. *Plant Cell Reports*, **7**: 262-265
- Spano, L., Pomponi, M., Constantino, P., Van Slogteren, G.M.S., Tempe, J. (1982) Identification of T-DNA in the root-inducing plasmid of the agropine type *Agrobacterium rhizogenes* 1855. *Plant Molecular biology*, **1**: 291-300
- Spanu, P., Grosskopf, D.G., Felix, G., Boller, T. (1994) The apparent turnover of 1-aminocyclopropane-1-carboxylate synthase in tomato cells is regulated by protein-phosphorylation and dephosphorylation. *Plant Physiology*, **106**: 529-535
- Stam, P., Van Ooijen, J.W. (1995) JoinMap (Tm) 2.0: software for the calculation of genetic maps. CPRO-Wageningen
- Tang, X., Wang, H., Brandt, A.S., Woodson W.R. (1993) Organisation and structure of the 1-aminocyclopropane-1-carboxylate oxidase gene family from *Petunia hybrida*. *Plant Molecular Biology*, **23**: 1151-1164
- Tempe J., Casse-Delbart, F. (1987) Plant gene vectors and genetic transformation: *Agrobacterium Ri* plasmids. In: Vasil I.K (ed) Cell culture and somatic cell genetics of plants, vol. 6, pp. 25-49
- Tepfer, D. (1990) Genetic transformation using *Agrobacterium rhizogenes*. *Physiologia Plantarum*, **79**: 140-146
- Terryn, N., Rouze, P. (2000) The sense of naturally transcribed antisense RNAs in plants. *Trends in Plant Science*, **5**: 394-396
- Thayer, S.S., Choe, H.T., Tang, A., Huffaker, R.C. (1987) Protein turnover during senescence. In: W.W. Thomson, E.A. Nothnagel, and R.C. Huffaker (eds) Plant senescence: Its biochemistry and physiology, pp 71-80. American Society of Plant Physiology, Rockville, Md
- Theologis, A. (1992) One rotten apple spoils the whole bushel: The role of ethylene in fruit ripening. *Cell*, **70**: 181-184

- Thompson, K.F. (1957) Self-incompatibility in marrow-stem Kale, *Brassica oleracea* var *acephala*. I. Demonstration of a sporophytic system. *Journal of Genetics*, **55**: 45-60
- Tian, M.S., Downs, C.G., Lill, R.E., King, G.A. (1994). A role for ethylene in the yellowing of broccoli after harvest. *Journal of the American Society of Horticultural Science*, **119**: 276-281
- U, N. (1935) Genome analysis in Brassica with special reference to the experimental formation of *B. napus* and peculiar mode of fertilisation. *Japanese Journal of Botany*, **7**: 389-452
- Van der Straeten, D., Van Wiemeersch, L., Goodman, H.M., Montagu, M. (1990) Cloning and sequence of two different cDNAs encoding 1-aminocyclopropane-1-carboxylate synthase. *Proceedings of the National Academy of Sciences USA*, **87**: 4859-4863
- Verma, S.C., Rees, H. (1974) Nuclear DNA and the evolution of allotetraploid Brassicae. *Heredity*, **33**: 61-68
- Vriezen, W.H., VanRijn, C.P.E., Voeselek, L.A.C.J., Mariani, C. (1997) A homolog of the *Arabidopsis thaliana* ERS gene is actively regulated in *Rumex palustris* upon flooding. *Plant Journal*, **11**: 1265-1271
- Wang, C.Y. (1977). Effect of aminoethoxy analog of rhizobitoxine and sodium benzoate on senescence of broccoli. *Hortscience*, **12**: 54-56
- Weisz, R., Saunders, M., Smilowitz, Z., Huang, H.W., Christ, B. (1994) Knowledge-based reasoning in integrated resistance management - the colorado potato beetle (*Coleoptera*, *Chrysomelidae*). *Journal of Economic Entomology*, **87**: 1384-1399
- White, F.F., Taylor, B.H., Huffman, G.A., Gordon, M.P., Nester, E.W. (1985) Molecular genetic analysis of the transferred DNA regions of the root-inducing plasmid of *Agrobacterium rhizogenes*. *Journal of Bacteriology*, **164**: 33-44
- Wilkinson, J., Lanahan, M., Yen, H.C., Giovannoni, J., Klee, H. (1995) An ethylene-inducible component of signal transduction encoded by Never-ripe. *Science*, **270**: 1807-1809
- Woodson, W.R. (1987) Changes in protein and mRNA populations during the senescence of carnation petals. *Physiologia Plantarum*, **71**: 495-502
- Woodson, W.R., Park, K.Y., Drory, A., Larsen, P.B., Wang, H. (1992) Expression of ethylene biosynthetic-pathway transcripts in senescing carnation flowers. *Plant Physiology*, **99**: 526-532
- Yamamoto, M., Miki, T., Ishiki, Y., Fujinami, K., Yanagisawa, Y., Nakagawa, H., Ogura, N., Hirabayashi, T., Sato, T. (1995) The synthesis of ethylene in

melon fruit during the early-stage of ripening. *Plant and Cell Physiology*, **36**: 591-596

Yang, S.F., Hoffman, N.E. (1984). Ethylene biosynthesis and its regulation in higher plants. *Annual Review of Plant Physiology*, **35**: 155-189

Yang, S.F., Oetiker, J.H. (1998) Molecular biology of ethylene biosynthesis and its application in horticulture. *Journal of Japanese Society of Horticultural Science*, **67**: 1209-1214

Zambyski, P., Joos, H., Genetello, C., Leemans, M., Van Montagu, M., Schell, J. (1983) *Ti* plasmid vector for the introduction of DNA into plant cells without alteration of their normal regeneration capacity. *The EMBO Journal*, **2**: 2143-2150

Zambryski, P., Tempe, J., Schell, J. (1989) Transfer and function of T-DNA genes from *Agrobacterium Ti* and *Ri* plasmids in plants. *Cell*, **56**: 193-201

Zarembinski, T.I., Theologis, A. (1994) Ethylene biosynthesis and action - a case of conservation. *Plant Molecular Biology*, **26**: 1579-1597

Zheng, X.Y., Wolff, D.W. (2000) Ethylene production, shelf-life and evidence of RFLP polymorphisms linked to ethylene genes in melon (*Cucumis melo* L.). *Theoretical And Applied Genetics*, **101**: 613-624

Zhuang, H., Hildebrand, D.F., Barth, M.M. (1995). Senescence of broccoli buds is related to changes in lipid peroxidation. *Journal of Agricultural and Food Chemistry*, **43**: 2585-2591